Universidad Miguel Hernández de Elche

# CRH-expressing neurons in the medial prefrontal cortex promote social submission

---

Paula Andrea Sierra Diaz

Director of the thesis
**Dr. Felix Raymond Michel Leroy**

Co-director of the thesis
**Dr. Noelia Sofia de León Reyes**

---

Doctoral programme in neuroscience
*Instituto de Neurociencias*
*Universidad Miguel Hernández de Elche*

- 2025 –

INSTITUTO DE NEUROCIENCIAS

EXCELENCIA SEVERO OCHOA

This Doctoral Thesis, entitled “CRH-expressing neurons in the medial prefrontal cortex regulate mouse social hierarchy”, is submitted under the format of **convention thesis by** with the following quality indicators:

de León Reyes NS, Sierra Díaz P, Nogueira R, Ruiz-Pino A, Nomura Y, de Solis CA, Schulkin J, Asok A, Leroy F. Corticotropin-releasing hormone signaling from prefrontal cortex to lateral septum suppresses interaction with familiar mice. Cell. 2023 Sep 14;186(19):4152-4171.e31. doi: 10.1016/j.cell.2023.08.010. Epub 2023 Sep 4. PMID: 37669667; PMCID: PMC7615103.

Sant Joan d'Alacant, April 1st, 2025

Dr. Felix Raymond Michel Leroy, director, and Dr. Noelia Sofia de León Reyes, co-director, of the Doctoral Thesis entitled "CRH-expressing neurons in the medial prefrontal cortex promote social submission**".**

**REPORTS**:

That *Paula Andrea Sierra Diaz* has performed, under the supervision of our Doctoral Programme, the work entitled **"CRH-expressing neurons in the medial prefrontal cortex promote social submission"** pursuant to the terms and conditions established in the Research Plan and following the Code of Good Practices of the Miguel Hernández University of Elche, successfully meeting the objectives planned for its public defense as a doctoral thesis.

In witness whereof I sign for all pertinent purposes, in San Juan de Alicante on April 1st, 2025

| Director of the thesis | Co-director of the thesis |
|---|---|
| Dr. Felix Leroy | Dr. Noelia Sofia de León Reyes |

Sant Joan d'Alacant, April 1st, 2025

Dr. *Cruz Morenilla Palao*, Coordinator of the Doctoral Programme in neuroscience.

**REPORTS**:

That *Paula Andrea Sierra Diaz* has performed, under the supervision of our Doctoral Programme, the work entitled **"CRH-expressing neurons in the medial prefrontal cortex promote social submission"** pursuant to the terms and conditions established in the Research Plan and following the Code of Good Practices of the Miguel Hernández University of Elche, successfully meeting the objectives planned for its public defense as a doctoral thesis.

In witness whereof I sign for all pertinent purposes, in San Juan de Alicante on April 1st, 2025

Prof. Dr. *Cruz Morenilla Palao*

Coordinator of the Doctoral Programme in neuroscience

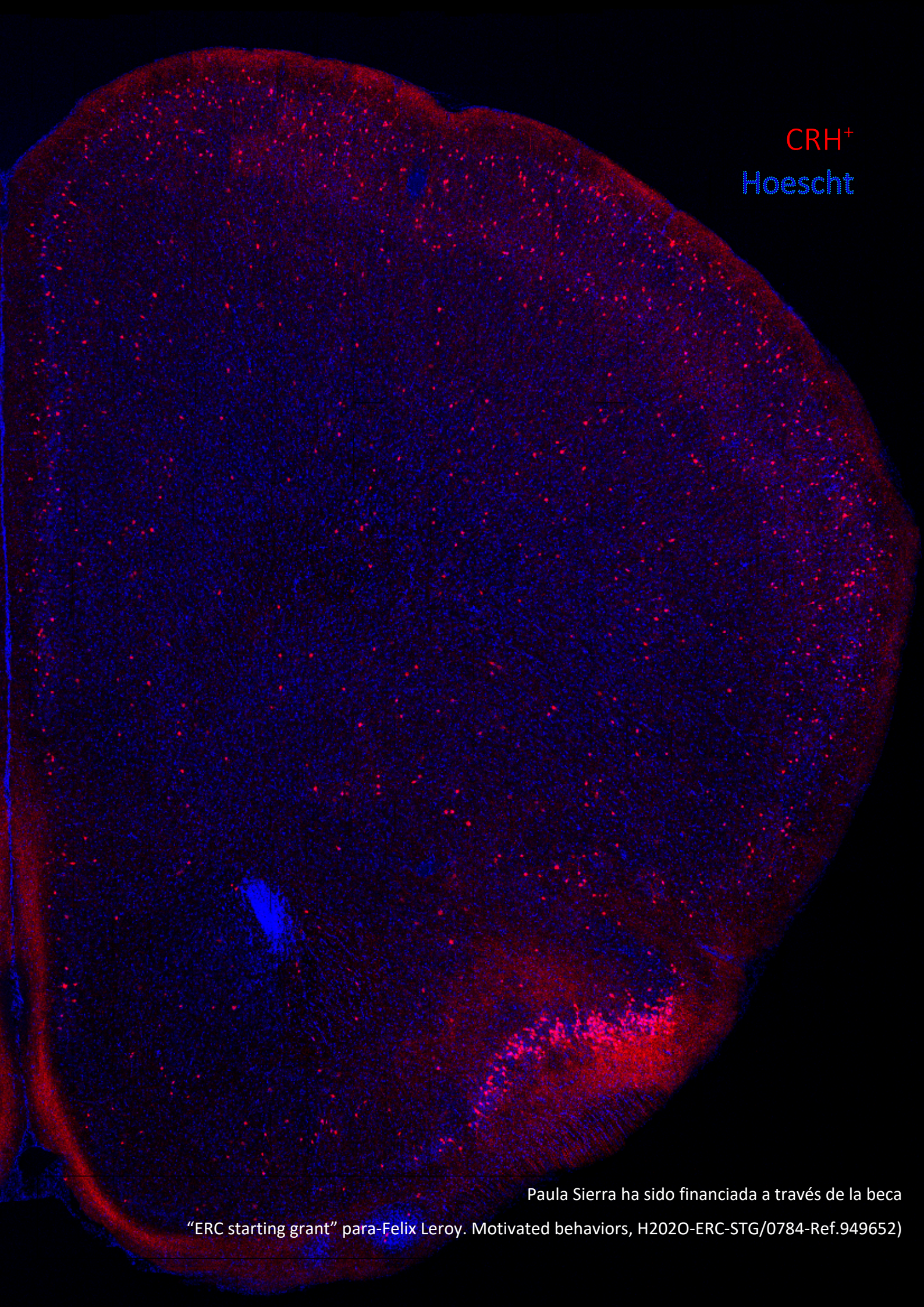


Paula Sierra ha sido financiada a través de la beca
"ERC starting grant" para-Felix Leroy. Motivated behaviors, H202O-ERC-STG/0784-Ref.949652)

# Contents

## List of abbreviations

**AAV:** Adeno-Associated Virus

**AAV2/1, AAV2/8, AAV2/9, AAV5**: Specific serotypes of Adeno-Associated Virus

**ACA**: Anterior Cingulate Area

**Ai9**: A transgenic mouse line that expresses tdTomato under the control of a CRE-responsive box

**ArchT**: Archaerhodopsin T, used to inhibit neurons with light

**c-Fos**: Proto-oncogene involved in gene transcription

**ChR2**: Channelrhodopsin-2, a light-sensitive protein used in optogenetics

**CRH**: Corticotropin-Releasing Hormone

**Crh-Cre**: Corticotropin-Releasing Hormone Cre mice

**CtB**: Cholera Toxin Subunit B, used as a neural tracer

**CMV**: Cytomegalovirus (used as a promoter in gene expression studies)

**DIO**: Double-Floxed Inverted Open reading frame (used for conditional gene expression)

**DREADD**: Designer Receptors Exclusively Activated by Designer Drugs

**eGFP**: Enhanced Green Fluorescent Protein

**eYFP**: Enhanced Yellow Fluorescent Protein

**FLEX**: A system for conditional gene expression

**hChR2**: Human Channelrhodopsin, used to activate neurons with light

**hM4Di**: Inhibitory DREADD variant (hM4D(Gi)) used to silence specific neurons

**ILA**: Infra-Limbic Area

**mCherry**: A red fluorescent protein

**mPFC**: Medial Prefrontal Cortex

**PL**: Peri-Limbic Area

**rAAV**: Recombinant Adeno-Associated Virus

**rLS**: Rostral Lateral Septum

**shRNA**: Short Hairpin RNA, used to silence specific genes

**SI:** Social Interaction

**GCaMP6f**: Genetically Encoded Calcium Indicator, version 6, fast

**TdTomato**: Tandem dimer tomato, a red fluorescent protein

**TT**: Tube Test

**VGAT**: Vesicular GABA Transporter

**WPREs**: Woodchuck Hepatitis Virus Posttranscriptional Regulatory Element

**CNO**: Clozapine-N-oxide, an agonist used in DREADD studies

**E123T/T159C**: Mutations of Channelrhodopsin-2

All images, figures, and diagrams were produced within the Cognition and Social Interactions Laboratory, except for the Allen Brain Atlas-Driven Visualizations (ABADV) of **Crh** gene expression in *Mus musculus* and those generated using the Artificial Intelligence Applied to Scientific Reviews tool.

## Abstract

The present thesis investigates the role of corticotropin-releasing hormone (CRH) release in regulating social interactions and social hierarchy in mice. Specifically, we investigated the function of medial prefrontal cortex (mPFC) neurons expressing CRH. Through a combination of electrophysiological recordings, chemogenetic and optogenetic manipulations, calcium imaging, and gene silencing techniques, we demonstrate that $CRH^{+}$ neurons in the infralimbic area (ILA) of the mPFC project to the rostral lateral septum (rLS) and that liberation of CRH suppresses social interactions with familiar mice. This neural circuit is therefore crucial for the familiarization process and underlies the social preference for novelty observed in mice, successfully modulating interactions between conspecifics. Motivated by these findings, I investigated the function of these cells of the mPFC for social hierarchy and showed that $mPFC^{CRH}$ neurons induce retreat during the tube test and therefore facilitate social submission (Graphical abstract (I).

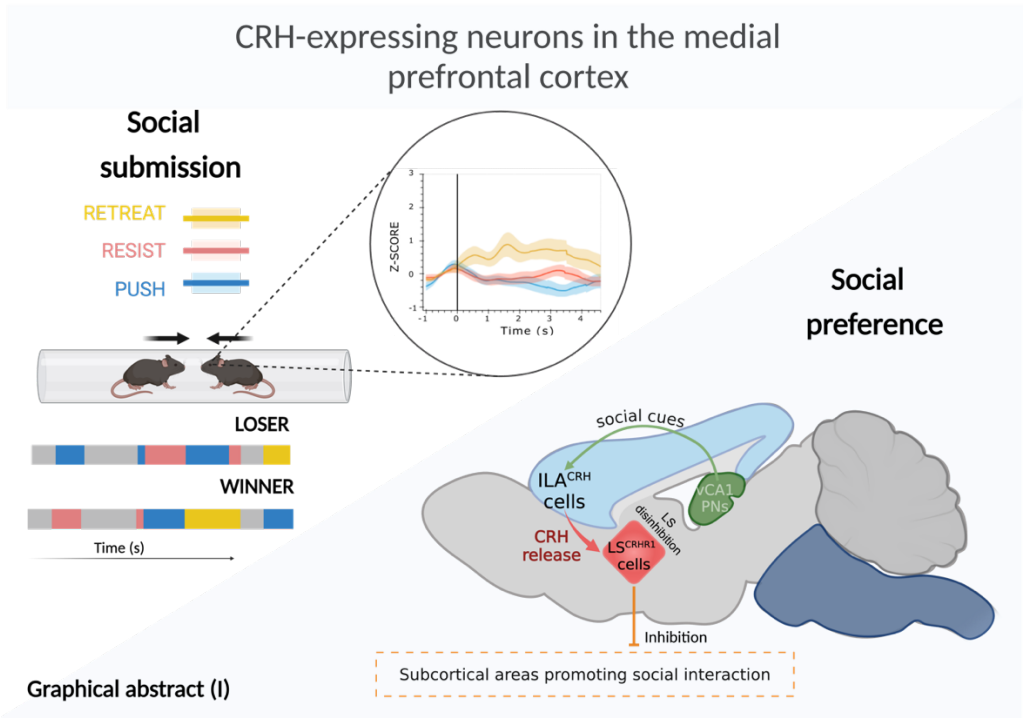


## Resumen

La presente tesis investiga el papel de la liberación de la hormona liberadora de corticotropina (CRH) en la regulación de las interacciones sociales y la jerarquía social en ratones. Específicamente, estudiamos la función de las neuronas de la corteza prefrontal medial (mPFC) que expresan CRH. A través de una combinación de registros electrofisiológicos, manipulaciones quimiogenéticas y optogenéticas, técnicas de imagen de calcio y silenciamiento génico, demostramos que las neuronas $CRH^{+}$ en el área infralímbica (ILA) de la mPFC proyectan al septum lateral rostral (rLS) y que la liberación de CRH suprime las interacciones sociales con ratones familiares. Por lo tanto, este circuito neuronal es crucial para el proceso de familiarización y sustenta la preferencia social por la novedad observada en ratones, modulando con éxito las interacciones entre congéneres. Motivados por estos hallazgos, investigué la función de estas células de la mPFC en la jerarquía social y demostré que las neuronas $mPFC^{CRH}$ inducen retirada durante la prueba del tubo y, por lo tanto, facilitan la sumisión social (Resumen gráfico (I).

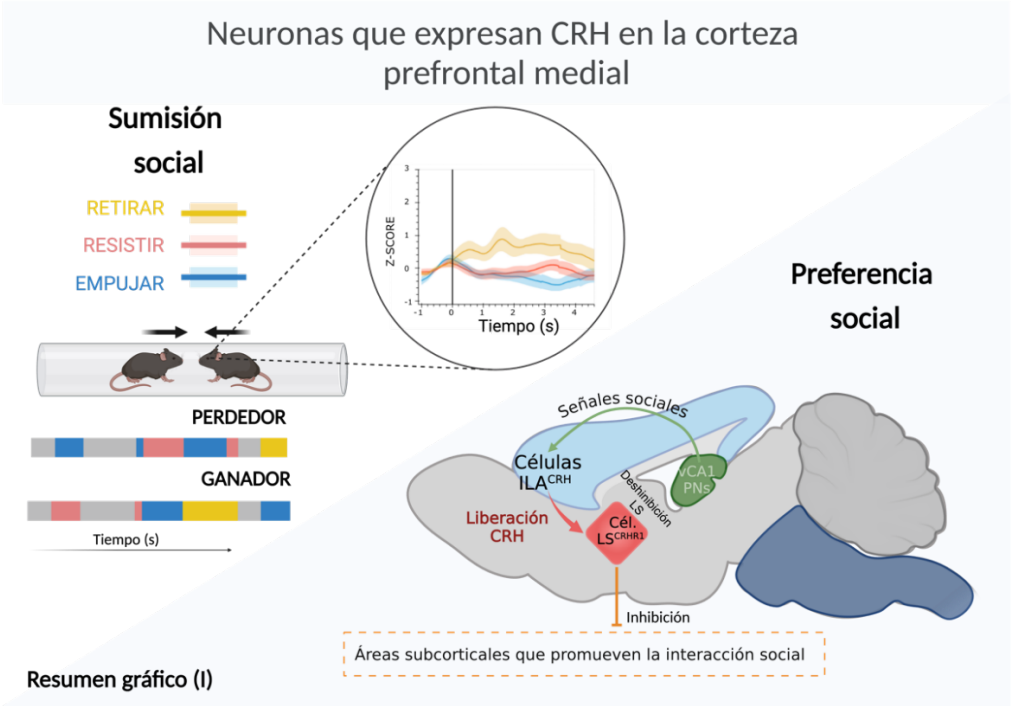


## Introduction

The present thesis encompasses and goes beyond the results presented in our publication "Corticotropin-releasing hormone signaling from prefrontal cortex to lateral septum suppresses interaction with familiar mice" (1). The motivation of this research was to investigate the neural circuits underlying social preference, the inclination to interact with one individual over another, which is crucial for successful social interactions. Previous work assigned a key role for CRH in the regulation of biological processes including homeostatic and allostatic neuroendocrine mechanisms, memory, and social behaviors (2–4) even in non-stressful contexts (5,6). In addition, the mPFC is critical (7,8) for decision-making, social cognition (9) and the establishment of social hierarchy in mice (10–14).

In the first chapter, we review the literature on social dominance and hierarchy, including the concept of submission using the Scopus data base (15). We also review the neurobiology of CRH

and its correlation with behavior. First, we provide an overview of CRH and related peptides, as well as the signaling mechanisms that trigger organic responses. This includes the classical role of CRH in the hypothalamic-pituitary-adrenal (HPA) axis and its impact on anxiety-like behaviors. Next, we focus on neuromodulation of CRH within the central nervous system, where it influences processes such as memory and social behaviors, affecting both distress and non-distress contexts (5,16), to finally visualize the gene expression in the mouse brain through data from the Allen Brain Atlas (ISH data (17).

The second chapter consists in a summary of the most recent work we published (1). We investigated whether CRH release from the mPFC could regulate social interaction and demonstrated that neurons from the infralimbic area (ILA) expressing corticotropin-releasing hormone (CRH) project to the rostral lateral septum (rLS) and are crucial in modulating social interactions between familiar mice. Utilizing a combination of electrophysiological recordings, chemogenetic and optogenetic manipulations, calcium imaging, and gene silencing techniques, we show that CRH release from ILA to rLS specifically suppresses social interactions with familiar mice. This neural circuit is key in regulating the familiarization process—the process by which interaction decreases as a novel rodent becomes familiar—and underlies the social novelty preference observed in adult mice. This mechanism is summarized in the graphical abstract shown below, adapted from our published work (1). Additionally, we showed how an increase in $ILA^{CRH}$ neuron density during the second postnatal week drives a developmental shift in social preference in young mice, favoring novel over familiar conspecifics.

The third chapter focuses on the role of mPFC$^{CRH}$ neurons in social hierarchy. Using chemogenetics, optogenetics, and in vivo calcium recordings, I demonstrated a clear association between mPFC$^{CRH}$ neuronal activity and submissive behaviors during the tube test. Activation of these neurons promotes retreat behavior, while their inhibition enhances social hierarchy. These results highlight the crucial role of mPFC$^{CRH}$ neurons in regulating social dominance and underscore the importance of the mPFC in modulating submissive behaviors. In the fourth chapter, the main conclusions emphasize that mPFC$^{CRH}$ neurons are essential for regulating social interactions by promoting social avoidance, along with future directions and implications for understanding and treating social disorders.

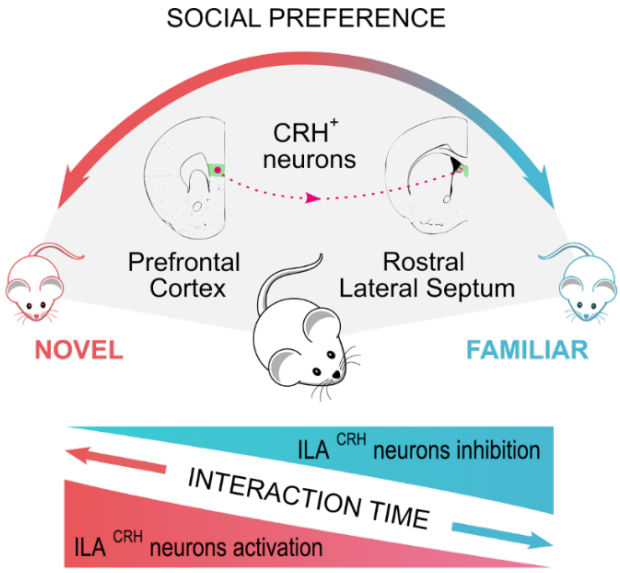


**Graphical abstract.** Corticotropin-releasing hormone signaling from prefrontal cortex to lateral septum suppresses interaction with familiar mice. (De león et. al, 2023)

# CHAPTER I

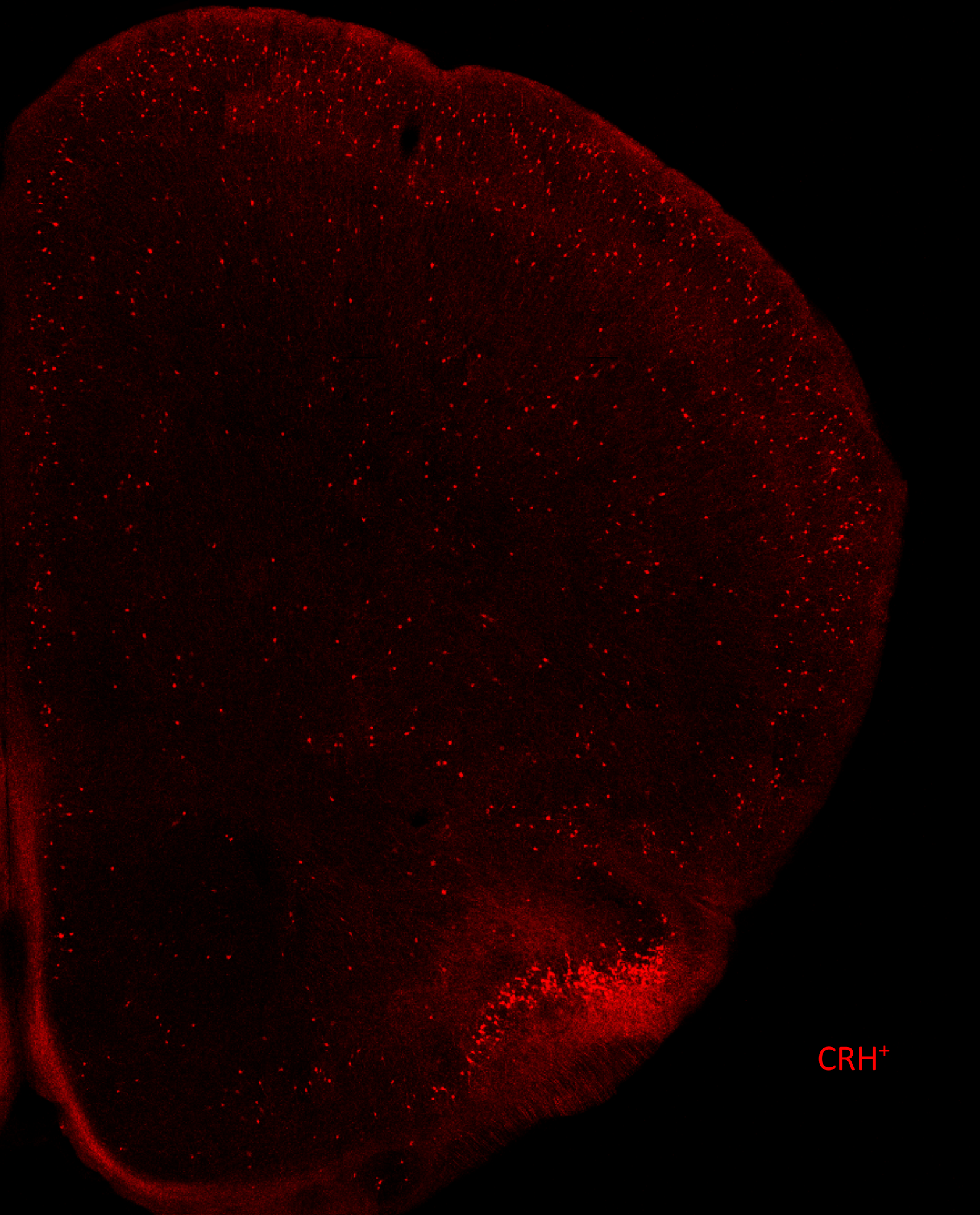

# CHAPTER I. Corticotropin-releasing hormone, gene expression mapping and Insights on Social Dominance and Hierarchy.

## Review on social dominance and hierarchy, including the concept of submission using the tool "Artificial Intelligence Applied to the Improvement of Scientific Reviews" (15)

In order to observe the general trends of the research efforts that have been carried out about dominance and social hierarchy, we used the tool "Artificial Intelligence Applied to the Improvement of Scientific Reviews" (15), developed by the Institute for research, development and innovation in health biotechnology of Elche (IDiBE). Using artificial intelligence applied to language processing, this tool analyses Scopus abstracts. In this way, it uses the K-mean technique to categorize the results and thus examine the information used in the abstracts, reflecting key concepts for exploring this search about dominance and social hierarchy constructs. To this end, we performed the search in the Scopus database with the entry (TITLE-ABS-KEY (dominance) AND TITLE-ABS-KEY (hierarchy) AND TITLE-ABS-KEY (submission) OR TITLE-ABS-KEY (cortex) OR TITLE-ABS-KEY (tube)). The results were downloaded in a .csv file, exporting the fields "Citation information" and "Abstract & keywords" to process the information.

The search yielded 330 results including 275 articles, 26 reviews, 18 book chapters, 9 conference papers or notes, and 2 short surveys until the year 2024. Following the k-means algorithm, an unsupervised clustering algorithm, to find groups of similar abstracts by calculating the distance between them to group the closest ones. Then, the Elbow method and the Average Silhouette method were used to define the optimal number of clusters, resulting in 5 clusters for the 330 results (Figure 1A-C). To evaluate the resulting categorization the tool used the Term Frequency - Inverse Document Frequency (TF-IDF) method. TF-IDF is a feature Statistical weighting of Words algorithm that calculates the importance of words in each abstract relative to own as well as to all

the abstracts in the Scopus results to assign each word in an abstract a score that ranges from zero to one.

The 75 most frequent words for all the abstracts are visualized on a word Cloud and the top keywords, based on their TFIDF score, for each cluster (Figure 1E) show the general trends on research regarding the Scopus search. Considering that the objective of this search was configured under the construct of social dominance and hierarchy, including the concept of submission, the TFIDF shows a variety of terms that include the neurobiological bases of these behaviors. Clusters 0, 2, 3 and 4 included the terms dominance, hierarchy or submission (Figure 1D dashed box), additionally these clusters involved the terms social, rank and behavior (Figure 1D asterisk) but just in the clusters 0, 2 and 3 appear animal, mice, rat or dog. However, cluster 4 has the highest score for the term social. Unlike, cluster 1 where mainly addresses concepts on brain functions and brain anatomy, associated with investigation like “Hierarchy of cortical responses underlying binocular” (ref) or “A Hierarchical Model of Binocular Rivalry”.

Based on these results, we analyzed the index keywords of the 248 abstracts corresponding to these four clusters (0, 2, 3 and 4) related to social dominance and hierarchy, including the concept of submission. The neuroanatomical bases included in these results mention brain regions such as the prefrontal cortex (10,18,19), hippocampus and the amygdala (20,21), as well as the hypothalamus (22) in 32%, 5%, and 6% respectively. These brain areas are mainly associated with decision-making, social cognition and regulation of social behavior, as well as fear, aggression or stress response (19,20). Less frequently, brain regions such as the striatum, thalamus and periaqueductal gray (PAG) are also included (23).

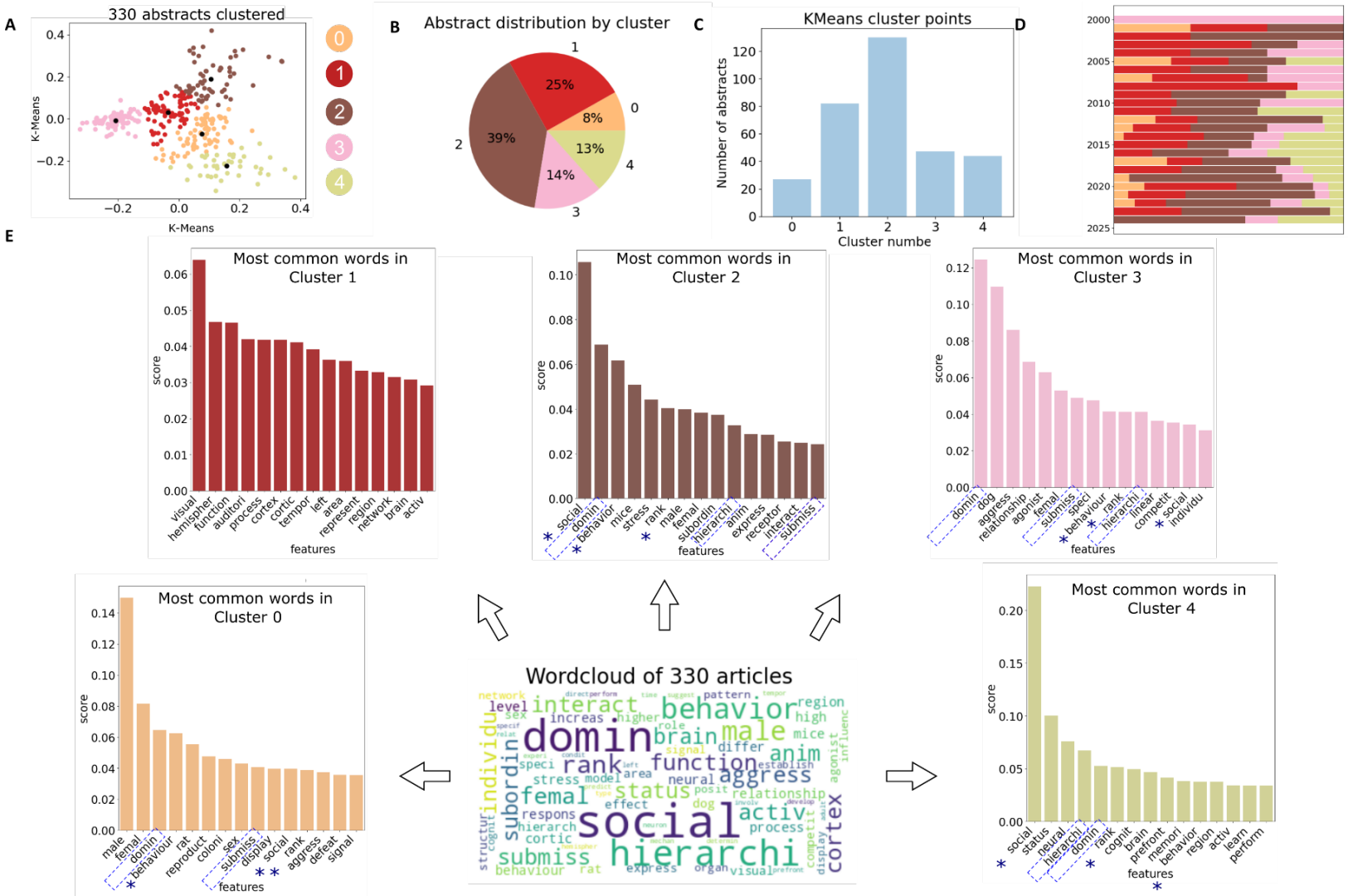


**Figure 1. Artificial Intelligence Applied to Scientific Reviews. A.** Scatter plot from PCA of the 330 articles collected from the Scopus entry: (TITLE-ABS-KEY (dominance) AND TITLE-ABS-KEY (hierarchy) AND TITLE-ABS-KEY (submission) OR TITLE-ABS-KEY (cortex) OR TITLE-ABS-KEY (tube)). Colors represent the items in each of the 5 clusters. The black dots represent the centroids of each cluster**. B.** Pie chart with the percentage distribution of distribution in each cluster. **C.** Number of abstracts on each cluster by using the K-means algorithm. **D.** Distribution of each cluster per year. **E.** Middle, Word cloud of the 75 most frequent words. A larger font size indicates a higher relative frequency. The arrows show the graph of the score assigned by the Term Frequency - Inverse Document Frequency (TF-IDF) algorithm in each of the cluster

Among the most cited works in this search, the impact of social hierarchy on the health of social species stands out (10,24–26). Interestingly, one of the species studied in this context is the dog (27,28), exhibiting social structures with hierarchies of dominance and submission, even in non-domesticated populations (29,30). The interest in understanding these behavioral patterns aims to provide knowledge about both dog-dog and dog-human interactions due to their long history of cohabitation. Similarly, hierarchical structures are observed in primates, both human and non-human (14,31,32). However, it has been argued that the concept of dominance is more complex than simply social relationships involving competition or agonistic behaviors (33–35)

Dominance (36,37) can be seen as a learned result of intragroup interactions that configure hierarchies of subordination (38). It is common to observe the formation of hierarchies under stressful conditions, especially in captivity, where animals in disadvantaged situations often respond to competitive situations to configure useful social dynamics in their group (37,39,40). Dominance must be distinguished from other factors such as territoriality, particularly for space, or learned behavior (40,41). Dominance relationships (based mainly on dyadic interactions) and social hierarchy (assigned ranks) are terms that are often blurred (37). While dominance/subordination describes a relationship in which one individual submits to another during a conflict and the dynamic represents an adaptive compromise, weighing the benefits and costs of submission versus resistance (38,41), social hierarchy is the outcome of behavior within a group, useful for categorizing and predicting group interactions (37,40). In this way, there are terms to differentiate and understand the dynamics in the continuum of social interactions, which fluctuate between passive behaviors, such as avoidance, and aggressive actions mostly related to maintaining territorial boundaries and securing access to resources (40,41). Thus, agonistic interactions emerge as a term within this continuum to describe social interactions linked to fight, not only aggression, but also behaviors like threats, displays, retreats, and efforts to confront aggressors (25,42).

To understand complex behaviors such as aggression or dominance, researchers have developed a comprehensive view of their biological foundations, including autonomous response and their evolutionary history regarding functionality (43). The four levels of behavioral analysis are often used to analyze this continuum in social interactions. This framework includes ontogeny, mechanism (focusing on the physiological or neurological causes), function, and phylogeny (44). Additionally, the importance of epigenetics in the development of traits during social interactions, which involves the way environmental factors influence gene expression, plays a significant role in shaping these behaviors during development (38,45). Advances in pharmacology and molecular biology offer new tools, such as drugs targeting specific neural circuits related to social behaviors. For example, 5-HT (serotonin) has been shown to alter aggressive behaviors (46,47). Serotonergic systems interact with dopamine, GABA, and neuropeptides, providing insights into brain function and aggression (34,47). In this way, understanding the dynamics and forms of social hierarchies emphasizes both brain regions and pathways (14,22) and physiological indicators in the context of social position (5,48)

Cortisol levels have been a target in the psychological process to understand their relationship with social status (48–50). Research on different primate species (36,51–53) reveals variations between cortisol levels and social status. Studies show that subdominant males often have higher cortisol levels (51–53) in species like squirrel monkeys or mandrills. In contrast, other species (54–57) such as white-faced capuchins or chimpanzees display the opposite pattern. This diversity highlights that cortisol levels in dominants versus subordinates depend on species-specific social systems and whether the hierarchy is unstable (48–50,55) where high cortisol helps manage social interactions by promoting vigilance and submissiveness to reduce aggression from higher-status individuals (58,59). Subordinate individuals generally experience higher cortisol levels when facing frequent stressors and having limited social support (50). This underscores the complex interplay between cortisol, social rank (49,55,58).

## Neurobiology of Corticotropin-releasing hormone (CRH), activation of hypothalamus-pituitary-adrenal (HPA) axis.

Corticotropin-releasing hormone (CRH), a 41-amino-acid peptide exists in a wide variety of mammalian species and is generated by proteolytic cleavage of a 194-amino acid precursor (60). CRH operates through receptors, CRHR1 and CRHR2, which are differentially distributed throughout the brain. The CRHR1 receptor activates various intracellular pathways by increasing cyclic AMP (cAMP). The most studied pathway downstream of CRHR1 is the MAPKs cascade, which plays a central role in stress (61–63).

The signaling mechanism activated by CRH receptors (CRHRs) involves a series of steps facilitated by G-protein-coupled receptors (GPCRs). CRHRs, embedded in the cell membrane, bind to CRH, leading to a conformational change in the receptor. This active conformation promotes the exchange of GDP for GTP on the Gα subunit of the associated heterotrimeric G-protein, which is composed of α, β, and γ subunits (64,65). Consequently, the Gα-GTP and Gβγ subunits dissociate and propagate different intracellular signaling pathways. These pathways can activate various enzymes and second messengers, influencing cellular responses (62). Following receptor endocytosis, the Gα subunit hydrolyzes GTP to GDP, leading to the reassembly of the heterotrimeric G-protein (66).

In addition to CRH, the neuropeptide family includes urocortin (UCN), which shares 45% sequence homology with CRH and is the main agonist of CRHR2. Indeed, UCN shows greater affinity for CRHR2 receptor subtype than CRH (62,67). UCN, is often associated with reduction in food intake (hypophagia) without being associated with toxic effects or conditioned taste aversion, highlighting its potential for stronger physiological effects in certain stress-related pathways (68). Both CRH and UCN are integral components of the stress response system, with implications in anxiety, depression (69), and immune modulation, underlining the complexity of the CRH receptor system and its significance in neuroendocrine regulation (68,70). Differentiation between UCN and CRH suggests

unique functional roles for each receptor subtype (67,71).

In this thesis, we focus on the role of CRH to regulate social behaviors with the underlying assumption that CRH released in different brain areas can modulate different behaviors. It is primarily associated with the neuroendocrine and behavioral response to stress, mainly by activating the hypothalamic-pituitary-adrenal (HPA) axis (2,4,71,72). When the body experiences stress—whether visceral, environmental, or psychological—the hypothalamus releases CRH and arginine vasopressin (AVP) by neurons in the paraventricular nucleus (PVN) of the hypothalamus. These hormones work together to stimulate the pituitary gland to produce and release adrenocorticotropic hormone (ACTH. Bonfiglio et al., 2011; Holsboer & Ising, 2010. ACTH acts on the adrenal cortex, stimulating the synthesis and release of glucocorticoids, primarily cortisol in primates and corticosterone in rodents. These glucocorticoids mediate functions designed to adapt to the demands of stress known as a crucial biological stress response system (74,75).

Cortisol plays a significant role in medical and psychobiological research due to its involvement in various pathological states. Hypercortisolism leads to Cushing's disease, which often presents with psychological disturbances linked to symptoms of major depression (76,77). Conversely, hypocortisolism, seen in Addison's disease (78), is also present in disorders like chronic fatigue syndrome (79) and is associated with mood alterations (80–83). Notably, cortisol serves as a biomarker for stress in psychobiological research. Investigations show that cortisol levels respond to both acute and chronic stressors (84,85) and are strongly correlated with the development and functioning of the HPA axis in adults (86). Environmental factors involved in stress exposure include loneliness, family conflicts, negative social evaluation, and social status (48,84). Additionally, major depression disease has been associated with differences in stress reactivity and cortisol responses (87–89). These findings highlight the impact of both somatic diseases and mental health conditions (80) on the functioning of the HPA axis (86,90,91).

**Beyond the HPA axis, role of CRH in Central Nervous System (CNS).**

CRH acts as a neuromodulator in the central nervous system, and its dysregulation is linked to psychiatric disorders. Also involved in process like memory and social behaviors even in non-distress context (4–6,16). An investigation in rats demonstrated that intracerebroventricular (ICV) injection of synthetic CRH elicited dose-dependent anxiogenic effects, which were not observed with peripheral administration. This suggests that CRH has direct effects on the central nervous system, independent of its known role in stimulation of the anterior pituitary gland (92).

Constitutive CRH knockout mice showed a significant glucocorticoid requirement for fetal lung maturation, highlighting the crucial role of CRH in fetal development. Remarkably, despite having marked glucocorticoid deficiency, these mice exhibited normal growth, fertility, and longevity after birth, demonstrating that glucocorticoids are far more essential during fetal life than postnatally (93,94). Conversely, in Sim1-Crh-KO mice, which lack CRH expression in the PVH but retain it in other brain regions, adrenal atrophy and reduced corticosterone levels were observed, reflecting the expected loss of neuroendocrine function associated to CRH. However, Sim1-Crh-KO mice displayed anxiolytic behavior even after corticosterone levels were restored, suggesting that the anxiolytic effect is independent of glucocorticoid levels (94,95).

Specific approaches through targeted deletions of CRHR1 in different neuronal populations have revealed the complex, bidirectional roles of this receptor in behavioral regulation (96–98). For instance, a conditional knockout experiment was conducted using a mouse line (Crhr1loxP/loxPCamk2a-cre) where the CRHR1 receptor was selectively inactivated postnatally in the anterior forebrain and limbic structures, while preserving pituitary function and the integrity of the HPA-axis. Behavioral findings showed that these mice displayed significantly reduced anxiety

levels compared to control mice, despite the basal activity of their HPA axis remained normal (96). Similar to these results, the absence of CRHR1 in forebrain glutamatergic neurons reduces anxiety, but this also disrupts neurotransmission in critical regions such as the amygdala and hippocampus, which are involved in emotion and memory processing. In contrast, deleting CRHR1 in midbrain dopaminergic neurons leads to increased anxiety-like behaviors and reduced dopamine release in the prefrontal cortex, an area essential for mood regulation and cognitive function (97). Based on these findings, it is suggested that an imbalance between these opposing CRHR1-regulated systems could contribute to emotional disorders like depression (96,97,99).

The synaptic physiology of CRH reveals that it can exert both tonic and phasic effects, modulating neurotransmission by either potentiating or inhibiting key neurotransmitters like glutamate, as well as neuromodulators like dopamine. These mechanisms further underscore the role of CRH as a key mediator in maintaining organismal homeostasis and adaptive behavioral responses (98,100). Further research has shown a connection between the CRH system and social behaviors in several species, including fish, birds, rodents, and primates (4,101). This suggests that the role of the CRH goes beyond stress responses, as it influences behaviors related to social interactions in these different species (102). Studies on poor social conditions, such as isolation or defeat, have shown activation in the PVN (103,104), CeA (105), cingulate cortex, piriform cortex, or cerebellum (106). However, these differences in brain regions seem to differ depending on the species, as well as the type of receptor (4) or sex (107). These results should consider that they were mainly examined in males, so their effects should consider experimental variations (4,108).

The CRH system is also involved in prosocial behaviors, such as parental care, maternal defense, sexual behavior, pair bonding, and social memory (4). For example, in male prairie voles, CRF administration facilitates the formation of mate preferences (109,110). Regarding social memory, CRH system plays a complex role in social memory and recognition (4), influencing both social

interactions and the memory processes (111) through various receptors and conditions (112).

A study in rats demonstrated bidirectional effects of pharmacological manipulation of the CRH system(6). First, adult female rats received intracerebroventricular injections of a CRF receptor antagonist (d-Phe CRF (12-41)) at varying doses (0.2, 1, or 5 μg). Subsequently, social recognition memory was assessed using a delay paradigm, where rats were presented with a familiar juvenile rat after a 30-minute delay. The results demonstrated that administration of the CRF receptor antagonist dose-dependently impaired social recognition performance. Then, they explored the effects of increasing CRF availability on social recognition memory, adult rats were administered intracerebroventricular injections of a CRF binding protein ligand inhibitor (r/h CRF (6-33)) at different doses (1 or 5 μg). Social recognition memory was then evaluated using a longer delay (120 minutes) to induce forgetting. The findings revealed that a 1 μg dose of the CRF binding protein ligand inhibitor successfully reversed the memory impairment caused by the extended delay. However, a higher 5 μg dose exhibited non-specific effects on social investigation, suggesting a potential dose-dependent effect on memory processes. Through these two main experiments demonstrated that brain CRF systems play a crucial role in social recognition memory in rats, even in the absence of stressor exposure (6).

In contrast, another investigation showed that mice overexpressing CRH (CRH-OE) exhibited increased social investigation during the first habituation to a juvenile (111). In subsequent habituation sessions, CRH-OE mice showed investigative behavior similar to wild-type mice. When tested 10 minutes after the last session, both groups preferred the novel juvenile, indicating normal short-term memory. However, 24 hours later, only CRH-OE mice retained social memory. This implies the CRH system in social recognition but leaves uncertainty as to whether its effects are specific to social stimuli or general memory. Further research on Ucn3 knockout (KO) mice revealed

slower extinction of social recognition memory but no impairments in object, social odor discrimination, or social interaction (112). Additionally, mice lacking CRHR2 also exhibited improved social memory, while Ucn2 KO mice had normal social memory, highlighting Ucn3's role in social memory via CRHR2 receptors (112). This intricate regulation aligns with the understanding that the central CRH system, beyond its traditional association with the HPA axis, plays a broader role in modulating emotional functions receptor (4). These findings highlight the neural mechanisms influenced by CRH and prompt further investigation into the circuits involved in social and motivated behaviors. Key brain regions, including the PFC, hippocampus, amygdala, and thalamus, play a central role in these processes, offering valuable insights for a more comprehensive understanding of their functions (113,114).

The role of CRH in the brain, particularly in the PFC, amygdala, and hippocampus, is linked to modulating social interactions (115), behavioral responses to challenges (99,116), and executive functions (117). However, the circuits involved across the brain remain largely unknown (97,99). Remarkably, the mPFC plays a crucial role in regulating social behaviors, decision-making, and navigating social status (8,9,11,14). Additionally, the prefrontal cortex has been consistently identified as one of the most affected regions in depressive disorders (118,119), where impairments in these circuits may contribute to affective dysregulation ((119,120). The role of CRH in the PFC has attracted increasing attention, both in its local dynamics (115–117) and in the circuits involved (97,99). In this way, modulation by CRH depend on the cell type where it is expressed but also on the specific circuit context in these brain regions. The hypothesis about the intracellular pathways activated by CRH vary by brain region due to specific ligand-receptor interactions, influencing synaptic transmission differently (97,98,100) showing the complex role of in shaping brain functions.

**Spatial and Quantitative Visualization of Crh Gene Expression Across Mouse Brain Regions using "Allen Brain Atlas-Driven Visualizations: a web-based gene expression energy visualization tool"** (17)**.**

In order to visualize the Crh gene expression in the mouse brain, we use the Allen Brain Atlas-Driven Visualizations (ABADV. Zaldivar & Krichmar, 2014). The Allen Brain Atlas (ABA) is a publicly accessible online resource that integrates gene expression, connectivity, and neuroanatomical data from adult and developing mouse, human, and nonhuman primate brains. It offers multiple data types, including in situ hybridization (ISH), microarrays, RNA sequencing, reference atlases, projection mapping, and MRI. As users, we can explore these datasets through interactive tools such as gene search methods, image viewers, 3D anatomical navigation, and cross-dataset searches (121,122). The ABA provides extensive data on gene expression and neuroanatomy for human and mouse brains (123), but its built-in tools can be limiting in terms of the number of genes and brain structures researchers can view simultaneously.

The Allen Brain Atlas-Driven Visualizations is a web-based tool designed to enhance the accessibility and analysis of gene expression data from the ABA API and D3 Javascript library (124). ABADV addresses this limitation by generating multiple visualizations, including pie charts, bar charts, and heat maps, which display expression energy values across various genes and brain structures. This allows for straightforward comparisons of gene expression patterns in different brain areas. Each visualization links back to the ABA, providing access to detailed experimental summaries. This tool facilitates immediate and comprehensive analysis of large datasets (17).

The gene expression energy values from the Allen Brain Atlas API, represents gene expression across 200 μm voxels in the mouse brain (125,126). This data is derived through a specialized processing pipeline developed by the Allen Institute to manage large-scale RNA in situ hybridization (ISH) data.

Each experiment image is divided into a 3D grid of 200µm sections, where expression pixels and their intensity are measured for each division. Two key metrics are derived from this division: expression density, which is the ratio of expressing pixels to total pixels, and expression intensity, which is the average intensity of expressing pixels (17,126,127).

Following the ABADV pipeline (17) we performed the search for the expression of the corticotropin-releasing hormone gene following as input the genetic symbols and the acronyms of the brain structure of Mouse Genome Informatics(128) In this way, we type “Genes (Symbol)” Crh; “Brain Structures (Acronym)”TH, MB, CB, STR, HPF, P, PAL, HY, Isocortex, CTXsp, MY, OLF; Color Scheme: Atlas; “Probe” Antisense; “Section” Both; “Visualization” All (Figure 2A).

Results showed three experiments for *Crh*, *Chr1* and *Chr2* each. First, the bar charts of expression energy and the colors show information about different sub-groups of brain structures to Crh gene expression. It means that the height of the bar is proportional to the amount of expression energy (Figure 2B). Pie charts demonstrating relative proportions in brain structures for Crh, Chr1 and Chr2 (Figure 2C: top, middle and bottom). The color intensity of the pie charts shows the expression energy relative to each gene, thus appear more transparent or opaque according to the expression energy. Furthermore, the width of a pie slice represents the total amount of expression energy. Finally, to compare the visualization with Brain Explorer 2 application (122), we consult the same query with ABADV (Figure 2A). After downloading each gene into Brain Explorer, we navigated through their structural hierarchical panel within the application, turning on all 3D polygonal brain structures associated with the ABADV query and turning off the brain structures (Figure 2D).

According to previous reports (94,129–131) this visualization is consistent with the highest amount of expression energy to Crh is observed in olfactory areas (OLF), Isocortex and hypothalamus (HY). Furthermore, as expected, there is higher expression of Crhr1 than Crhr2 and their regions associated are the cerebellum, olfactory areas and isocortex (Figure 3B. (94). Pie charts (Figure 3C)

provide stronger color intensity and wider portion corresponding to expression energy in the anterior olfactory nucleus (AON) and paraventricular hypothalamic nucleus (PVH) subregions. Interestingly, the greater intensity in the isocortex includes the Anterior Cingulate Area (ACA), Agranular Insular Area (AI), Prelimbic Area (PL), Ectorhinal Area (ECT), Gustatory Areas (GU), and Orbital Area (ORB. Figure 2C). Based on a study that analyzed the distribution of CRH neurons in CRH-IRES-Cre;Ai3 mice using automatic imaging and stereoscopic cell counting, a higher density of these neurons was found in specific regions, revealing intricate details about their spatial organization in the glomerular (Gl) and external plexiform (EPl) layers of the main olfactory bulb. The same study reported that expression in the PVH, as expected, was distributed throughout the entire rostro-caudal extent, from the suprachiasmatic nucleus to the rostral portion of the arcuate nucleus. Finally, in the cerebral cortex, the distribution included the rostro-caudal extent, primarily in layers 2 and 3 of the neocortex, with some presence in deeper layers (4 and 5). These neurons exhibited bipolar or multipolar shapes, with bipolar neurons often having dendritic processes traversing multiple cortical layers (129).

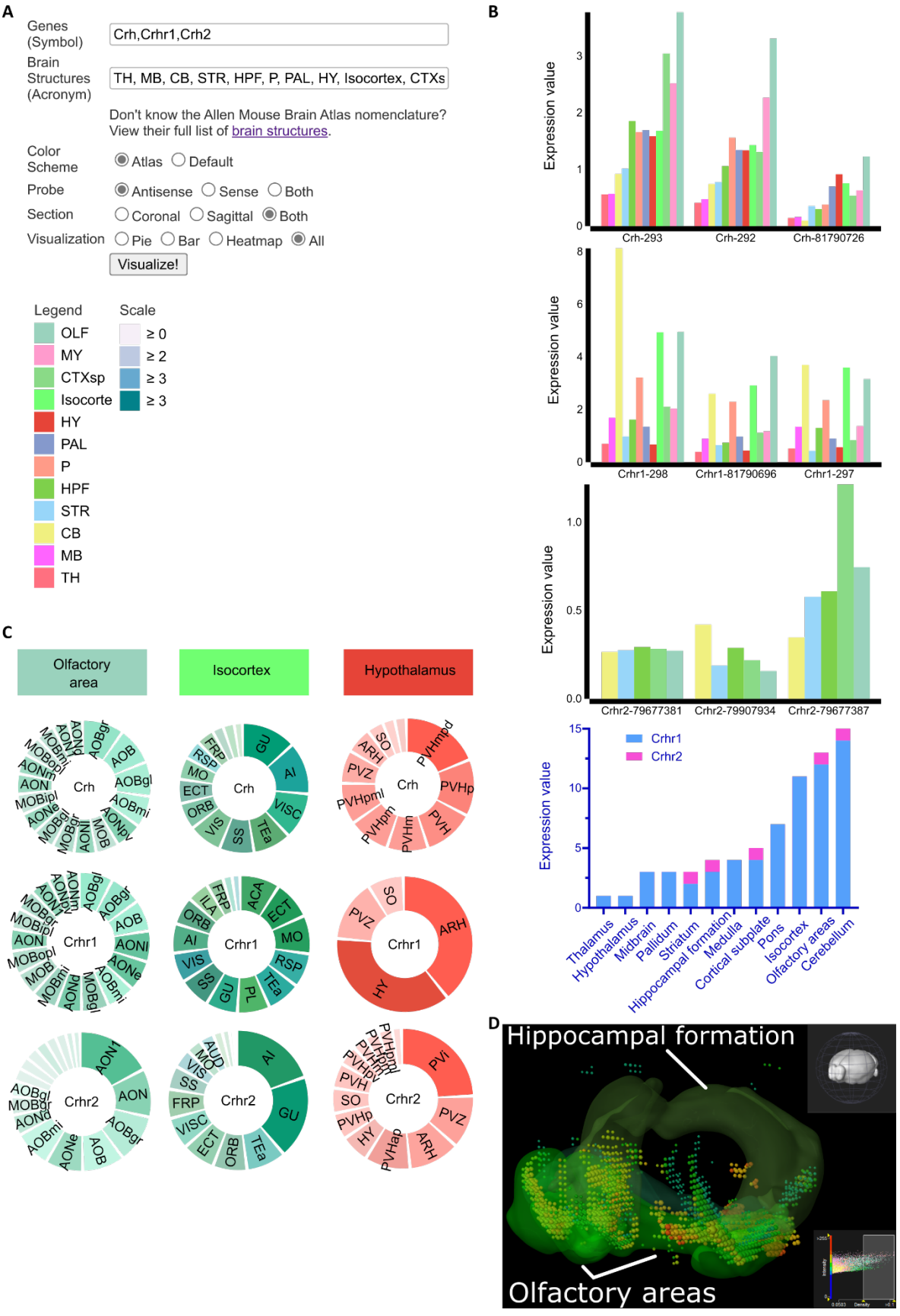
A
Genes (Symbol)
Crh,Crhr1,Crh2
Brain Structures (Acronym)
TH, MB, CB, STR, HPF, P, PAL, HY, Isocortex, CTXs
Don't know the Allen Mouse Brain Atlas nomenclature? View their full list of brain structures.
Color Scheme
Atlas
Default
Probe
Antisense
Sense
Both
Section
Coronal
Sagittal
Both
Visualization
Pie
Bar
Heatmap
All
Visualize!
Legend
OLF
MY
CTXsp
Isocorte
HY
PAL
P
HPF
STR
CB
MB
TH
Scale
≥ 0
≥ 2
≥ 3
≥ 3
B
Expression value
Crh-293
Crh-292
Crh-81790726
Crhr1-298
Crhr1-81790696
Crhr1-297
Crhr2-79677381
Crhr2-79907934
Crhr2-79677387
Crhr1
Crhr2
Thalamus
Hypothalamus
Midbrain
Pallidum
Striatum
Hippocampal formation
Medulla
Cortical subplate
Pons
Isocortex
Olfactory areas
Cerebellum
C
Olfactory area
Isocortex
Hypothalamus
Crh
Crhr1
Crhr2
D
Hippocampal formation
Olfactory areas

**Figure 2. Allen Brain Atlas-Driven Visualizations (ABADV) of Crh gene expression in mouse (mus muscullus).**

**A.** Searching for corticosteroid-releasing gene (*Crh, Crhr1, Crhr2*) expression through the ABA databases. Brain structures: Thalamus (TH), Midbrain (MB), Cerebellum (CB), Striatum (STR), Hippocampal formation (HPF), Pons (P), Pallidum (PAL), Hypothalamus (HY), Isocortex (Isocortex), Cortical subplate (CTXsp), Medulla (MY), Olfactory areas (OLF) **B.** Bars represent a different gene expression experiment, each bar within a group of bars represents a different brain structure. Left-up, *Crh*. Right-up, *Crh1*. Left-down, *Crhr2*. Right-down, *Crhr1-Crhr2*. Bar height denotes the amount of expression energy to *Crhr1* and *Crhr2*. **C.** Pie chart to brain structures in OLF, ISO and HY brain structures. *Crh*-up, *Crhr1*-middle and *Crhr2*-dowm. Width of a pie slice represents the total amount of expression energy, and the opacity of each slice denotes the amount of expression corresponding to brain regions. **D.** Crh expression in brain structures, colored spheres represent the amount of expression in each brain structure, where blue green is low, yellow is medium, and red is high. The spheres also represent each 200 µm3 voxel detected in expression. Density observation is above 0.053.

# CHAPTER II

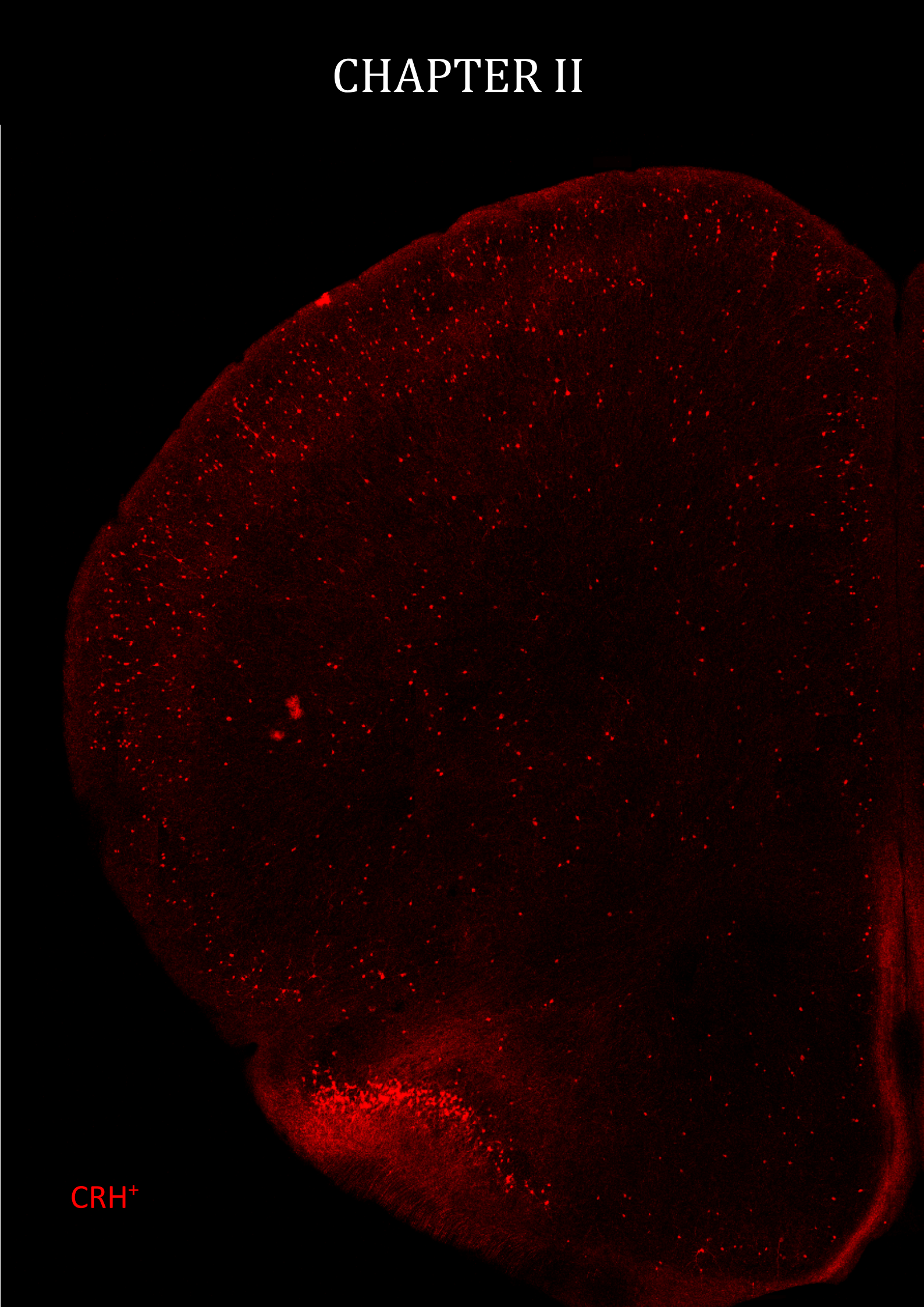

## CHAPTER II. Summary of *"Corticotropin-releasing hormone signalling from* prefrontal cortex to lateral septum suppresses interaction with familiar mice" (1) research.

Social preference is a fundamental trait in gregarious animals, defined by the tendency to interact with one conspecific over another, which is crucial for navigating social environments. In adult rodents, this preference is shaped by kinship, strain identity, and sex, leading to increased engagement with relatives and opposite-sex individuals. While innate factors play a role, additional influences further shape these social choices (132–134), Social preference is not only driven by innate factors but is also shaped by social memory, hierarchy, and the affective state of conspecifics, influencing how individuals navigate and engage within their social environment. (135,136). Adult rodents exhibit a social novelty preference (SNP), favoring interactions with unfamiliar individuals over familiar ones. SNP has served as a key behavioral assay to measure of social memory, although the underlying neural circuits remain unclear. It is still uncertain whether this preference arises purely from the rewarding nature of novel social interactions or if it also involves an active suppression of engagement with familiar individuals. We proposed that specific neural circuits may drive the avoidance of familiar conspecifics, thereby reinforcing social novelty preference when both familiar and novel mice are present.

Memory-driven preferences, including social novelty preference, develop within specific time windows and can evolve throughout the lifespan of altricial animals (137) For instance, before weaning, young mice show a strong preference for their mother over unfamiliar dams, but this preference reverses afterward, favoring novel dams. Likewise, rat pups initially prefer their familiar siblings during the first two postnatal weeks, then gradually shift their preference toward unfamiliar pups (132,138). While the mechanisms driving these developmental transitions are not yet fully understood, the lateral septum (LS) —a brain region involved in regulating motivated behaviors, including social interactions—plays a crucial role. It is essential for kinship and familiarity preference

in young rats and contributes to social novelty preference in adult rodents. (132). Additionally, the infralimbic area (ILA) of the medial prefrontal cortex (mPFC) plays a key role in decision-making, responds to social stimuli, and is essential for social novelty preference. The mPFC connects with the lateral septum (LS) to modulate food-seeking behavior, but how these regions process social memory cues and coordinate to regulate social interactions remains unclear.

In humans, CRH is linked to psychiatric disorders characterized by social impairments, including depression and social phobia. In rodents, altering the CRH system disrupts social behavior. Since CRH is expressed in the infralimbic area (ILA) and its receptor, CRHR1, is present in the lateral septum (LS), we propose that CRH signaling from the ILA to the LS plays a role in regulating social interactions and influencing social novelty preference.

## Projection from ILA$^{CRH}$ to the lateral septum in rostro-dorsal area

To explore the neural mechanisms underlying social novelty preference, we targeted infralimbic area (ILA) neurons expressing corticotropin-releasing hormone (CRH). We injected CRH-Cre mice in the ILA with a Cre-dependent adeno-associated virus (AAV) encoding membranous GFP and synaptophysin tagged with mRuby, enabling visualization of axons and synaptic terminals (Fig. 3A-B). GFP$^+$ fibers were detected in the rostral-dorsal region of the lateral septum (rdLS), and mRuby-labeled axon terminals were confirmed (Fig. 3D-E). Retrograde labeling with CtB-488 in the rdLS of CRH-Cre mice crossed with a Cre-dependent tdTomato reporter line revealed tdTomato$^+$ cells across the rostro-caudal axis of the ILA (Fig. 3F-G). Further verification with a retrograde monosynaptic herpes simplex virus expressing GFP showed that 79% of CRH/GFP$^+$ cells were located in the ILA, with 66% in layer 2/3 (Fig. S1 A-D). In situ hybridization confirmed that 92% of ILA$^{CRH}$ cells expressed Gad2 mRNA, identifying them as GABAergic neurons (Fig. S1 E-H). In septal slices from CRH-Cre mice injected with Channelrhodopsin, blue light stimulation induced outward currents at +10 mV, but no inward currents at -70 mV, and light-evoked IPSCs were blocked by GABAA and GABAB receptor

antagonists (Fig. 3 L-N). These findings indicate that ILA$^{CRH}$ neurons projecting to rdLS are a specific population of GABAergic neurons.

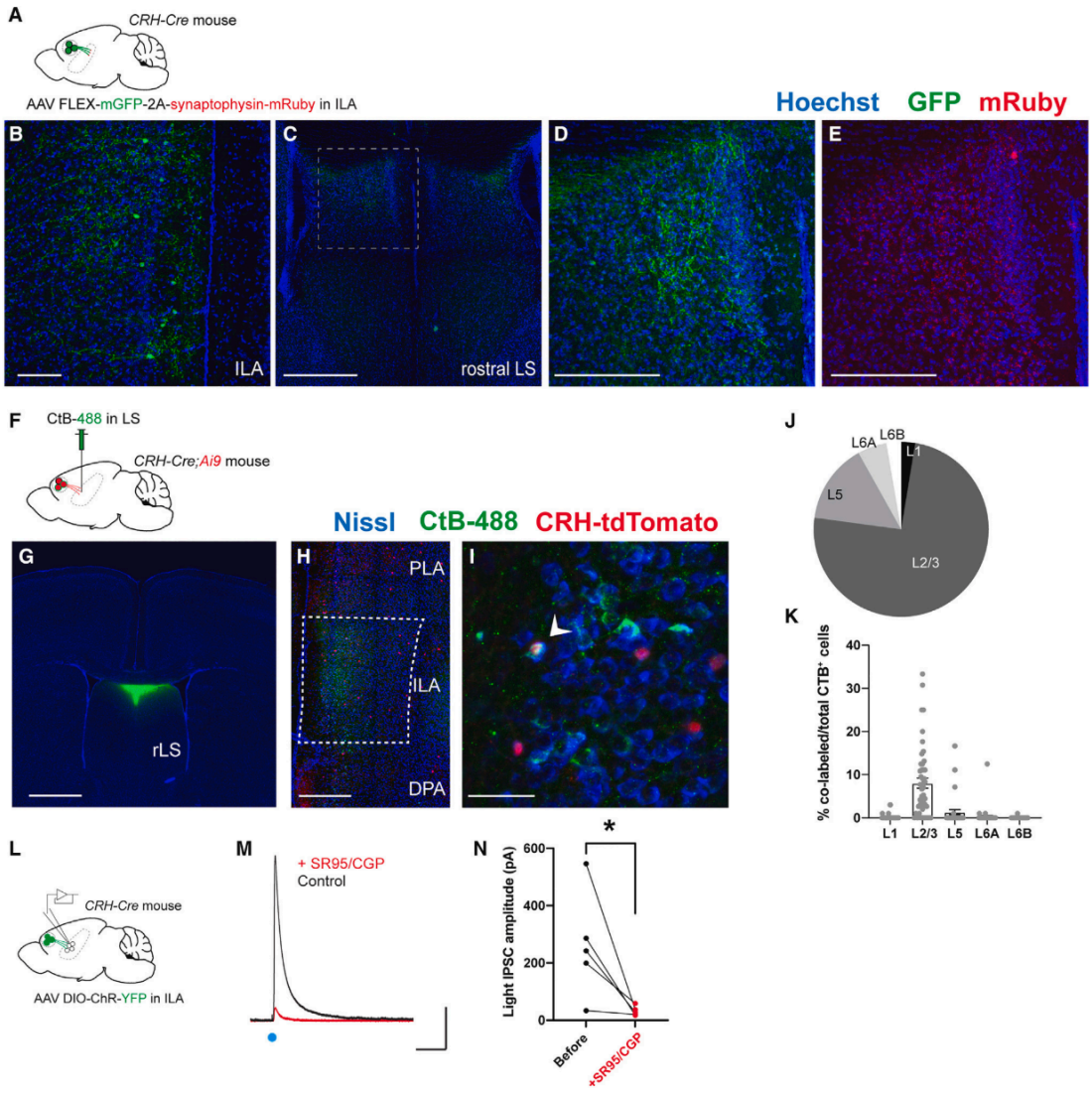


**Figure 3. According to Figure 1 in reference** (1)**, ILA$^{CRH}$ cells project to rostro-dorsal LS**

(A) Viral Tracing: CRH-Cre mice were injected with AAV constructs in the infralimbic area (ILA) to label CRH-expressing neurons and their synaptic terminals with GFP and mRuby.
(B–E) Immunohistochemistry confirmed labeled projections in the lateral septum (LS).
(F-K) Retrograde Tracing: Injection of CtB-488 in rdLS of CRH-Cre;Ai9 mice revealed retrogradely labeled CRH$^{+}$ neurons in ILA, showing their distribution across cortical layers.
(L–N) Electrophysiology: Optogenetic stimulation of Channelrhodopsin-expressing ILA$^{CRH}$ axons in rdLS evoked inhibitory postsynaptic currents (IPSCs), which were blocked by GABAA/B receptor antagonists (SR95 & CGP).
Reproduced from reference (1), under CC BY 4.0 license.

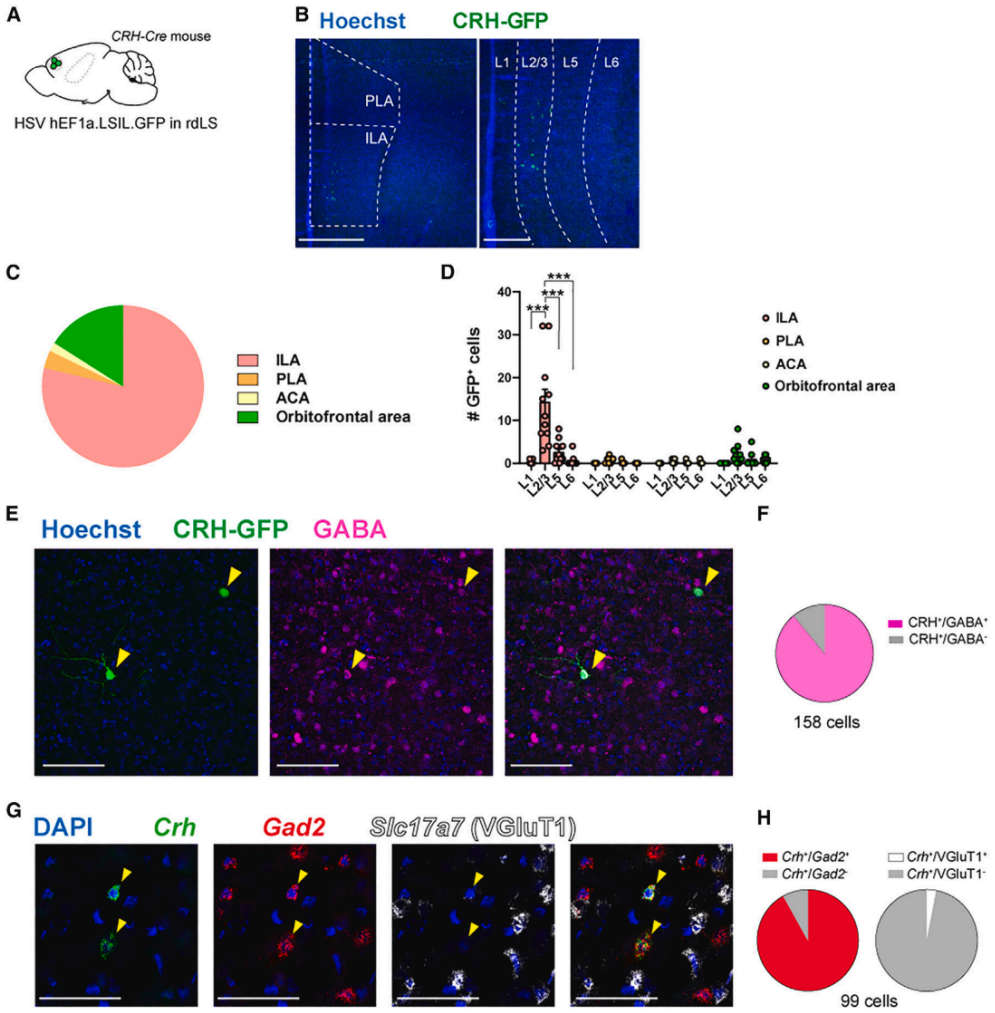


**Figure S1. According to Figure S3, related to figure 1 in reference** (1)**, Molecular identity of ILA$^{CRH}$ cells**

(A-B) Retrograde Labeling: CRH-Cre mice were injected with HSV-GFP in rdLS, revealing CRH$^{+}$ neurons in the infralimbic area (ILA) of the mPFC.
(C-D) Cell Distribution: GFP$^{+}$ cells were primarily found in layer 2/3 of the ILA, with significant differences across layers and regions.
(E-F) Neurochemical Identity: Immunohistochemistry confirmed that ILA$^{CRH}$ cells are GABAergic.
(G-H) Gene Expression: In situ hybridization showed that most ILA$^{CRH}$ cells express Crh and Gad2 (GABAergic marker) but not Slc17a7 (glutamatergic marker), confirming their inhibitory nature.
Reproduced from reference (1), under CC BY 4.0 license.

## ILA$^{CRH}$ cells regulate the duration of social interaction with a familiar mouse during SNP.

To understand the behavioral function of ILA$^{CRH}$ neurons, we used a chemogenetic approach to modulate their activity. Then, injecting *Crh*-Cre mice in ILA with Cre-dependent AAVs expressing an inhibitory DREADD (designer receptor exclusively activated by designer drugs) tagged with mCherry

(iDREADD) or mCherry only as a control (Fig. 4A-B). Next, we tested for social novelty preference (SNP), we found that silencing ILA$^{CRH}$ cells abolished SNP (Fig. 4C). Control groups exhibited a higher interaction time with the novel mouse compared to the familiar one, indicating intact SNP (Fig. 4D). In contrast, the test group with silenced ILA$^{CRH}$ cells explored the novel and familiar mice to the same extent, resulting in a decrease in the discrimination index for SNP (Fig. 4E). Following these results, we hypothesized that ILA$^{CRH}$ cells leverage social memory cues to promote SNP by regulating interactions with novel and familiar mice. Observing that during the learning phase of the SNP test, test mice explored each novel conspecific to the same extent as control mice, suggesting that silencing ILA$^{CRH}$ cells does not impair interactions with novel animals (Fig. S2 D-F). This experiment shows that ILA$^{CRH}$ cells are necessary for social novelty preference.

Then, to determine whether ILA$^{CRH}$ cells support SNP by promoting interactions with novel mice or suppressing interactions with familiar ones we conducted the repetitive social presentation test, where a novel mouse is presented multiple times to the test mouse (Fig. 4F). Control mice showed a progressive decrease in interaction time with repeated presentations, indicating social familiarization animals (Fig. 4G-H). However, mice expressing inhibitory DREADD (iDREADD) showed no decrease in interaction time, suggesting that ILA$^{CRH}$ cells are necessary for social familiarization (Fig. 4G). Conversely, over-activating ILA$^{CRH}$ cells with excitatory DREADD (eDREADD) slightly facilitated the decrease in social interaction, indicating that ILA$^{CRH}$ cells can bidirectionally modulate interaction time with familiar mice (Fig. 4H).

Silencing ILA$^{CRH}$ cells had no effect on locomotion, anxiety, or feeding-related behaviors, suggesting that these neurons are functionally distinct (Fig. S2 A-M). Additionally, we tested ILA$^{CRH}$ cells during social interactions. Founding that silencing ILA$^{CRH}$ cells did not affect sociability (preference for a mouse compared to an object. (Fig. S3 A-C) where both groups exhibited a strong preference for the mouse.

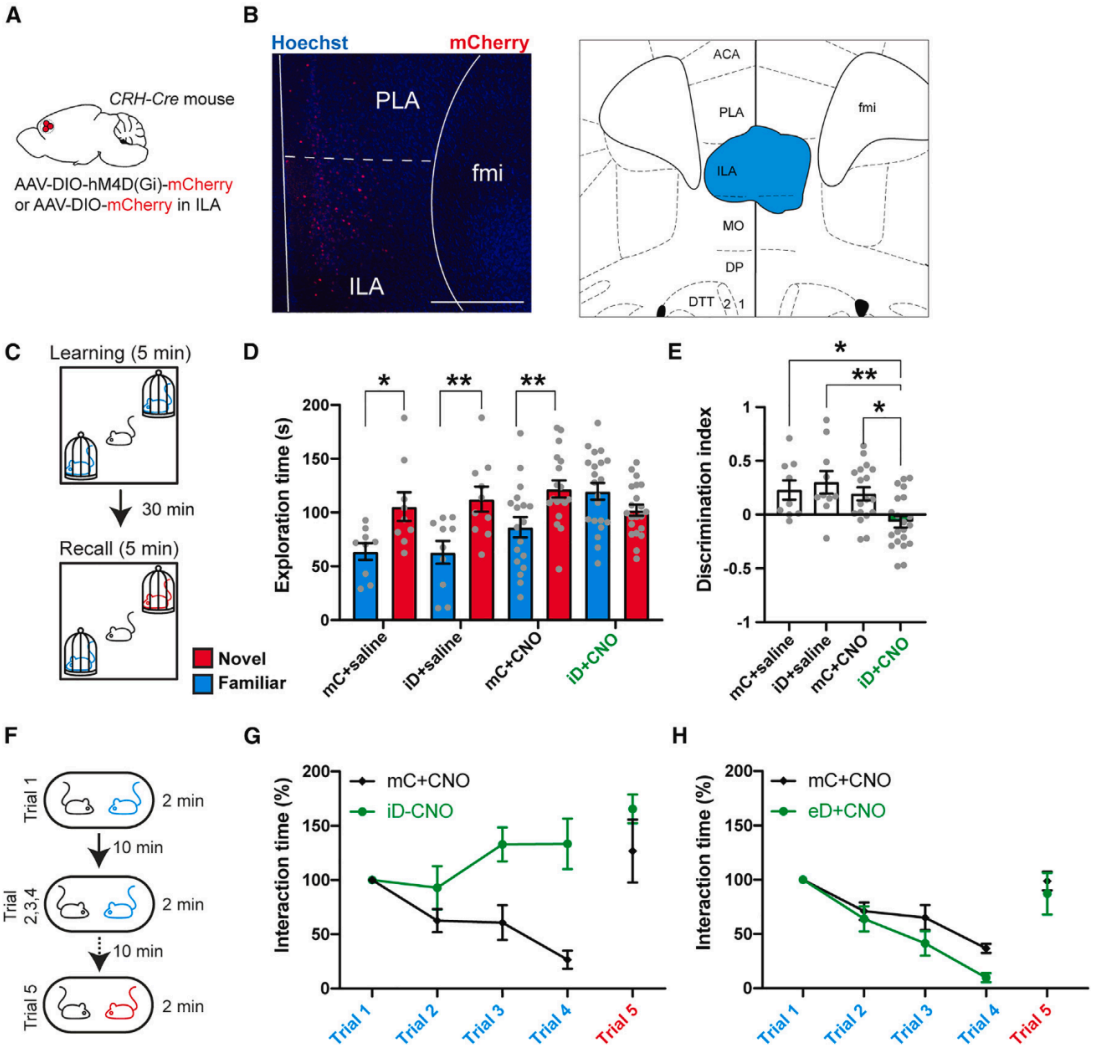


**Figure 4.** [According to Figure 2 in reference ](1)[, ILA$^{CRH}$ cells support social novelty preference and familiarization]

(A) Targeting ILA$^{CRH}$ Neurons for Chemogenetic Manipulation. CRH-Cre mice were injected in the ILA with hM4Di (inhibitory DREADD) or mCherry (control) virus.
(B) Immunohistochemistry confirmed the extent of iDREADD expression in the mPFC.
(C-E) Social Novelty Preference Test. (C) Mice were exposed to a familiar and a novel mouse. Control (mCherry) mice preferred novel mice over familiar ones. (D) Silencing ILA$^{CRH}$ neurons (iDREADD + CNO) abolished this preference. (E) Discrimination index confirmed that ILA$^{CRH}$ activity is necessary for social novelty preference.
(F-H) Repetitive Social Presentation Test. (F) Mice were repeatedly exposed to the same social partner until trial 4. (G) Control mice gradually reduced interaction, indicating familiarization. Silencing ILA$^{CRH}$ neurons impaired familiarization, with iDREADD-expressing mice maintaining high interaction times across trials. (H) Activating ILA$^{CRH}$ Neurons enhances familiarization using hM3Dq (excitatory DREADD) in ILA$^{CRH}$ neurons led to a more rapid reduction in interaction times, supporting the role of ILA$^{CRH}$ neurons in social adaptation.
Reproduced from reference (1), under CC BY 4.0 license.

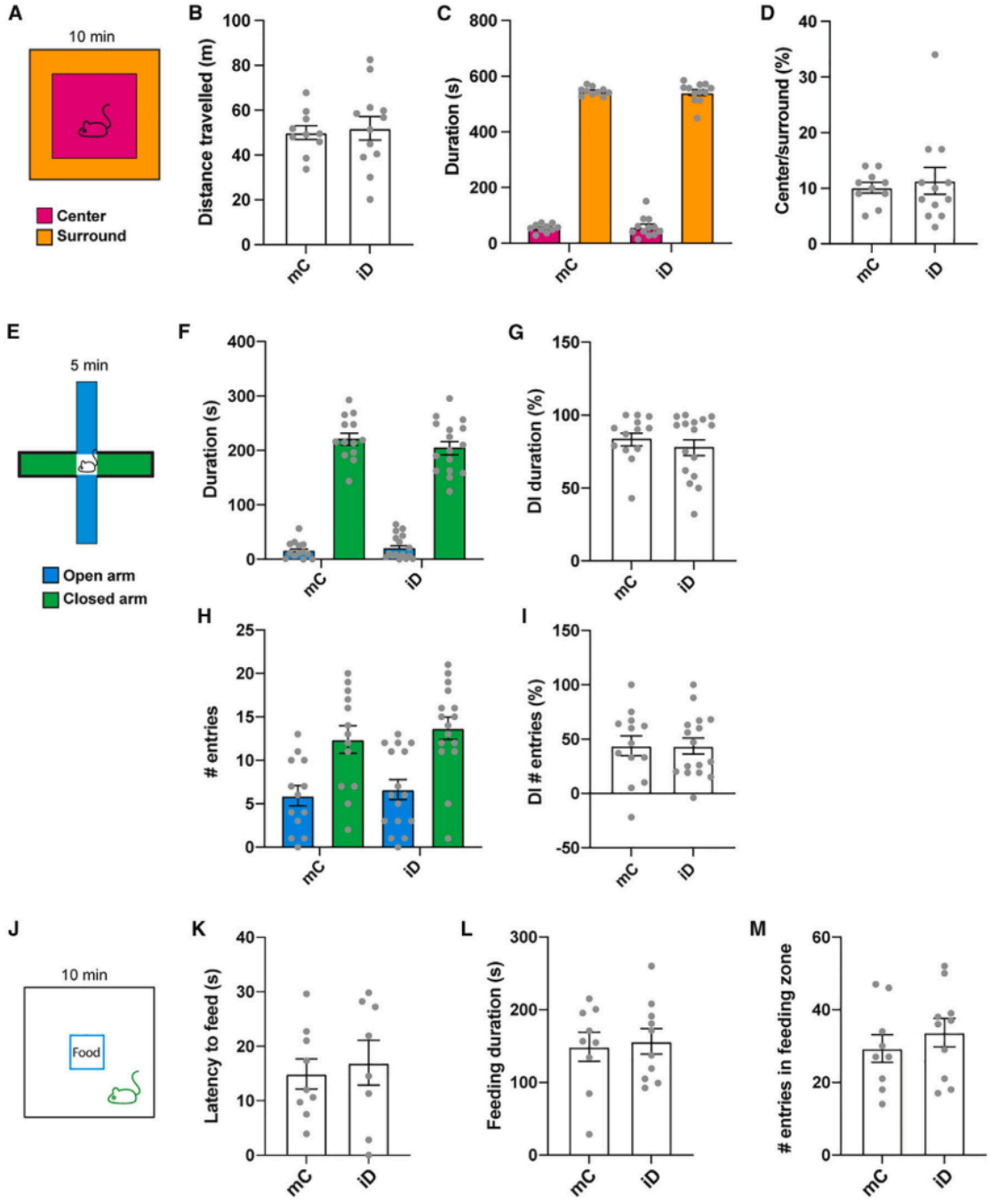


**Figure S2. As shown in figure S4** (1)**, Locomotion, anxiety, and feeding behavior are not affected by chemogenetic silencing of ILA$^{CRH}$ neurons, related to Figure 2.**

(A-D) Open-Field Test. Locomotion and anxiety. Total distance traveled was similar between groups, indicating no effect on locomotion. Time spent in the center vs. surround and the center/surround ratio showed no differences, suggesting no impact on anxiety-like behavior.
(E-I) Elevated Plus Maze. Anxiety-Like Behavior. Time spent in open vs. closed arms and closed arm preference were unaffected by ILA$^{CRH}$ silencing. Number of entries into arms showed no differences, further supporting no anxiety-related changes.

(J-M) Novelty-Suppressed Feeding Test. Feeding Behavior. Latency to feed, feeding duration, and feeding zone entries were similar between groups, indicating no effect on feeding motivation or anxiety-related feeding suppression.

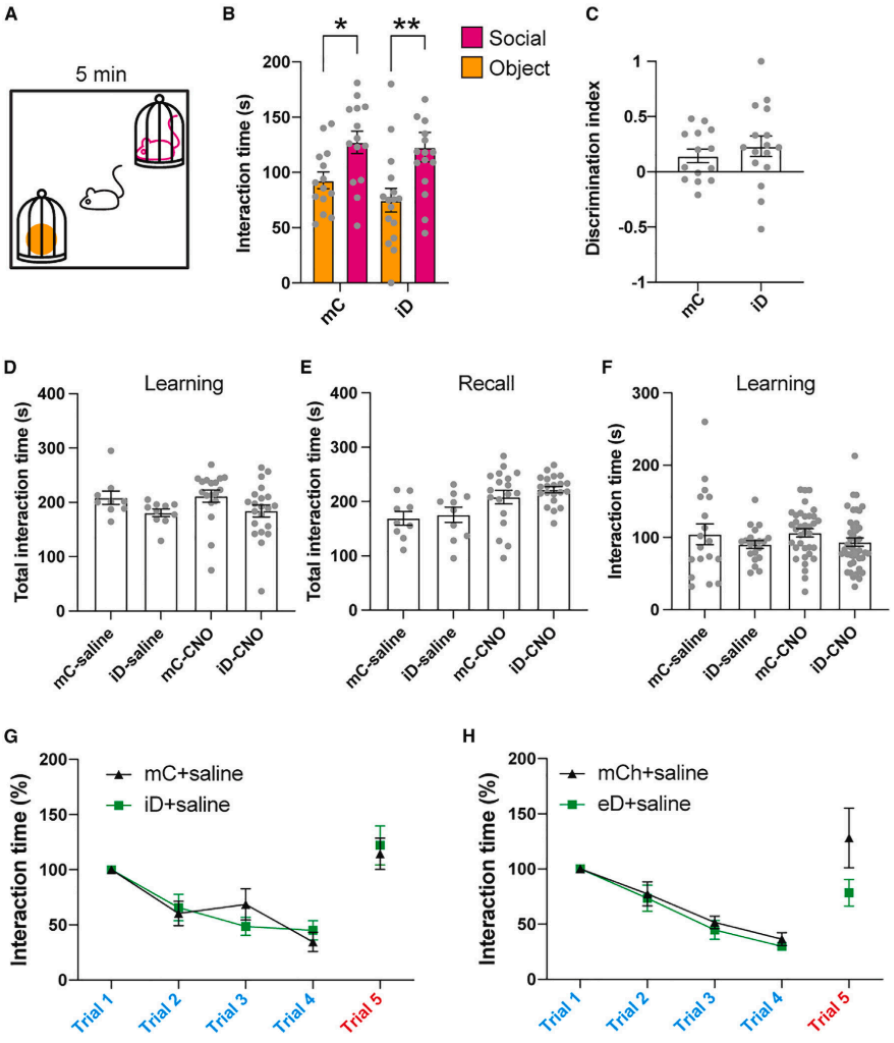


**Figure S3. According to Figure S3, related to figure 2 in reference** (1)**, Social behavior controls for chemogenetic silencing of ILA$^{CRH}$ cells**

(A-C) Sociability Test. Preference for a Social Stimulus. Mice spent more time interacting with a conspecific mouse than an object (p = 0.01, 0.009), confirming intact sociability despite ILA$^{CRH}$ silencing. Social preference discrimination index was positive in both groups (p = 0.03, 0.02), with no significant difference between them (p = 0.4), showing that sociability remains unchanged.
(D-F) Social Novelty Preference Test. Learning and Recall Phases. Total interaction time during the learning trial was not affected by ILA$^{CRH}$ silencing (p = 0.7). However, during the recall trial, ILA$^{CRH}$-silenced mice spent less time interacting with novel mice (p = 0.0004), indicating an effect on social novelty preference but not on social exploration itself. Interaction with each novel mouse during learning was unchanged (p = 0.7), confirming that the impairment is specific to recall.
(G-H) Repetitive Social Presentation Test. Social Recognition. Inhibitory DREADD-expressing mice vs. controls: No significant effect across trials (p = 0.39), suggesting no major deficits in social recognition. Excitatory DREADD-expressing mice vs. controls: No significant difference between groups (p = 0.4), but overall interaction times decreased over repeated trials, as expected.

## $ILA^{CRH}$ neurons are more actively engaged during interactions with familiar littermates

To determine if $ILA^{CRH}$ neurons are more active during familiar social interactions, we conducted fiber-photometry recordings in $ILA^{CRH}$ cells. This was achieved by injecting CRH-Cre mice with a Cre-dependent AAV encoding the calcium sensor GCaMP6f and placing an optical ferrule above the ILA (Fig. 5A). Subject mice were presented with novel and familiar mice while calcium activity was recorded (Fig. 5B-C). When a familiar mouse was presented, there was a significant increase in calcium response, whereas a novel mouse led to a slight decrease (Fig. 5D). The peak responses were notably higher during familiar mouse interactions (Fig. 5E-F), though event frequency remained unchanged (Fig. 5G). These findings indicate that $ILA^{CRH}$ neuron activity is more pronounced during familiar social encounters than novel ones. To further validate this difference, we used fiber-photometry recordings to train linear classifiers to distinguish between interactions with novel and familiar mice. Most recording sessions showed decoding performance above chance, averaging 68% accuracy. When analyzing pseudo-simultaneous data, decoding accuracy increased to 79%, demonstrating that $ILA^{CRH}$ neurons encode social familiarity (Fig. 5I).

Additionally, when mice were exposed to both novel and familiar objects, their neural activity remained unchanged from baseline, with no difference between the two object types (Fig. 5J). By analyzing peak amplitudes, we calculated discrimination indexes (DI) to assess familiarity preference after object and social interactions. The DI for social interactions demonstrated a strong preference for familiar social encounters, whereas object interactions showed no such bias (Fig. 3K). During repeated social presentations, $ILA^{CRH}$ cell recordings revealed an increase in peak amplitude as mice became familiar with their social partner (Fig. 5L), while event frequency remained consistent (Fig. 5M).

To further assess neuronal activity, we examined the expression of the immediate-early gene c-fos. CRH-Cre; Ai9 mice were exposed to either a novel or familiar mouse for two minutes (Fig. 5N). As expected, mice spent more time interacting with novel mice than with familiar ones (Fig. 5O). However, despite the reduced interaction time, ILA$^{CRH}$ cells in layer 2/3 showed greater c-fos expression following familiar encounters compared to novel ones. Moreover, the activation of these ILA$^{CRH}$ cells was inversely correlated with the duration of social interaction (Fig. 5P-Q). These findings indicate that ILA$^{CRH}$ cells are more active during familiar social interactions than novel ones. Furthermore, ILA$^{CRH}$ cells play a role in limiting social interactions with familiar mice while reinforcing social novelty preference (Fig. 5R). This neural circuit also contributes to developmental changes in social preference in young mice.

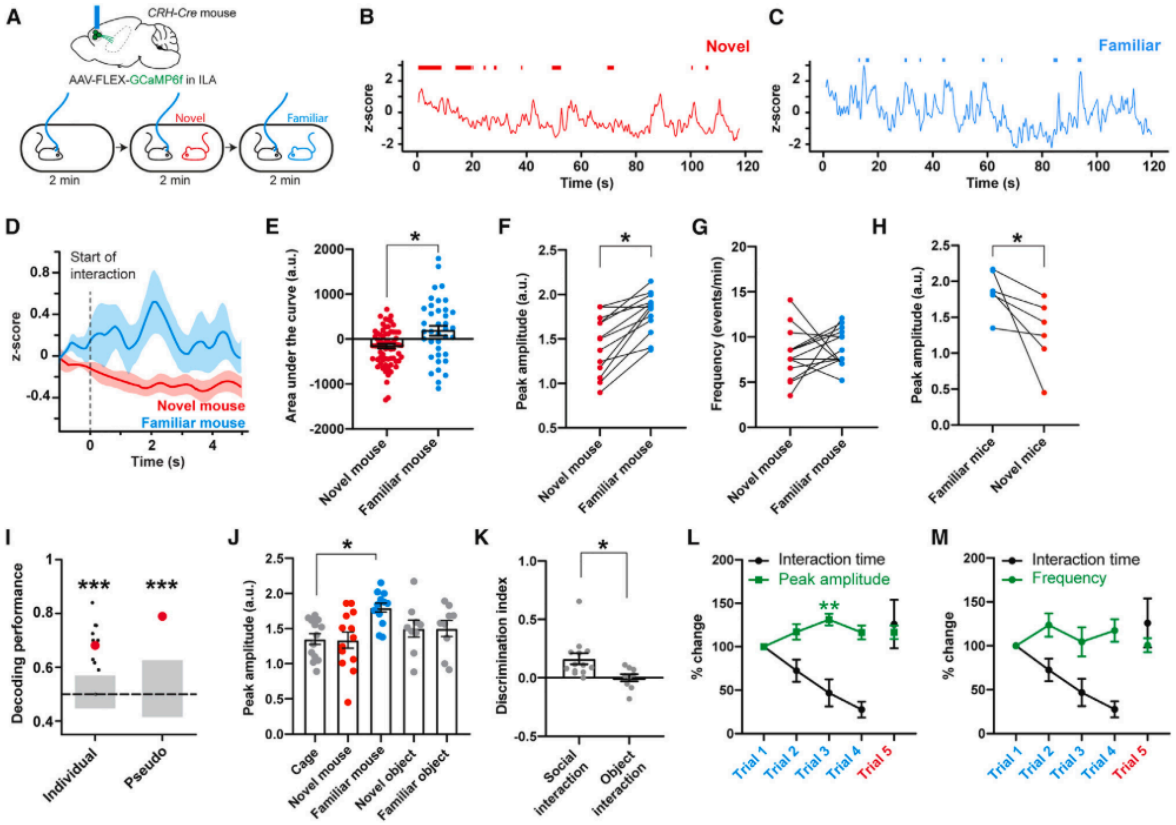

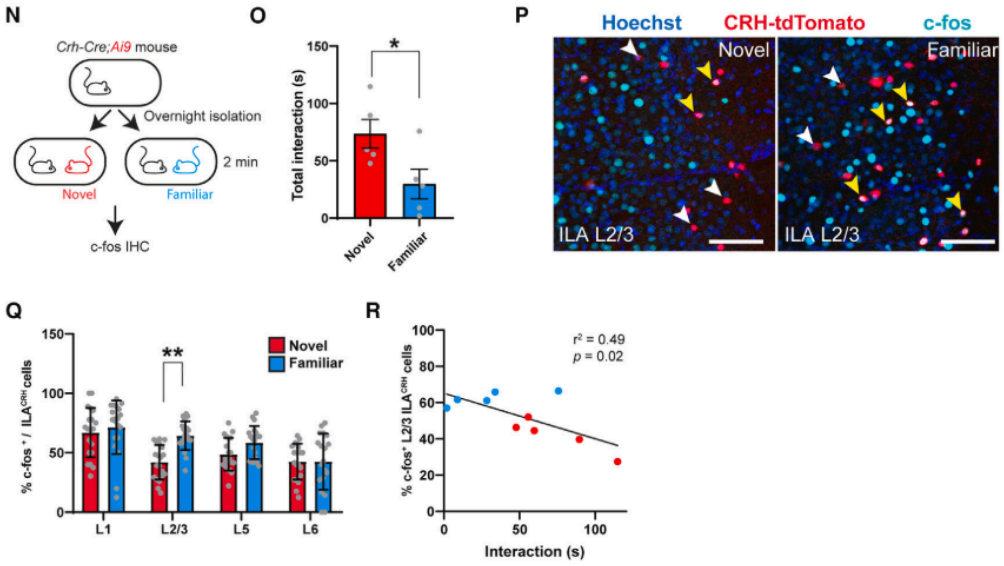


**Figure 5. According to Figure 3 in reference** (1) **ILA$^{CRH}$ cells respond preferentially to familiar mouse presentation**

(A) CRH-Cre mice were injected with AAV2/1 syn.FLEX.GCaMP6f in the ILA and implanted with optical ferrules for fiber photometry recording during social interactions.
(B-C) Example Traces: (B) novel mouse and (C) familiar mouse presentation elicited calcium event responses in ILA$^{CRH}$ cells during social interaction, with interaction intervals marked above each trace.
(D) Calcium Activity During Social Interactions: peri-stimulus time histograms show increased calcium activity during interactions with both novel and familiar mice.
(E) Area under the curve analysis revealed significant increases in calcium signals during both types of interactions compared to baseline (p = 0.001 for both novel and familiar), with higher activity during the familiar mouse interaction (p = 0.01 between groups).
(F) Calcium Signal Amplitude and (G) Frequency: peak amplitude of the calcium signal was higher when a familiar mouse was presented after a novel one (p = 0.02). Frequency of calcium events during novel and familiar presentations did not differ significantly (p = 0.4).
(H) Inverted Social Presentation: when the order of presentation was inverted (familiar first, then novel), the peak amplitude of the calcium signal increased during the novel mouse presentation (p = 0.03).
(I) Decoding Novelty vs. Familiarity: decoding performance of familiarity vs. novelty from individual recordings or pseudo-population data was successful, with average decoding accuracy above chance levels. Red dots indicate the average and pseudo-population analysis results, with gray areas showing chance levels.
(J) Amplitude of Z-Scores During Various Presentations: peak amplitude was analyzed during different trial conditions, revealing significant differences between familiar mouse presentations and object controls (p = 0.03 for familiar).
(K) Discrimination Indexes for Social Preference: discrimination indexes for familiarity preference showed significant preference for social stimuli over objects during mouse presentations (p = 0.01)
(L-M) Repetitive Social Presentation Test: fiber photometry during repetitive social presentations demonstrated changes in calcium event frequency across multiple trials (p = 0.02), suggesting neural response adaptation. Frequency of calcium events was consistent throughout trials (p = 0.63 in a one-way ANOVA).
(N-P) After overnight isolation Cre;Ai9 mice were presented with novel or familiar mice c-fos Expression in ILA: c-fos labeling in ILA layer 2/3 neurons (yellow arrowheads indicate

cfos$^+$/tdTomato$^+$ cells) confirmed that ILA$^{CRH}$ cells are activated by social interactions with both novel and familiar mice.
(Q) Percentage of ILA$^{CRH}$ cells positive for c-fos was higher in Layer 2/3 ($p = 0.003$) and correlated with interaction time with the familiar mouse (R) ($p = 0.02$).


## The release of CRH in the rLS inhibits social interactions with familiar mice, thereby enhancing novelty preference.

Observations of ILA$^{CRH}$ cells reveal projections to the rLS, a region expressing CRH type-1 receptors (CRHR1) that regulate social interactions. This led us to investigate whether CRH release from ILA to rLS is essential for familiarization and social novelty preference (SNP). To test this, we used a Cre-dependent shRNA targeting Crh, selectively reducing CRH expression in ILA$^{CRH}$ neurons (Fig. 6A). Mice expressing the anti-Crh shRNA showed a significant decrease in Crh levels, confirming successful gene silencing (Fig. 6B). These mice exhibited deficits in familiarization during repeated social encounters compared to control mice expressing a scrambled shRNA (Fig. 6C). Furthermore, mice with reduced Crh expression in ILA$^{CRH}$ neurons failed to show a preference for social novelty in recall trials, unlike controls (Fig. 6D). This effect was specific to CRH, as silencing vGAT, a GABA transporter, in ILA$^{CRH}$ neurons did not disrupt familiarization or social novelty preference (Fig. 6E).

We confirmed that removing Crh from rLS-projecting cells in the ILA impaired familiarization and social novelty preference. CRH release in rLS was higher during familiar social interactions compared to novel ones, as demonstrated using a CRH-biosensor (CRF 1.0). In this experiment, WT mice were injected in the rLS with an adeno-associated virus (AAV) expressing the CRH biosensor CRF 1.0. An optical ferrule was implanted above the injection site to record CRH activity events (Fig. 6F). Then, was presented novel and familiar mice to the WT mice in a random order while recording CRH activity (Fig. 6G). The results showed that the presentation of a familiar mouse induced responses of larger amplitude compared to the presentation of a novel mouse, despite the mice interacting less with the familiar mouse (Fig. 6H-I). There was no change in the frequency of CRH activity events

between the presentations of novel and familiar mice (Fig. 6J). The discrimination index, based on the z-score peak amplitude, showed a significant preference for the response to familiar mice (Fig. 6K). These findings align with previous calcium recordings of $ILA^{CRH}$ cells and demonstrate that CRH release in the rLS is higher during familiar social interactions compared to novel social interactions. This suggests that CRH release in the rLS plays a crucial role in mediating social interactions with familiar mice, promoting social novelty preference.

We validated that the removal of Crh from ILA cells projecting to the rLS disrupted both familiarization and the preference for social novelty. Using the CRH-biosensor (CRF 1.0), we observed that CRH release in the rLS was significantly higher during interactions with familiar mice compared to novel ones. In this experiment, wild-type (WT) mice were injected with an adeno-associated virus (AAV) expressing the CRH biosensor CRF 1.0 in the rLS. An optical ferrule was implanted above the injection site to record CRH activity during social interactions (Fig. 6F). The mice were then presented with either a novel or a familiar mouse in a randomized order while CRH activity was recorded (Fig. 6G). The results showed that familiar mouse presentations triggered CRH responses with a larger amplitude than those seen with novel mouse presentations, even though the mice spent less time interacting with the familiar mouse (Fig. 6H-I). No difference was found in the frequency of CRH activity events between the two types of presentations (Fig. 6J). The discrimination index, based on peak amplitude z-scores, revealed a clear preference for the CRH response to familiar mice (Fig. 6K). These results are consistent with previous calcium recordings from $ILA^{CRH}$ cells and confirm that CRH release in the rLS is elevated during interactions with familiar mice. This indicates that CRH release in the rLS plays a critical role in modulating social interactions with familiar mice, supporting the preference for social novelty.

After this, using optogenetics to silence $ILA^{CRH}$ cell terminals in rLS, injecting AAVs expressing Archaerhodopsin (Arch) tagged with tdTomato (Arch mice) or tdTomato only as a control (tdT mice.

(Fig. 6L). Light from a 561-nm laser was applied continuously during either the learning or recall trials of the SNP test. When light was applied during the learning trial, both groups exhibited SNP during the recall trial. However, when light was applied during the recall trial, mice ex- pressing Arch failed to show a preference for the novel mouse while mice expressing tdTomato only did (Fig. 6N-N). Besides, during repetitive social presentations stimulation after first trial. Arch mice exposed to light failed to familiarization (Fig. 6O). This suggests that CRH release from $ILA^{CRH}$ cells in rLS is necessary for mediating familiarization and social novelty preference. Combining Arch-mediated silencing and CRH recording, we showed that activating Arch decreased the frequency and amplitude of CRH-related transients. Importantly, turning on the laser increased social interaction with the familiar mouse, indicating that $ILA^{CRH}$ fibers regulate the amount of social interaction with familiar mice. Overall, the study demonstrates that CRH release from $ILA^{CRH}$ cells in rLS during social encounters suppresses social interactions with familiar mice to promote social novelty preference, highlighting the role of CRH in regulating social behavior and providing insights into the neural circuits underlying social interactions.

Afterward, we used optogenetics to silence $ILA^{CRH}$ cell terminals in the rLS by injecting AAVs expressing Archaerhodopsin (Arch) tagged with tdTomato (Arch mice) or tdTomato alone as a control (tdT mice) (Fig. 6L). A 561-nm laser was applied continuously during either the learning or recall phases of the social novelty preference (SNP) test. When light was applied during the learning phase, both groups exhibited a preference for the novel mouse during the recall phase. However, when light was applied during the recall phase, Arch-expressing mice did not show a preference for the novel mouse, whereas the tdT control mice did (Fig. 6N). Additionally, during repetitive social presentations, Arch mice exposed to light failed to show proper familiarization after the first trial (Fig. 6O). This suggests that CRH release from $ILA^{CRH}$ cells in rLS is essential for mediating familiarization and social novelty preference. By combining Arch-mediated silencing with CRH recording, we demonstrated that activating Arch reduced both the frequency and amplitude of CRH-

related transients. Notably, turning on the laser increased social interactions with the familiar mouse, indicating that ILA$^{CRH}$ fibers regulate the level of social interaction with familiar mice. Overall, these results highlight the crucial role of CRH release from ILA$^{CRH}$ cells in the rLS during social encounters, as it suppresses interactions with familiar mice to promote social novelty preference, providing deeper insight into the neural circuits governing social behavior.

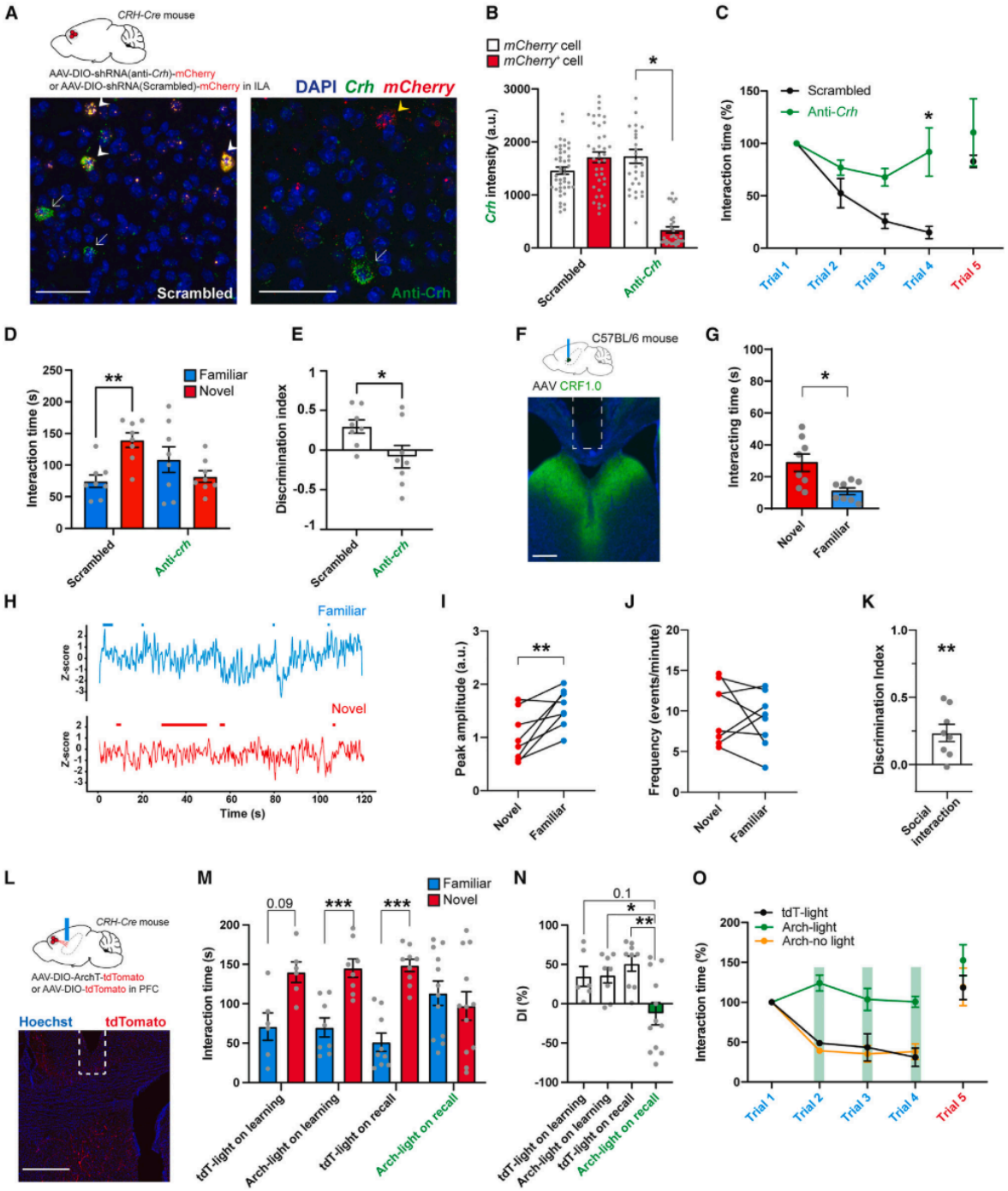

**Figure 6. According to Figure 4 in reference** (1)**, CRH release from ILA in rdLS suppresses social interactions with familiar mice and supports social novelty preference**

(A) Downregulation of Crh Expression in ILA: CRH-Cre mice were injected with AAV2/9 expressing shRNA to downregulate Crh or control scrambled shRNA in ILA. In situ hybridization showed reduced Crh expression in cells expressing anti-Crh shRNA (yellow arrowhead) and intact expression in cells expressing scrambled shRNA (white arrowheads).
(B) Quantification of Crh Expression: CRH expression was significantly reduced in neurons expressing the anti-Crh shRNA compared to scrambled shRNA ($p = 0.03$).
(C) Repetitive Social Presentation Test: mice expressing anti-Crh shRNA spent significantly less time interacting with familiar mice in later trials compared to scrambled shRNA controls ($p = 0.009$ in trial 4).
(D) Social Novelty Preference Test: Social novelty preference during recall was significantly impaired in anti-Crh shRNA-expressing mice for familiar mouse interactions ($p = 0.004$ for novel vs. familiar).
(E) Discrimination index analysis confirmed that anti-Crh mice showed reduced preference for social novelty ($p = 0.03$).
(F) CRF1.0 Expression in rdLS and Optical Ferrule Implantation: CRF1.0 expression was induced in rdLS in wild-type mice, with optical ferrules implanted for fiber photometry.
(G) Social Interaction with Familiar vs. Novel Mice: CRF1.0-expressing mice showed significant preference for interaction with novel over familiar mice ($p = 0.002$).
(H-I) Fiber Photometry Recording of Social Interaction: fiber photometry recordings during interaction with novel or familiar mice showed increased (I) peak amplitude during novel presentations ($p = 0.008$).
(J) Frequency of calcium events did not differ significantly ($p = 0.5$).
(K) Discrimination Index for Familiarity Preference: discrimination index analysis confirmed a preference for novelty during social interaction with the novel mouse ($p = 0.008$).
(L) ArchT-tdTomato Expression in ILA: CRH-Cre mice were injected with ArchT-tdTomato in ILA to enable optogenetic silencing during social interaction experiments.
(M-N) Social Novelty Preference Test with ArchT: optogenetic silencing during social novelty preference test (M) significantly reduced interaction with the novel mouse and impaired novelty preference (N) ($p = 0.03$ for the ArchT group vs. controls).
(O) Repetitive Social Presentation Test with ArchT: ArchT silencing during repetitive social presentation tests significantly decreased interaction times in ArchT-expressing mice compared to controls ($p < 0.0001$).


## Activation of CRHR1 in the rdLS reduces social interactions with familiar mice and promotes social novelty preference.

CRH receptor 1 (CRHR1) is known to regulate social interaction and social novelty preference (3,139), prompting us to investigate whether CRHR1 is expressed near the $ILA^{CRH}$ cell terminals in the rLS. We injected CRHR1-Cre mice with a Cre-dependent AAV expressing GFP and observed several neurons in the rdLS (Fig. 7A). By crossing the CRHR1-Cre line with the Ai9 tdTomato reporter, we were able to visualize $CRHR1^{+}$ neurons. Whole-cell patch-clamp recordings from $rdLS^{CRHR1}$

neurons demonstrated that application of stressin-1, a CRHR1 agonist, induced an inward current, consistent with previous findings (140), suggesting that CRH release in the rdLS depolarizes $CRHR1^{+}$ neurons. To further explore this, mice were implanted with a cannula in the rdLS and infused with either the CRHR1 antagonist antalarmin or DMSO before conducting the social novelty preference test. Mice infused with DMSO exhibited normal novelty preference, whereas those infused with antalarmin showed no preference for the novel mouse (Fig. 7C-D). There was no difference in total exploration time during the learning or recall phases between the groups.

We then performed chemogenetic silencing of CRHR1+ neurons in the rdLS by injecting CRHR1-Cre mice with Cre-dependent AAVs expressing inhibitory DREADD tagged with mCherry, or mCherry alone as a control (Fig. 7E). Social novelty preference tests revealed that control groups showed a preference for the novel mouse, while the test group did not (Fig. 7F). The discrimination index for the test group was not significantly different from 0, unlike the control groups. Total interaction times during the learning or recall phases, as well as interaction time with the novel mouse during learning, were similar across all groups. The repetitive social presentation test showed no evidence of familiarization in the test group, suggesting that CRHR1 activation in the rdLS is crucial for familiarization and the preference for social novelty (Fig. 7H).

To determine whether $CRHR1^{+}$ neurons in the rdLS were preferentially activated during interactions with familiar mice, we presented CRHR1-Cre; Ai9 mice with either novel or familiar mice before perfusing them and performing c-fos labeling (Fig. 7I-J). The percentage of $rdLS^{CRHR1}$ neurons expressing c-fos during familiar interactions was three times higher than during novel interactions. These findings confirm that $rdLS^{CRHR1}$ neurons are preferentially activated during familiar encounters and play a role in regulating both familiarization and social novelty preference.

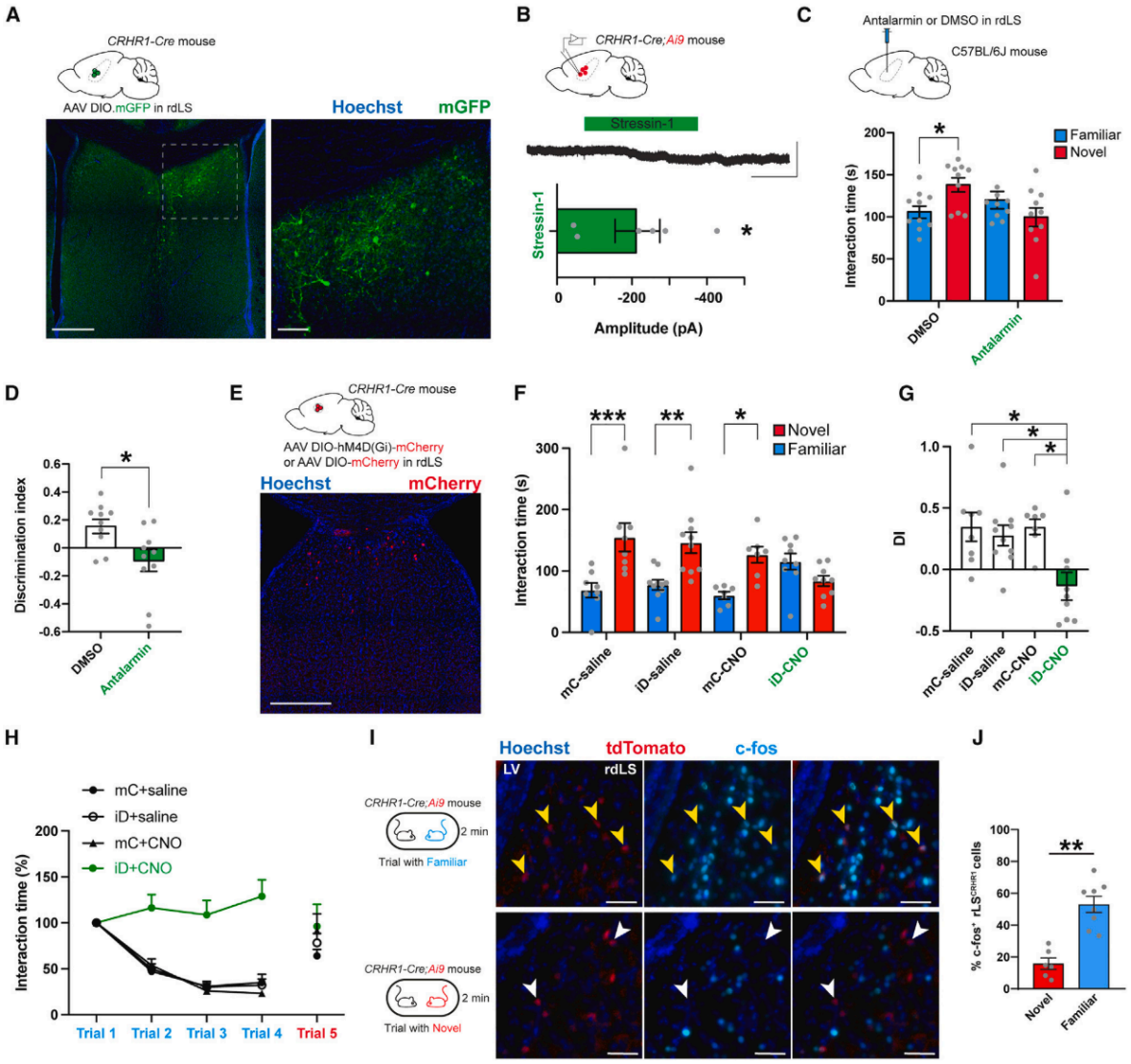


**Figure 7. According to Figure 5 in reference (1) CRHR1⁺ neurons in rdLS are activated by social familiarity and regulate SNP and familiarization**

(A) CRHR1-Cre Mice in rdLS: CRHR1-Cre mice were injected in rdLS with AAV2/5 expressing mGFP (green fluorescent protein). Immunohistochemistry confirmed mGFP expression in the rdLS.
(B) Patch-Clamp Recording from CRHR1-tdTomato Cells: whole-cell patch-clamp recordings were performed on CRHR1-tdTomato cells in CRHR1-Cre;Ai9 mice. Stressin-1 (a CRH receptor agonist) was applied, resulting in a decrease in the amplitude of the response, confirming activation of CRHR1+ neurons by stressin-1 ($p = 0.02$).
(C) Antalarmin Treatment in Wild-Type Mice: C57BL/6J wild-type mice were infused with antalarmin (CRHR1 antagonist) or control DMSO into rdLS. During the social novelty preference test, antalarmin-treated mice showed reduced preference for novel mice, indicating that CRHR1 is involved in social novelty preference ($p = 0.04$ for novel vs. familiar).
(D) Discrimination Index for Social Novelty Preference: discrimination index for social novelty preference was significantly reduced in antalarmin-treated mice ($p = 0.01$).
(E) iDREADD Expression in CRHR1-Cre Mice: CRHR1-Cre mice were injected with AAV2/8 hSyn.DIO.hM4D(Gi)-mCherry (iDREADD) or control mCherry virus in rdLS. Immunohistochemistry confirmed expression of iDREADD-mCherry in rdLS.

(F) Social Novelty Preference Test with iDREADD and CNO: CNO (designer drug) was administered to activate iDREADD in CRHR1+ neurons. iDREADD mice (activated with CNO) spent significantly less time interacting with the novel mouse during the social novelty preference test ($p = 0.0003$, $p = 0.01$ for different trials).
(G) Discrimination Index with iDREADD and CNO: Social novelty preference was significantly impaired in iDREADD+CNO group, as shown by the discrimination index ($p = 0.009$).
(H) Repetitive Social Presentation Test: iDREADD mice treated with CNO showed significantly reduced interaction times during the repetitive social presentation test ($p < 0.0001$).
(I) Immunohistochemistry for c-fos in $CRHR1^+$ Neurons: c-fos labeling in CRHR1-tdTomato mice was used to identify activated neurons after interaction with familiar or novel mice. $c\text{-}fos^+$ CRHR1 neurons were more abundant in response to novel mouse interactions.
(J) Percentage of $CRHR1^+$ Neurons Expressing c-fos: The percentage of $CRHR1^+$ neurons expressing c-fos was significantly higher following novel mouse interaction ($p = 0.007$).


**Activation of CRHR1 in the rLS disinhibits the region, leading to a reduction in social interactions with familiar mice.**

To examine the effects of CRHR1 in the rLS, acute slices from the lateral septum (LS) of wild-type mice were treated with the CRHR1 agonist stressin-1 (Fig. 8A-B). This treatment resulted in a reduction in the frequency and integrated charge of spontaneous inhibitory post-synaptic currents (IPSCs), with a trend toward decreased amplitude as well (Fig. 8C-E). Importantly, this effect was observed specifically in the rLS and not in the ventral lateral septum (vLS), consistent with the localized expression of CRHR1. To investigate whether CRH release from other regions might also influence this effect, we focused on the release of CRH from ILA fibers into the rLS. To do this, we expressed channelrhodopsin in $ILA^{CRH}$ neurons and prepared rdLS slices (Fig. 8F). Upon light stimulation, CRH release from ILA fibers, induced by channelrhodopsin, also led to a decrease in the frequency, amplitude, and charge of spontaneous inhibitory events in rLS neurons, similar to the effect of stressin-1 application. This disinhibition was confirmed to be CRH-dependent, as it was blocked by the CRHR1 antagonist antalarmin (Fig. 8G-J). Overall, these findings suggest that CRH release, whether induced pharmacologically or via optogenetic stimulation, reduces inhibitory synaptic activity in rLS neurons, emphasizing the specific modulatory role of CRHR1 in this brain region.

The next step was to investigate whether the rLS is disinhibited during social interactions with familiar mice and to explore the effects of this disinhibition. Using fiber-photometry, we recorded the responses of rLS neurons in wild-type C57BL/6J mice injected with an AAV expressing the calcium indicator GCaMP6f (Fig. 8K-L). During interactions with familiar mice, larger amplitude transients were observed compared to interactions with novel mice, even though the interaction time with familiar mice was shorter (Fig. 8M). The frequency of transients remained unchanged (Fig. 6N). A significant preference for familiar mice was observed through a discrimination index based on peak amplitude (Fig. 8O). Additionally, linear classifiers trained on fiber-photometry data were able to differentiate between novel and familiar mice with 59% accuracy for individual sessions and 81% accuracy for pooled sessions, indicating that rLS neurons encode social familiarity (Fig. 6P).

Further, we examined c-fos expression in the LS following interactions with novel or familiar mice (Fig. 8Q). The results showed that the rLS responded more strongly to familiar mice, with c-fos expression being upregulated in a specific region of rLS cells near the lateral ventricle. This activation was not observed with novel mice (Fig. 8R-S). Both fiber-photometry recordings and c-fos labeling revealed that a subset of rLS neurons is preferentially activated during familiar interactions, similar to the activation seen in layer 2/3 $ILA^{CRH}$ neurons. The activation of rLS neurons was negatively correlated with the amount of social interaction, while the activation of layer 2/3 $ILA^{CRH}$ cells showed a strong positive correlation with rLS neuron activation (Fig. 8T), suggesting a potential regulatory relationship between the two. In contrast, the posterior dorsal LS (dLS) and posterior ventral LS (vLS) did not show preferential activation or any correlation with the amount of social interaction during familiar encounters.

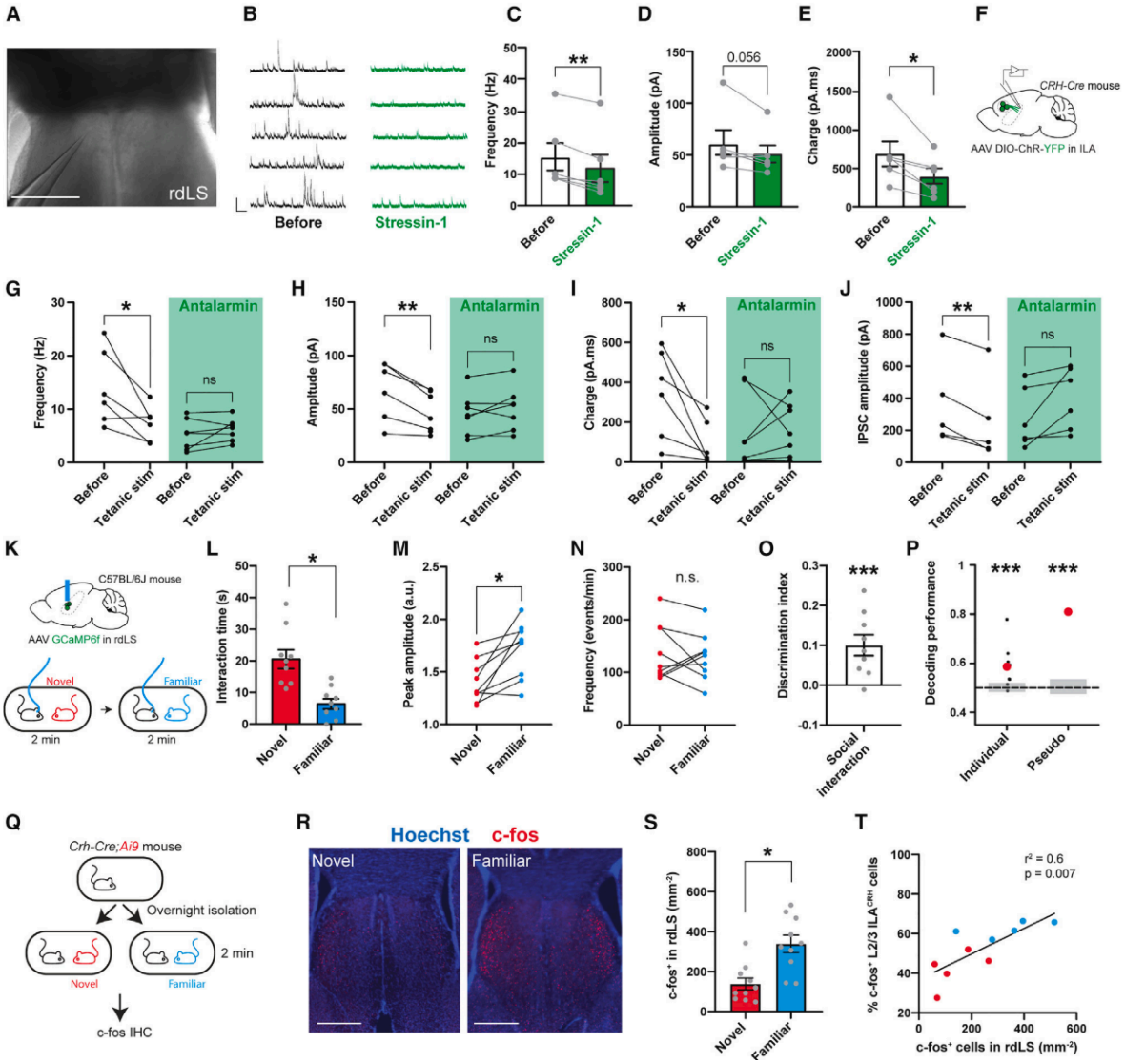


**Figure 8. As shown in figure 6 (1), CRH signaling from ILA and familiar social interaction disinhibit rdLS**

(A) Patch-clamp recordings were performed on rdLS neurons, with differential interference contrast microscopy images showing the recording setup.
(B-E) Stressin-1 and IPSCs in rdLS: Application of 300-nM stressin-1 (a CRH receptor agonist) significantly reduced inhibitory postsynaptic currents (IPSCs) in rdLS neurons 15 minutes post application. Frequency of IPSCs increased ($p = 0.003$). IPSC area under the curve also increased ($p = 0.02$), but IPSC amplitude showed no significant change ($p = 0.056$).
(F) CRH-Cre Mice in ILA: CRH-Cre mice were injected with AAV2/9 EF1a.DIO.hChR2(E123T/T159C)-eYFP in ILA, allowing for light activation of CRH+ neurons in ILA (F).
(G-I) Effects of Tetanic Light Stimulation on rdLS Neurons: Tetanic light stimulation of $CRH^{+}$ neurons from ILA led to increased spontaneous inhibitory events in rdLS neurons, as seen in frequency, amplitude, and charge. The application of 300-nM antalarmin (CRH receptor antagonist) reduced the effects of light stimulation on spontaneous inhibitory events (G-I). Frequency and charge were significantly affected by antalarmin ($p = 0.03$, $p = 0.0003$), while amplitude remained unaffected ($p = 0.2$ and $p = 0.9$).

(J) Electrically Evoked IPSC After Tetanic Light Stimulation: electrically evoked IPSCs in rdLS neurons showed similar results to spontaneous inhibitory events when tetanic light stimulation was applied, with significant effects on IPSC frequency ($p = 0.006$) and charge ($p = 0.07$).
(K) Fiber Photometry in Wild-Type Mice: Wild-type mice were injected with GCaMP6f in rdLS and implanted with an optical ferrule to record calcium activity during social interactions (novel vs. familiar mouse).
(L-N) Social Interaction and Calcium Activity: during the social presentation test, interaction time with a familiar mouse was significantly reduced ($p = 0.01$), and calcium activity in rdLS neurons was higher during the presentation of a novel mouse ($p = 0.03$ for peak amplitude).
(O) Discrimination Index for Social Familiarity Preference: the discrimination index for social novelty preference was calculated based on calcium activity, showing a significant preference for the novel mouse ($p = 0.0005$).
(P) Decoding Familiarity vs. Novelty: decoding performance showed that rdLS neurons could distinguish between novel and familiar social interactions, with results significantly better than chance ($p < 0.001$).
(Q-T) c-fos Activation in rdLS: CRH-Cre;Ai9 mice were presented with novel or familiar mice to study neuronal activation in rdLS. c-fos labeling showed increased activation of rdLS neurons after social interaction with a novel mouse. The density of c-fos$^+$ neurons in rdLS was significantly greater after social interaction ($p = 0.02$) (S), and there was a significant correlation between c-fos expression in ILA and rdLS after social interactions (T) ($p = 0.007$).

**CRH release in the rdLS reduce the inhibitory signaling in the rLS, thereby limiting social interactions with familiar mice.**

To examine whether rLS activation during familiar encounters relies on CRH release from ILA$^{CRH}$ cells, we measured c-fos expression in mice with Crh knockdown in the ILA. Cre-dependent AAVs expressing anti-Crh shRNA or a scrambled shRNA control were injected into the ILA (Fig. 9A-C). Mice with reduced Crh expression showed increased interaction with familiar mice, suggesting that CRH inhibits social novelty interaction (Fig. 9D). Although the loss of Crh did not affect c-fos expression in ILA$^{CRH}$ cells, it significantly reduced c-fos in the rLS (Fig. 9E-H). To investigate if CRHR1$^+$ neurons in the rdLS control disinhibition during familiar encounters, inhibitory DREADD was expressed in rdLS$^{CRHR1}$ neurons (Fig. 9H). Silencing these neurons led to decreased c-fos expression in the rLS and an increase in social interaction (Fig. 9I-L), indicating that CRH release from ILA$^{CRH}$ cells and activation of rdLS$^{CRHR1}$ neurons suppress social interactions.

Additionally, optogenetic activation of rLS neurons was tested by injecting an AAV expressing

Channelrhodopsin (ChR) tagged with mCherry, or mCherry alone, into the rLS of C57BL/6J wild-type mice. Mice were then presented with a familiar mouse for 2 minutes while ChR was stimulated using a 445 nm laser (1 ms pulse at 20 Hz) (Fig. 9M). This activation resulted in decreased social interaction with familiar mice, due to shorter interaction durations, without affecting locomotion (Fig. 9M-P, Fig. 9Q). These findings show that rLS activation can reduce social interactions. In conclusion, ILA$^{CRH}$ cells are activated during interactions with familiar mice, releasing CRH in the rdLS, which causes disinhibition and suppresses social interaction, ultimately promoting a preference for social novelty when presented with both novel and familiar mice.

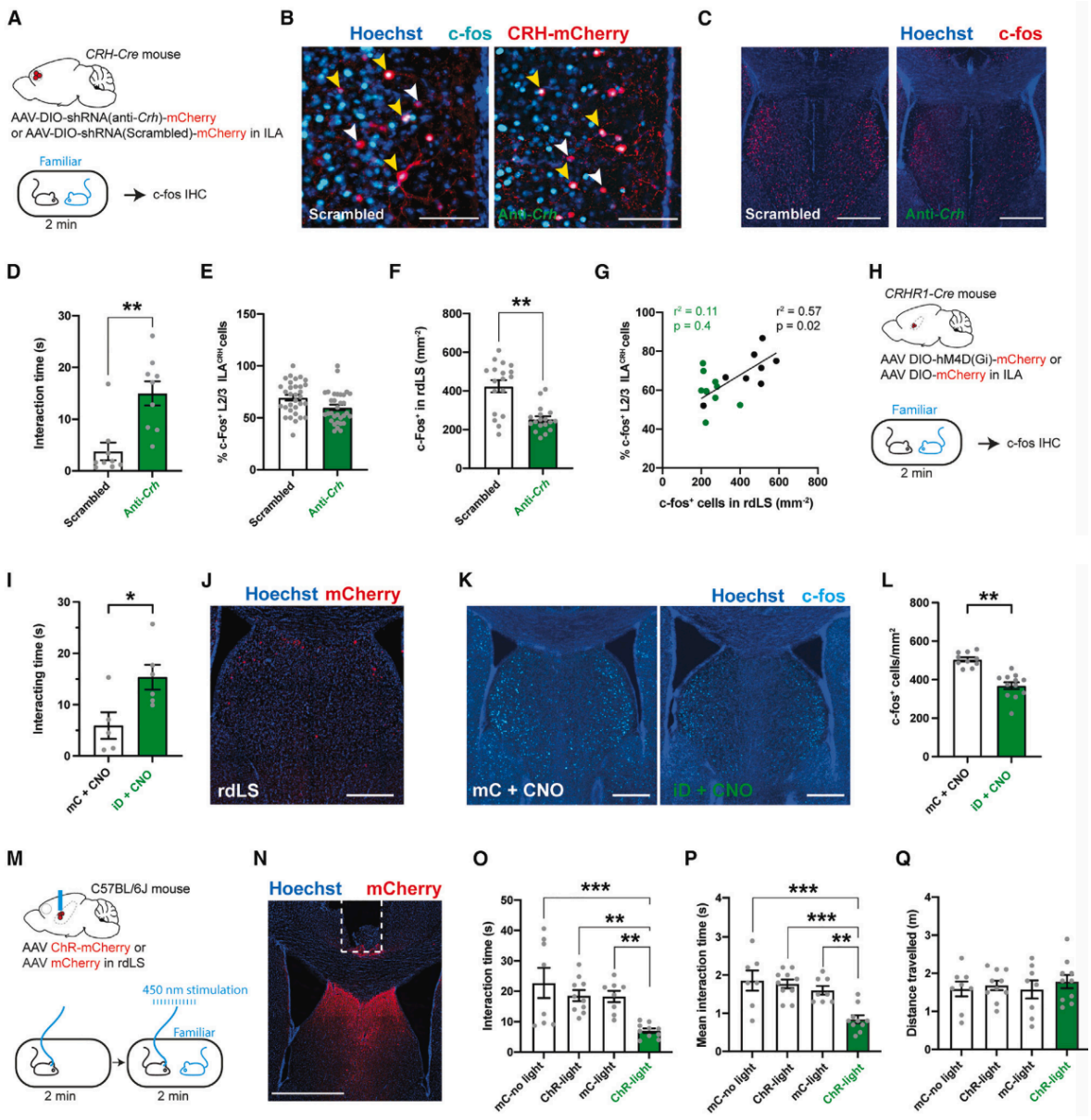

**Figure 9. According to Figure 7 in reference (1), CRH release from ILA and rdLS$^{CRHR1}$ neurons regulate rdLS disinhibition and social interaction with a familiar mouse.**

(A) CRH-Cre Mice and ShRNA Injection: CRH-Cre mice were injected in ILA with AAV2/9 CMV-DIO-(mCherry-U6)-shRNA(anti-Crh) or scrambled shRNA to downregulate CRH expression. Mice were presented with a familiar mouse before c-fos labeling.
(B and C) c-fos Labeling in ILA and rdLS: Immunohistochemistry for c-fos in ILA and rdLS showed increased c-fos expression following social interaction with a familiar mouse. c-fos$^{+}$ / tdTomato$^{+}$ cells in ILA and rdLS were observed. Scale bars for ILA and rdLS images were 100 µm and 300 µm, respectively.
(D) Interaction Duration with Familiar Mouse: interaction duration with a familiar mouse was significantly reduced in mice expressing anti-Crh compared to the control group ($p = 0.001$).
(E) c-fos Expression in ILA and rdLS: Percentage of layer 2/3 ILA CRH$^{+}$ neurons positive for c-fos showed a trend toward increased activity ($p = 0.06$).
(F) Density of rdLS neurons positive for c-fos was significantly higher following interaction with a familiar mouse ($p = 0.002$).
(G) Correlation Between c-fos in ILA and rdLS: a correlation analysis between c-fos+ CRH$^{+}$ neurons in ILA and c-fos+ neurons in rdLS showed a significant relationship in the scrambled group ($p = 0.02$), but no significant relationship in the anti-Crh group ($p = 0.4$).
(H-K) CRHR1-Cre Mice with iDREADD in rdLS: CRHR1-Cre mice were injected with AAV2/8 hSyn.DIO.hM4D(Gi)-mCherry (iDREADD) in rdLS, and presented with a familiar mouse before c-fos labeling.(I) Interaction time with the familiar mouse was significantly reduced in the iDREADD group ($p = 0.03$) (J). Immunohistochemistry confirmed mCherry expression in rdLS, and c-fos expression was observed in rdLS neurons (K).
(L) Density of c-fos+ rdLS neurons was significantly higher in control mice compared to the iDREADD group ($p = 0.002$).
(M-Q) Light Stimulation in Wild-Type Mice: Wild-type mice were injected with AAV2/2 hSyn1.hChR2(H134R)-mCherry or control mCherry, and an optical fiber was implanted to deliver light (450 nm) during a social interaction with a familiar mouse. (O-P) Total and mean interaction time with the familiar mouse was significantly reduced in the ChR2 light stimulation group ($p = 0.0005$, $p = 0.006$, and $p = 0.01$) (Q) Total distance traveled did not differ significantly between groups.


## Increased CRH expression in ILA supports a shift in social preference in young mice.

Previous investigations have sown that unlike to adult's mice, young ones prefer to interact with their familiar siblings compared to novel pups (132,139). Thus, we explore when the shift in social preference occurs in mice. The Young C57BL/6J wild-type mice were given a choice to interact with familiar siblings or unfamiliar non-siblings from P7 to P21. Initially, they preferred siblings, but this preference shifted towards novel mice after P16 (Fig. 10A-B). To examine when ILA neurons begin to express CRH and if this contributes to the shift in social preference. CRH-tdTomato$^{+}$ cells were counted at different ages (Fig. 10C-D), showing a strong increase in ILA$^{CRH}$ cells from P7 to P21,

especially in layer 2/3 of ILA (Fig. 10E-G). Next, to test if the emergence of the ILA to rdLS circuit causes the shift in preference, P5 pups were injected with AAVs expressing anti-Crh or scrambled shRNAs. Control group preference shifted at P14, while Crh-depleted group continued to prefer familiar mice until P20 (Fig. 10I). Overall, the results suggests that increased CRH expression in ILA is responsible for the shift in social preference in young mice, as demonstrated by the strong decrease in Crh labelling intensity in cells expressing anti-Crh shRNA.

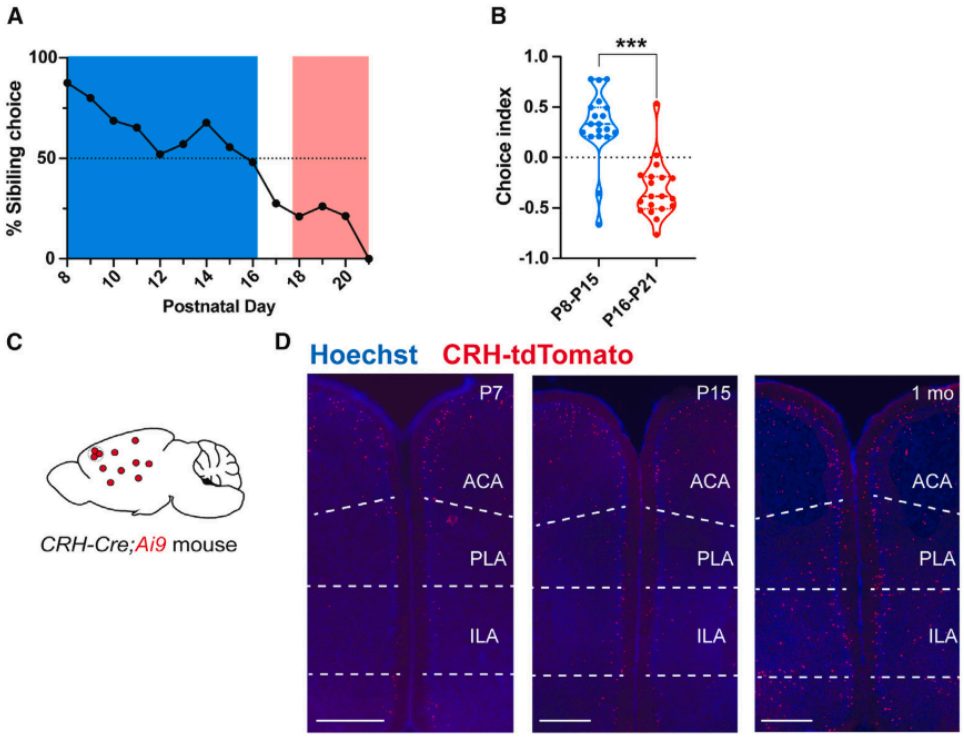

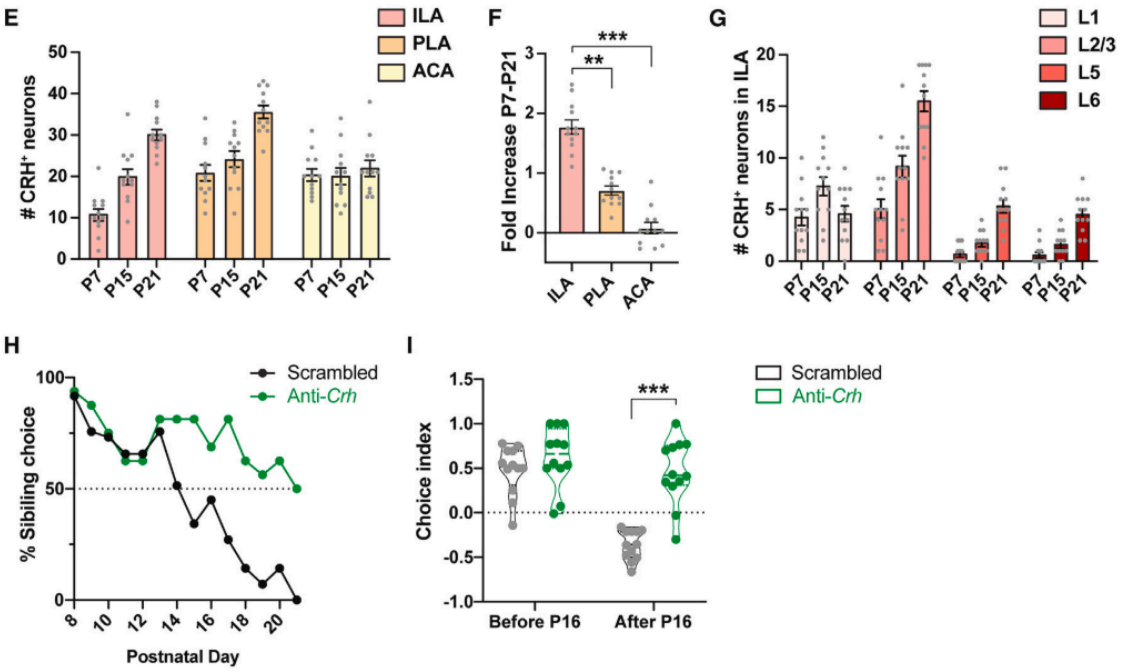


**Figure 10. According to Figure 8 in reference** (1) **Increased CRH expression in ILA supports a shift in social preference in young mice.**

(A) Social Preference During Development: the percentage of familiar choice was measured during development in 19 mice. The figure shows changes in social preference as the mice age.
(B) Discrimination Index for Familiar Kin: discrimination index for familiar kin was assessed before and after post-natal day 16. A significant shift in preference was observed after post-natal day 16 ($p < 0.0001$), indicating a developmental change in social preference.
(C) CRH-Cre;Ai9 Mouse: CRH-Cre;Ai9 mice were used to examine the expression of CRH and its effects during development.
(D) mPFC Imaging of CRH-Cre;Ai9 Mice: immunohistochemistry images of the medial prefrontal cortex (mPFC) in CRH-Cre;Ai9 mice were taken at P7, P15, and P21. The images show changes in $CRH^+$ cell expression over time. Scale bars were 500 µm.
(E) $CRH^+$ Cells in Brain Regions: the number of CRH+ cells in the ILA, PLA (prelimbic area), and ACA (anterior cingulate area) was quantified during development (P7, P15, and P21). A significant increase in $CRH^+$ cells was observed in the ILA and PLA ($p = 0.003$ and $p = 0.009$), but no significant change in the ACA ($p = 0.8$).
(F) Fold-Increase of $CRH^+$ Cells (P7 to P21): the fold-increase in CRH+ cells between P7 and P21 was significant in the ILA (F). P21 values were significantly higher compared to P7 values ($p < 0.0001$).
(G) Number of $CRH^+$ Cells per ILA Layer: the number of CRH+ cells in different layers of the ILA was analyzed during development. Data from 4 observations per mouse across 3 mice per group were used.
(H) Social Preference in CRH-Cre Mice with CRH Knockdown: CRH-Cre mice were injected in ILA with AAV2/9 CMV-DIO-(mCherry-U6)-shRNA(anti-Crh) or control shRNA (scrambled) to downregulate Crh expression. The percentage of familiar choice during social interaction was measured in 12 pups per group. Results showed a significant reduction in preference for the familiar mouse when CRH was downregulated ($p < 0.0001$).
(I) Discrimination Index with CRH Knockdown: the discrimination index for familiar kin was assessed in CRH-Cre mice before and after post-natal day 16. A significant effect was found in social preference following CRH downregulation. Statistical analysis with two-way ANOVA showed significant effects of virus and age on preference shifts ($p < 0.0001$).

Reproduced from reference (1), under CC BY 4.0 license.

## Conclusions

My contributions to this work included conducting behavioral tests such as food seeking and sibling choice, as well as providing constructive input throughout the conceptualization, data collection, and analysis stages. As part of the pioneering Cognition and Social Interaction research group at the Neuroscience Institute of Alicante, I had the opportunity to delve into basic sciences and the use of molecular tools with experimental animals for the first time. This experience enriched my psychology background, enhancing my understanding of research methodology and allowing me to explore vital phenomena such as social interactions.

This study elucidates a critical role for ILA$^{CRH}$ neurons in regulating social novelty preference in mice. By integrating social familiarity cues (140), ILA$^{CRH}$ cells are activated by social interactions with familiar mice, leading to the release of CRH into the rLS, which suppresses further social interaction with the familiar mouse by disinhibiting the LS. As a mouse becomes more familiar, these ILA$^{CRH}$ cells increasingly regulate the reduction in interaction (Figure 11).

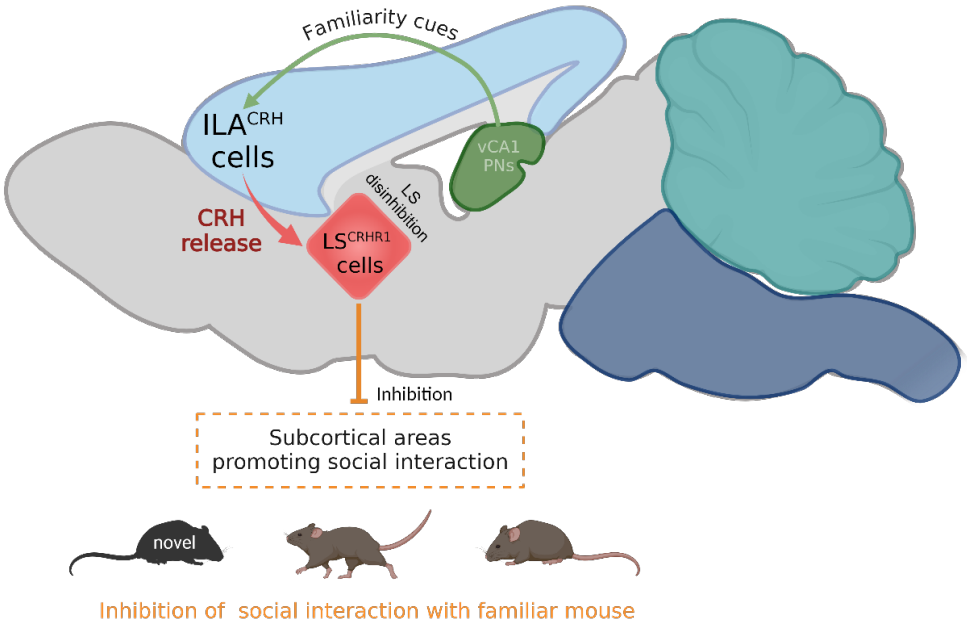


**Figure 11. Circuit diagram promoting social interactions.** CRH release during familiar encounters

disinhibit rLS neurons, suppressing social interactions with familiar mice and promoting preference for social novelty (1).

In other words, this research investigated whether ILA$^{CRH}$ cells are involved in social memory formation or in downstream processes like social novelty preference that rely on social memory cues. Silencing ILA$^{CRH}$ cell terminals in the rdLS during the recall trial, but not during the learning trial, disrupts SNP. This suggests that ILA$^{CRH}$ cells are not involved in forming social memory. Instead, ILA$^{CRH}$ neurons seem to integrate social familiarity cues and release CRH to regulate social interactions with familiar mice. Knocking down Crh expression in ILA increases interaction with familiar mice, further supporting this role.

Previous theories suggested that social novelty preference is driven by a circuit that promotes interactions with novel mice, likely influenced by the rewarding aspects of social novelty. Young mice's kin preferences indicate that other circuits may also control social preferences (137,141). However, the mechanisms behind the rewarding nature of social cues are not well understood. Brain regions like the lateral habenula, nucleus accumbens, dorsal raphe nucleus, and ventral tegmental area are known to modulate social rewards, often under the influence of oxytocin. Future research should explore how social novelty facilitates interactions with novel mice, with the lateral septum (LS) being a key area of interest due to its modulation by dopamine, vasopressin, and oxytocin. Studies have shown that different regions within the LS may regulate distinct types of social interactions, working together to promote SNP.

The regulation of social preference by ILA$^{CRH}$ cells is specific to memory-based SNP and does not extend to memory-based novel object preference. In the social novelty preference test, mice distinguished between novel and familiar siblings based on individual recognition rather than general class recognition. It remains unclear whether ILA$^{CRH}$ cells influence other social preferences, such as those based on sex, strain, kinship, or anxiety. ILA$^{CRH}$ cells likely integrate various social cues

from multiple brain regions, including the ventral CA1 (vCA1) of the hippocampus, which is known to store social memories (140). Rabies tracing shows that $ILA^{CRH}$ cells receive inputs from vCA1 pyramidal neurons, suggesting a role in processing social familiarity information, although this connection requires further confirmation.

Young rats and mice show a strong preference for their mother and siblings during the first weeks of life. This study shows that young mice prefer their siblings over age-matched pups until the maturation of the CRH circuit, which shifts their behavior to the adult norm of preferring novel social interactions. This shift supports behaviors like exploring and interacting with unfamiliar conspecifics, which are important for feeding and reproduction. The lateral septum plays a crucial role in prioritizing these various motivated behaviors. In contrast, monogamous prairie voles exhibit social novelty preference only in short-term tests, but show partner preference in long-term tests, potentially due to differences in CRH expression in the mPFC (109,142). These findings highlight the role of CRH in regulating social preferences across different rodent species.

Humans can suffer from social separation anxiety disorder, characterized by an intense fear or anxiety about separating from attachment figures, and avoidant personality disorder, where individuals avoid interacting with new people, preferring familiar interactions instead. CRH is implicated in various anxiety disorders, including social phobia (143,144). The study suggests that, like mice, familiarity cues activate the human prefrontal cortex and septal regions, indicating that the neural circuit observed in mice might be conserved in humans.

## Future directions

Following the described results on a population of mPFC neurons expressing corticotropin-releasing hormone (CRH. Vale et al., 1981), the key role involved in the regulation of many biological processes including homeostatic and allostatic neuroendocrine mechanisms, memory, and social behaviors (3,4)) even in non-stressful contexts (5,6) and the known role of the mPFC leading in the

establishment of social hierarchy in mice (7,10–13), prompted us to test the function of these cells for the regulation of social hierarchy. Thus, the main results of this doctoral project answer the questions about how $CRH^{+}$ neurons in the medial prefrontal cortex facilitate social submission. Using chemogenetic, optogenetic and calcium recordings in vivo, we show that $mPFC^{CRH}$ neurons promote retreat during the tube test of social hierarchy, therefore promoting social submission. Overall, our study contributes to a better understanding of the neural substrates regulating complex social behaviors and may suggest novel therapeutic approaches to treat mental health disorders associated with impaired social interactions such as social anxiety disorder or avoidant personality disorder.

# CHAPTER III

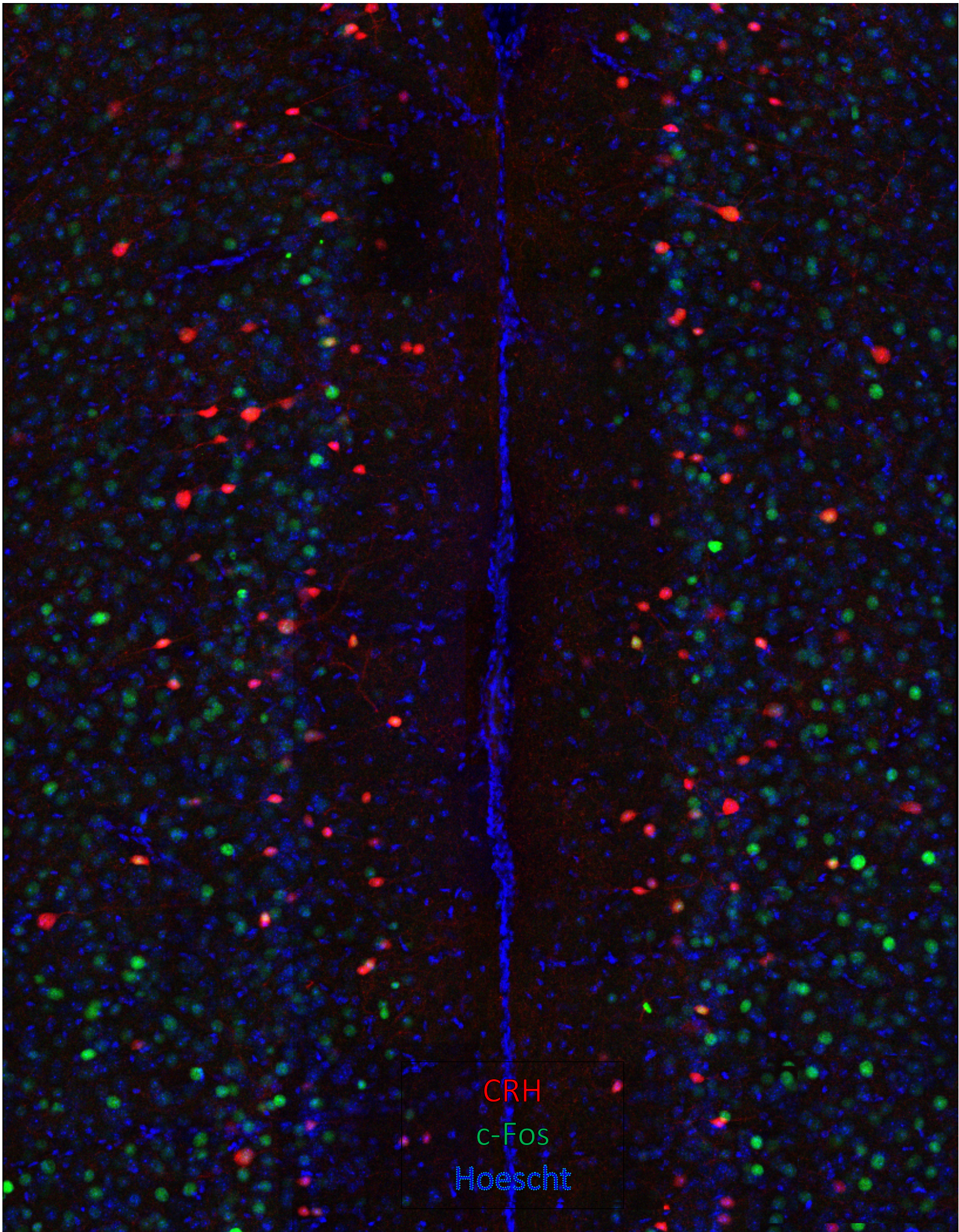

# CHAPTER III. CRH-expressing neurons in the medial prefrontal cortex promote social submission.

## Introduction

Social hierarchy (14,23,145) occurs in most gregarious species (146–150). The rank occupied by everyone within a group influences its survival, reproductive success and health (26,48,151,152). An animal rank depends on two opposing behavioral traits: social dominance (20,153–155), which promotes winning social conflicts when incompatible motivational goals exist among individuals and leads to a higher social ranking (156) and social submission, which promotes defeat and leads to a lower social ranking. Difference in social ranking is therefore due to the tendency of dominant animals to monopolize resources such as food, water, space and mates (135,157,158). Alternatively, agonistic interactions between subordinate animals are attenuated to avoid conflict, thus reducing intragroup fights which helps maintain the group stability (13,159,160). While many studies have investigated the neuronal mechanisms underlying social dominance (10–13,161), only a handful of studies have looked at the mechanisms facilitating social submission (18,162,163)

Investigating social hierarchy in mice(164,165) relies on the tube test, which is based on the use of space, an ecological relevant resource (166) Although this test was first used to assess dominance tendencies between different mouse strains (167), it recently became a key paradigm to assess social hierarchy within a group of cage mate male mice (168). Manipulation of mPFC activity or thalamic inputs to the mPFC (11,169,170) during the tube test have shown that the mPFC is an important neural substrate for the establishment of social hierarchy (11). Thus, synaptic efficacy through mediodorsal thalamic input to the dorsal-medial PFC mediates long-lasting changes in social dominance status that affect the history of social ranking of the mouse (10,11). Neural projections from mPFC to the hypothalamus, amygdala or limbic circuit in general exert top-down controls on serotonin and dopamine release, endocrine function and fear response, which

influences distinct features of dominance behaviors (10,171). This is part of a larger role for the mPFC in the regulation of social behaviors (172) of rodents (8) and humans (18,145), necessary in decision-making and the regulation of the social status (8,11). While most studies have focused on mPFC pyramidal neurons (11,173,174), a recent study began investigated the contribution of other neuronal populations within the highly heterogenous mPFC (9) Thus, vasoactive intestinal peptide-expressing neurons from the mPFC promote social dominance while parvalbumin-expressing interneurons prevent it (12). Furthermore, it has been observed that mPFC astrocytes enhance presynaptic neuronal excitation or reduce postsynaptic inhibitory excitation in dominant and subordinate mice, respectively (13). How other mPFC neurons contribute to social hierarchy remains however unknown.

Here, we focused on a population of mPFC GABAergic neurons expressing the corticotropin-releasing hormone (CRHVale et al., 1981), a 41-amino acid peptide widely expressed in the brain and involved in the regulation of many biological processes including homeostatic and allostatic neuroendocrine mechanisms, memory and social behaviors (3,4,48,136,175) even in non-stressful contexts (5,6,176). We first used c-Fos immunohistochemistry to demonstrate that $mPFC^{CRH}$ neurons are recruited during the tube test compared to social interaction. Then, we used fiber-photometry to record calcium activity and found that $mPFC^{CRH}$ neurons are active during retreat episodes. We then leveraged chemogenetic to silence the $mPFC^{CRH}$ neurons during the tube test and observed an increase in social ranking, suggesting $mPFC^{CRH}$ neurons promote social submission. Knocking-down CRH or GABAergic transmission recapitulated this effect. Finally, optogenetic activation of $mPFC^{CRH}$ neurons lead to an increase in retreat behaviors. Overall, our results demonstrate that $mPFC^{CRH}$ neurons facilitate retreat behavior, therefore promoting social submission and a lower social ranking.

**Results**

## mPFC$^{CRH}$ cells are recruited during the tube test of social dominance

*Crh-Cre* mice were crossed with the Cre-dependent TdTomato reporter line Ai9 to generate the *Crh*-TdTomato mouse line and visualize CRH$^+$ cells. Following habituation to the cage and training, *Crh*-TdTomato male mice interacted with a littermate male mouse under a pencil cup at the end of a tube or fought for social dominance with a littermate mouse in the same tube (Fig. 12A). 1 hour later, we perfused the mice and processed their brain for immunohistochemistry against c-Fos (Fig. 1B). Then, we measured the density c-Fos$^+$ cells in mPFC showed an elevated tendency in the tube test condition compared to social interaction (Fig. 12C), similar to previous observations (11,25). This tendency was originated from all mPFC subregions (Fig. 12D). The density of CRH$^+$ cells expressing c-Fos (Fig. 12E) had an increase in the tube test condition compared to social interaction. This increase originated from mPFC sub-regions: the anterior cingulate area (ACA), the infra-limbic area (ILA) and the pre-limbic area (PL, Fig. 12F). Then, we looked at the ratio of the total CRH$^+$ cells expressing c-Fos and we found an increase in the tube test condition compared to social interaction (Fig. 12G). We found positive correlation between the duration of social interaction and the number of CRH$^+$ cells expressing c-Fos ($p$ = 0.05). While interaction time correlated with CRH$^+$ cells activation following tube test, this was not the case following control condition (Fig. 12F). Additionally, we used a consistent behavioral protocol with a novel C57BL/6J wild-type male mouse as stimuli in each condition (Fig. S1A). In the mPFC, we observed an elevated trend in the number of CRH$^+$ cells during the TT condition compared to the SI condition (Fig. S4C-F). Similarly, as in the familiar condition (Fig.12), the proportion of CRH$^+$ cells expressing c-Fos was significantly increased in the experimental condition compared to the control (Fig. S4G). Furthermore, we found a positive correlation between the duration of social interaction and the number of CRH$^+$ cells expressing c-Fos during the tube test but not in the social interaction condition, suggesting that mPFC$^{CRH}$ cells are

specifically recruited during the tube test (Fig. S1H).

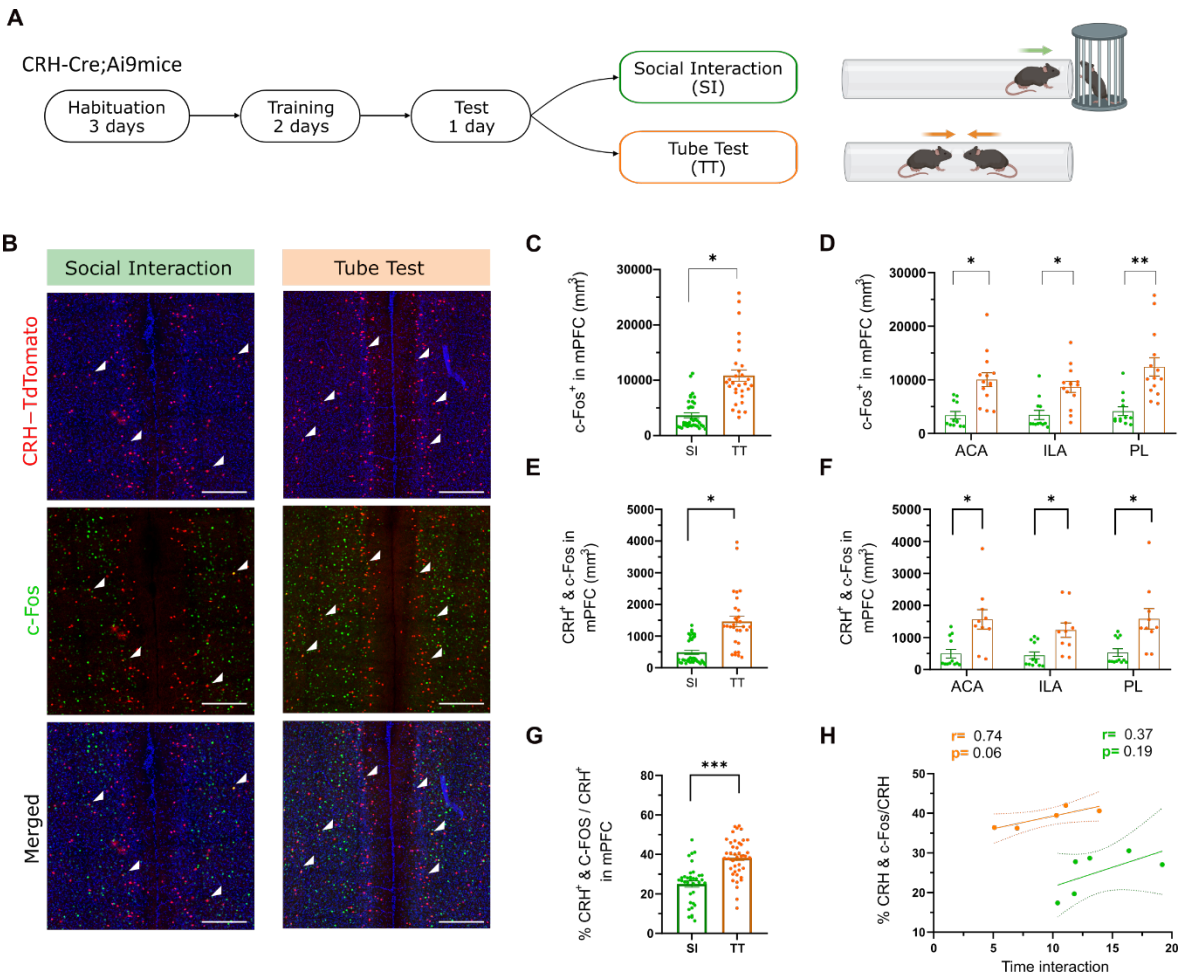


**Figure 12: PFC$^{CRH}$ cells are recruited during tube test.**

**A.** Left, timeline of behavioral protocol with *Crh-Cre* mice crossed with a Cre-dependent TdTomato reporter line (*Crh*-TdTomato mice). Right, schematic of social interaction (SI) and tube test (TT) with littlemate male mice. **B.** Immunohistochemistry images of mPFC. Scale bar: 300 µm.

**C.** Density of c-Fos+ cells. Nested t test: $p = 0.01$. **D.** Density of c-Fos$^+$ cells in ACA, ILA and PL. Nested t tests: $p = 0.01$, 0.02 and 0.007. **E.** Density of CRH$^+$ cells positive for c-Fos. Nested t tests: $p = 0.04$. **F.** Density of CRH$^+$ cells positive for c-Fos in ACA, ILA and PL. Nested t tests: $p = 0.03$, 0.04 and 0.04 **G.** Percentage of CRH$^+$ cells positive for c-Fos. Nested t test: $p = 0.0005$. **H.** Percentage of CRH$^+$ cells positive for c-Fos vs. interaction time following SI and TT. Pearson's tests. Each point is one

observation. Two observations per mouse. SI: 6 mice and TT: 5 mice. ACA: anterior cingulate area, ILA: infra-limbic area and PLA: peri-limbic area. For the entire figure, bar graphs represent mean ± S.E.M.

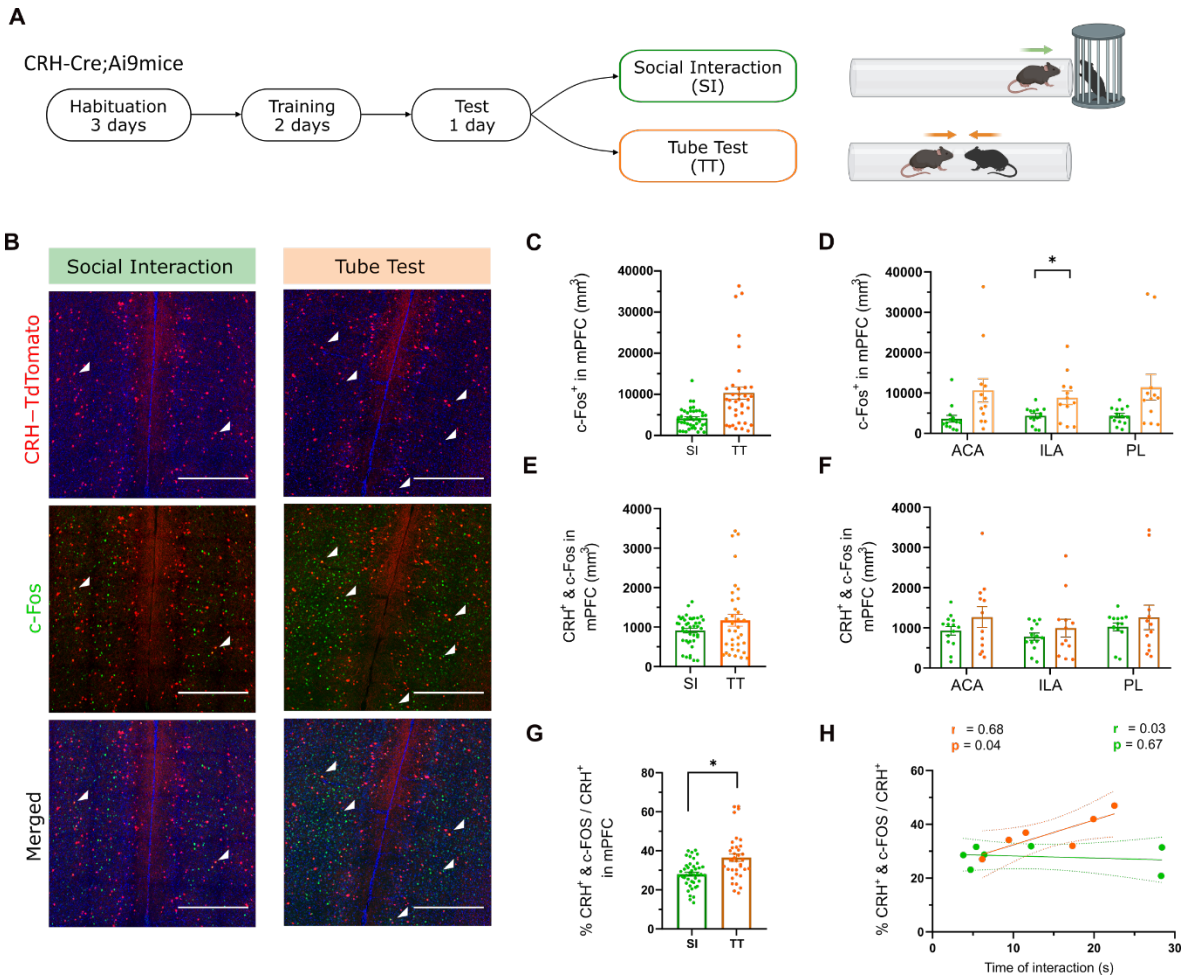


**Figure S4 related to Figure 3: PFC$^{CRH}$ cells are recruited during tube test.**

**A.** Left, timeline of behavioral protocol with *Crh-Cre* mice crossed with a Cre-dependent TdTomato reporter line (*Crh*-TdTomato mice). Right, schematic of social interaction (SI) and tube test (TT) between novel C57BL/6J wild-type male mouse. **B.** Immunohistochemistry images of mPFC. Scale bar: 300 µm. **C.** Density of c-Fos$^+$ cells. Nested t test: $p$ = 0.08. **D.** Density of c-Fos$^+$ cells in ACA, ILA and PL. Nested t tests: $p$ = 0.1, 0.03 and 0.13. **E.** Density of CRH$^+$ cells positive for c-Fos. Nested t tests: $p$ = 0.41. **F.** Density of CRH$^+$ cells positive for c-Fos in ACA, ILA and PL. Nested t tests: $p$ = 0.26, 0.51 and 0.6. **G.** Percentage of CRH$^+$ cells positive for c-Fos. Nested t test: $p$ = 0.02. **H.** Percentage

of $CRH^+$ cells positive for c-Fos vs. interaction time following SI and TT. Pearson's tests. Each point is one observation. Two observations per mouse. SI: 6 mice and TT: 5 mice. ACA: anterior cingulate area, ILA: infra-limbic area and PLA: peri-limbic area. For the entire figure, bar graphs represent mean ± S.E.M.

## $mPFC^{CRH}$ neurons are activated during retreat behavior

To record $mPFC^{CRH}$ cell activity, we injected the PFC of *Crh-Cre* mice with a Cre-dependent AAV expressing the calcium sensor GCaMP6f and implanted an optic fiber above the injection site one week later (Fig. 13A). Mice were habituated to the patch-cord and trained to walk through the tube without an opponent. Then, mice were presented against their littermates in the tube test (Fig. 13B), and we quantified the duration of tube test behavioral parameters: push, resist and retreat episodes (Fig. 13C). First, we aligned the fiber-photometry recordings trace to the push, resist and retreat episodes in order to build peri-stimulus time histograms (PSTH) and quantified their area under the curve as well as the amplitude of the event (Fig. 13D-F). Retreat episodes were associated with increased activity while push events were associated with a slight but significant decrease in activity (Fig. 13H-I). In addition, we looked at the frequency and mean amplitude of calcium transients during the entire test and found a higher frequency of transients in subordinate mice (the mouse that lose their encounter) compared to the dominant mice (Fig. 13G-J) with no difference in total test duration (Fig. S5A). Finally, we also looked at the activity when mice walked through the tube and found that it is associated with a small decrease in activity (Fig. S5C-E).

As previous work from our lab demonstrated that social familiarity activated $ILA^{CRH}$ cell activity (1), we ran mice for the tube test against a novel male mouse from a different cage while recording the $mPFC^{CRH}$ cells calcium activity (Fig. S6A). We first quantified the duration of each tube test behavior (Fig. S6B). and aligned the fiber-photometry recordings trace to the push, resist and retreat episodes

to build PSTH (Fig. S5C). Similar to the previous results during familiar encounters (Fig. 13I), mPFC$^{CRH}$ cells were active during retreat episodes (Fig. S6D). In addition, we separated the behavioral episodes and calcium recordings according to the outcome of the test (winner or loser). As expected, the winner mice pushed more and retreated less than looser mice (Fig. S6E). However, the duration of push, resist and retreat was similar between winners and losers (Fig. S6F-H). The frequency and amplitude of calcium events was also similar (Fig. S6I-J). Finally, we compared the PSTHs and found that push episodes were associated with less activity in losers compared to winners (Fig. S6K). The response to resist episode was similar (Fig. S6L). Finally, during retreat episode the calcium response of winners were transient while the one of losers was sustained (Fig. S6M). Overall, these results show that the CRH$^{+}$ cell activity in losing mice decreases during the push phase compared to winning mice but increases during the retreat phase (Fig. S6N-P).

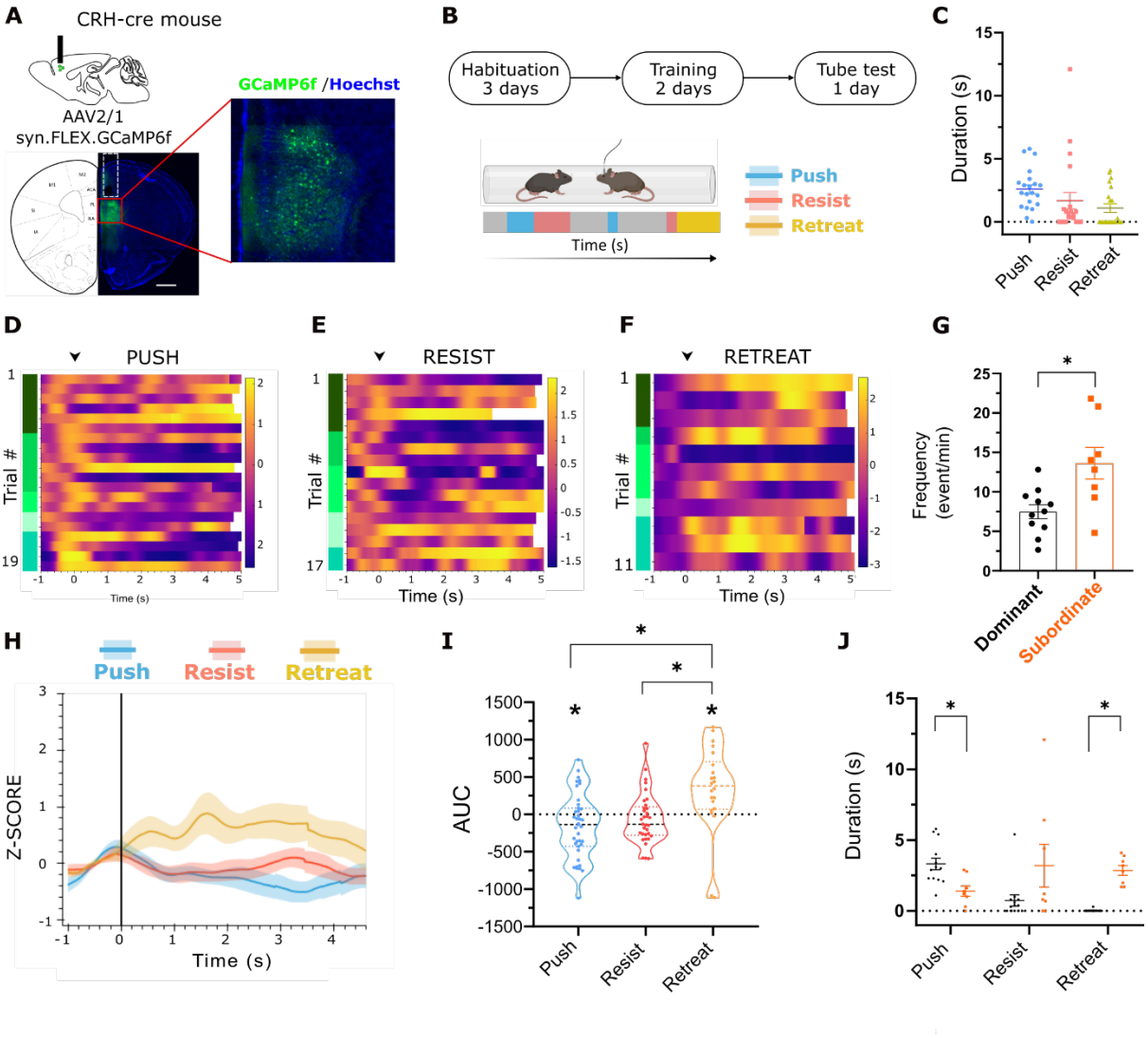


**Figure 13: mPFC$^{CRH}$ cells are active during retreat.**

**A.** *Crh-Cre* mice injected in mPFC with AAV2/1 Syn.GCaMP6f and implanted with an optical ferrule above mPFC. Scale bar: 1 mm **B.** Experimental timeline and schematic of the behavior. **C.** Duration of each behavior (5 mice). Nested *t* test: push vs. resist, $p = 0.35$; push vs. retreat, $p = 0.1$; resist vs. retreat, $p = 0.45$. Each point is one trial. **D-F.** Heatmap of z-score aligned at the onset of push (D), resist (E) and retreat events (F). Each line is a trial grouped by mouse (green bars on the left, 5 mice). **G.** Frequency of calcium events. Nested *t* test: $p = 0.02$. **E.** Amplitude of calcium events. Nested *t* test: $p = 0.5$. Each point is one trial. 4 dominant and 4 subordinate. **H.** Peri-stimulus time histograms of the z-score during each behavior. **I.** Area under the curve (AUC). One-sample nested *t* tests

compared to 0: $p$ = 0.02, $p$ = 0.3 and $p$ = 0.01. Nested $t$ tests: push vs. resist, $p$ = 0.3; push vs. retreat, $p$ = 0.04 and resist vs. retreat, $p$ = 0.01. **J.** Duration of push, resist and retreat. Nested $t$ tests: $p$ = 0.03, 0.1, 0.0008. For the entire figure, bar graphs represent mean ± S.E.M.

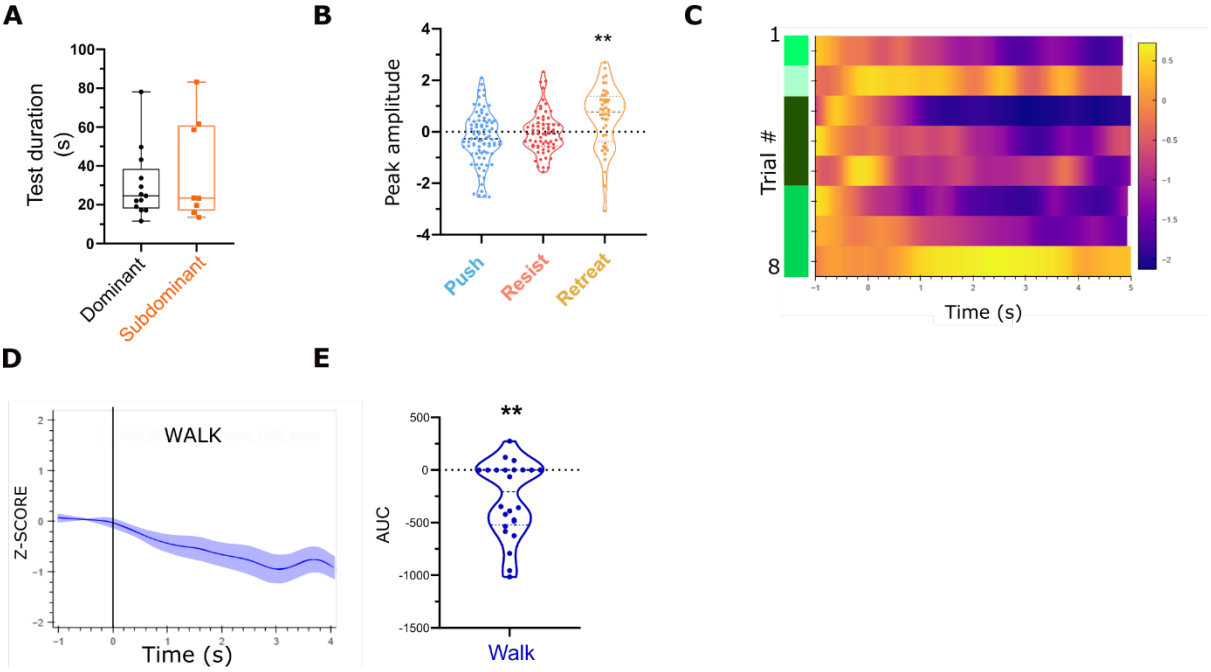


**Figure S5 related to Figure 4: mPFC$^{CRH}$ cells are active during retreat.**

**A.** Test duration for dominant and subordinate mice. Each point represents one observation. Nested $t$ test: $p$ = 0.6. **B.** Average peak amplitudes during push, resist and retreat events. Each point represents one calcium event. One-sample nested $t$ tests compared to 0: $p$ = 0.07, 0.8 and 0.004. **C.** Heatmap of z-score when the mouse walks alone in the tube. Green bars on the left represent different mice (4 mice). **D.** Peri-stimulus time histogram when mice are walking alone through the tube (4 mice, mean ± S.E.M). **E.** Area under the curve during walking. Each point is one observation. One-sample nested $t$ test compared to 0: $p$ = 0.001.

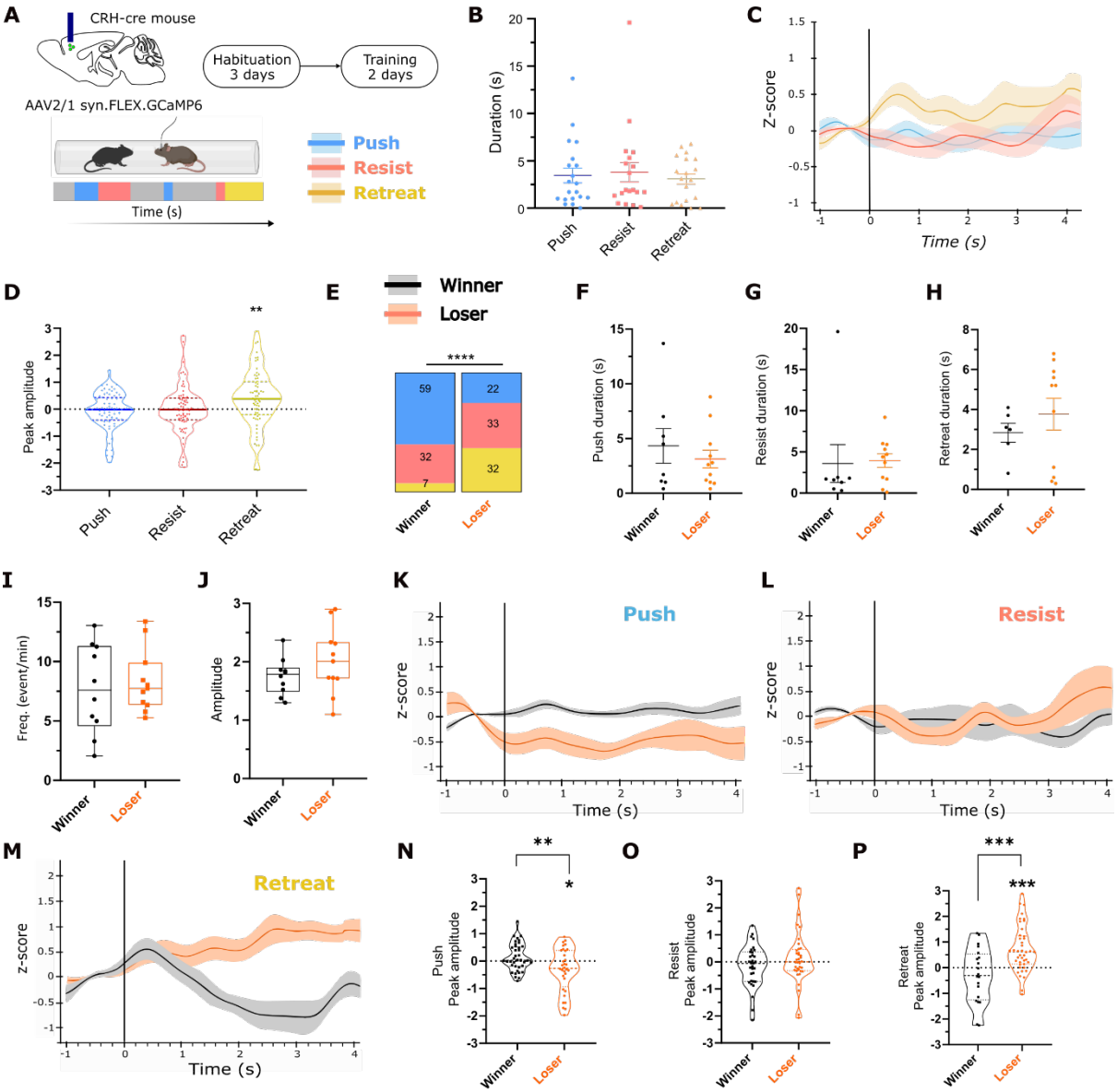


**Figure S6 related to Figure4: mPFC$^{CRH}$ cells of subordinate mice respond more during retreat than mPFC$^{CRH}$ cells of dominant mice.**

**A.** *Crh-Cre* mice injected in mPFC with AAV2/1 Syn.GCaMP6f and implanted with an optical ferrule above mPFC. A novel stimulus mouse from a different cage was presented to the test mouse. The outcome of the test determined whether the mouse was dominant or subordinate. **B.** Duration of push, resist and retreat behaviors. **C.** Peri-stimulus time histogram of z-score signals (6 mice). **D.** Average peak amplitudes during push, resist and retreat events. One-sample nested *t* tests compared to 0: $p$ = 0.3, 0.9, 0.005. **E.** Distribution of push, resist and retreat behaviors (3 winner mice and 3 loser mice). $\chi 2$ tests, $p$ = 0.0001. **F-H.** Duration of push (F), resist (G) and retreat (H)

behaviors. Each point is one trial, 3 mice per group. Nested t tests winner vs loser mice: $p$ = 0.8, 0.9 and 0.4. **I.** Frequency of calcium events. Nested $t$ test, $p$ = 0.7. **J.** Peak amplitude of calcium events. Nested $t$ test, $p$ = 0.5. **K-M.** Peri-stimulus time histograms of z-score signals during push (K), resist (L), retreat (M). **N-P.** Peak amplitude of calcium recording during push (N), resist (O) and retreat (P). One-sample $t$ tests compared to 0: push $p$ = 0.08 and 0.01 resist $p$ = 0.3 and 0.4 and retreat $p$ = 0.2 and $p < 0.0001$. Unpaired t tests between winner vs loser mice: push $p$ = 0.003, resist $p$ = 0.2 and retreat $p$ = 0.0002. For the entire figure, bar graphs represent mean ± S.E.M.

### mPFC$^{CRH}$ neurons promote social submission.

We used a chemogenetic silencing approach to test the function of mPFC$^{CRH}$ cells. Every mouse in a cage of four *Crh-Cre* male mice were injected with a Cre-dependent AAVs expressing an inhibitory DREADD tagged with mCherry (iDREADD) in PFC (Fig. 14A). We tested each pair of mice every day for the tube test until we obtained a stable ranking for 4 consecutive days. We then proceeded to inject the mouse ranked #2 or #3 with Clozapine-N-oxide (CNO) while the other three mice received saline and then tested each pair 30 min, 1.30h, 3h, 6h and 24h after injection (Fig. 14B). Injecting CNO increase the rank in 6/9 mice and the increase in ranking was maximal 3-6 hours following the injection (Fig. 14C-D). Then, we analyzed tube test behaviors before and after CNO injection. Because CNO injection changed the average test duration (Fig. 14E), we plotted the percentage of time for each behavior rather than absolute duration. We observed an increase in the number of pushes and their duration as well as in the proportion of the time pushing back (Fig. 14F-I). Besides, the decrease in the proportion of time spent retreating (Fig. 14K), consistent with the fact that CNO injection increase the mouse ranking. Saline injections on the other hand did not affect the behavioral parameters (Fig. 14L-Q). We also tested the effect of silencing mPFC$^{CRH}$ cells during the resident-intruder test of aggression and saw no effect (Fig. S7). Our previous characterization of these cells showed that chemogenetic silencing had no impact on locomotion or anxiety (Chapter

2, Figure S2 (1)) Overall, our results show that mPFC$^{CRH}$ cells contribute to social submission without affecting social aggression.

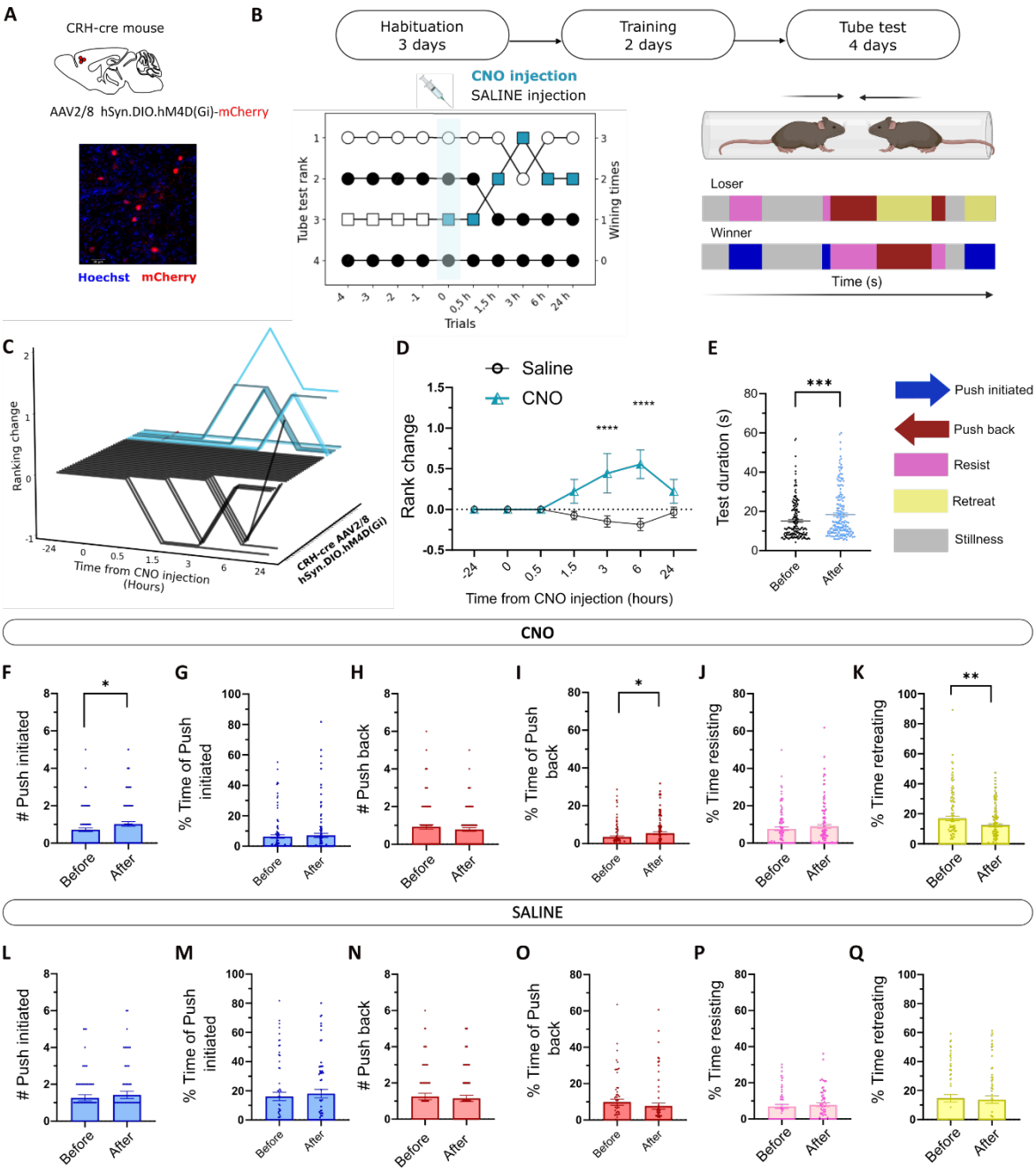


**Figure 14: CRH cells are necessary for social submission on rank male mice.**

**A.** *Crh*-Cre mice injected in mPFC with AAV2/8 hSyn.DIO.hM4D(Gi)-mCherry (iDREADD). Below, immunohistochemistry image showing viral expression in the mPFC. Scale bar: 30 µM. **B.** Schematic

of the experimental protocol with an example of a stable ranking five days in a row and consecutive trials after the injection. **C.** Rank change following 5 mg/kg CNO or saline injection. Each line represents a different mouse that showed change in the rank. **D.** Average rank change after CNO or saline injection of *Crh*-Cre mice. Two-way ANOVA: F (injection x time)$_{7,260}$ = 7.5 $p$ < 0.0001, F(injection)$_{1,260}$ = 40.9 $p$ < 0.0001 and F(time)$_{7,260}$ = 1.8 $p$ = 0.07 followed with Bonferroni multiple comparisons post-hoc tests: saline vs. CNO at 0h $p$ = 0.9, 30 min $p$ = 0.9, 1h30 $p$ = 0.05, 3h $p$ < 0.0001, 6h $p$ < 0.0001 and 24h $p$ = 0.02. **E.** Test duration before and after CNO injection. Each point represents one trial. Paired $t$ test: $p$ = 0.0002 **F-K.** Tube test behaviors before and after CNO injection. Each point is one tube test trial. Number (F) and proportion (G) of pushes initiated. Paired $t$ tests: $p$ = 0.02 and $p$ = 0.5. Number (H) and proportion of pushes back (I). Paired $t$ tests: $p$ = 0.3 and $p$ = 0.02. Percentage of time resisting (J). Paired $t$ test: $p$ = 0.3. Percentage of time retreating (K). Paired $t$ test: $p$ = 0.001. **L-Q.** Tube test behaviors before and after CNO injection. Paired $t$ tests: $p$ = 0.3, 0.5, 0.1, 0.3, 0.5 and 0.4. For the entire figure, bar graphs represent mean S.E.M

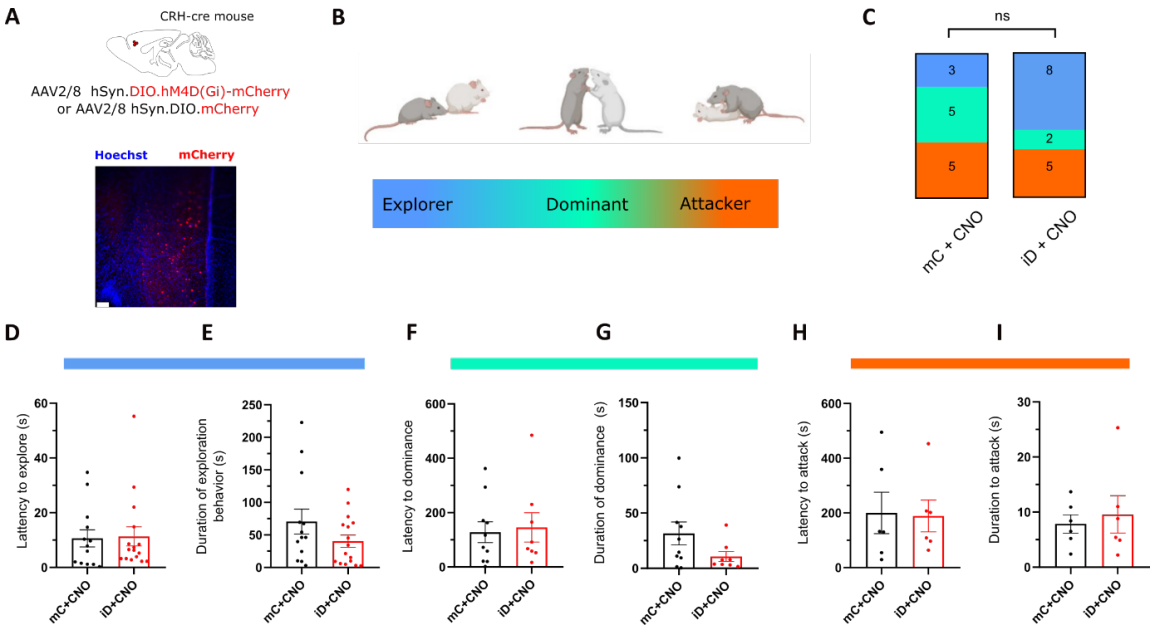

**Figure S7 related to Figure 5: mPFC$^{CRH}$ cells do not regulate social aggression.**

**A.** Top, *Crh*-Cre mice injected in mPFC with AAV2/8 hSyn.DIO.hM4D(Gi)-mCherry (iDREADD) or AAV2/8 hSyn.DIO.mCherry. Bottom, immunohistochemistry image showing viral expression in the mPFC. Scale bar: 100 µM. **B.** Schematic of the exploration, dominance and attack behaviors during resident-intruder test **C.** Number of mice exhibiting only social exploration (blue), social dominance but no aggression (green), or social aggression (at least one biting attack, orange). χ2 tests: $p = 0.2$. **D.** Latency to explore, p = 0.8. **E.** Duration of exploration behavior. Unpaired *t* test: $p = 0.1$. **F.** Latency to dominance behavior. Unpaired *t* test: $p = 0.6$. **G.** Duration of dominance behavior. Unpaired *t* test: $p = 0.1$. **H.** Latency to attack. Unpaired *t* test: $p = 0.5$. **I.** Duration of attack. Unpaired *t* test: $p = 0.8$. For the entire graph, each point is one mouse and bar graphs represent mean S.E.M.

## mPFC$^{CRH}$ cells promote social submission through the release of GABA and CRH.

mPFC$^{CRH}$ cells express GABA and CRH peptides (Chapter 2, Fig. S1 E-H (1). We previously showed the importance of CRH release to LS to suppress social interaction with familiar mice, but the identity of the neurotransmitter released from these cells to promote social submission remains unclear. To tackle with this question, we leveraged shRNAs to silence the expression of *vGAT* or *Crh* and therefore impair GABA or CRH release from mPFC$^{CRH}$ cells. Having previously established the efficiency of shRNAs (Chapter 2, Fig. 4A-B (1) we used the tube test to measure social hierarchy in cages of four *Crh*-Cre male mice every day until a stable ranking was obtained for 4 consecutive days. The mouse ranked #3 was subsequently injected with a Cre-dependent AAV expressing a shRNA against *vGAT* or *Crh* while mice ranked #1, #2 and #4 were injected with Cre-dependent AAVs expressing scramble shRNAs (Fig. 15A- 7A). Two days after the surgery, we resumed the daily testing the mice social ranking.

shRNA-mediated silencing of *vGAT* caused all mice to go up in ranking. Two mice moved up to second place and maintained their position, while the other eventually even moved up to first place (Fig. 15B). The increase in ranking was maximal 4 days after AAV expression, which is consistent with the fast expression pattern of shRNA under control of U6 promoters (177) Fig. 15C). We analyzed the mice tube test behavioral parameters before and after mice expressed the shRNA against *vGAT* and observed a significant increase in the number and proportion of pushes as well as a tendency for a decrease in the proportion of time spent retreating is observed (Fig. 15E-J), reminiscent of the chemogenetic silencing results. In contrast, mice injected with the scramble shRNA showed a decrease in the proportion of the pushes back with no changes in other parameters (Fig. 15J-O). These results indicate GABA release from $mPFC^{CRH}$ cells promotes social submission.

Following shRNA-mediated silencing of *Crh*, 3 of 5 mice increased their rank while the other remain at the same rank (5 cages, Fig. 16B). The increase in ranking was maximal 2 days following AAV injection (Fig. 16C). The behavioral parameters before and after revealed an increase in the number and the proportion of the pushes initiated accompanied with a decreased tendency in the time spent retreating (Fig. 16E-J). In contrast, mice injected with the scramble shRNA did not change behavioral (Fig. 16J-O). These results indicate that CRH release from $mPFC^{CRH}$ cells also facilitates social submission.

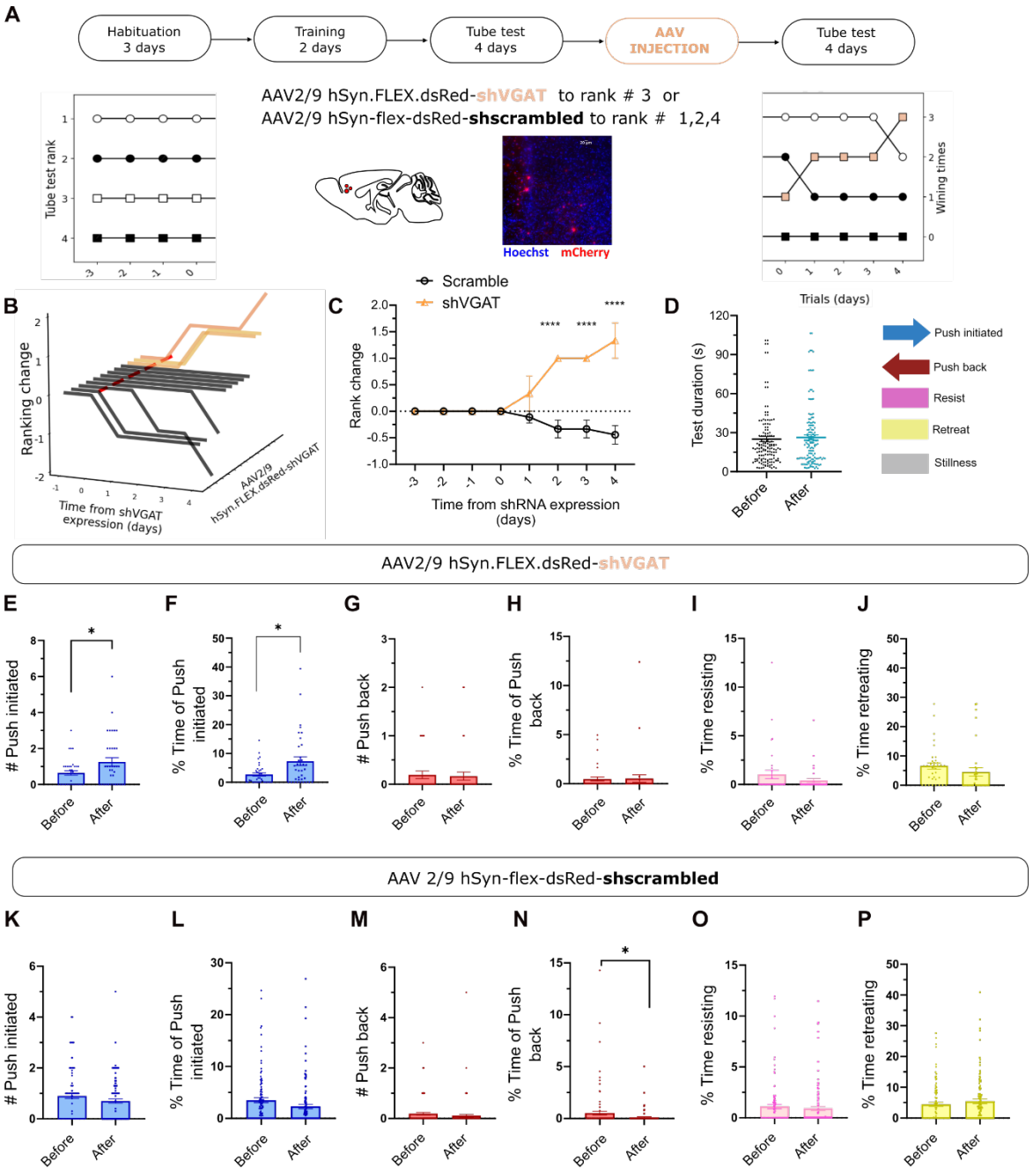


**Figure 15: GABA release from mPFC$^{CRH}$ neuros promotes social submission.**

**A.** Experimental protocol. After obtaining a stable ranking, mouse #3 received *Crh*-Cre mice received an injection of AAV2/9 hSyn.FLEX.dsRed-shVGAT in mPFC while mice #1, 2 and 4 received AAV2/9hSyn-flex-dsRed-shscrambled. **B.** Rank change following viral injection. Each line is one mouse. **C.** Average rank changes mice following viral injection. Two-way ANOVA: F (group x time)$_{7,70}$ =16.3, $p$ < 0.0001; F(group)$_{1,10}$ = 22.2, $p$ = 0.0008; F(time)$_{7,70}$ = 4.1, $p$ = 0.0008 followed with

Bonferroni multiple comparisons post-hoc tests comparing anti-*vgat* to Scrambled at day 1 $p = 0.3$, day 2 $p < 0.0001$, day 3 $p < 0.0001$, day 4 $p < 0.0001$. **D.** Test duration before and after AVV injection. Each point represents one trial. Paired *t* test: $p = 0.6$. **E-J.** Tube test behaviors before and after injection of an AAV expressing the anti-*vgat* shRNA. Each point is one tube test trial. Number (E) and duration (F) of pushes initiated. Paired *t* tests: $p = 0.01$ and $p = 0.01$. Number (G) and duration of time spent pushing back (H). Paired *t* tests: $p = 0.8$ and $p = 0.7$. Time spent resisting (I). Paired *t* test: $p = 0.2$. Time spent retreating (J). Paired *t* test: $p = 0.01$. **J-O.** Tube test behaviors before and after injection of an AAV expressing a scrambled shRNA. Paired t tests: $p = 0.08$, 0.0007, 0.2, 0.1, 0.5 and 0.3. For the entire figure, bar graphs represent mean S.E.M.

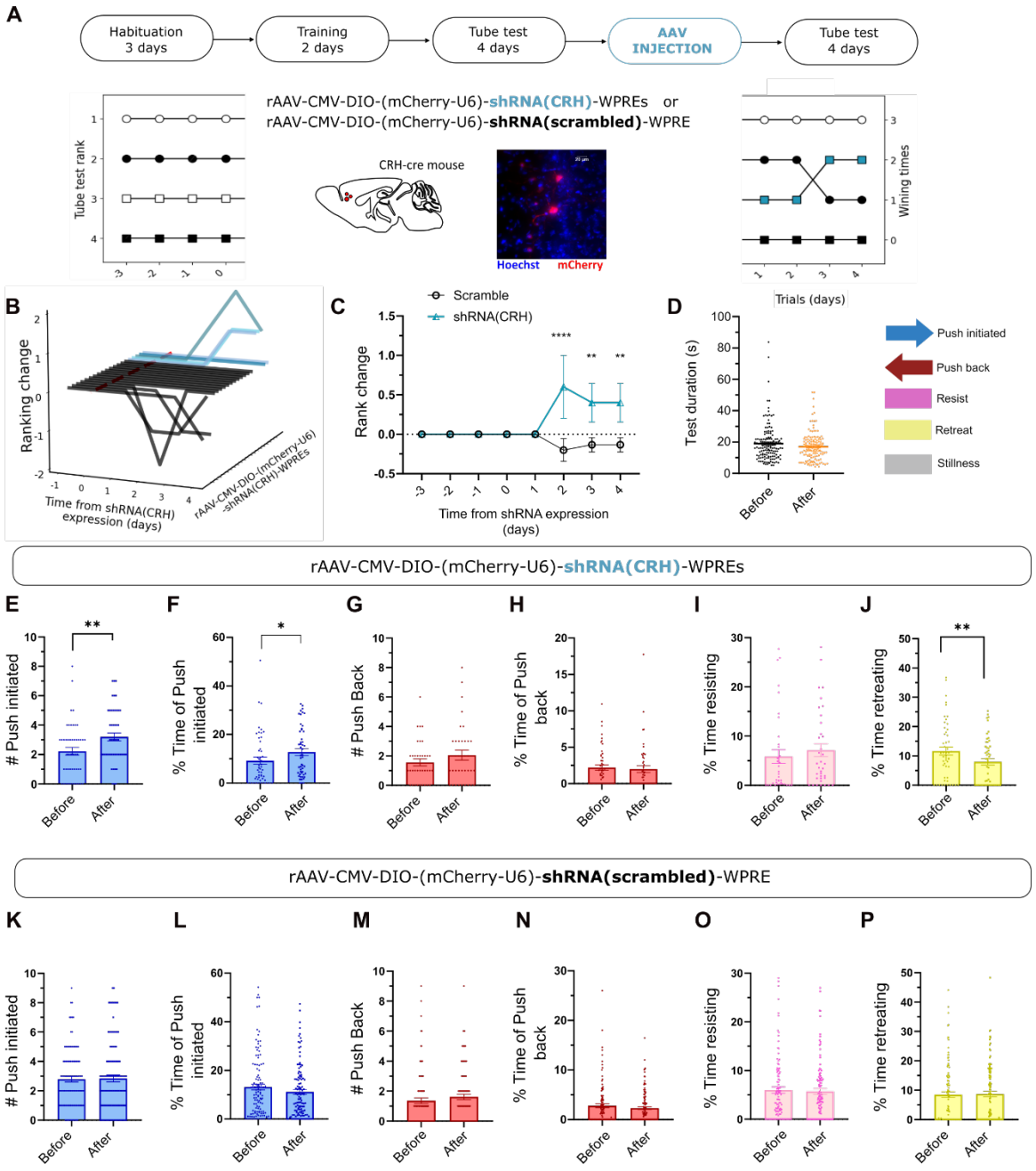


**Figure 16: CRH release from mPFC$^{CRH}$ neuros promotes social submission.**

**A.** Experimental protocol. After obtaining a stable ranking, mouse #3 received *Crh*-Cre mice received an injection of rAAV-CMV-DIO-(mCherry-U6)-shRNA(CRH)-WPREs in mPFC while mice #1, 2 and 4 received rAAV-CMV-DIO-(mCherry-U6)-shRNA(scrambled)-WPRE. **B.** Rank change following viral injection. Each line is one mouse. **C.** Average rank changes mice following viral injection. Two-way

ANOVA: F(virus x time)$_{7,126}$ = 3.5, $p$ = 0.001*;* F(group)$_{1,18}$ = 7.8, $p$ = 0.01; F(Time)$_{7,126}$ = 0.7, $p$ = 0.6 followed with Bonferroni multiple comparisons post-hoc tests comparing anti-*Crh* to Scrambled at day 1 *p = 0.9,* day *p = 0.9*, day 3 $p$ < 0.0001, day 4 $p$ = 0.06. **D.** Test duration before and after AVV injection. Each point represents one trial. Paired *t* test: $p$ = 0.2 **E-J.** Tube test behaviors before and after injection of an AAV expressing the anti-*Crh* shRNA. Each point is one tube test trial. Number (E) and duration of pushes initiated (F). Paired *t* tests: $p$ = 0.03 and $p$ = 0.3. Number (G) and duration of time spent pushing back (H). Paired *t* tests: $p$ = 0.2 and $p$ = 0.8. Time spent resisting (I). Paired *t* test: $p$ = 0.4. Time spent retreating (J). Paired *t* test: $p$ = 0.04. **K-P.** Tube test behaviors before and after injection of an AAV expressing a scrambled shRNA. Paired t tests: $p$ = 0.8, 0.05, 0.2, 0.8, 0.4 and 0.7. For the entire figure, bar graphs represent mean S.E.M.

## mPFC$^{CRH}$ neurons promote retreat during the tube test

How can mPFC$^{CRH}$ cells promote social submission? Fiber-photometry recordings revealed that the neurons are active during retreat, so we leveraged optogenetics to stimulate them during the tube test. Cages of four *Crh*-Cre mice received mPFC bilateral injections of a Cre-dependent AAV expressing Channelrhodopsin-2 (ChR2) tagged with YFP (Fig. 17A). One week later, an optical ferrule was implanted above the injection site and mice were habituated to the patch cord and empty tube. Each pair of mice was tested daily until a stable hierarchy formed for four consecutive days. First, one mouse was plugged to the patch-cord with the laser off and tested against the other 3 mice. The next day we plugged another mouse and ran it against the others. We repeated this daily until all 4 mice from the cage had performed with the laser off. We observed no changes in ranking with the laser off and proceeded to apply the 20 Hz stimulation during the entire duration of each tube test. Analysis of the tube test behaviors with or without light indicated that light application had no effect on the duration of the test (Fig. 17B), the time spent pushing (Fig. 17C) and the time spent

resisting (Fig. 17D). However, turning on the light increased the time spent retreating (Fig. 17E). When comparing the effect of laser stimulation between winner or loser mice as determined by each encounter (Fig. S8A-C) or across social rank (Fig. S8D-E), we saw that the increase in retreat was driven by all mice, independent of their rank or trial outcome.

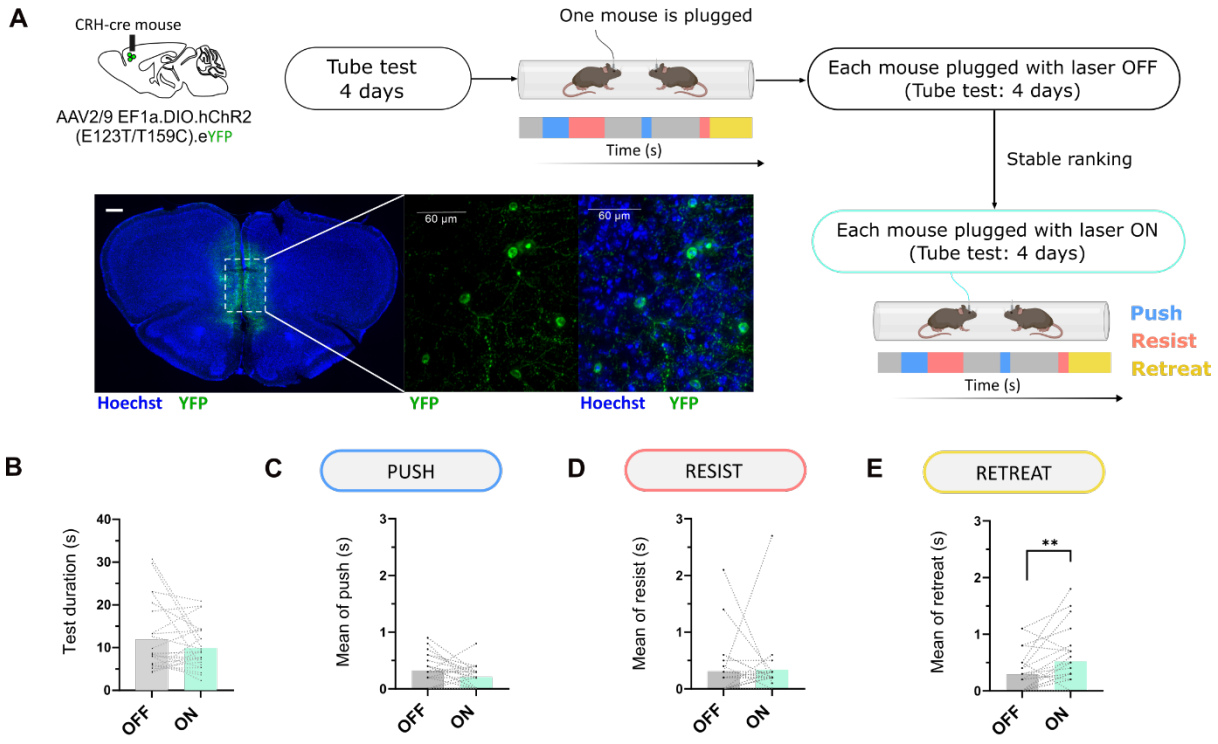


**Figure 17: PFC$^{CRH}$ cells promote retreat during tube test.**

**A.** Schematic of the protocol. *Crh*-Cre mice injected with AAV2/9EF1a.DIO.hChR2 (E123T/T159C). eYFP in mPFC. Scale bar: 500 µm. One mouse is connected to a patch-cord with the laser off and tested against three others, repeating daily until all four mice were tested. No changes in ranking were observed with the laser off. Subsequently, 20 Hz stimulation is applied during testing, following the same procedure, with each mouse connected to a patch-cord and tested against the others. **B.** Test duration. Paired *t* test, $p = 0.1$. **C-E.** Tube test behaviors with or without light. Paired t tests: $p = 0.009$, $p = 0.9$ and $p = 0.05$. For the entire figure: each point is one tube test trial (8 mice) and bar graphs represent mean S.E.M.

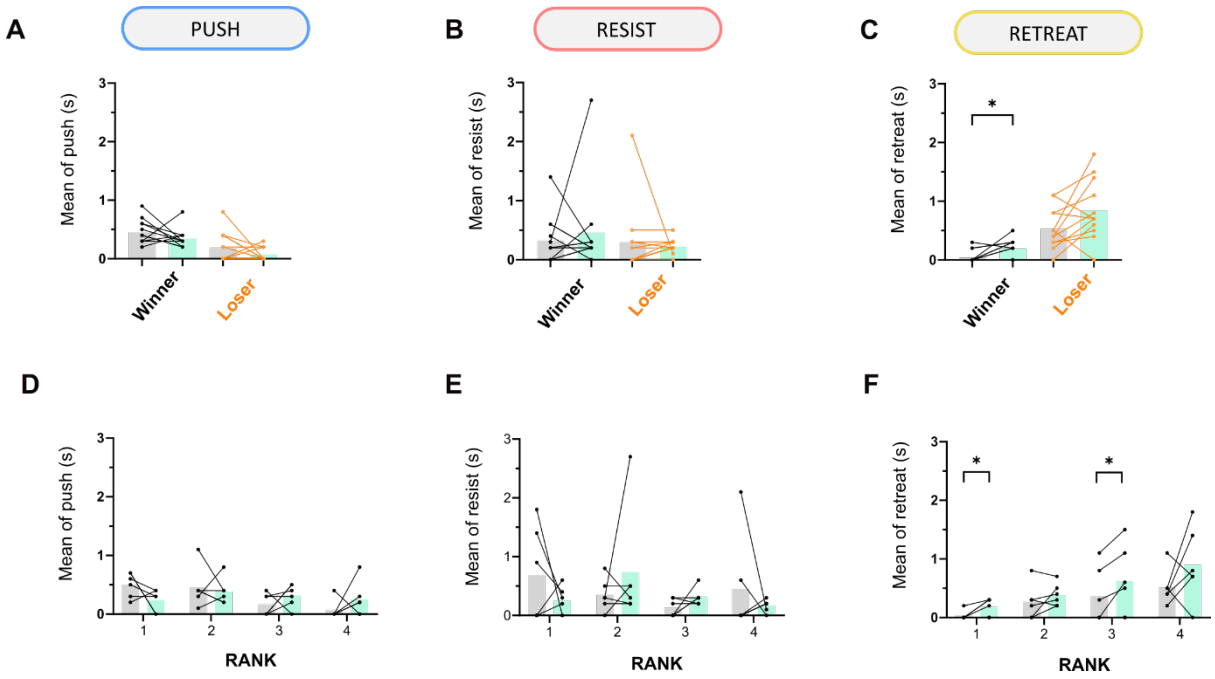


**Figure S8 related to Figure 8: mPFC$^{CRH}$ cells promote retreat during tube test.**

**A-C.** Tube test behaviors for winners and losers. Paired *t* tests: $p = 0.02$, $p = 0.05$, $p = 0.6$, $p = 0.6$, $p = 0.2$ and $p = 0.1$. **D-F.** Tube test behaviors for each social rank. Paired *t* tests for push: $p = 0.1$, 0.7, 0.3 and 1 (D). Paired *t* tests for resist: $p = 0.2$, 0.4, 0.1 and 0.4 (E). Paired *t* tests for retreat: $p = 0.04$, 0.2, 0.04 and 0.2 (F). For the entire figure: each point is one tube test trial (8 mice) and bar graphs represent mean S.E.M.

## Discussion

We found that mPFC$^{CRH}$ cells exhibit significant activation in dominance-related contexts, particularly during bouts in the tube test. Interestingly, these cells show distinct activation patterns based on the behavioral parameters throughout the test. CRH$^{+}$ cells were more active during retreat episodes and inhibited during pushing episodes. This is consistent with a reduction, but not complete elimination, of retreat behaviors when mPFC$^{CRH}$ cells were silenced through chemogenetic methods. This suggests a direct correlation between mPFC$^{CRH}$ activity and submissive behaviors. The

same pattern persisted even when the bouts involved novel mice, further supporting the link between mPFC$^{CRH}$ activity and submissiveness.

Additionally, inhibiting CRH signaling in the mPFC led to an increase in social hierarchy status, characterized by a decrease in retreat time and an increase in pushing episodes. Both reducing neuronal transmission and genetically knocking out mPFC$^{CRH}$ expression resulted in an upward shift in hierarchy, with the maximum effect on social hierarchy observed two trials after CRH silencing. However, the impact on hierarchy changes was 100% when GABA release was impaired, compared to 60% (3 out of 5 mice) in genetically modified mPFC shRNA (CRH) mice. In contrast, optogenetic stimulation of mPFC$^{CRH}$ cells in ranked mice significantly increased the time spent retreating, an effect observed consistently across all mice, regardless of their social rank or outcomes in previous encounters.

Overall, these findings demonstrate a clear association between mPFC$^{CRH}$ neuronal activity and submissive behaviors during the tube test. The activation of these cells promotes retreat behavior, while their inhibition enhances social hierarchy. These results highlight the crucial role of PFC$^{CRH}$ neurons in regulating social dominance and underscore the importance of the mPFC in modulating submissive behaviors.

## Material and methods

### Key resources table

| REAGENT or RESOURCE | SOURCE | IDENTIFIER |
|---|---|---|
| **Antibodies** | | |
| Anti-c-Fos antibody produced in rabbit | Abcam | #ab190289 |
| Anti-GFP antibody produced in chicken | AVES Labs | #GFP-1020<br>RRID: AB_10000240 |
| Anti-GFP polyclonal antibody, Alexa Fluor 488 | Thermo-Fisher Scientific | #A21311 |
| Goat anti-rabbit IgG (H+L) secondary antibody, Alexa Fluor 568 conjugate | Thermo-Fisher Scientific | #A11011;<br>RRID: AB_143157 |
| **Chemicals** | | |
| CNO | Cayman Chemical | #16882 |
| **Experimental models: Organisms/strains** | | |
| C57BL/6J Mus musculus | Jackson Laboratories | RRID:<br>IMSR_JAX:000664 |
| B6(Cg)-Crh$^{tm1(cre)Zjh/J}$ | Jackson Laboratories | RRID:<br>IMSR_JAX:012704 |
| B6.Cg-Gt (ROSA)26Sor$^{tm9(CAG-tdTomato)Hze/J}$ | Jackson Laboratories | RRID:<br>IMSR_JAX:007909 |
| **Recombinant DNA** | | |
| AAV2/9 EF1a.DIO.hChR2(E123T/T159C).eYFP | Addgene | #35505-AAV9 |
| AAV2/8 hSyn.DIO.hM4D(Gi)-mCherry | Addgene | #44362-AAV8 |
| AAV2/8 hSyn.DIO.mCherry | Addgene | #50459-AAV8 |
| AAV2/1 syn. FLEX.GCaMP6f.WPRE.SV40 | Addgene | #100833-AAV1 |
| AAV2/9 CMV-DIO-(mCherry-U6)-shRNA(anti-Crh) | Brain VTA | #PT-2787 |
| AAV2/9 CMV-DIO-(mCherry-U6)-shRNA(scrambled) | Brain VTA | #PT-2788 |
| AAV2/9 hSyn.FLEX.dsRed-sh vGAT | Addgene | #67845 |

| | | |
|---|---|---|
| AAV 2/9 hSyn-flex-dsRed-shscrambled | Addgene | #71383 |
| Software | | |
| PRISM 8 | GraphPad | 8.0.1 |
| Microsoft Office Word | Microsoft | 2019 16.56 |
| Microsoft Office Excel | Microsoft | 2019 |
| Inkscape | | 1.1 |
| FIDJI | GPL v2 | 2.3.0/1.53f |
| Python | | 3.10.2 |
| Guppy | Lerner Lab | 1.1.4 |
| Leica Application Suite X | Leica | v3.7.4 |
| ANY-maze | Stoelting Co. | 4.99 |
| Doric Neuroscience Studio | Doric | 5.4.1.23 |

**Virus injections**

For all injections, animals were anesthetized using isoflurane and given analgesics. A craniotomy was performed above the target region and a glass pipette was stereotaxically lowered down the desired depth. Injections were performed using a nano-inject II (Drummond Scientific). 23 nL were delivered 10 seconds apart until the total amount was reached. The pipette was retracted after 5 min. With homozygous animals (Crh-Cre mice), the injection of the virus expressing DREADD, shRNA (anti-Crh) was in subdominants (third or fourth place) and its control viruses (fluorophore only) in dominants (first or second place). Injection coordinates were the following (in mm from Bregma): AP: 1.65, ML: ±0.1, DV: -2.6. Injections were done bilaterally with 100 nl injected per site. We injected AAV2/8 hSyn.DIO.hM4D(Gi)-mCherry (Addgene #44362-AAV8), AAV2/8 hSyn.DIO.mCherry (Addgene #50459-AAV8), AAV2/1 syn.FLEX.GCaMP6f.WPRE.SV40 (Addgene #100833-AAV1), AAV2/9 CMV-DIO-(mCherry-U6)-shRNA(anti-Crh) (VTA brain) and AAV2/9 CMV-DIO-(mCherry-U6)-shRNA(scrambled) (VTA brain), AAV2/9 hSyn.FLEX.dsRed-shVGAT (Addgene #67845) and AAV 2/9

hSyn-flex-dsRed-shscrambled (Addgene #71383) into the mPFC of Crh-Cre mice. Viruses expressed for a minimum of 2 weeks.

**Optical ferrule implants**

Animals were anesthetized using isoflurane and given analgesics. The scalp was removed, and we applied Vetbond™ (3M™ #7000002814) along the cut. A craniotomy was performed above the target region and the optical ferrule was lowered until the desired depth. Superglue was applied to hold the lens in position and then dental cement (GC FujiCEM 2) was applied to cover the exposed skull and keep the optical ferrule in position. Animals were allowed to recover for at least 2 days before being used. For fiber photometry recording of $PFC^{CRH}$ cells in the right hemisphere we implanted the optical ferrule (B280-4419-3, Doric) at the following coordinates: AP: 1.65, ML: 0.1, DV: -2.4.

**Immunohistochemistry (IHC)**

Mice were anesthetized using isoflurane then perfused in the heart with 10 mL saline and their brains were quickly extracted and incubated in 4% PFA overnight. After 1 h washing in PBS, 60 µm slices were prepared using a Leica VT1000S vibratome (Leica Biosystems). The slices were incubated overnight at 4°C with primary antibodies diluted in PBS with 0.5% Triton-X in PBS. Then, the slices were incubated overnight at 4°C with secondary antibodies from Thermo-Fisher Scientific at a concentration of 1:500 diluted in PBS with 0.1% Triton-X. Hoechst counterstain was applied (Hoechst 33342 at 1:1000 for 30 min in PBS at RT) prior to mounting the slice using fluoromount (Sigma-Aldrich). Images were acquired using inverted confocal microscopes (lsm 900, Zeiss and SPII, Leica) or an epifluorescent microscope (Thunder, Leica).

Figures 1B: For c-Fos labelling, primary incubation was performed overnight at 4°C with anti-c-Fos antibody (1:1000, Abcam, #ab190289). Secondary incubation was performed with an anti-rabbit antibody conjugated to Alexa 568 (#A11036).

Figures 1B, 3B: For tdTomato or mCherry labelling, primary incubation was performed overnight at 4°C with an anti-RFP antibody (1:500, Rockland Antibody, 600-401-379). Secondary incubation was performed with anti-rabbit antibody conjugated to Alexa 568 (#A11036).

Figures 2A For GFP or GCaMP6f labelling, incubation was performed overnight at 4°C with an anti-GFP antibody conjugated to Alexa 488 (1:500, Thermo-Fisher Scientific, #A21311).

**Fluorescence quantification in Crh-Cre;Ai9 mice**

Images were acquired using an epifluorescent microscope (Thunder, Leica). Images at 8 bits (0 to 255 intensity units/pixel) were analyzed using the software Image J. For each picture, mPFC was divided into regions. We measured the number of $CRH^+$ cells, the number of $CRH^+$ expressing c-Fos and then we calculated the ratio of CRH activation. We also counted afterwards the number of cells expressing c-Fos.

**Behavioral tests**

The observer was blind to the identity of the mice while performing the behavioral experiments and later analyses.

**Tube test**

The tube test assay was applied as described before (Fan et al., 2019). Previously, the mice were habituated and trained to go through the tube. In test days, each pair of mice was released from the two ends of a tube (30 cm in length, 3 cm in diameter), meet at the middle, and the mouse that

retreated first from the tube was appointed as the ‘‘loser.’’ Tube test trials were carried out between groups of 4 cage mates using a round robin design. The ranks were determined by total numbers of winning on each test day. Only mouse cages with stable ranks for over 4 successive days were used for chemogenetic manipulation. The different behavioral states of mice during the test trial: push (mouse initiates shoving its head under the opponent), pushback (mouse realizes a counter-push after being pushed by the opponent), resistance (hold on to their territory when being pushed) and retreat (goes backward after being pushed or voluntarily withdraw). Stillness is when the mouse has no movement. Tests were quantified using ANY maze software.

**Social interaction**

To perform this test the mice were habituated and trained to go through the tube. In test days, the experimental mouse was released from the one end of a tube (30 cm in length, 3 cm in diameter) to meet at the stimulus mouse under a pencil cup on the other side of the tube. Once the mice interacted and the experimental mouse retreated to leave the tube it was placed in a box for subsequent perfusion.

**Resident-Intruder test**

The resident–intruder paradigm was used to assess social aggression as previously described (178). Experimental male mice were individually housed for a minimum of 1 week. Intruder mice were BALB/cJ housed and used for only a single encounter per day. No intruder was used for more than three aggressive episodes. Feeding and water apparatuses were removed before habituation to allow unimpeded interaction and better recording. Ten-minute presentations of age- and weight-matched intruders occurred in the home cages of the resident mice after a one-hour habituation to the behavioral room. On the encounter where the intruder mouse attacked the resident the trial was halted, and this intruder was excluded from the study.

# CHAPTER IV

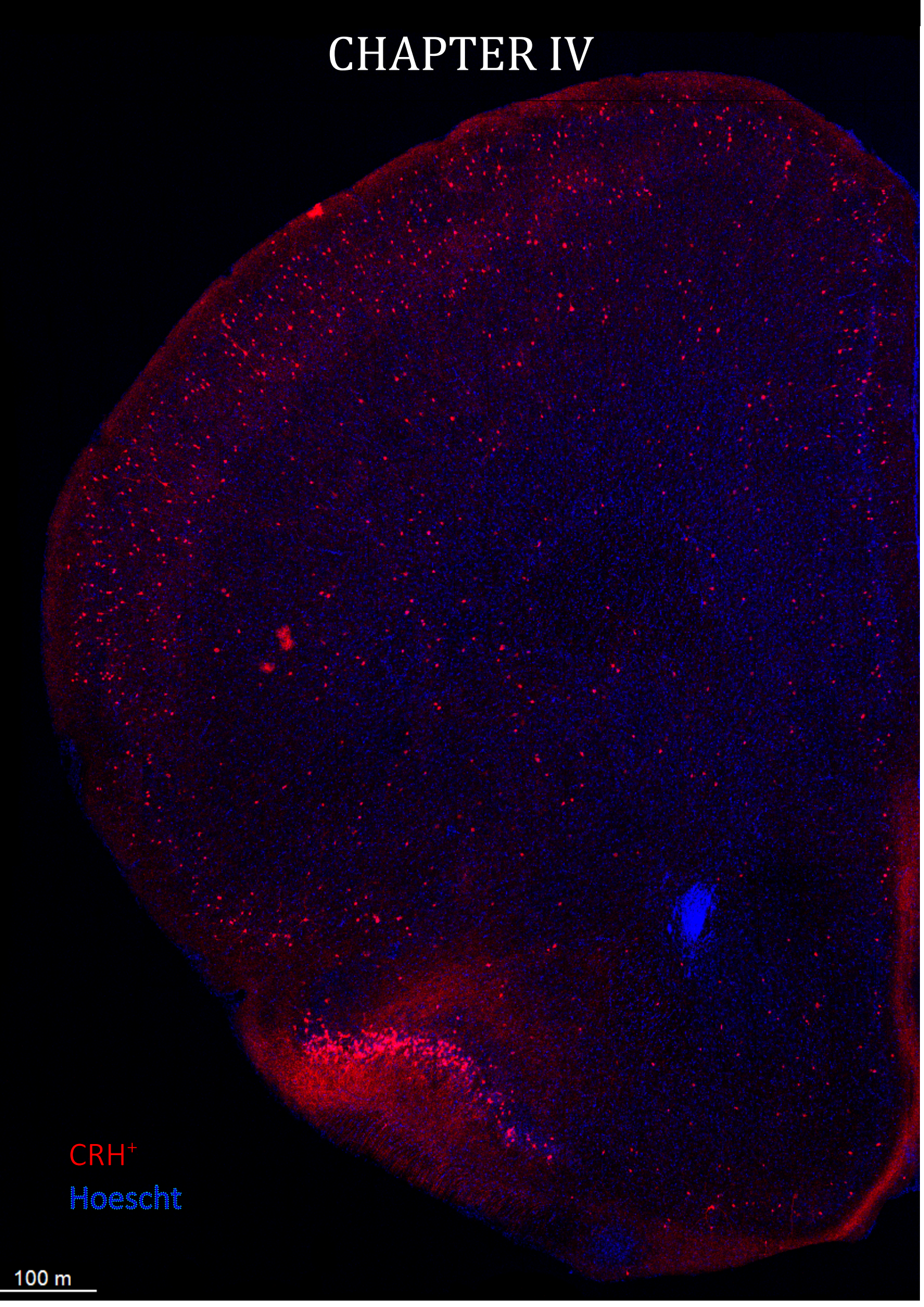

# CHAPTER IV: conclusion

## Hightlights

1. Neural circuit between ILA and rLS modulates the familiarization process, where social interaction decreases as a novel rodent becomes familiar and supports social novelty preference.
2. $mPFC^{CRH}$ neurons regulate social hierarchy, balancing submission and dominance during tube test encounters.
3. CRH-expressing neurons in the mPFC promote retreat behavior both novel and familiar peers.
4. $mPFC^{CRH}$ cells regulate social interactions by suppressing confrontation during tube test as characteristic of social submission.
5. CRH signaling in the mPFC interacts with GABAergic signaling, finely tuning social behaviors and submission-dominance dynamics.
6. The findings suggest new research avenues into neural circuits governing social dominance and submission, related to engage or avoidance in social contexts.

## Conclusions

The thesis explores the role of the CRH in regulating both familiar and novel social interactions in mice, as well as its influence on social hierarchy and submissive behaviors. The main conclusions involve:

1. $ILA^{CRH}$ cells regulate interactions with familiar and novel mice, promoting novelty preference and suppressing interactions with familiar ones, encouraging engagement with new individuals as they become familiar through changes in $ILA^{CRH}$ cell activity.

2. $ILA^{CRH}$ cells influence social novelty preference (SNP), not directly forming social memory but using this memory to regulate interactions, especially promoting engagement with novel mice during recall, as shown by disrupting their recall-phase activity.

3. $ILA^{CRH}$ cells release CRH into the rLS to disinhibit the lateral septum, reducing social interactions with familiar mice and enhancing social exploration by suppressing engagement with known individuals, promoting novelty-seeking behavior.

4. Reducing CRH expression in ILA increased social interaction with familiar mice, without affecting ILA activation, suggesting that $ILA^{CRH}$ cells use CRH to process familiarity cues and regulate social interactions based on familiarity.

5. As mice mature, their preference shifts from kin-based interactions to social novelty, regulated by the CRH circuit, which suppresses kin interactions, promoting exploration and socializing with novel conspecifics in line with adult behavioral priorities.

6. Chemogenetic silencing of $mPFC^{CRH}$ neurons during an aggression test showed no change in aggression, indicating CRH in mPFC does not regulate aggression in this context, suggesting a more specialized role in other social behaviors.

7. During the tube test, $mPFC^{CRH}$ neurons were activated, implicating them in dominance-related behaviors and social hierarchy, suggesting that these neurons influence spatial behavior in assessing social rank.

8. $mPFC^{CRH}$ neurons showed increased activity during retreat episodes (submissive behavior)

and decreased activity during pushing (dominant behavior), indicating their association with submission rather than familiarity in social interactions.

9. Silencing mPFC$^{CRH}$ neurons reduced retreat behaviors (submissiveness) but did not eliminate them, increasing social rank, which reinforces the idea that these neurons promote submission during confrontations.

10. ShRNA-induced silencing of CRH or GABA release from mPFC$^{CRH}$ neurons altered social hierarchy, increasing dominance behaviors like pushing, highlighting the critical role of GABA-CRH interactions in modulating social rank.

11. Optogenetic activation of mPFC$^{CRH}$ neurons consistently increased retreat time across all mice, indicating that activation directly promotes submissive behaviors regardless of social rank, underscoring the role of these neurons in submission.

12. mPFC$^{CRH}$ neurons regulate the balance between submission and dominance in social hierarchies, promoting retreat behaviors (submission) when activated and leading to more dominant behaviors when silenced, crucial for understanding social ranking dynamics.

13. ILA$^{CRH}$ cells may integrate diverse social cues, including sex, strain, and hierarchy, suggesting their role in mediating complex social interactions, with input from the mPFC contributing to the regulation of various social behaviors.

## Conclusiones

Esta tesis explora el papel de la hormona liberadora de corticotropina (CRH) en la regulación de

interacciones sociales tanto con individuos familiares como novedosos en ratones, así como su influencia en la jerarquía social y comportamientos de sumisión. Las principales conclusiones son:

1. Las células $ILA^{CRH}$ regulan las interacciones con ratones familiares y novedosos, promoviendo la preferencia por la novedad y suprimiendo las interacciones con los conocidos, fomentando la interacción con nuevos individuos a medida que se vuelven familiares mediante cambios en la actividad de las células $ILA^{CRH}$.

2. Las células $ILA^{CRH}$ influyen en la preferencia por la novedad social (SNP), no formando directamente la memoria social, pero utilizando esta memoria para regular las interacciones, especialmente promoviendo el compromiso con ratones nuevos durante la fase de recuerdo, como se muestra al interrumpir su actividad en la fase de recuerdo.

3. Las células $ILA^{CRH}$ liberan CRH en el rLS para desinhibir el septo lateral, reduciendo las interacciones sociales con ratones familiares y mejorando la exploración social al suprimir la interacción con individuos conocidos, promoviendo el comportamiento de búsqueda de novedad.

4. La reducción de la expresión de CRH en el ILA aumentó la interacción social con ratones familiares, sin afectar la activación del ILA, lo que sugiere que las células $ILA^{CRH}$ utilizan CRH para procesar señales de familiaridad y regular las interacciones sociales basadas en la familiaridad.

5. A medida que los ratones maduran, su preferencia cambia de las interacciones basadas en el parentesco a la novedad social, regulada por el circuito CRH, que suprime las

interacciones con los familiares, promoviendo la exploración y la socialización con conspecíficos novedosos.

6. El silenciamiento quimogenético de las neuronas mPFC$^{CRH}$ durante una prueba de agresión no mostró cambios en la agresión, lo que indica que el CRH en el mPFC no regula la agresión en este contexto, sugiriendo un papel más especializado en otros comportamientos sociales.

7. Durante la prueba del tubo, las neuronas mPFC$^{CRH}$ se activaron, implicándolas en comportamientos relacionados con la dominancia y la jerarquía social, lo que sugiere que estas neuronas influyen en el comportamiento espacial para evaluar el rango social.

8. Las neuronas mPFC$^{CRH}$ mostraron mayor actividad durante los episodios de retirada (comportamiento sumiso) y menor actividad durante los empujes (comportamiento dominante), lo que indica su asociación con la sumisión más que con la familiaridad en las interacciones sociales.

9. El silenciamiento de las neuronas mPFC$^{CRH}$ redujo los comportamientos de retirada (sumisión), pero no los eliminó, aumentando el rango social, lo que refuerza la idea de que estas neuronas promueven la sumisión durante los enfrentamientos.

10. El silenciamiento inducido por shRNA de la liberación de CRH o GABA de las neuronas mPFC$^{CRH}$ alteró la jerarquía social, aumentando los comportamientos de dominancia como los empujes, destacando el papel crucial de las interacciones GABA-CRH en la modulación del rango social.

11. La activación optogenética de las neuronas mPFC$^{CRH}$ aumentó consistentemente el tiempo de retirada en todos los ratones, lo que indica que la activación promueve directamente los comportamientos sumisos independientemente del rango social, subrayando el papel de estas neuronas en la sumisión.

12. Las neuronas mPFC$^{CRH}$ regulan el equilibrio entre sumisión y dominancia en las jerarquías sociales, promoviendo comportamientos de retirada (sumisión) cuando se activan y conduciendo a comportamientos más dominantes cuando se silencia, lo que es crucial para entender las dinámicas del rango social.

13. Las células ILA$^{CRH}$ pueden integrar diversas señales sociales, incluyendo sexo, cepa y jerarquía, lo que sugiere su papel en la mediación de interacciones sociales complejas, con la entrada del mPFC contribuyendo a la regulación de diversos comportamientos sociales.

**Future direction**

Understanding these mechanisms not only advances our knowledge of social behavior in animals but may also have implications for understanding and treating social disorders in humans. The study provides significant insights into the neural mechanisms underlying the regulation of social interactions, promoting successful approaches to exploring conspecifics. mPFC$^{CRH}$ cells play a pivotal role in decreasing social interactions with familiar mice and in avoidance behaviors in contexts of conflicts. This research enhances our understanding of the neural basis of social behavior and has potential implications for studying social behavior disorders where dominance and submissiveness have implications for the individual's adaptation.

The psychological processes of submission, social interaction, and familiarization are intricately intertwined and can be significantly affected by various mental health conditions. Individuals with social anxiety disorder (SAD), avoidant personality disorder (APD), and dependent personality disorder often exhibit submissive behaviors to avoid social situations, negative evaluations, or the need to be independent. These disorders can lead to pervasive patterns of social inhibition, feelings of inadequacy, and excessive reliance on others. Such emotional and behavioral characteristics can significantly impact an individual's ability to engage in healthy social interactions and form meaningful relationships (179,180).

Finally, attachment theory and studies on rodent social behavior both underscore the critical role of early relationships in shaping social interactions and preferences, which can have lasting effects on mental health. Attachment theory suggests that early experiences with caregivers form attachment styles that influence future relationships and behaviors; individuals with insecure attachment may struggle with social interactions, often exhibiting submissive behaviors and emotional distress. This aligns with findings in young rats and mice, which display a strong preference for maternal figures and siblings in early life, indicative of the foundational role of these relationships (132,139). As these rodents mature, their preference shifts towards novel social interactions, influenced by the maturation of the CRH circuit, which is crucial for regulating motivated behaviors (1). This dynamic mirrors how the neural circuits involved in human attachment can affect social cognition and emotion regulation. Additionally, the contrast seen in prairie voles (142), who prefer long-term partners over novel interactions, emphasizes the complexity of social preferences across species, reinforcing the idea that understanding these neural and behavioral connections is vital for addressing mental health disorders tied to attachment and social interaction challenges.

## References


1. de León Reyes NS, Sierra Díaz P, Nogueira R, Ruiz-Pino A, Nomura Y, de Solis CA, et al. Corticotropin-releasing hormone signaling from prefrontal cortex to lateral septum suppresses interaction with familiar mice. Cell [Internet]. 2023 Sep 14 [cited 2024 Sep 18];186(19):4152-4171.e31. Available from: https://pubmed.ncbi.nlm.nih.gov/37669667/
2. Vale W, Spiess J, Rivier C, Rivier J. Characterization of a 41-residue ovine hypothalamic peptide that stimulates secretion of corticotropin and beta-endorphin. Science [Internet]. 1981 [cited 2024 Sep 18];213(4514):1394–7. Available from: https://pubmed.ncbi.nlm.nih.gov/6267699/
3. Zhao Y, Valdez GR, Fekete ÉM, Rivier JE, Vale WW, Rice KC, et al. Subtype-selective corticotropin-releasing factor receptor agonists exert contrasting, but not opposite, effects on anxiety-related behavior in rats. J Pharmacol Exp Ther [Internet]. 2007 Dec [cited 2024 Sep 18];323(3):846–54. Available from: https://pubmed.ncbi.nlm.nih.gov/17855476/
4. Hostetler CM, Ryabinin AE. The CRF system and social behavior: a review. Front Neurosci [Internet]. 2013 [cited 2024 Sep 18];7(7 MAY):92. Available from: http://www.ncbi.nlm.nih.gov/pubmed/23754975
5. Schulkin J. The CRF signal: Uncovering an information molecule. The CRF Signal: Uncovering an Information Molecule [Internet]. 2017 Jan 1 [cited 2024 Sep 18];1–324. Available from: https://academic.oup.com/book/10092
6. Heinrichs SC. Modulation of social learning in rats by brain corticotropin-releasing factor. Brain Res. 2003 Dec 19;994(1):107–14.
7. Franklin TB, Silva BA, Perova Z, Marrone L, Masferrer ME, Zhan Y, et al. Prefrontal cortical control of a brainstem social behavior circuit. Nat Neurosci. 2017 Feb 1;20(2):260–70.
8. Kingsbury L, Huang S, Wang J, Gu K, Golshani P, Wu YE, et al. Correlated Neural Activity and Encoding of Behavior across Brains of Socially Interacting Animals. Cell. 2019 Jul 11;178(2):429-446.e16.
9. Lui JH, Nguyen ND, Grutzner SM, Darmanis S, Peixoto D, Wagner MJ, et al. Differential encoding in prefrontal cortex projection neuron classes across cognitive tasks. Cell. 2021 Jan 21;184(2):489-506.e26.
10. Wang F, Zhu J, Zhu H, Zhang Q, Lin Z, Hu H. Bidirectional control of social hierarchy by synaptic efficacy in medial prefrontal cortex. Science [Internet]. 2011 Nov 4 [cited 2024 Sep 18];334(6056):693–7. Available from: https://pubmed.ncbi.nlm.nih.gov/21960531/
11. Zhou T, Zhu H, Fan Z, Wang F, Chen Y, Liang H, et al. History of winning remodels thalamo-PFC circuit to reinforce social dominance. Science (1979) [Internet]. 2017 Jul 14 [cited 2024 Sep 18];357(6347):162–8. Available from: https://www.science.org/doi/10.1126/science.aak9726
12. Zhang C, Zhu H, Ni Z, Xin Q, Zhou T, Wu R, et al. Dynamics of a disinhibitory prefrontal microcircuit in controlling social competition. Neuron. 2021 Nov;
13. Noh K, Cho WH, Lee BH, Kim DW, Kim YS, Park K, et al. Cortical astrocytes modulate dominance behavior in male mice by regulating synaptic excitatory and inhibitory balance. Nat Neurosci. 2023 Sep 1;26(9):1541–54.
14. Utevsky A V., Platt ML. Status and the Brain. PLoS Biol. 2014 Jan 1;12(9).
15. Álvarez-Martínez FJ, Borrás-Rocher F, Micol V, Barrajón-Catalán E. Artificial Intelligence Applied to Improve Scientific Reviews: The Antibacterial Activity of Cistus Plants as Proof of Concept. Antibiotics [Internet]. 2023 Feb 1 [cited 2024 Sep 18];12(2). Available from: /pmc/articles/PMC9952093/
16. Pournajafi-Nazarloo H, Partoo L, Sanzenbacher L, Paredes J, Hashimoto K, Azizi F, et al. Stress differentially modulates mRNA expression for corticotrophin-releasing hormone receptors in hypothalamus, hippocampus and pituitary of prairie voles. Neuropeptides [Internet]. 2009

Apr [cited 2024 Sep 18];43(2):113–23. Available from: https://pubmed.ncbi.nlm.nih.gov/19185916/
17. Zaldivar A, Krichmar JL. Allen Brain Atlas-Driven Visualizations: a web-based gene expression energy visualization tool. Front Neuroinform [Internet]. 2014 May 21 [cited 2024 Sep 17];8(MAY). Available from: https://pubmed.ncbi.nlm.nih.gov/24904397/
18. Marsh AA, Blair KS, Jones MM, Soliman N, Blair RJR. Dominance and submission: the ventrolateral prefrontal cortex and responses to status cues. J Cogn Neurosci [Internet]. 2009 Apr [cited 2024 Sep 18];21(4):713–24. Available from: https://pubmed.ncbi.nlm.nih.gov/18578604/
19. Bicks LK, Koike H, Akbarian S, Morishita H. Prefrontal Cortex and Social Cognition in Mouse and Man. Front Psychol [Internet]. 2015 [cited 2024 Sep 16];6(NOV). Available from: /pmc/articles/PMC4659895/
20. Watanabe N, Yamamoto M. Neural mechanisms of social dominance. Front Neurosci [Internet]. 2015 [cited 2024 Sep 16];9(APR). Available from: https://pubmed.ncbi.nlm.nih.gov/26136644/
21. Kumaran D, Banino A, Blundell C, Hassabis D, Dayan P. Computations Underlying Social Hierarchy Learning: Distinct Neural Mechanisms for Updating and Representing Self-Relevant Information. Neuron [Internet]. 2016 Dec 7 [cited 2024 Sep 18];92(5):1135–47. Available from: https://pubmed.ncbi.nlm.nih.gov/27930904/
22. Noonan MAP, Sallet J, Mars RB, Neubert FX, O'Reilly JX, Andersson JL, et al. A Neural Circuit Covarying with Social Hierarchy in Macaques. PLoS Biol. 2014 Jan 1;12(9).
23. Isogai Y. Transcriptional programming of social hierarchy. Neuron [Internet]. 2024 Feb 21 [cited 2024 Sep 18];112(4):523–5. Available from: https://pubmed.ncbi.nlm.nih.gov/38387437/
24. Boyce WT. Social stratification, health, and violence in the very young. Ann N Y Acad Sci [Internet]. 2004 [cited 2024 Sep 18];1036:47–68. Available from: https://pubmed.ncbi.nlm.nih.gov/15817730/
25. Wang F, Kessels HW, Hu H. The mouse that roared: Neural mechanisms of social hierarchy. Vol. 37, Trends in Neurosciences. Elsevier Ltd; 2014. p. 674–82.
26. Sapolsky RM. The influence of social hierarchy on primate health. Science [Internet]. 2005 Apr 29 [cited 2024 Sep 18];308(5722):648–52. Available from: https://pubmed.ncbi.nlm.nih.gov/15860617/
27. Van Der Borg JAM, Schilder MBH, Vinke CM, De Vries H, Petit O. Dominance in Domestic Dogs: A Quantitative Analysis of Its Behavioural Measures. PLoS One [Internet]. 2015 Aug 26 [cited 2024 Sep 18];10(8):e0133978. Available from: https://journals.plos.org/plosone/article?id=10.1371/journal.pone.0133978
28. Trisko RK, Smuts BB. Dominance relationships in a group of domestic dogs (Canis lupus familiaris). Behaviour. 2015 Mar 20;152(5):677–704.
29. Pal SK, Ghosh B, Roy S. Agonistic behaviour of free-ranging dogs (Canis familiaris) in relation to season, sex and age. Appl Anim Behav Sci. 1998 Sep 1;59(4):331–48.
30. Cafazzo S, Valsecchi P, Bonanni R, Natoli E. Dominance in relation to age, sex, and competitive contexts in a group of free-ranging domestic dogs. Behavioral Ecology [Internet]. 2010 May 1 [cited 2024 Sep 16];21(3):443–55. Available from: https://dx.doi.org/10.1093/beheco/arq001
31. de Waal FBM. The integration of dominance and social bonding in primates. Q Rev Biol [Internet]. 1986 Dec 1 [cited 2024 Sep 16];61(4):459–79. Available from: https://pubmed.ncbi.nlm.nih.gov/3543991/
32. Fichtel C, Dinter K, Ratsoavina F. Benefits but not the dual functions of submissive signals differ between two Malagasy primates. Philosophical Transactions B [Internet]. 2024 May 20 [cited 2024 Sep 18];379(1905). Available from:

https://royalsocietypublishing.org/doi/10.1098/rstb.2023.0197
33. Terranova ML, Laviola G, de Acetis L, Alleva E. A description of the ontogeny of mouse agonistic behavior. J Comp Psychol [Internet]. 1998 [cited 2024 Sep 18];112(1):3–12. Available from: https://pubmed.ncbi.nlm.nih.gov/9528111/
34. Kudriavtseva NN, Bakshtanovskaia I V. [The neurochemical control of aggression and submission]. Zh Vyssh Nerv Deiat Im I P Pavlova [Internet]. 1991 May [cited 2024 Sep 18];41(3):459–66. Available from: https://pubmed.ncbi.nlm.nih.gov/1681631/
35. Koenig A, Larney E, Lu A, Borries C. Agonistic behavior and dominance relationships in female Phayre's leaf monkeys -- preliminary results. Am J Primatol [Internet]. 2004 Nov [cited 2024 Sep 18];64(3):351–7. Available from: https://pubmed.ncbi.nlm.nih.gov/15538761/
36. Sapolsky RM. The endocrine stress-response and social status in the wild baboon. Horm Behav [Internet]. 1982 [cited 2024 Sep 18];16(3):279–92. Available from: https://pubmed.ncbi.nlm.nih.gov/6890939/
37. Rowell TE. The concept of social dominance. Behav Biol. 1974 Jun 1;11(2):131–54.
38. Ashizuka A, Mima T, Sawamoto N, Aso T, Oishi N, Sugihara G, et al. Functional relevance of the precuneus in verbal politeness. Neurosci Res. 2015 Feb 1;91:48–56.
39. Deag JM. Aggression and submission in monkey societies. Anim Behav. 1977 May 1;25(PART 2):465–74.
40. Bernstein IS. Dominance: The baby and the bathwater. Behavioral and Brain Sciences [Internet]. 1981 [cited 2024 Sep 18];4(3):419–29. Available from: https://www.cambridge.org/core/journals/behavioral-and-brain-sciences/article/abs/dominance-the-baby-and-the-bathwater/C1CC73E4CBE20C77360D9E5CA50FA087
41. Kaufmann JH. ON THE DEFINITIONS AND FUNCTIONS OF DOMINANCE AND TERRITORIALITY. Biological Reviews [Internet]. 1983 Feb 1 [cited 2024 Sep 16];58(1):1–20. Available from: https://onlinelibrary.wiley.com/doi/full/10.1111/j.1469-185X.1983.tb00379.x
42. Barratt ES. Agonistic Behavior. International Encyclopedia of the Social & Behavioral Sciences. 2001 Jan 1;326–9.
43. Holekamp KE, Strauss ED. Aggression and dominance: an interdisciplinary overview. Curr Opin Behav Sci. 2016 Dec 1;12:44–51.
44. Tinbergen N. On aims and methods of Ethology. Z Tierpsychol [Internet]. 1963 Jan 12 [cited 2024 Sep 17];20(4):410–33. Available from: https://onlinelibrary.wiley.com/doi/full/10.1111/j.1439-0310.1963.tb01161.x
45. Verhulst S, Geerdink M, Salomons HM, Boonekamp JJ. Social life histories: jackdaw dominance increases with age, terminally declines and shortens lifespan. Proceedings of the Royal Society B: Biological Sciences [Internet]. 2014 Aug 6 [cited 2024 Sep 17];281(1791). Available from: https://royalsocietypublishing.org/doi/10.1098/rspb.2014.1045
46. Ase AR, Reader TA, Hen R, Riad M, Descarries L. Altered serotonin and dopamine metabolism in the CNS of serotonin 5-HT(1A) or 5-HT(1B) receptor knockout mice. J Neurochem [Internet]. 2000 [cited 2024 Sep 18];75(6):2415–26. Available from: https://pubmed.ncbi.nlm.nih.gov/11080193/
47. Helmy M, Zhang J, Wang H. Neurobiology and Neural Circuits of Aggression. Adv Exp Med Biol [Internet]. 2020 [cited 2024 Sep 17];1284:9–22. Available from: https://pubmed.ncbi.nlm.nih.gov/32852736/
48. Sherman GD, Mehta PH. Stress, cortisol, and social hierarchy. Vol. 33, Current Opinion in Psychology. Elsevier B.V.; 2020. p. 227–32.
49. Abbott DH, Keverne EB, Bercovitch FB, Shively CA, Mendoza SP, Saltzman W, et al. Are subordinates always stressed? A comparative analysis of rank differences in cortisol levels among primates. Horm Behav [Internet]. 2003 [cited 2024 Sep 18];43(1):67–82. Available from: https://pubmed.ncbi.nlm.nih.gov/12614636/

50. Mendonça-Furtado O, Edaes M, Palme R, Rodrigues A, Siqueira J, Izar P. Does hierarchy stability influence testosterone and cortisol levels of bearded capuchin monkeys (Sapajus libidinosus) adult males? A comparison between two wild groups. Behavioural processes [Internet]. 2014 Nov 1 [cited 2024 Sep 18];109 Pt A(Part A):79–88. Available from: https://pubmed.ncbi.nlm.nih.gov/25239540/
51. Manogue KR, Leshner AI, Candland DK. Dominance status and adrenocortical reactivity to stress in squirrel monkeys (Saimiri sciureus). Primates [Internet]. 1975 Dec [cited 2024 Sep 18];16(4):457–63. Available from: https://link.springer.com/article/10.1007/BF02382742
52. Eberhart JA, Keverne EB, Meller RE. Social influences on circulating levels of cortisol and prolactin in male talapoin monkeys. Physiol Behav [Internet]. 1983 [cited 2024 Sep 18];30(3):361–9. Available from: https://pubmed.ncbi.nlm.nih.gov/6683410/
53. Setchell JM, Smith T, Wickings EJ, Knapp LA. Stress, social behaviour, and secondary sexual traits in a male primate. Horm Behav. 2010 Nov 1;58(5):720–8.
54. Muller MN, Wrangham RW. Dominance, cortisol and stress in wild chimpanzees (Pan troglodytes schweinfurthii). Behav Ecol Sociobiol. 2004 Feb;55(4):332–40.
55. Schoof VAM, Jack KM, Carnegie SD. Rise to power: a case study of male fecal androgen and cortisol levels before and after a non-aggressive rank change in a group of wild white-faced capuchins (Cebus capucinus). Folia Primatol (Basel) [Internet]. 2011 May [cited 2024 Sep 18];82(6):299–307. Available from: https://pubmed.ncbi.nlm.nih.gov/22488354/
56. Czoty PW, Gould RW, Nader MA. Relationship between Social Rank and Cortisol and Testosterone concentrations in Male Cynomolgus Monkeys (Macaca fascicularis). J Neuroendocrinol [Internet]. 2009 [cited 2024 Sep 18];21(1):68. Available from: /pmc/articles/PMC2709846/
57. Fichtel C, Kraus C, Ganswindt A, Heistermann M. Influence of reproductive season and rank on fecal glucocorticoid levels in free-ranging male Verreaux's sifakas (Propithecus verreauxi). Horm Behav. 2007 May 1;51(5):640–8.
58. Goymann W, Wingfield JC. Allostatic load, social status and stress hormones: The costs of social status matter. Anim Behav. 2004;67(3):591–602.
59. Lynch JW, Ziegler TE, Strier KB. Individual and seasonal variation in fecal testosterone and cortisol levels of wild male tufted capuchin monkeys, Cebus apella nigritus. Horm Behav [Internet]. 2002 [cited 2024 Sep 18];41(3):275–87. Available from: https://pubmed.ncbi.nlm.nih.gov/11971661/
60. Dautzenberg FM, Hauger RL. The CRF peptide family and their receptors: yet more partners discovered. Trends Pharmacol Sci [Internet]. 2002 Feb 1 [cited 2024 Sep 18];23(2):71–7. Available from: https://pubmed.ncbi.nlm.nih.gov/11830263/
61. Bonfiglio JJ, Inda C, Refojo D, Holsboer F, Arzt E, Silberstein S. The corticotropin-releasing hormone network and the hypothalamic-pituitary-adrenal axis: molecular and cellular mechanisms involved. Neuroendocrinology [Internet]. 2011 Jul [cited 2024 Sep 18];94(1):12–20. Available from: https://pubmed.ncbi.nlm.nih.gov/21576930/
62. Inda C, Bonfiglio JJ, Dos Santos Claro PA, Senin SA, Armando NG, Deussing JM, et al. cAMP-dependent cell differentiation triggered by activated CRHR1 in hippocampal neuronal cells. Sci Rep [Internet]. 2017 Dec 1 [cited 2024 Sep 18];7(1). Available from: https://pubmed.ncbi.nlm.nih.gov/28512295/
63. Teli T, Markovic D, Levine MA, Hillhouse EW, Grammatopoulos DK. Regulation of corticotropin-releasing hormone receptor type 1alpha signaling: structural determinants for G protein-coupled receptor kinase-mediated phosphorylation and agonist-mediated desensitization. Mol Endocrinol [Internet]. 2005 Feb [cited 2024 Sep 18];19(2):474–90. Available from: https://pubmed.ncbi.nlm.nih.gov/15498832/
64. Lefkimmiatis K, Zaccolo M. cAMP signaling in subcellular compartments. Pharmacol Ther [Internet]. 2014 [cited 2024 Sep 18];143(3):295. Available from:

/pmc/articles/PMC4117810/
65. Tresguerres M, Levin LR, Buck J. Intracellular cAMP signaling by soluble adenylyl cyclase. Kidney Int [Internet]. 2011 Jun 2 [cited 2024 Sep 18];79(12):1277–88. Available from: http://www.kidney-international.org/article/S0085253815547613/fulltext
66. Halm ST, Zhang J, Halm DR. β-Adrenergic activation of electrogenic K+ and Cl - secretion in guinea pig distal colonic epithelium proceeds via separate cAMP signaling pathways. Am J Physiol Gastrointest Liver Physiol [Internet]. 2010 Jul [cited 2024 Sep 18];299(1):81–95. Available from: https://journals.physiology.org/doi/10.1152/ajpgi.00035.2010
67. Steckler T, Holsboer F. Corticotropin-releasing hormone receptor subtypes and emotion. Biol Psychiatry [Internet]. 1999 Dec 1 [cited 2024 Sep 18];46(11):1480–508. Available from: https://pubmed.ncbi.nlm.nih.gov/10599478/
68. Pan W, Kastin AJ. Urocortin and the Brain. Prog Neurobiol [Internet]. 2008 Feb [cited 2024 Sep 18];84(2):148. Available from: /pmc/articles/PMC2267723/
69. Raadsheer FC, Hoogendijk WJG, Stam FC, Tilders FJH, Swaab DF. Increased numbers of corticotropin-releasing hormone expressing neurons in the hypothalamic paraventricular nucleus of depressed patients. Neuroendocrinology [Internet]. 1994 [cited 2024 Sep 18];60(4):436–44. Available from: https://pubmed.ncbi.nlm.nih.gov/7824085/
70. Koob GF, Heinrichs SC. A role for corticotropin releasing factor and urocortin in behavioral responses to stressors. Brain Res [Internet]. 1999 Nov 27 [cited 2024 Sep 18];848(1–2):141–52. Available from: https://pubmed.ncbi.nlm.nih.gov/10612706/
71. Owens MJ, Nemeroff CB. Physiology and pharmacology of corticotropin-releasing factor. Pharmacol Rev [Internet]. 1991 [cited 2024 Sep 18];43(4):425–73. Available from: https://pubmed.ncbi.nlm.nih.gov/1775506/
72. De Souza EB. Corticotropin-releasing factor receptors: Physiology, pharmacology, biochemistry and role in central nervous system and immune disorders. Psychoneuroendocrinology [Internet]. 1995 [cited 2024 Sep 18];20(8):789–819. Available from: https://pubmed.ncbi.nlm.nih.gov/8834089/
73. Holsboer F, Ising M. Stress hormone regulation: biological role and translation into therapy. Annu Rev Psychol [Internet]. 2010 Jan 10 [cited 2024 Sep 18];61:81–109. Available from: https://pubmed.ncbi.nlm.nih.gov/19575614/
74. Herman JP, Figueiredo H, Mueller NK, Ulrich-Lai Y, Ostrander MM, Choi DC, et al. Central mechanisms of stress integration: Hierarchical circuitry controlling hypothalamo-pituitary-adrenocortical responsiveness. Front Neuroendocrinol [Internet]. 2003 [cited 2024 Sep 18];24(3):151–80. Available from: https://pubmed.ncbi.nlm.nih.gov/14596810/
75. Sapolsky RM, Romero LM, Munck AU. How do glucocorticoids influence stress responses? Integrating permissive, suppressive, stimulatory, and preparative actions. Endocr Rev [Internet]. 2000 Feb 1 [cited 2024 Sep 18];21(1):55–89. Available from: https://pubmed.ncbi.nlm.nih.gov/10696570/
76. Sonino N, Fava GA. Psychosomatic aspects of Cushing's disease. Psychother Psychosom. 1998 May;67(3):140–6.
77. Bratek A, Koźmin-Burzyńska A, Górniak E, Krysta K. Psychiatric disorders associated with Cushing's syndrome. Psychiatr Danub [Internet]. 2015 Sep 1 [cited 2024 Sep 18];27(5):S339–43. Available from: https://link.springer.com/article/10.2165/00023210-200115050-00003
78. Henry M, Thomas KGF, Ross IL. Sleep, Cognition and Cortisol in Addison's Disease: A Mechanistic Relationship. Front Endocrinol (Lausanne) [Internet]. 2021 Aug 27 [cited 2024 Sep 15];12. Available from: https://pubmed.ncbi.nlm.nih.gov/34512546/
79. Heim C, Ehlert U, Hellhammer DH. The potential role of hypocortisolism in the pathophysiology of stress-related bodily disorders. Psychoneuroendocrinology [Internet]. 2000 Jan [cited 2024 Sep 15];25(1):1–35. Available from: https://pubmed.ncbi.nlm.nih.gov/10633533/

80. Levine A, Zagoory-Sharon O, Feldman R, Lewis JG, Weller A. Measuring cortisol in human psychobiological studies. Physiol Behav [Internet]. 2007 Jan 30 [cited 2024 Sep 15];90(1):43–53. Available from: https://pubmed.ncbi.nlm.nih.gov/17055006/
81. Van Londen L, Goekoop JG, Van Kempen GMJ, Frankhuijzen-Sierevogel AC, Wiegant VM, Van Der Velde EA, et al. Plasma levels of arginine vasopressin elevated in patients with major depression. Neuropsychopharmacology [Internet]. 1997 Oct [cited 2024 Sep 15];17(4):284–92. Available from: https://pubmed.ncbi.nlm.nih.gov/9326754/
82. Michael A, Jenaway A, Paykel ES, Herbert J. Altered salivary dehydroepiandrosterone levels in major depression in adults. Biol Psychiatry [Internet]. 2000 Nov 15 [cited 2024 Sep 15];48(10):989–95. Available from: https://pubmed.ncbi.nlm.nih.gov/11082473/
83. Anglin RE, Rosebush PI, Mazurek MF. The neuropsychiatric profile of Addison's disease: revisiting a forgotten phenomenon. J Neuropsychiatry Clin Neurosci [Internet]. 2006 [cited 2024 Sep 15];18(4):450–9. Available from: https://pubmed.ncbi.nlm.nih.gov/17135373/
84. Dickerson SS, Kemeny ME. Acute stressors and cortisol responses: a theoretical integration and synthesis of laboratory research. Psychol Bull [Internet]. 2004 May [cited 2024 Sep 18];130(3):355–91. Available from: https://pubmed.ncbi.nlm.nih.gov/15122924/
85. Russell G, Lightman S. The human stress response. Nature Reviews Endocrinology 2019 15:9 [Internet]. 2019 Jun 27 [cited 2024 Sep 15];15(9):525–34. Available from: https://www.nature.com/articles/s41574-019-0228-0
86. Lupien SJ, McEwen BS, Gunnar MR, Heim C. Effects of stress throughout the lifespan on the brain, behaviour and cognition. Nature Reviews Neuroscience 2009 10:6 [Internet]. 2009 Apr 29 [cited 2024 Sep 18];10(6):434–45. Available from: https://www.nature.com/articles/nrn2639
87. Burke HM, Davis MC, Otte C, Mohr DC. Depression and cortisol responses to psychological stress: a meta-analysis. Psychoneuroendocrinology [Internet]. 2005 Oct [cited 2024 Sep 18];30(9):846–56. Available from: https://pubmed.ncbi.nlm.nih.gov/15961250/
88. Swaab DF, Bao AM, Lucassen PJ. The stress system in the human brain in depression and neurodegeneration. Ageing Res Rev. 2005 May 1;4(2):141–94.
89. Claes SJ. CRH, Stress, and Major Depression: A Psychobiological Interplay. Vitam Horm [Internet]. 2004 [cited 2024 Sep 15];69:117–50. Available from: https://pubmed.ncbi.nlm.nih.gov/15196881/
90. Chida Y, Steptoe A. Cortisol awakening response and psychosocial factors: a systematic review and meta-analysis. Biol Psychol [Internet]. 2009 Mar [cited 2024 Sep 15];80(3):265–78. Available from: https://pubmed.ncbi.nlm.nih.gov/19022335/
91. Hellhammer DH, Wüst S, Kudielka BM. Salivary cortisol as a biomarker in stress research. Psychoneuroendocrinology [Internet]. 2009 Feb [cited 2024 Sep 15];34(2):163–71. Available from: https://pubmed.ncbi.nlm.nih.gov/19095358/
92. Sutton RE, Koob GF, Le Moal M, Rivier J, Vale W. Corticotropin releasing factor produces behavioural activation in rats. Nature [Internet]. 1982 [cited 2024 Sep 18];297(5864):331–3. Available from: https://pubmed.ncbi.nlm.nih.gov/6978997/
93. Muglia L, Jacobson L, Dikkest P, Majzoub JA. Corticotropin-releasing hormone deficiency reveals major fetal but not adult glucocorticoid need. Nature [Internet]. 1995 Feb 2 [cited 2024 Sep 18];373(6513):427–32. Available from: https://pubmed.ncbi.nlm.nih.gov/7830793/
94. Deussing JM, Chen A. The Corticotropin-Releasing Factor Family: Physiology of the Stress Response. Physiol Rev [Internet]. 2018 Oct 1 [cited 2024 Sep 18];98(4):2225–86. Available from: https://pubmed.ncbi.nlm.nih.gov/30109816/
95. Zhang R, Asai M, Mahoney CE, Joachim M, Shen Y, Gunner G, et al. Loss of hypothalamic corticotropin-releasing hormone markedly reduces anxiety behaviors in mice. Mol Psychiatry [Internet]. 2017 May 1 [cited 2024 Sep 18];22(5):733–44. Available from:

https://pubmed.ncbi.nlm.nih.gov/27595593/
96. Müller MB, Zimmermann S, Sillaber I, Hagemeyer TP, Deussing JM, Timpl P, et al. Limbic corticotropin-releasing hormone receptor 1 mediates anxiety-related behavior and hormonal adaptation to stress. Nat Neurosci [Internet]. 2003 Oct 1 [cited 2024 Sep 18];6(10):1100–7. Available from: https://pubmed.ncbi.nlm.nih.gov/12973355/
97. Refojo D, Schweizer M, Kuehne C, Ehrenberg S, Thoeringer C, Vogl AM, et al. Glutamatergic and dopaminergic neurons mediate anxiogenic and anxiolytic effects of CRHR1. Science [Internet]. 2011 Sep 30 [cited 2024 Sep 18];333(6051):1903–7. Available from: https://pubmed.ncbi.nlm.nih.gov/21885734/
98. Henckens MJAG, Deussing JM, Chen A. Region-specific roles of the corticotropin-releasing factor-urocortin system in stress. Nat Rev Neurosci [Internet]. 2016 Sep 19 [cited 2024 Sep 18];17(10):636–51. Available from: https://pubmed.ncbi.nlm.nih.gov/27586075/
99. Lv SS, Lv XJ, Cai YQ, Hou XY, Zhang ZZ, Wang GH, et al. Corticotropin-releasing hormone neurons control trigeminal neuralgia-induced anxiodepression via a hippocampus-to-prefrontal circuit. Sci Adv [Internet]. 2024 [cited 2024 Sep 17];10(3). Available from: https://pubmed.ncbi.nlm.nih.gov/38241377/
100. Gallagher JP, Orozco-Cabal LF, Liu J, Shinnick-Gallagher P. Synaptic physiology of central CRH system. Eur J Pharmacol [Internet]. 2008 Apr 7 [cited 2024 Sep 18];583(2–3):215–25. Available from: https://pubmed.ncbi.nlm.nih.gov/18342852/
101. Radulovic J, Rühmann A, Liepold T, Spiess J. Modulation of learning and anxiety by corticotropin-releasing factor (CRF) and stress: differential roles of CRF receptors 1 and 2. J Neurosci [Internet]. 1999 Jun 15 [cited 2024 Sep 15];19(12):5016–25. Available from: https://pubmed.ncbi.nlm.nih.gov/10366634/
102. Bale TL, Vale WW. CRF and CRF receptors: role in stress responsivity and other behaviors. Annu Rev Pharmacol Toxicol [Internet]. 2004 [cited 2024 Sep 15];44:525–57. Available from: https://pubmed.ncbi.nlm.nih.gov/14744257/
103. Pan Y, Liu Y, Young KA, Zhang Z, Wang Z. Post-weaning social isolation alters anxiety-related behavior and neurochemical gene expression in the brain of male prairie voles. Neurosci Lett [Internet]. 2009 Apr 17 [cited 2024 Sep 18];454(1):67–71. Available from: https://pubmed.ncbi.nlm.nih.gov/19429056/
104. Grippo AJ, Gerena D, Huang J, Kumar N, Shah M, Ughreja R, et al. Social isolation induces behavioral and neuroendocrine disturbances relevant to depression in female and male prairie voles. Psychoneuroendocrinology [Internet]. 2007 Sep [cited 2024 Sep 15];32(8–10):966–80. Available from: https://pubmed.ncbi.nlm.nih.gov/17825994/
105. Chauke M, de Jong TR, Garland T, Saltzman W. Paternal responsiveness is associated with, but not mediated by reduced neophobia in male California mice (Peromyscus californicus). Physiol Behav [Internet]. 2012 Aug 20 [cited 2024 Sep 18];107(1):65–75. Available from: https://pubmed.ncbi.nlm.nih.gov/22634280/
106. Ehlers CL, Kaneko WM, Owens MJ, Nemeroff CB. Effects of gender and social isolation on electroencephalogram and neuroendocrine parameters in rats. Biol Psychiatry [Internet]. 1993 Mar 1 [cited 2024 Sep 19];33(5):358–66. Available from: https://pubmed.ncbi.nlm.nih.gov/8471694/
107. Lim MM, Nair HP, Young LJ. Species and sex differences in brain distribution of corticotropin-releasing factor receptor subtypes 1 and 2 in monogamous and promiscuous vole species. J Comp Neurol [Internet]. 2005 Jun 20 [cited 2024 Sep 19];487(1):75–92. Available from: https://pubmed.ncbi.nlm.nih.gov/15861459/
108. Schmidt M V., Scharf SH, Liebl C, Harbich D, Mayer B, Holsboer F, et al. A novel chronic social stress paradigm in female mice. Horm Behav [Internet]. 2010 Apr [cited 2024 Sep 16];57(4–5):415–20. Available from: https://pubmed.ncbi.nlm.nih.gov/20100488/
109. DeVries AC, Guptaa T, Cardillo S, Cho M, Carter CS. Corticotropin-releasing factor induces

social preferences in male prairie voles. Psychoneuroendocrinology. 2002 Aug 1;27(6):705–14.
110. Lim MM, Liu Y, Ryabinin AE, Bai Y, Wang Z, Young LJ. CRF receptors in the nucleus accumbens modulate partner preference in prairie voles. Horm Behav [Internet]. 2007 Apr [cited 2024 Sep 19];51(4):508–15. Available from: https://pubmed.ncbi.nlm.nih.gov/17320879/
111. Kasahara M, Groenink L, Kas MJH, Bijlsma EY, Olivier B, Sarnyai Z. Influence of transgenic corticotropin-releasing factor (CRF) over-expression on social recognition memory in mice. Behavioural brain research [Internet]. 2011 Apr 15 [cited 2024 Sep 19];218(2):357–62. Available from: https://pubmed.ncbi.nlm.nih.gov/21192987/
112. Deussing JM, Breu J, Kühne C, Kallnik M, Bunck M, Glasl L, et al. Urocortin 3 modulates social discrimination abilities via corticotropin-releasing hormone receptor type 2. J Neurosci [Internet]. 2010 Jul 7 [cited 2024 Sep 19];30(27):9103–16. Available from: https://pubmed.ncbi.nlm.nih.gov/20610744/
113. Swanson LW. Cerebral hemisphere regulation of motivated behavior. Brain Res. 2000 Dec 15;886(1–2):113–64.
114. Chen P, Hong W. Neural Circuit Mechanisms of Social Behavior. Neuron [Internet]. 2018 Apr 4 [cited 2024 Sep 19];98(1):16–30. Available from: https://pubmed.ncbi.nlm.nih.gov/29621486/
115. Riad MH, Park K, Ibañez-Tallon I, Heintz N. Local production of corticotropin-releasing hormone in prefrontal cortex modulates male-specific novelty exploration. Proc Natl Acad Sci U S A [Internet]. 2022 Dec 12 [cited 2024 Sep 19];119(49). Available from: /pmc/articles/PMC9894189/
116. Chen P, Lou S, Huang ZH, Wang Z, Shan QH, Wang Y, et al. Prefrontal Cortex Corticotropin-Releasing Factor Neurons Control Behavioral Style Selection under Challenging Situations. Neuron [Internet]. 2020 Apr 22 [cited 2024 Sep 19];106(2):301-315.e7. Available from: https://pubmed.ncbi.nlm.nih.gov/32101698/
117. Uribe-Mariño A, Gassen NC, Wiesbeck MF, Balsevich G, Santarelli S, Solfrank B, et al. Prefrontal Cortex Corticotropin-Releasing Factor Receptor 1 Conveys Acute Stress-Induced Executive Dysfunction. Biol Psychiatry. 2016 Nov 15;80(10):743–53.
118. Howard DM, Adams MJ, Clarke TK, Hafferty JD, Gibson J, Shirali M, et al. Genome-wide meta-analysis of depression identifies 102 independent variants and highlights the importance of the prefrontal brain regions. Nature Neuroscience 2019 22:3 [Internet]. 2019 Feb 4 [cited 2024 Sep 19];22(3):343–52. Available from: https://www.nature.com/articles/s41593-018-0326-7
119. Pizzagalli DA, Roberts AC. Prefrontal cortex and depression. Neuropsychopharmacology [Internet]. 2022 Jan 1 [cited 2024 Sep 18];47(1):225–46. Available from: https://pubmed.ncbi.nlm.nih.gov/34341498/
120. Roberts A. Prefrontal Regulation of Threat-Elicited Behaviors: A Pathway to Translation. Annu Rev Psychol [Internet]. 2020 Jan 4 [cited 2024 Sep 18];71:357–87. Available from: https://pubmed.ncbi.nlm.nih.gov/31622562/
121. Hawrylycz MJ, Lein ES, Guillozet-Bongaarts AL, Shen EH, Ng L, Miller JA, et al. An anatomically comprehensive atlas of the adult human brain transcriptome. Nature 2012 489:7416 [Internet]. 2012 Sep 19 [cited 2024 Sep 19];489(7416):391–9. Available from: https://www.nature.com/articles/nature11405
122. Sunkin SM, Ng L, Lau C, Dolbeare T, Gilbert TL, Thompson CL, et al. Allen Brain Atlas: an integrated spatio-temporal portal for exploring the central nervous system. Nucleic Acids Res [Internet]. 2013 Jan 1 [cited 2024 Sep 19];41(Database issue). Available from: https://pubmed.ncbi.nlm.nih.gov/23193282/
123. Jones AR, Overly CC, Sunkin SM. The Allen Brain Atlas: 5 years and beyond. Nat Rev Neurosci [Internet]. 2009 Nov [cited 2024 Sep 18];10(11):821–8. Available from:

https://pubmed.ncbi.nlm.nih.gov/19826436/
124. Bostock M, Ogievetsky V, Heer J. D3 data-driven documents. IEEE Trans Vis Comput Graph. 2011;17(12):2301–9.
125. Lein ES, Hawrylycz MJ, Ao N, Ayres M, Bensinger A, Bernard A, et al. Genome-wide atlas of gene expression in the adult mouse brain. Nature 2006 445:7124 [Internet]. 2006 Dec 6 [cited 2024 Sep 19];445(7124):168–76. Available from: https://www.nature.com/articles/nature05453
126. Dang C, Sodt A, Lau C, Youngstrom B, Ng L, Kuan L, et al. The Allen Brain Atlas: Delivering Neuroscience to the Web on a Genome Wide Scale. Lecture Notes in Computer Science (including subseries Lecture Notes in Artificial Intelligence and Lecture Notes in Bioinformatics) [Internet]. 2007 [cited 2024 Sep 19];4544 LNBI:17–26. Available from: https://link.springer.com/chapter/10.1007/978-3-540-73255-6_4
127. Ng L, Pathak SD, Kuan C, Lau C, Dong H, Sodt A, et al. Neuroinformatics for genome-wide 3D gene expression mapping in the mouse brain. IEEE/ACM Trans Comput Biol Bioinform [Internet]. 2007 Jul [cited 2024 Sep 19];4(3):382–92. Available from: https://pubmed.ncbi.nlm.nih.gov/17666758/
128. Eppig JT, Blake JA, Bult CJ, Kadin JA, Richardson JE, Anagnostopoulos A, et al. The Mouse Genome Database (MGD): facilitating mouse as a model for human biology and disease. Nucleic Acids Res [Internet]. 2015 Jan 1 [cited 2024 Sep 18];43(Database issue):D726. Available from: /pmc/articles/PMC4384027/
129. Kono J, Konno K, Talukder AH, Fuse T, Abe M, Uchida K, et al. Distribution of corticotropin-releasing factor neurons in the mouse brain: a study using corticotropin-releasing factor-modified yellow fluorescent protein knock-in mouse. Brain Struct Funct [Internet]. 2017 May 1 [cited 2024 Sep 18];222(4):1705–32. Available from: https://pubmed.ncbi.nlm.nih.gov/27638512/
130. Wang Y, Hu P, Shan Q, Huang C, Huang Z, Chen P, et al. Single-cell morphological characterization of CRH neurons throughout the whole mouse brain. BMC Biol [Internet]. 2021 Dec 1 [cited 2024 Sep 18];19(1). Available from: https://pubmed.ncbi.nlm.nih.gov/33722214/
131. Zhao C, Ries C, Du Y, Zhang J, Sakimura K, Itoi K, et al. Differential CRH expression level determines efficiency of Cre- and Flp-dependent recombination. Front Neurosci [Internet]. 2023 [cited 2024 Sep 18];17. Available from: https://pubmed.ncbi.nlm.nih.gov/37599997/
132. Clemens AM, Wang H, Brecht M. The lateral septum mediates kinship behavior in the rat. Nature Communications 2020 11:1 [Internet]. 2020 Jun 22 [cited 2024 Sep 18];11(1):1–11. Available from: https://www.nature.com/articles/s41467-020-16489-x
133. Kogo H, Kiyokawa Y, Takeuchi Y. Rats show a preference for certain unfamiliar strains of rats. bioRxiv [Internet]. 2021 Feb 18 [cited 2024 Sep 19];2021.02.18.431764. Available from: https://www.biorxiv.org/content/10.1101/2021.02.18.431764v1
134. Mossman CA, Drickamer LC. Odor Preferences of Female House Mice (Mus domesticus) in Seminatural Enclosures. J Comp Psychol. 1996;110(2):131–8.
135. Watanabe S. The dominant/subordinate relationship between mice modifies the approach behavior toward a cage mate experiencing pain. Behavioural processes [Internet]. 2014 [cited 2024 Sep 18];103:1–4. Available from: https://pubmed.ncbi.nlm.nih.gov/24184143/
136. van der Kooij MA, Sandi C. Social memories in rodents: methods, mechanisms and modulation by stress. Neurosci Biobehav Rev [Internet]. 2012 Aug [cited 2024 Sep 18];36(7):1763–72. Available from: https://pubmed.ncbi.nlm.nih.gov/22079398/
137. Laham BJ, Diethorn EJ, Gould E. Newborn mice form lasting CA2-dependent memories of their mothers. Cell Rep [Internet]. 2021 Jan 26 [cited 2024 Sep 19];34(4). Available from: http://www.cell.com/article/S2211124720316570/fulltext
138. Blaustein AR, O'Hara RK. Genetic control for sibling recognition? Nature 1981 290:5803

[Internet]. 1981 [cited 2024 Sep 19];290(5803):246–8. Available from: https://www.nature.com/articles/290246a0
139. Clemens AM, Brecht M. Neural representations of kinship. Curr Opin Neurobiol. 2021 Jun 1;68:116–23.
140. Okuyama T, Kitamura T, Roy DS, Itohara S, Tonegawa S. Ventral CA1 neurons store social memory. Science (1979) [Internet]. 2016 Sep 30 [cited 2024 Sep 19];353(6307):1536–41. Available from: https://www.science.org/doi/10.1126/science.aaf7003
141. Menon R, Süß T, Oliveira VE de M, Neumann ID, Bludau A. Neurobiology of the lateral septum: regulation of social behavior. Vol. 45, Trends in Neurosciences. Elsevier Ltd; 2022. p. 27–40.
142. Beery AK, Christensen JD, Lee NS, Blandino KL. Specificity in sociality: Mice and prairie voles exhibit different patterns of peer affiliation. Front Behav Neurosci [Internet]. 2018 Mar 19 [cited 2024 Sep 21];12:355168. Available from: www.frontiersin.org
143. Risbrough VB, Stein MB. Role of corticotropin releasing factor in anxiety disorders: A translational research perspective. Horm Behav. 2006 Nov 1;50(4):550–61.
144. Laryea G, Arnett MG, Muglia LJ. Behavioral Studies and Genetic Alterations in Corticotropin-Releasing Hormone (CRH) Neurocircuitry: Insights into Human Psychiatric Disorders. Behavioral Sciences 2012, Vol 2, Pages 135-171 [Internet]. 2012 Jun 21 [cited 2024 Sep 19];2(2):135–71. Available from: https://www.mdpi.com/2076-328X/2/2/135/htm
145. Zink CF, Tong Y, Chen Q, Bassett DS, Stein JL, Meyer-Lindenberg A. Know your place: neural processing of social hierarchy in humans. Neuron [Internet]. 2008 Apr 24 [cited 2024 Sep 18];58(2):273–83. Available from: https://pubmed.ncbi.nlm.nih.gov/18439411/
146. Ferreira-Fernandes E, Peça J. The Neural Circuit Architecture of Social Hierarchy in Rodents and Primates. Front Cell Neurosci [Internet]. 2022 May 12 [cited 2024 Sep 18];16. Available from: https://pubmed.ncbi.nlm.nih.gov/35634473/
147. Byrne RW, Bates LA. Primate social cognition: uniquely primate, uniquely social, or just unique? Neuron [Internet]. 2010 Mar [cited 2024 Sep 18];65(6):815–30. Available from: https://pubmed.ncbi.nlm.nih.gov/20346757/
148. Bergman TJ, Beehner JC, Cheney DL, Seyfarth RM. Hierarchical classification by rank and kinship in baboons. Science [Internet]. 2003 Nov 14 [cited 2024 Sep 18];302(5648):1234–6. Available from: https://pubmed.ncbi.nlm.nih.gov/14615544/
149. Grosenick L, Clement TS, Fernald RD. Fish can infer social rank by observation alone. Nature [Internet]. 2007 Jan 25 [cited 2024 Sep 18];445(7126):429–32. Available from: https://pubmed.ncbi.nlm.nih.gov/17251980/
150. Guillermo Paz-Y-Miño C, Bond AB, Kamil AC, Balda RP. Pinyon jays use transitive inference to predict social dominance. Nature [Internet]. 2004 Aug 12 [cited 2024 Sep 18];430(7001):778–81. Available from: https://pubmed.ncbi.nlm.nih.gov/15306809/
151. Milewski TM, Lee W, Champagne FA, Curley JP. Behavioural and physiological plasticity in social hierarchies. Philosophical Transactions of the Royal Society B [Internet]. 2022 Feb 28 [cited 2024 Sep 18];377(1845). Available from: https://royalsocietypublishing.org/doi/10.1098/rstb.2020.0443
152. Drews C. The concept and definition of dominance in animal behaviour. Behaviour. 1993;125(3–4):283–313.
153. Mehrabian A. Pleasure-Arousal-Dominance: A general framework for describing and measuring individual differences in temperament. Current Psychology. 1996;14(4):261–92.
154. Morgan D, Grant kathleen A, Gage HD, Mach RH, Kaplan JR, Prioleau O, et al. Social dominance in monkeys: dopamine D2 receptors and cocaine self-administration. Nat Neurosci [Internet]. 2002 [cited 2024 Sep 18];5(2):169–74. Available from: https://pubmed.ncbi.nlm.nih.gov/11802171/
155. Mascaro O, Csibra G. Representation of stable social dominance relations by human infants.

Proc Natl Acad Sci U S A [Internet]. 2012 May 1 [cited 2024 Sep 18];109(18):6862–7. Available from: https://pubmed.ncbi.nlm.nih.gov/22509020/
156. Hand JL. Resolution of Social Conflicts: Dominance, Egalitarianism, Spheres of Dominance, and Game Theory. https://doi.org/101086/414899 [Internet]. 1986 Jun 1 [cited 2024 Sep 18];61(2):201–20. Available from: https://www.journals.uchicago.edu/doi/10.1086/414899
157. Li SW, Zeliger O, Strahs L, Báez-Mendoza R, Johnson LM, McDonald Wojciechowski A, et al. Frontal neurons driving competitive behaviour and ecology of social groups. Nature [Internet]. 2022 Mar 24 [cited 2024 Sep 18];603(7902):661–6. Available from: https://pubmed.ncbi.nlm.nih.gov/35296863/
158. Hou XH, Hyun M, Taranda J, Huang KW, Todd E, Feng D, et al. Central Control Circuit for Context-Dependent Micturition. Cell [Internet]. 2016 Sep 22 [cited 2024 Sep 18];167(1):73-86.e12. Available from: https://pubmed.ncbi.nlm.nih.gov/27662084/
159. Dwortz MF, Curley JP, Tye KM, Padilla-Coreano N. Neural systems that facilitate the representation of social rank. Philos Trans R Soc Lond B Biol Sci [Internet]. 2022 Feb 28 [cited 2024 Sep 18];377(1845). Available from: https://pubmed.ncbi.nlm.nih.gov/35000438/
160. Curley JP. Temporal pairwise-correlation analysis provides empirical support for attention hierarchies in mice. Biol Lett [Internet]. 2016 May 1 [cited 2024 Sep 18];12(5). Available from: https://pubmed.ncbi.nlm.nih.gov/27194290/
161. Barabas AJ, Lucas JR, Erasmus MA, Cheng HW, Gaskill BN. Who's the Boss? Assessing Convergent Validity of Aggression Based Dominance Measures in Male Laboratory Mice, Mus Musculus. Front Vet Sci [Internet]. 2021 Jul 9 [cited 2024 Sep 18];8. Available from: https://pubmed.ncbi.nlm.nih.gov/34307534/
162. Šabanović M, Liu H, Mlambo V, Aqel H, Chaudhury D. What it takes to be at the top: The interrelationship between chronic social stress and social dominance. Brain Behav [Internet]. 2020 Dec 1 [cited 2024 Sep 18];10(12). Available from: https://pubmed.ncbi.nlm.nih.gov/33070476/
163. Jing P, Shan Q. Exogenous oxytocin microinjection into the nucleus accumbens shell attenuates social dominance in group-housed male mice. Physiol Behav [Internet]. 2023 Oct 1 [cited 2024 Sep 18];269. Available from: https://pubmed.ncbi.nlm.nih.gov/37270150/
164. So N, Franks B, Lim S, Curley JP. A Social Network Approach Reveals Associations between Mouse Social Dominance and Brain Gene Expression. PLoS One [Internet]. 2015 Jul 30 [cited 2024 Sep 18];10(7). Available from: https://pubmed.ncbi.nlm.nih.gov/26226265/
165. Lee W, Dwortz MF, Milewski TM, Champagne FA, Curley JP. Social status mediated variation in hypothalamic transcriptional profiles of male mice. Horm Behav [Internet]. 2022 Jun 1 [cited 2024 Sep 18];142. Available from: https://pubmed.ncbi.nlm.nih.gov/35500322/
166. Vermande MM, Sterck EHM. How to Get the Biggest Slice of the Cake. A Comparative View of Social Behaviour and Resource Access in Human Children and Nonhuman Primates. Front Psychol [Internet]. 2020 Nov 3 [cited 2024 Sep 18];11. Available from: https://pubmed.ncbi.nlm.nih.gov/33250823/
167. Lindzey G, Winston H, Manosevitz M. Social Dominance in Inbred Mouse Strains. Nature 1961 191:4787 [Internet]. 1961 Jul 1 [cited 2024 Sep 18];191(4787):474–6. Available from: https://www.nature.com/articles/191474a0
168. Fan Z, Zhu H, Zhou T, Wang S, Wu Y, Hu H. Using the tube test to measure social hierarchy in mice. Nature Protocols 2019 14:3 [Internet]. 2019 Feb 15 [cited 2024 Sep 18];14(3):819–31. Available from: https://www.nature.com/articles/s41596-018-0116-4
169. Padilla-Coreano N, Batra K, Patarino M, Chen Z, Rock RR, Zhang R, et al. Cortical ensembles orchestrate social competition through hypothalamic outputs. Nature [Internet]. 2022 Mar 24;603(7902):667–71. Available from: https://www.nature.com/articles/s41586-022-04507-5
170. Choi TY, Jeon H, Jeong S, Kim EJ, Kim J, Jeong YH, et al. Distinct prefrontal projection activity

and transcriptional state conversely orchestrate social competition and hierarchy. Neuron [Internet]. 2024 Feb 21 [cited 2024 Sep 18];112(4):611-627.e8. Available from: https://pubmed.ncbi.nlm.nih.gov/38086372/

171. Lee W, Dowd HN, Nikain C, Dwortz MF, Yang ED, Curley JP. Effect of relative social rank within a social hierarchy on neural activation in response to familiar or unfamiliar social signals. Sci Rep [Internet]. 2021 Dec 1 [cited 2024 Sep 18];11(1). Available from: https://pubmed.ncbi.nlm.nih.gov/33536481/
172. Gutzeit VA, Ahuna K, Santos TL, Cunningham AM, Sadsad Rooney M, Muñoz Zamora A, et al. Optogenetic reactivation of prefrontal social neural ensembles mimics social buffering of fear. Neuropsychopharmacology [Internet]. 2020 May 1 [cited 2024 Sep 19];45(6):1068–77. Available from: https://pubmed.ncbi.nlm.nih.gov/32035426/
173. Ma M, Xiong W, Hu F, Deng MF, Huang X, Chen JG, et al. A novel pathway regulates social hierarchy via lncRNA AtLAS and postsynaptic synapsin IIb. Cell Res [Internet]. 2020 Feb 1 [cited 2024 Sep 18];30(2):105–18. Available from: https://pubmed.ncbi.nlm.nih.gov/31959917/
174. Yin YY, Lai ZK, Yan JZ, Wei QQ, Wang B, Zhang LM, et al. The interaction between social hierarchy and depression/anxiety: Involvement of glutamatergic pyramidal neurons in the medial prefrontal cortex (mPFC). Neurobiol Stress [Internet]. 2023 May 1 [cited 2024 Sep 18];24. Available from: https://pubmed.ncbi.nlm.nih.gov/37057073/
175. Beery AK, Bicks L, Mooney SJ, Goodwin NL, Holmes MM. Sex, social status, and CRF receptor densities in naked mole-rats. J Comp Neurol [Internet]. 2016 Feb 1 [cited 2024 Sep 18];524(2):228–43. Available from: https://pubmed.ncbi.nlm.nih.gov/26100759/
176. Guo H, Fang Q, Huo Y, Zhang Y, Zhang J. Social dominance-related major urinary proteins and the regulatory mechanism in mice. Integr Zool [Internet]. 2015 Nov 1 [cited 2024 Sep 18];10(6):543–54. Available from: https://pubmed.ncbi.nlm.nih.gov/26331981/
177. Lambeth LS, Moore RJ, Muralitharan M, Dalrymple BP, McWilliam S, Doran TJ. Characterisation and application of a bovine U6 promoter for expression of short hairpin RNAs. BMC Biotechnol [Internet]. 2005 May 11 [cited 2024 Sep 19];5(1):1–9. Available from: https://bmcbiotechnol.biomedcentral.com/articles/10.1186/1472-6750-5-13
178. Koolhaas JM, Coppens CM, de Boer SF, Buwalda B, Meerlo P, Timmermans PJA. The Resident-intruder Paradigm: A Standardized Test for Aggression, Violence and Social Stress. J Vis Exp [Internet]. 2013 [cited 2024 Sep 19];(77):4367. Available from: /pmc/articles/PMC3731199/
179. Stefania C, Rogier G, Beomonte Zobel S, Velotti P. The Relation of Anxiety and Avoidance Dimensions of Attachment to Intimate Partner Violence: A Meta-Analysis About Victims. https://doi.org/101177/15248380211050595 [Internet]. 2021 Nov 13 [cited 2024 Sep 21];24(2):1047–62. Available from: https://journals.sagepub.com/doi/10.1177/15248380211050595?url_ver=Z39.88-2003&rfr_id=ori%3Arid%3Acrossref.org&rfr_dat=cr_pub++0pubmed
180. Fearon RMP, Roisman GI. Attachment theory: progress and future directions. Curr Opin Psychol. 2017 Jun 1;15:131–6.

# ANNEX

## Corticotropin-releasing hormone signaling from prefrontal cortex to lateral septum suppresses interaction with familiar mice

Authors Noelia Sofia de Leo´ n Reyes, Paula Sierra Diaz, Ramon Nogueira, ..., Jay Schulkin, Arun Asok, Felix Leroy

Correspondence felxfel@aol.com

In brief Corticotropin-releasing hormone release from the infra-limbic area of the prefrontal cortex to the lateral septum suppresses social interaction with familiar but not novel mice to support the social novelty preference exhibited by adult mice. The maturation of this circuit during the first two post-natal weeks enables the developmental shift from a preference for littermates in juveniles to a preference for novel mice in adults.

Highlights

- Release of CRH from PFC to LS suppresses social interaction with familiar mice d
- Suppression of social interaction with familiar mice supports social novelty preference d
- Maturation of this circuit induces a shift in social preference in young mice

**SUMMARY**

Social preference, the decision to interact with one member of the same species over another, is critical to optimize social interactions. Thus, adult rodents favor interacting with novel conspecifics over familiar ones, but whether this social preference stems from neural circuits facilitating interactions with novel individuals or suppressing interactions with familiar ones remains unknown. Here, we identify neurons in the infralimbic area (ILA) of the mouse prefrontal cortex that express the neuropeptide corticotropin-releasing hormone (CRH) and project to the dorsal region of the rostral lateral septum (rLS). We show how release of CRH during familiar encounters disinhibits rLS neurons, thereby suppressing social interactions with familiar mice and contributing to social

novelty preference. We further demonstrate how the maturation of CRH expression in ILA during the first 2 post-natal weeks enables the developmental shift from a preference for littermates in juveniles to a preference for novel mice in adults.

**INTRODUCTION**

Social preference, the decision to interact with one conspecific over another, is a feature displayed by gregarious animals, which is critical to navigate their social space.[1,2] Adult rodents prefer to interact with their kin,[3,4] individuals from specific strains,[5] and members of the opposite sex.[6–9] In addition to innate factors (e.g., kin, strain, and sex), social preference is also influenced by social memory,[10] social hierarchy,[9,11,12] and the affective state of the conspecific.[13] Thus, adult rodents display social novelty preference (SNP), choosing to interact with novel individuals over familiar ones.[10] For the last two decades, SNP has been used as a proxy to assess social memory,[14–16] but the neuronal circuits mediating SNP remain elusive. In particular, it is unknown whether SNP is due solely to a rewarding signal for novel social interactions[17] or also involves the suppression of exploration of familiar individuals. We hypothesized the existence of neuronal circuits promoting the avoidance of familiar mice and therefore contributing to SNP when novel and familiar mice are presented simultaneously. Memory-based preferences, such as SNP, also have a developmental window[18] and can change during the life of altricial animals. For example, young mice prefer their mother to unfamiliar dams until weaning when they begin to prefer unfamiliar dams over their mother.[19] Similarly, rat pups display a preference for their familiar siblings during the first 2 post-natal weeks, after which the preference shifts toward novel pups.[3,4] Although the mechanisms that regulate these developmental shifts remain elusive, the lateral septum (LS), a brain region associated with the regulation of motivated behaviors including social interactions,[20] is necessary for kinship/familiarity preference in young rats3 as well as for SNP in adult rodents.[20–22] Moreover, the ventral aspect of medial prefrontal cortex (mPFC), the infralimbic area (ILA), is known for its

involvement in decision-making, responds to social stimuli[23–25] and is also necessary for SNP.[26,27] The mPFC projects to LS to regulate food-seeking behavior,28 but how these regions integrate social memory cues and communicate to regulate social interactions is still unclear. Corticotropin-releasing hormone (CRH),[29] a 41-amino-acid peptide, regulates several processes including homeostatic and allostatic neuroendocrine mechanisms, memory,30 and social behaviors in non-stressful context.[31,32] In humans, CRH is implicated in psychiatric disorders associated with social

deficits such as depression[33,34] and social phobia.[35] In rodents, systemic manipulations of the CRH system impair social interactions.[32,36–44] Given that CRH is expressed in ILA[45] and CRH receptor 1 (CRHR1) is expressed in LS,46 we hypothesized that CRH release from ILA to LS is involved in regulating social interactions and therefore SNP. We demonstrate through a combination of electrophysiological, chemogenetic, optogenetic, calcium recording, and gene silencing techniques that the release of CRH from ILA neurons ($ILA^{CRH}$ neurons) into the rostral region of LS (rLS) suppresses social interaction with familiar mice. This circuit therefore regulates familiarization (decrease in interaction as a novel rodent becomes familiar) and contributes to the SNP exhibited by adult mice. In addition, we find that the increase in $ILA^{CRH}$ neuron density during the second post-natal week is responsible for a developmental shift in the social preference of young mice from familiar to novel conspecifics.

## RESULTS

### $ILA^{CRH}$ cells project to the rostro-dorsal lateral septum

We injected CRH-Cre mice in ILA[47] with a Cre-dependent adeno-associated virus (AAV) expressing membranous GFP and synaptophysin tagged with mRuby in order to visualize axons and synaptic terminals, respectively (Figures 1A and 1B). We observed $GFP^+$ fibers in the rostro-dorsal region of the LS (rdLS) (Figures 1C and 1D). A closer examination confirmed the presence of mRuby-labeled

axon terminals in this region (Figure 1E). We did not observe fibers going to posterior LS or any other brain regions (Figures S1A–S1C). In addition, we did not observe fibers in rdLS following injections into nearby mPFC regions (pre-limbic or anterior cingulate area, Figure S1D). Next, we injected the retrograde marker CtB-488 in rdLS of CRH-Cre mice crossed with a Cre-dependent tdTomato reporter line to visualize $CRH^+$ cells (Figures 1F and 1G). $tdTomato^+$ cells were distributed evenly throughout the rostro-caudal axis of ILA (Figure S2). CtB retrogradely labeled ILA neurons mostly located in layer 2/3 (Figures 1H and 1J). Some CtB+ cells co-expressed tdTomato (Figure 1I) and were mainly found in layer 2/3 of ILA (Figure 1K). We confirmed this result by injecting a Cre-dependent retrograde monosynaptic herpes simplex virus (HSV) expressing GFP in the rdLS of CRH-Cre mice (Figure S3A). Consistent with our CtB injections, 79% of $CRH/GFP^+$ cells were located in ILA (Figures S3B and S3C). Within ILA, 66% of $GFP^+$ cells were located in layer 2/3 (Figure S3D). Overall, these experiments show that $CRH^+$ cells from layer 2/3 of ILA project to rdLS. We labeled sections from the same mice for GABA and observed that 89% of $GFP^+$ $ILA^{CRH}$ cells are positive for GABA (Figure S3E). Furthermore, using markers for excitatory and inhibitory neurons, we found that 92% of $ILA^{CRH}$ cells expressed the mRNA for glutamic acid decarboxylase 2 (Gad2) while only 3% expressed the mRNA for the vesicular glutamate transporter 1 (Slc17a7/vGlut1) (Figures S3G and S3H), confirming the identity of these neurons as GABAergic. We also patched rdLS neurons in septal slices obtained from CRH-Cre mice injected with a Cre-dependent AAV expressing Channelrhodopsin (ChR) in ILA (Figure 1L). Stimulation with blue light elicited a large outward current when holding the neurons at +10 mV (Figure 1M). No inward currents were detected at 70 mV. The light-induced IPSCs were abolished upon application of SR95531 and CGP55845, which block GABAA and GABAB receptors, respectively (Figure 1N). Overall, these results show that $ILA^{CRH}$ neurons projecting to rdLS are a sub-population of GABAergic neurons making functional synapses in rLS.

**$ILA^{CRH}$ neurons suppress social interactions with familiar mice and support SNP**

Next, we used a chemogenetic approach to modulate the activity of $ILA^{CRH}$ neurons and probe their behavioral function. We injected CRH-Cre mice in ILA with Cre-dependent AAVs expressing an iDREADD (inhibitory designer receptor exclusively activated by designer drugs) tagged with mCherry or mCherry only (Figures 2A and 2B). 3 weeks later, mice were intra-peritoneally injected with the DREADD agonist clozapine N-oxide (CNO) prior to conducting the behavioral tests. Since a previous study associated $CRH^{+}$ cells in the pre-limbic area of the mPFC with anxiety,45 we first tested the mice in the open field to assess locomotion and anxiety (Figure S4A). Silencing $ILA^{CRH}$ cells had no effect on the distance traveled, the time spent in the center or the surround, or the ratio of time spent in the center vs. surround (Figures S4B–S4D). Next, we examined the effect of silencing in the elevated plus maze test of anxiety and found no effect on the number of entries or time spent in the open arms relative to the closed ones (Figures S4E–S4I). Finally, since glutamatergic cells in the PFC projecting to LS have been reported to be involved in food-seeking behavior,[28] we performed the anxiety-suppressed feeding behavior test, where a food-deprived mouse must venture into the center of an open field in order to eat (Figure S4J). Silencing $ILA^{CRH}$ cells had no effect on the latency to feed, the time spent feeding, or the number of entries into the food zone (Figures S4K–S4M). These controls suggest that $ILA^{CRH}$ cells are functionally distinct neurons without a prominent function in locomotion, anxiety, or feeding-related behaviors. We next tested whether $ILA^{CRH}$ cells regulate social interactions. The mPFC is known to regulate sociability, social preference, social hierarchy, as well as emotion discrimination,[13,26,27] but it remains unclear whether specific sub-regions or populations control different facets of social interactions. First, we silenced $ILA^{CRH}$ cells and assessed the sociability of the mice (preference for a mouse compared with an object, Figure S5A).14 Both groups exhibited a strong preference for the mouse compared with the object (Figures S5B and S5C). Next, we tested whether $ILA^{CRH}$ cells regulate SNP (Figure 2C). We injected CNO or saline 30 min before the beginning of the test in mice expressing iDREADD or mCherry only. During recall, the three control groups exhibited a higher interaction time with the novel compared with

the familiar mouse (Figure 2D), which translated into a positive discrimination index (DI) preference for the novel mouse (Figure 2E). However, in the test group, in which ILA$^{CRH}$ cells were silenced, the subject mice explored novel and familiar mice to the same extent (Figure 2D). As a result, the DI for SNP was not different from zero (Figure 2E). During learning or recall, the total exploration time of the mice was similar across groups (Figures S5D and S5E), suggesting that ILA$^{CRH}$ cell silencing does not affect the motivation to explore. Overall, this experiment shows that ILA$^{CRH}$ cells are necessary for SNP.

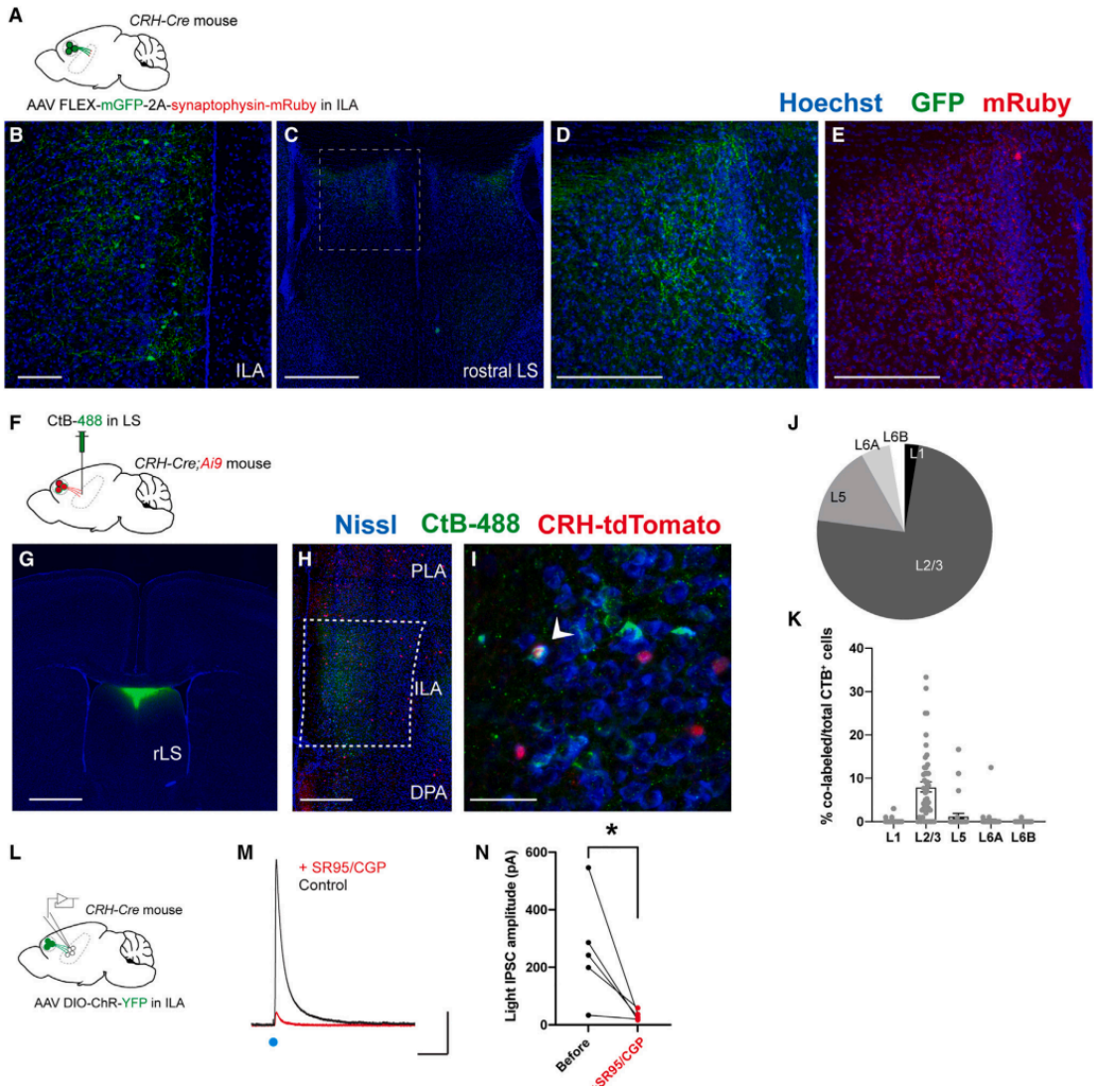


**Figure 1. ILA$^{CRH}$ cells project to rostro-dorsal LS**

(A) CRH-Cre mice injected in ILA with AAV2/DJ hSyn.FLEX.mGFP.2A.Synatophysin-mRuby. (B–E) Immunohistochemistry images of an ILA (B) and LS (C–E) sections labeled for GFP (B–D) or

mRuby (E). Scale bars: 100 mm in (B), 500 mm in (C), and 200 mm in (D) and (E).
(F) CRH-Cre;Ai9 mice injected in rdLS with CtB-488.
(G) Image of a coronal brain section containing the injection site. Scale bars, 1 mm.
(H and I) Images of coronal brain sections containing the mPFC. White arrowheads indicate CtB+/CRH$^+$ cells. Scale bars, 400 mm in (H) and 50 mm in (I).
(J) Distribution of CtB$^+$ cells in ILA (6 mice).
(K) Percentage of co-labeled tdTomato$^+$ and CtB$^+$ over the total number of CtB$^+$ cells per ILA layer. 8 observations per mouse, 6 mice per group. Bar graph represents mean ± SEM. Nested one-way ANOVA, $F_{4,25} = 13.95$, $p < 0.0001$.
(L) CRH-Cre mice injected in ILA with AAV2/9 EF1a.DIO.hChR2(E123T/T159C)-eYFP.
(M) Electrophysiological traces from a rdLS neuron recorded in voltage-clamp configuration at +10 mV. Blue dot, stimulation of CRH$^+$ fibers expressing Channelrhodopsin using 1-ms pulse of blue light to elicit an IPSC before and after application of SR95 and CGP. Scale bars, 100 pA and 100 ms.
(N) IPSC amplitude before and after SR95 and CGP application (5 cells from 4 mice; paired t test, $p = 0.04$). See also Figures S1, S2, and S3.

How ILA$^{CRH}$ cells regulate SNP is however unclear. Are they regulating social memory or rather processes that utilize social memory cues such as SNP? Because the mPFC is involved in executive functions,[27] we hypothesized that ILA$^{CRH}$ cells leverage social memory cues to promote SNP by regulating social interactions with novel and/or familiar mice. Specifically, do ILA$^{CRH}$ cells support SNP ‘‘by promoting interactions with the novel mouse or by suppressing interactions with the familiar one’’? During the learning phase of the SNP test, test mice explored each novel conspecific to the same extent than control mice (Figure S5F), suggesting that silencing ILA$^{CRH}$ cells does not impair social interactions with novel animals. We therefore tested the role of ILA$^{CRH}$ cells during the repetitive social interaction test, where a sex- and age-matched novel mouse is presented four times to the test mouse (Figure 2F). This test offers the advantage of observing the evolution of social interaction with a single novel mouse becoming gradually familiar. Control mice showed a progressive decrease in interaction time with repeated presentations of the mouse (Figure 2G). When a novel mouse was presented in the final trial, the interaction time jumped back to its initial level, demonstrating that the decrease was not due to a loss of engagement in the task. In contrast, mice expressing iDREADD showed no decrease in interaction time during the repeated

presentations, suggesting that $ILA^{CRH}$ cells are necessary for social familiarization (Figure 2G). We repeated the experiment with saline instead of CNO, and both groups exhibited a steady decrease in interaction (Figure S5G). Next, we asked whether over-activating $ILA^{CRH}$ cells could promote social familiarization and repeated the repetitive social presentation test with mice expressing an excitatory DREADD (eDREADD) in $ILA^{CRH}$ neurons. Increasing the activity of $ILA^{CRH}$ cells slightly facilitated the decrease in social interaction (Figures 2H and S5H), indicating that $ILA^{CRH}$ cells can bidirectionally modulate the interaction time with familiar mice. Taken together, these experiments suggest that $ILA^{CRH}$ cells suppress social interactions with familiar mice. To confirm our chemogenetic approach, CRH-Cre mice expressing eDREADD or iDREADD in ILA were injected with CNO or saline before presenting them with a familiar animal (Figure S6A). We measured the overlap between c-fos and mCherry expression in ILA (Figures S6B and S6C). iDREADD-expressing mice given CNO exhibited less c-fos/$mCherry^{+}$ cells compared with the saline control, suggesting $ILA^{CRH}$ cells silencing. By contrast, eDREADD-expressing mice injected with CNO showed an increased c-fos/mCherry+ overlap, suggesting $ILA^{CRH}$ cell excitation. Finally, we asked whether ILACRH cells specifically control social interactions, or does it extend to objects as well? We performed tests of novel object recognition, repetitive object presentation, and familiar food preference while silencing $ILA^{CRH}$ cells and found no effect (Figure S7), indicating that $ILA^{CRH}$ neurons specifically regulate social preferences.

**$ILA^{CRH}$ neurons respond preferentially during familiar social interactions**

If $ILA^{CRH}$ cells regulate social interactions with familiar mice, we can expect the cells to be more active when the mouse interacts with familiar mice than with novel ones. To test this prediction, we performed fiber photometry of $ILA^{CRH}$ cell population. We injected the ILA of CRH-Cre mice with a Cre-dependent AAV expressing the calcium sensor GCaMP6f and implanted an optical ferrule above ILA (Figures 3A and S8A). Subject mice were presented with novel then familiar mice as we recorded calcium activity (Figures 3A–3C). First, we calculated the peri-stimulus time histogram using the start

of social interaction to synchronize traces (Figure 3D) and found that familiar mouse presentation elicited a large increase of the calcium response while presentation of a novel mouse elicited a small decrease (Figure 3E). Then, we automatically detected calcium transients throughout the 2-min presentations and measured their average amplitude and frequency during each trial. The peaks were higher during familiar compared with novel mouse presentation (Figure 3F), but we saw no difference in the frequency of events (Figure 3G). We inverted the order of social presentation and obtained the same results (Figure 3H). These observations suggest that $ILA^{CRH}$ neuron population activity is increased during familiar encounters compared with novel ones.

To confirm whether $ILA^{CRH}$ cell activity differs during novel and familiar mouse presentation, we trained linear classifiers to discriminate between interactions with a novel or familiar mouse using our fiber photometry recordings. We implemented 2 classifiers using either individual recording sessions (individual) or a meta-session pooling all sessions (pseudo-simultaneous, Figure 3I).48 For each classifier, we also computed chance levels using permutation tests (gray bars). Most individual recording sessions yielded a decoding performance above chance with an average 68% accuracy. The pseudo-simultaneous data yielded a decoding performance even higher (79%). These results show that the $ILA^{CRH}$ cell population can code for social familiarity. We also presented novel and familiar objects and saw no change in activity compared with baseline (Figure 3J) or between novel and familiar object (Figures S8B–S8D). Using the peak amplitudes, we calculated the DIs for familiarity preference following object or social presentation (Figure 3K). DIs of social interaction showed a strong preference for social familiarity, unlike the one for object interaction. We then recorded $ILA^{CRH}$ neurons during the repetitive social presentation test and found the peak amplitude to increase during familiarization (Figure 3L). The frequency of events however remained stable (Figure 3M), similar to what was observed previously (Figure 3G). As a further assay of neuronal activity, we measured the expression of the immediate-early gene c-fos. CRH-Cre;Ai9 mice were presented with a novel or familiar mouse for 2 min (Figure 3N). As expected, mice interacted more

with novel than familiar mice (Figure 3O). Mice were perfused 1 h later and processed for c-fos immunohistochemistry in order to count the number of ILA$^{CRH}$ neurons expressing c-fos (Figure 3P). Despite shorter interactions, ILA$^{CRH}$ cells in layer 2/3 exhibited higher c-fos expression following encounters with familiar mice compared with novel (Figure 3Q), similar to what was already reported for the entire ILA cell population.23 Indeed, the activation of layer 2/3 ILA$^{CRH}$ cells negatively correlated with the amount of social interaction (Figure 3R). Overall, our experiments demonstrate that the ILA$^{CRH}$ cell population is more active during interaction with a familiar mouse than a novel one.

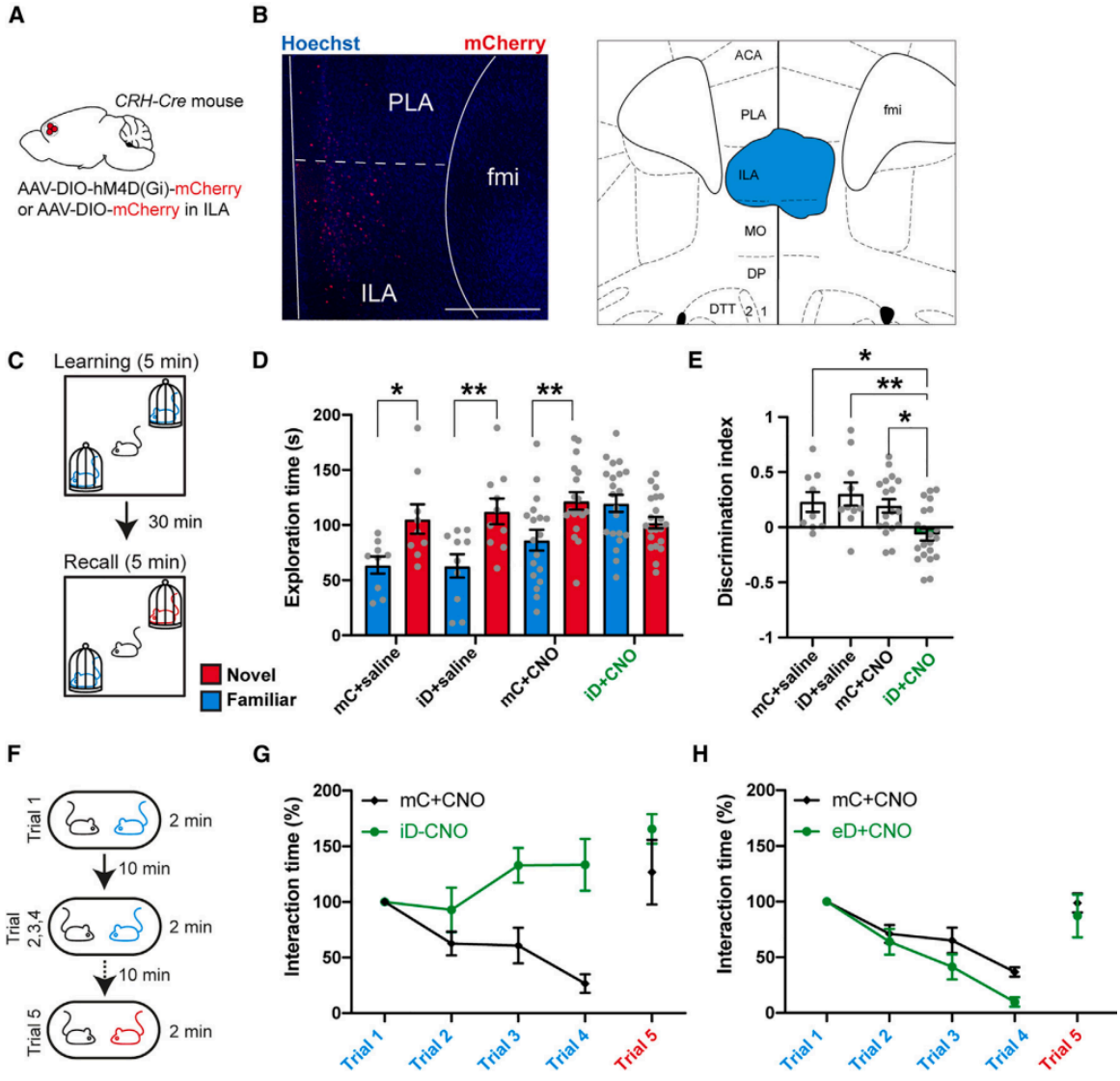

**Figure 2. ILA$^{CRH}$ cells support social novelty preference and familiarization**

(A) CRH-Cre mice injected in ILA with AAV2/8 hSyn.DIO.hM4D(Gi)-mCherry (iDREADD) or AAV2/8 hSyn.DIO.mCherry.

(B) Left, immunohistochemistry image showing the extent of iDREADD expression. Scale bars, 500 mm. Right, maximal extent of iDREADD expression across several mPFC sections.

(C) Schematic of the social novelty preference test.

(D) Interaction time with novel or familiar mice during recall in mice expressing mCherry (mC) or hM4Di (iD) injected with saline or CNO. Each dot is one mouse. Three-way ANOVA: F(novelty x injection x virus)1,108 = 3.471, p = 0.02. Sida´k's multiple comparison tests novel vs. familiar: p = 0.04, 0.006, 0.008, and 0.3.

(E) Discrimination indexes for social novelty preference of the four groups during recall trial. One-sample t tests vs. 0: p = 0.04, 0.02, 0.006, and 0.2. Two-way ANOVA: F(virus x injection)1,54 = 4.7, p = 0.03; F(virus )1,54 = 7.1, p = 0.01; F(injection)1,54 = 1.5, p = 0.2. Tukey's multiple comparison tests compared with the iD +CNO group: p = 0.04, 0.004, and 0.02.

(F) Schematic of the repetitive social presentation test.

(G) Normalized interaction times during social presentations (iDREADD-expressing and control mice injected with CNO). 8 mice per group. Two-way ANOVA: F(trial1-4 x virus)3,55 = 5.44, p = 0.002; F(trial)3,55 = 1.28, p = 0.2; F(virus)3,55 = 26.82, p < 0.0001. Post-hoc Sida´k's multiple comparison tests between mC and iD groups: trial 2, p = 0.4; trial 3, p = 0.004; and trial 4, p < 0.0001.

(H) Normalized interaction times during repetitive social presentation test in CRH-Cre mice injected in ILA with AAV5 hSyn.DIO.hM3D(Gq)-mCherry or with AAV5 hSyn.DIO.mCherry as a control. 8 mice per group. Two-way ANOVA: F(trial1–4 x virus)3,56 = 1.36, p = 0.3; F(trial)3,56 = 33.05, p < 0.0001; and F(virus)1,56 = 6.765, p = 0.01. For the entire figure, bar graphs represent mean ± SEM. See also Figures S4, S5, S6, and S7.

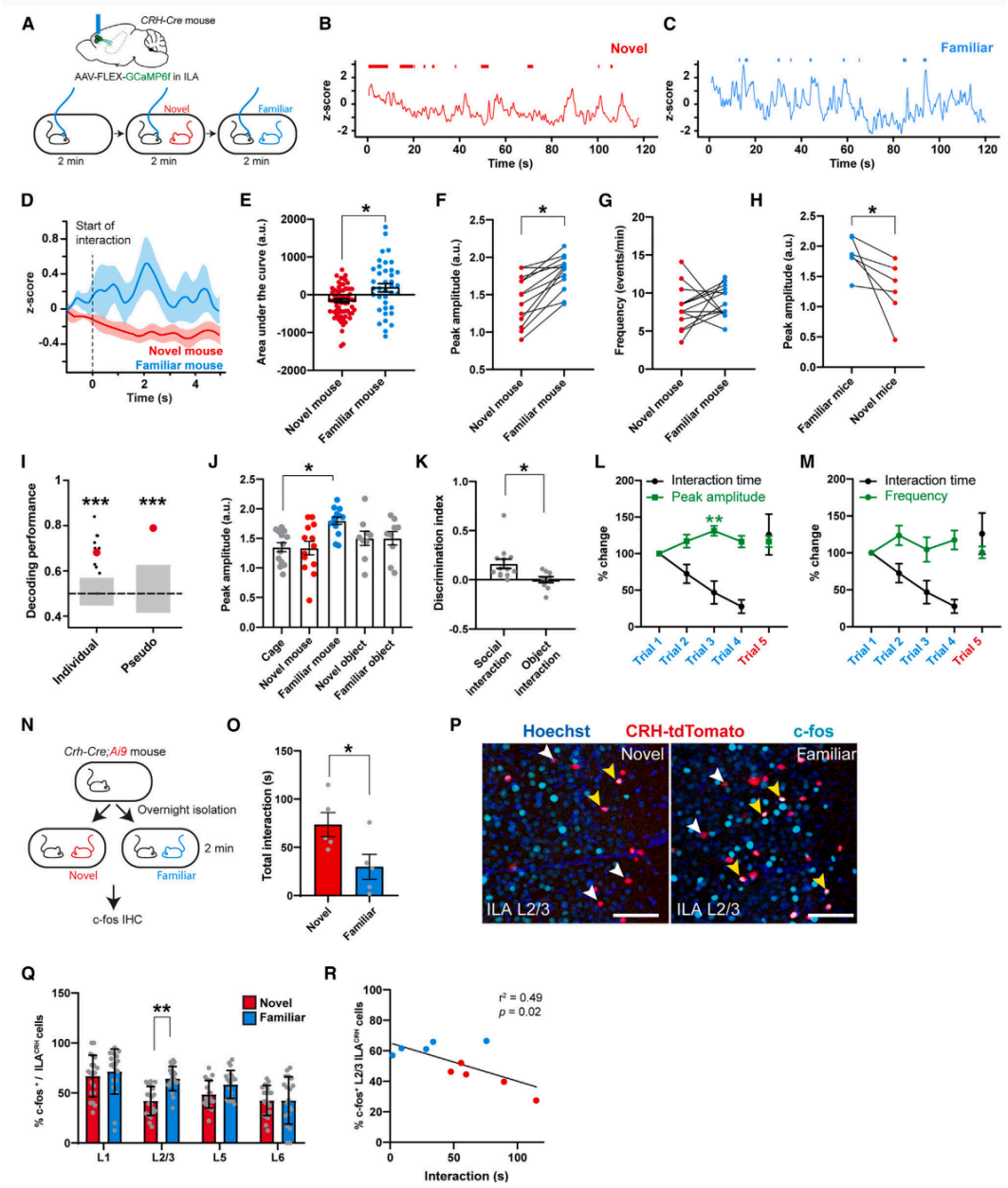


**Figure 3. ILA$^{CRH}$ cells respond preferentially to familiar mouse presentation**

(A) CRH-Cre mice injected in ILA with AAV2/1 syn.FLEX.GCaMP6f and implanted with an optical ferrule over ILA (top). Schematic of the fiber photometry recording experiment (bottom). (B and C) Example traces of recording during presentation of a novel (B) or familiar (C) mouse to the same test mouse. Interaction bouts intervals are shown above each trace. (D) Peri-stimulus time histogram during social interaction with novel or familiar mouse (5 mice). (E) Area under the curve during familiar and novel mouse interaction. Each dot is one interaction (5 mice). One-sample nested t test: familiar vs. 0, p = 0.001, novel vs. 0, p = 0.001. Nested t test between groups: p = 0.01.

(F) Average peak amplitude of the Zscore during social presentations of a novel then familiar mouse. For (F)–(K), each dot is a different recording session (5 mice in total). Nested t test between groups: p =0.02.

(G) Frequency of calcium events during presentation of a novel then familiar mouse. Nested t test: p = 0.4.
(H) Average peak amplitude of the Zscore during inverted presentation of a familiar then a novel mouse. 3 mice per groups. 2 observations per mice. Nested t test,p = 0.03.
(I) Decoding performance for familiarity vs. novelty from individual recordings or pseudo-simultaneous data. Small black dots on the left are individual recording sessions (5 mice). Red dot is the average. Red dot on the right is the result of pseudo-population analysis. Gray areas denote chance levels computed using permutation tests.
(J) Average peak amplitude during each type of presentation (novel then familiar experiments only). Nested one-way ANOVA Z score x trials: F4,16 = 2,933, p =0.05. Dunnett's multiple comparison cage vs. novel: p = 0.9, familiar: p = 0.03, novel object: p = 0.7, familiar object: p = 0.7.
(K) Discrimination indexes for familiarity preference calculated from Z scores during mouse or object presentation. One-sample t test: p = 0.004 and 0.9. Nested t test social vs. object: p = 0.01.
(L) Fiber photometry recording during repetitive social presentation test (10 sessions in 5 mice). Nested one-way ANOVA: F3,36 = 3.48, p = 0.02. Dunnett's multiple comparison tests: T1 vs. T2, p = 0.2; T1 vs. T3, p = 0.008; T1 vs. T4 p = 0.2.
(M) Frequency of calcium events during repetitive social presentation test (10 sessions in 5 mice). Nested one-way ANOVA Z score x trials: F3,16 = 0.63 N. CRH-Cre;Ai9 mice were presented with novel or familiar mice after overnight isolation before being processed for immunohistochemistry.
(O) Interaction times following 2 min social presentation. Each dot is one mouse. Unpaired t test, p = 0.04.
(P) Immunohistochemistry images of c-fos labeling in ILA layer 2/3. Yellow arrowheads: c-fos$^+$/tdTomato$^+$ cells. White arrowheads: c-fos$^+$/tdTomato+ cells. Scale bars, 100 mm.
(Q) Percentage of ILA$^{CRH}$ cells positive for c-fos per layer. 4 observations per mouse, 5 mice per group. Nested t test: p = 0.003.
(R) Percentage of layer 2/3 ILA$^{CRH}$ cells positive for c-fos vs. interaction time during social interaction with novel or familiar mouse. Each dot is one mouse. Pearson's test, p = 0.02. For the entire figure, bar graphs represent mean ± SEM. See also Figure S8.

**CRH release in rLS suppresses social interactions with familiar mice to promote SNP**

How could ILA$^{CRH}$ cells suppress social interactions with a familiar mouse? ILA$^{CRH}$ cells projects to rLS which expresses the CRHR120 and regulates social interactions.20 This led us to ask whether CRH release from ILA into rLS is necessary for familiarization. We designed a Cre-dependent short hairpin RNA (shRNA) against Crh (see STAR Methods) and expressed it into ILA$^{CRH}$ neurons (Figure 4A, top). To assess the efficacy of Crh silencing, we quantified Crh and mCherry levels using in situ hybridization (Figure 4A, bottom). ILA$^{CRH}$ cells expressing the anti-Crh shRNA and mCherry showed a 4-fold decrease in the intensity of Crh labeling compared with nearby non-infected CRH$^+$ cells that did not express mCherry (Figures 4A and 4B). No change was detected in cells expressing the

scrambled shRNA (Figures 4A and 4B). These results indicate that our strategy to reduce Crh level in $ILA^{CRH}$ neurons is both specific and efficient. Next, we tested CRH-Cre mice expressing scrambled or antiCrh shRNAs during repetitive social presentations. Mice expressing the anti-Crh shRNA in $ILA^{CRH}$ cells showed very little familiarization unlike mice expressing the scrambled shRNA (Figure 4C). Then, we tested the mice for SNP. Mice expressing anti-Crh shRNA showed no preference during the recall trial (Figure 4D) and the DI of this group was null (Figure 4E). Total exploration during learning or recall trials was not different between groups (Figures S9A and S9B). Given that $ILA^{CRH}$ neurons co-express GABA (Figures S3E and S3F), we repeated the same experiments using a shRNA against vesicular GABA transporter (vGAT) mRNA (Figures S9C and S9D),[49] which had been used previously to knock down vGAT expression in hypothalamic CRH+ neurons.50 Unlike knocking down Crh, knocking down vGAT expression in $ILA^{CRH}$ cells failed to impair familiarization or SNP (Figures S9E–S9H). Even though we did not observe $ILA^{CRH}$ projections in any region other than rdLS (Figure S1C), we sought to validate our previous results using a retrograde targeting approach. We injected a monosynaptic retrograde virus expressing Cre in rdLS (HSVCre) and the Cre-dependent viruses expressing the anti-Crh shRNA or the scrambled shRNA in the ILA of wild-type (WT) mice (Figure S9I). Removing Crh from rdLS-projecting cells in ILA impaired familiarization and SNP (Figures S9J–S9N), similar to our previous results. We then asked whether CRH release from $ILA^{CRH}$ in rLS cells was necessary to mediate familiarization and SNP. First, we sought to confirm that CRH release in LS occurs preferentially during familiar social interaction and leveraged the recently developed CRH-biosensor CRF1.0.51 WT mice were injected in rdLS with an AAV expressing CRF1.0, and an optical ferrule was implanted above it (Figure 4F). We presented novel and familiar mice in a random order meanwhile recording CRH activity events (Figure 4H). Presentation of a familiar mouse induced responses of larger amplitude compared with the presentation of a novel mouse (Figure 4I), despite the mice interacting less (Figure 4G). There was no change in the frequency of events (Figure 4J). The DI based on Z score peak amplitude (see STAR Methods) showed a significant preference for

the response for familiar mice (Figure 4K). This experiment fits with our calcium recordings of $ILA^{CRH}$ cells and demonstrates that CRH release in rLS is higher during familiar social interactions compared with novel social interactions. Next, we used optogenetics to silence $ILA^{CRH}$ cell terminals in rdLS. CRH-Cre mice were injected in ILA with Cre-dependent AAVs expressing Archaerhodopsin (Arch) tagged with tdTomato (Arch mice) or tdTomato only as a control (tdT mice), and an optical ferrule was implanted above rdLS (Figure 4L). Light from a 561-nm laser was applied continuously during either the learning or recall trials of the SNP test. When light was applied during the learning trial, both groups exhibited SNP during the recall trial. However, when light was applied during the recall trial, mice expressing Arch failed to show a preference for the novel mouse while mice expressing tdTomato only did (Figures 4M and 4N). All groups showed the same extent of total interaction during learning and recall (Figures S9O and S9P). We also tested the mice during repetitive social presentations and applied the light stimulation during trials 2–4 or no light. Arch mice exposed to light failed to familiarize to the novel mouse unlike tdT mice exposed to light or Arch mice with no light (Figure 4O). We tested the efficiency of our terminal silencing approach combining Arch-mediated silencing and CRH recording. CRHCre mice were injected with a Cre-dependent virus expressing Arch in the ILA and a virus expressing the biosensor CRF1.0 in rdLS (Figures S10A and S10B). Two optical ferrules were implanted above rdLS. Then, we exposed the mice to a familiar mouse for 3 sessions of 2 min separated by 10 min intervals. The 561 nm laser was turned on only during the middle presentation in order to stimulate Arch in $ILA^{CRH}$ terminals in rdLS (Figure S10C). Activating Arch efficiently decreased the frequency of CRH-related transients (Figure S10D). The amplitude of the transients followed a similar trend (Figure S10E). Importantly, turning on the laser increased the amount of social interaction with the familiar mouse, suggesting that $ILA^{CRH}$ fibers regulate the amount of social interaction with familiar mice (Figure S10F). Taken together, these experiments show that CRH release from $ILA^{CRH}$ cells in rdLS during social encounters suppress social interactions with familiar mice to promote SNP.

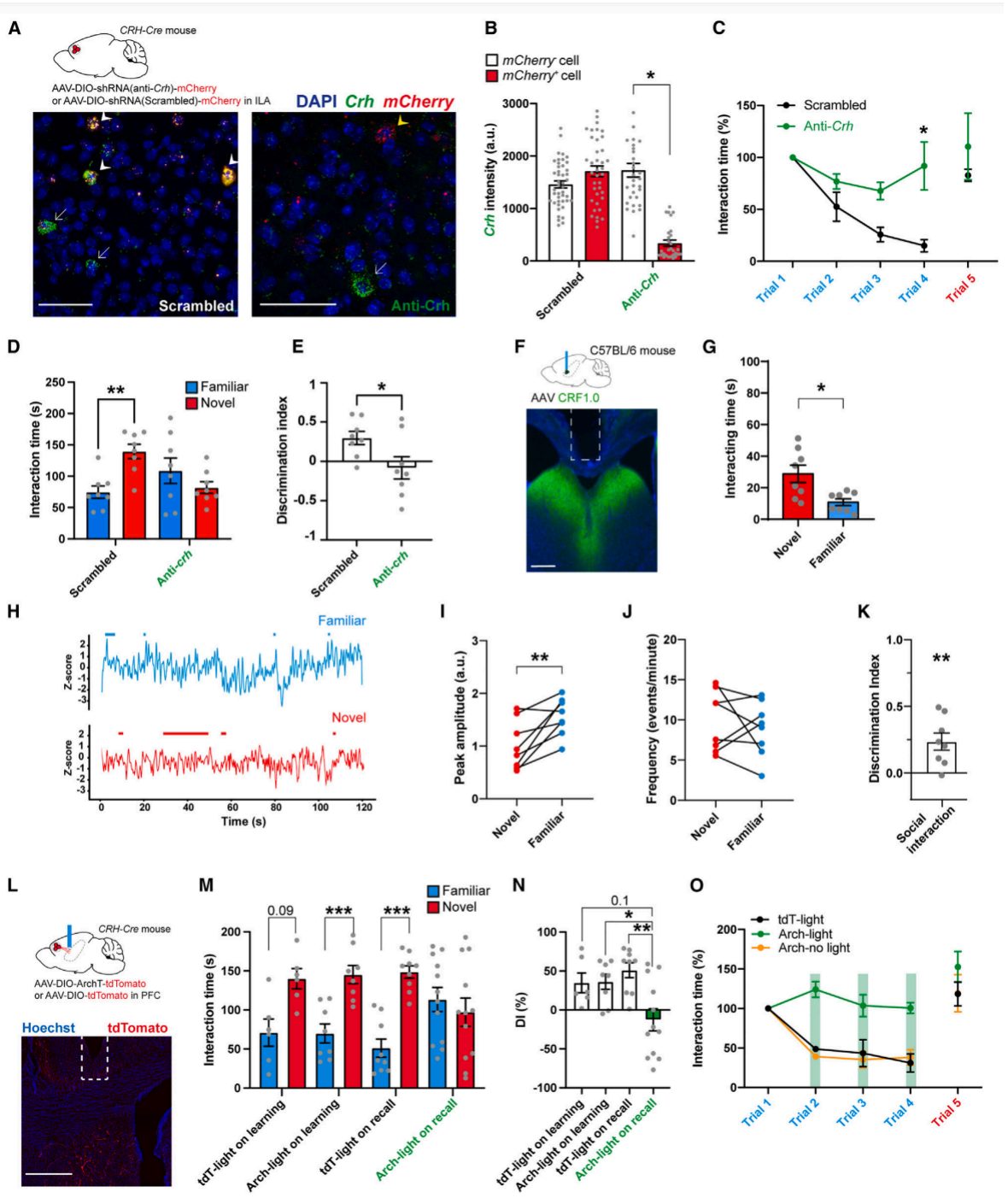


**Figure 4. CRH release from ILA in rdLS suppresses social interactions with familiar mice and supports social novelty preference**

(A) CRH-Cre mice injected in ILA with AAV2/9 CMV-DIO-(mCherry-U6)-shRNA(anti-Crh) to downregulate Crh or control AAV2/9 CMV-DIO-(mCherry-U6)-shRNA(scrambled) (top). In situ hybridization images of ILA slices expressing the scrambled shRNA (right) or the shRNA against Crh (left) labeled for mCherry and Crh. White arrows denote CRH+ neurons that do not express the virus. Yellow arrowhead denotes $CRH^+$ cells expressing the anti-Crh shRNA, with reduced level of Crh. White arrowheads denote $CRH^+$ neurons expressing the scrambled shRNA, with intact Crh level.

Scale bars, 50 mm.

(B) Quantification of Crh expression. In each slice neurons were classified as to whether they were uninfected or infected with virus based on mCherry expression (each dot is a different neuron, 3 mice per group). Nested one-way ANOVA $F_{3,8} = 6.41$, $p = 0.016$. Tukey's multiple comparison test between anti-Crh groups, $p = 0.03$.
(C) Normalized interaction time during the repetitive social presentation test in mice expressing scrambled or anti-Crh shRNAs. 4 mice per group. Two-way ANOVA: F(trial x virus)$_{3,24} = 4.4$, $p = 0.01$; F(trial)$_{3,24} = 9.6$, $p = 0.0002$; F(virus)$_{1,24} = 21.9$, $p < 0.0001$. Tukey's multiple comparison test between scrambled and anti-Crh groups: trial 2, $p = 0.8$; trial 3, $p = 0.2$; trial 4, $p = 0.009$.
(D) Interaction time with familiar or novel mouse during the recall trial of the social novelty preference test in mice expressing scrambled or anti-Crh shRNAs. Each dot is one mouse. Two-way ANOVA F(novelty x virus)$_{1,28} = 11.53$, $p = 0.002$. Sida´k's multiple comparison tests novel vs. familiar: $p = 0.004$ and 0.3.
(E) Discrimination indexes for social novelty preference during recall trial. One-sample t test vs 0: $p = 0.009$ and 0.6. Unpaired t test: $p = 0.03$.
(F) Top, C57BL/6J wild-type mice injected in rdLS with AAV2/9 Syn.CRF1.0 and implanted with an optical ferrule above rdLS. Bottom, immunohistochemistry image showing CRF1.0 expression in rdLS and the optical ferrule implanted above the injection site. Scale bars, 300 mm.
(G) Bar graph showing the interaction time with novel and familiar mice (8 mice). Paired t test, $p = 0.002$.
(H) Trace of a representative fiber photometry recording during interaction with a familiar mouse or a novel mouse. Interaction bouts are shown above each trace.
(I) Average peak amplitude of the Z score during presentation of a novel or familiar mouse (8 mice). Paired t test: $p = 0.008$.
(J) Frequency of events during presentation of a novel or a familiar mouse. Paired t test: $p = 0.5$.
(K) Discrimination index for social familiarity preference calculated from Z scores. One-sample t test: $p = 0.008$.
(L) CRH-Cre mice injected in ILA with AAV2/2 CAG.FLEX.ArchT-tdTomato or control AAV2/2 CAG.FLEX.tdTomato. Optical ferrule implant is above rdLS. Scale bars, 500 mm.
(M) Interaction time with familiar (blue) or novel (red) mouse during the recall trial of the social novelty preference test in the same mice. Laser was on during the learning or recall trial. Each dot is a mouse. Three-way ANOVA F(novelty x light x virus)$_{1,62} = 14{,}44$, $p = 0.007$. Sida´k's multiple comparison tests novel vs. familiar: $p = 0.03$, 0.004, <0.0001, and 0.8.
(N) Discrimination index for social novelty preference during recall trial of the social novelty preference test. One-sample t test: $p = 0.04$, 0.007, 0.0007, and 0.4. Two-way ANOVA: F(virus x light)$_{1,31} = 6.232$, $p = 0.01$; F(light)$_{1,31} = 1.578$, $p = 0.2$; F(virus)$_{1,31} = 5.701$, $p = 0.02$. Sida´k's multiple comparison tests: $p = 0.09$, 0.04, and 0.003.
(O) Normalized interaction time during the repetitive social presentation test. The laser was on during trials 1 to 4 of the Arch-light and mC-light groups (4 and 3 mice, respectively). Laser was not on for the Arch-no light group (4 mice). Two-way ANOVA: F(trial1-4 x virus)$_{6,32} = 5.84$, $p = 0.0003$; F(trial)$_{3,32} = 14.35$, $p < 0.0001$; F(group)$_{2,32} = 49.32$, $p < 0.0001$. For the entire figure, bar graphs represent mean ± SEM. See also Figure S9 and S10.

**CRHR1 activation in rdLS suppresses social interaction with familiar mice and support SNP**

Since CRHR1 regulates social interaction and SNP,[20,32,42] we looked whether it was expressed in the vicinity of the $ILA^{CRH}$ cells terminals in LS. We injected CRHR1-Cre mice (courtesy of Jan Deussing)52 with a Cre-dependent AAV expressing GFP and labeled several neurons in rdLS (Figure 5A), the same region targeted by terminals of $ILA^{CRH}$ cells (Figures 1C and 1D). Then, we crossed the CRHR1-Cre line with the Ai9 tdTomato reporter in order to visualize $CRHR1^{+}$ neurons, prepared acute LS slices and obtained whole-cell patch-clamp recordings from rdLSCRHR1 neurons clamped at 60 mV. Application of 300 nM stressin-1, a CRHR1 agonist, induced an inward current (Figure 5B), similar to previous results.53 This experiment suggests that CRH release in rdLS depolarizes $CRHR1^{+}$ neurons. Then, we implanted WT mice with a cannula in rdLS and infused them with the CRHR1 antagonist antalarmin diluted in DMSO54 or DMSO only before running them for the SNP test (Figure 5C). Mice infused with DMSO exhibited normal preference for the novel mouse whereas mice infused with antalarmin showed no novelty preference (Figures 5C and 5D). Total exploration time during learning or recall was not different between groups (Figures S11A and S11B). Next, we performed chemogenetic silencing of $CRHR1^{+}$ neurons in rdLS. We injected CRHR1-Cre mice with a Cre-dependent AAVs expressing iDREADD tagged with mCherry or mCherry only (Figure 5E). Then, we tested the mice for SNP and observed a preference for the novel mouse in the 3 control groups but not in the test group (Figure 5F). Consequently, the DI of the test group was not different from 0 unlike the ones of the control groups (Figure 5G). The total interaction times during learning or recall or the interaction time with each novel mouse during learning were similar across all groups (Figures S11C– S11E). We also ran the mice for the repetitive social presentation test and observed no familiarization in the test group (Figure 5H). Overall, these experiment shows that activation of the CRHR1 receptor in rdLS is necessary for familiarization and SNP. Then, we tested whether $CRHR1^{+}$ neurons in rdLS were preferentially activated during familiar encounters compared with novel ones. We presented CRHR1-Cre;Ai9 mice with either novel or familiar mice before perfusing

them and labeling for c-fos (Figure 5I). The percentage of rdLSCRHR1 neurons expressing c-fos during familiar interaction was 3-fold higher than the one during novel interaction (Figure 5J). Overall, these experiments demonstrate that rdLSCRHR1 neurons are preferentially recruited during familiar encounters in order to regulate familiarization and SNP.

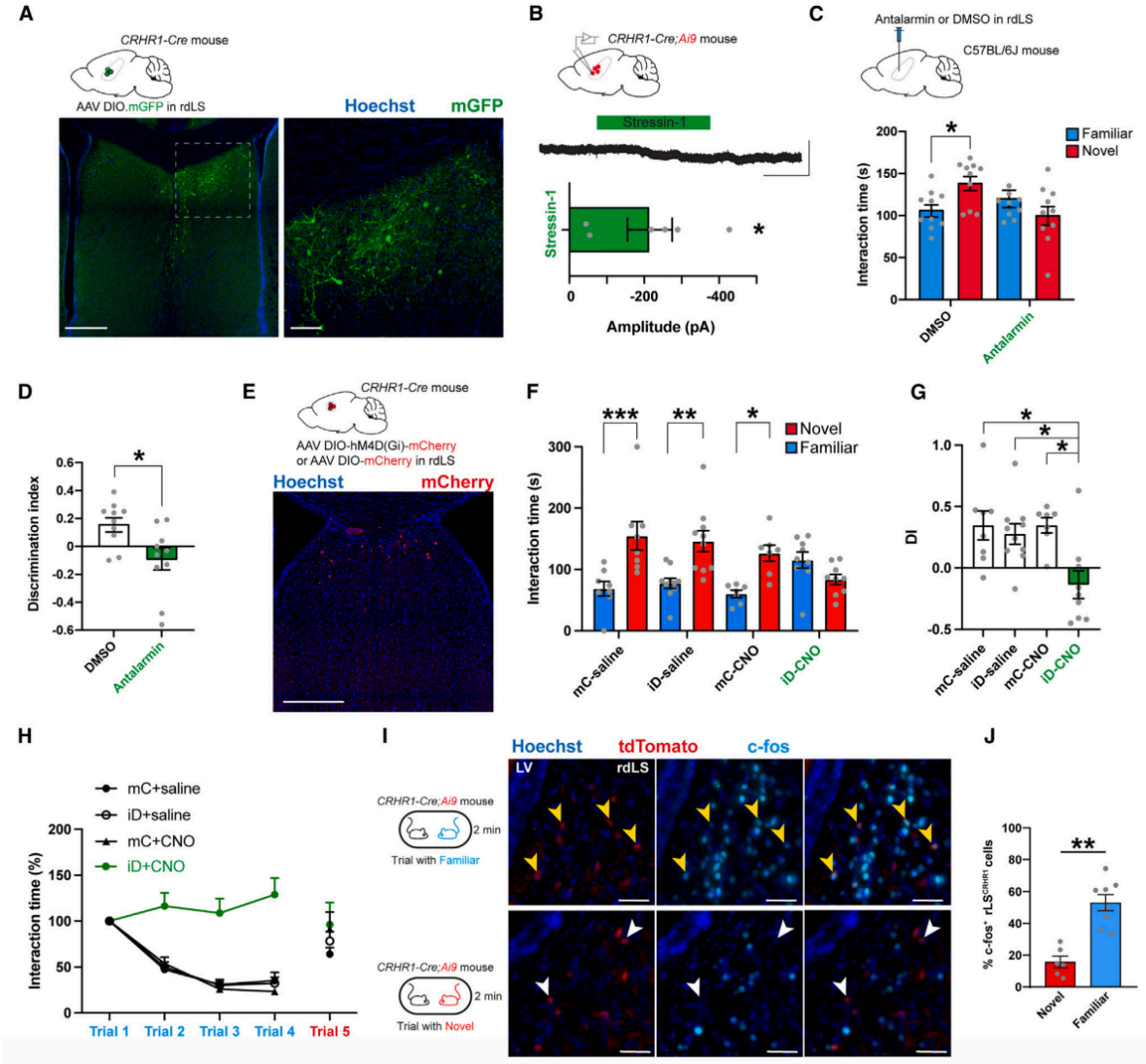


**Figure 5. CRHR1$^{+}$ neurons in rdLS are activated by social familiarity and regulate SNP and familiarization**

(A) CRHR1-Cre mice injected in rdLS with AAV2/5 hSyn.DIO.mGFP. Scale bars: 300 mm in (left) and 50 mm in (right).

(B) Whole-cell patch-clamp recording of CRHR1-tdTomato cells in rdLS of CRHR1-Cre; Ai9 mice (top). Voltage-clamp trace during bath application of 300 nM

stressin-1 (middle). Scale bars: 100 pA and 2 min. Bar graph showing the amplitude of the decrease (bottom). 6 observations from 3 mice. One-sample t test, p = 0.02.
(C) C57BL/6J wild-type mice infused in rdLS with 2 mg of antalarmin dissolved in 0.6 mL of DMSO or DMSO as a control (top). Interaction time with familiar (blue) or
novel (red) mouse during the recall trial of the social novelty preference test in mice infused with antalarmin or DMSO (bottom). Each dot is a mouse. Two-way ANOVA F (novelty x injection)1,36 = 7.699, p = 0.009. Sida´k's multiple comparison tests novel vs. familiar: p = 0.04 and 0.3.
(D) Discrimination index for social novelty preference during recall trial. One-sample t test: p = 0.003 and p = 0.2. Unpaired t test: p = 0.01.
(E) CRHR1-Cre mice injected in rdLS with AAV2/8 hSyn.DIO.hM4D(Gi)-mCherry (iDREADD) or AAV2/8 hSyn.DIO.mCherry (top). Immunohistochemistry pictures of iD-mCherry expression in rdLS. Scale bars, 300 mm (bottom).
(F) Interaction time with novel (red) or familiar (blue) mouse during the recall trial of the social novelty preference test in mice expressing mCherry (mC) or hM4Di
(iD) and injected with saline or CNO. Each dot is a mouse. Three-way ANOVA F (novelty x injection x virus)1,60 = 4.137, p = 0.04. Sida´k's multiple comparison tests novel vs. familiar: p = 0.0003, 0.001, 0.01, and 0.4.
(G) Discrimination indexes for social novelty preference during recall trial. One-sample t test: p = 0.02, 0.009, 0.001, and 0.3. Two-way ANOVA: F (virus x injection)1, 30 = 4.3, p = 0.04; F(virus )1, 30 = 7.654, p= 0.009; F(injection)1, 30 = 4.263, p= 0.05. Tukey's multiple comparison tests compared with the iD +CNO group: p = 0.009, 0.02, and 0.01. (H) Normalized interaction times during repetitive social presentations. 7–8 mice per group. Two-way ANOVA, F(trial1-4 x virus)9,104 = 6.612, p < 0.0001; F(trial)3,104 = 28.05, p < 0.0001; F(virus)3,104 = 52.74, p < 0.0001.
(I) Immunohistochemistry pictures against c-fos of CRHR1-tdTomato mouse rdLS of following interaction with a familiar or novel mice. Scale bars, 50 mm.
(J) Percentage of $CRHR1^{+}$ neurons expressing c-fos. 2 observations per mice, 3 and 4 mice per group. Nested t test, p = 0.007.
See also Figure S11.

**CRHR1 activation disinhibits rLS to suppress social interactions with familiar mice**

What is the effect of CRHR1 activation in rLS? We prepared acute LS slices from WT mice and recorded spontaneous inhibitory post-synaptic currents (IPSCs) from rdLS cells in whole-cell configuration before applying the CRHR1 agonist stressin-1 (300 nM) (Figures 6A and 6B).53 Stressin-1 application for 15 min decreased the frequency and integrated charge of spontaneous IPSCs (Figures 6B, 6C, and 6E). IPSC amplitude also exhibited a trend toward a decrease (Figure 6D). This effect was not seen when rLS neurons were recorded for 15 min without application of the agonist (Figure S12A). In addition, application of stressin-1 while recording from ventral LS (vLS) neurons in posterior LS slices had no effect (Figure S12B), suggesting that the agonist effect was not

generalized to the entire LS and consistent with the pattern of CRHR1 expression (Figure 5A).20 Taken together, these results suggests that CRH release disinhibits rLS neurons. Next, we thought of eliciting CRH release in rdLS from ILA fibers since CRH could originate from other regions. We expressed ChR in $ILA^{CRH}$ neurons and prepared rdLS slices (Figure 6F). We obtained whole-cell recordings of rdLS neurons and recorded spontaneous inhibitory events (sIPSC) before and after applying a tetanic light stimulation. Light stimulation induced a decrease in sIPSC frequency, amplitude and charge (Figures 6G–6I), similar to stressin-1 application. In addition, we applied a local electrical stimulation to induce a large IPSC, the amplitude of which was also decreased following tetanic light stimulation (Figure 6J). We repeated these recordings with 300-nM antalarmin in the bath to confirm that the decrease in inhibition following light stimulation was CRHR1 dependent. Indeed, antalarmin application blocked the decrease in frequency, amplitude, charge, and electrical stimulation, thereby blocking the disinhibition (Figures 6G–6J). Taken together, these results demonstrate that CRH release from ILA disinhibits rLS neurons. Is rLS disinhibited during social interactions with familiar mice and what is the effect of this disinhibition? To answer these questions, we recorded the calcium activity from rLS neuron population using fiber photometry. WT mice were injected in rLS with an AAV expressing GCaMP6f and an optical ferrule was implanted above it (Figures 6K and S13A–S13C). We presented novel and familiar mice and measured the interaction time, average peak amplitude, and peak frequency (Figures 6L–6N). Similar to our recordings of $ILA^{CRH}$ neurons, presentation of a familiar mouse induced transients of larger amplitude compared with the presentation of a novel mouse (Figure 6M), despite the mice interacting less (Figure 6L). There was no change in the frequency of transients however (Figure 6N). The DI based on the peak amplitude (see STAR Methods) showed a significant preference in response to a familiar mouse (Figure 6O). To determine further whether rLS activity alone can differentiate between novel and familiar mouse presentation, we trained linear classifiers to discriminate between interactions with a novel or familiar mouse based on our fiber photometry

recordings. We implemented 2 classifiers using either individual recording sessions (individual) or creating a meta-session pooling all sessions (pseudo-simultaneous, Figure 6P). For each classifier, we also computed chance levels using permutation tests (gray bars). Most individual recording session yielded a decoding performance above chance with an average of 59% accuracy while the pseudosimultaneous data yielded a decoding performance even higher (81%). This shows that rLS neuron population can encode for social familiarity. We also measure rLS activity during the repetitive social presentation test and observed that the peak amplitude of calcium events increased from trial 1 to trial 3 when familiarization is taking place (Figures S13D and S13E). Similar to the percentage of c-fos+ L2/3 ILA$^{CRH}$ cells (Figure 3R), the calcium activity anti-correlated with the amount of social interaction (Figure S13F). Which LS neurons are activated by familiar presentation? We examined c-fos expression in LS following novel or familiar social encounters (Figure 6Q) in the same cohort of mice than the one used to look at c-fos expression in ILA (Figure 3N). rLS responded preferentially to familiar mouse presentation (Figures 6R and 6S), similar to layer 2/3 ILA$^{CRH}$ neurons (Figure 3Q). Interestingly, familiar presentation specifically upregulated c-fos in a spatially defined band of rLS cells bordering the lateral ventricle (Figure 6R, right) while exposure to a novel mouse failed to activate the same population (Figure 6R, left). Taken together, the fiber photometry recordings and c-fos labeling demonstrate that a population of rLS neurons is activated preferentially during a familiar encounter compared with a novel one. Similar to L2/3 ILA$^{CRH}$ neurons, activation of rLS neurons tended to correlate negatively with the amount of social interaction (Figure S14A). Noteworthy, activation of layer 2/3 ILA$^{CRH}$ cells plotted against rdLS activation demonstrated a strong positive correlation, suggesting that one population might control the other (Figure 6T). We also quantified c-fos expression in posterior dLS and posterior vLS and observed no preferential response to familiar presentation compared with novel nor correlation with the amount of interaction (Figures S14B–S14G).

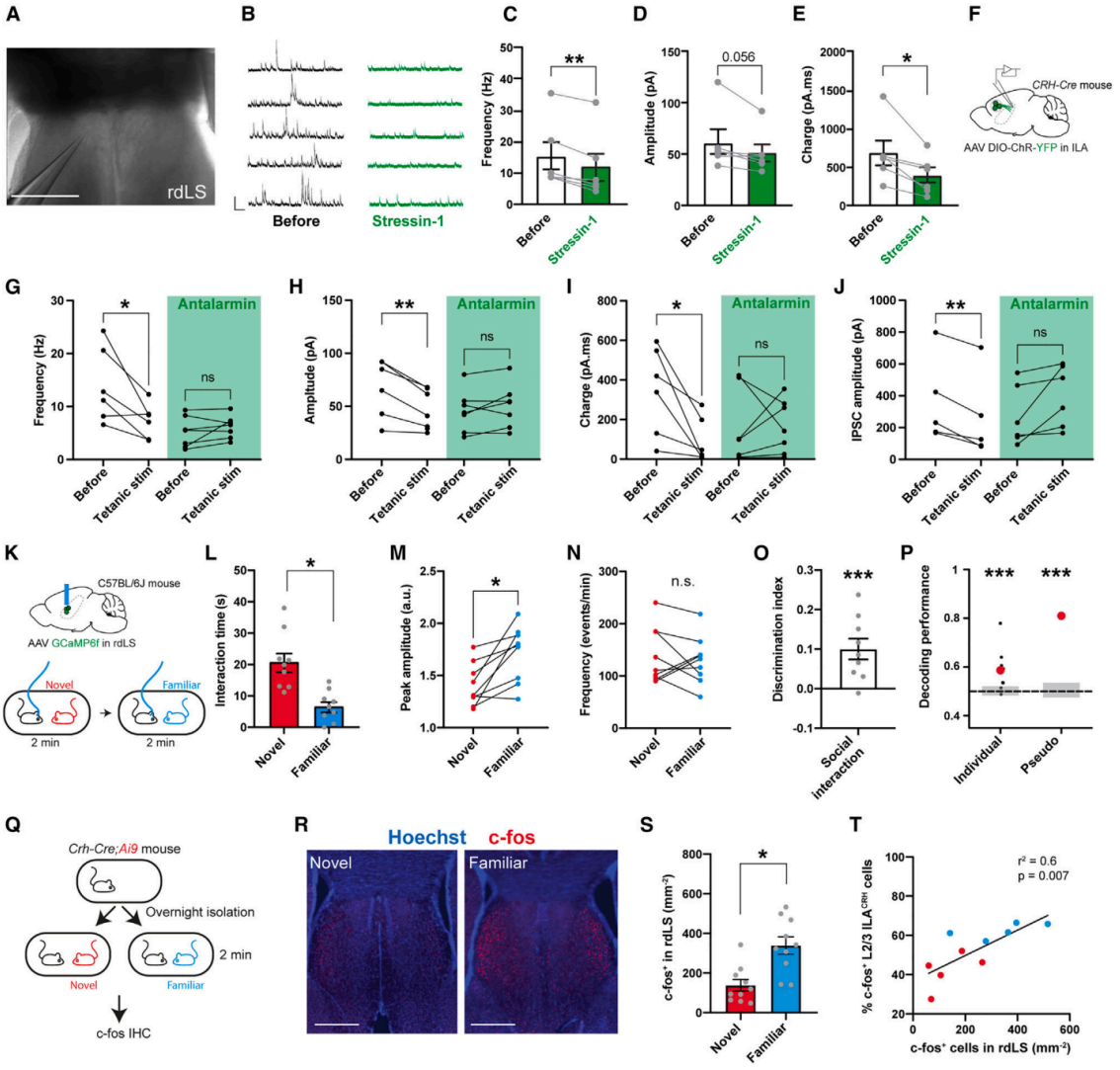


**Figure 6. CRH signaling from ILA and familiar social interaction disinhibit rdLS**

(A) Differential interference contrast microscopy image of rdLS during patch-clamp recording. Scale bars, 500 mm.

(B) Example traces of IPSCs before or 15 min after application of 300-nM stressin-1.

(C) Frequency of IPSCs. Paired t test, p = 0.003.

(D) Amplitude of IPSCs. Paired t test, p = 0.056.

(E) IPSCs area under the curve. For (C)–(E), points are cells recorded from separate slices in 6 mice. Paired t test, p = 0.02.

(F) CRH-Cre mice injected with AAV2/9 EF1a.DIO.hChR2(E123T/T159C)-eYFP in ILA.

(G–I) Frequency (G), amplitude (H), and charge (I) of rdLS neuron spontaneous inhibitory events before and after tetanic light stimulation with or without 300-nM antalarmin in the bath. Each observation is from a different cell in separate brain slices obtained from 6 mice and 5 mice, respectively. Paired t test: p = 0.03, 0.2, 0.0003, 0.2, 0.03, and 0.9.

(J) Electrically evoked IPSCof rdLS neuron spontaneous inhibitory events before and after tetanic

light stimulation with or without 300-nM antalarmin in the ACSF. Paired t test: p = 0.006 and 0.07.
(K) C57BL/6J wild-type mice injected in rdLS with AAV2/1 Syn.GCaMP6f and implanted with an optical ferrule above rdLS. Implanted mice were presented with novel then familiar mice.
(L) Interaction time during social presentation (9 recording sessions in 5 mice). Nested t test, p = 0.01.
(M) Average peak amplitude of the Z score during presentation of a novel or familiar mouse. Nested t test: p = 0.03.
(N) Frequency of events during presentation of a novel or a familiar mouse. Nested t test: p = 0.8.
(O) Discrimination index for social familiarity preference calculated from Z scores. One-sample t test: p = 0.0005.
(P) Decoding performance for familiarity vs. novelty from individual recordings or pseudo-simultaneous data. Small black dots on the left are the results from each individual recording sessions, large red dot is the average. Red dot on the right is the result of pseudo-population analysis. Gray areas denote chance level. Two-tailed permutation tests, p < 0.001 and p < 0.001.
(Q) CRH-Cre;Ai9 mice presented with novel or familiar mice before c-fos labeling.
(R) Immunohistochemistry images of c-fos labeling in rdLS following social presentation with a novel or familiar mouse (cf. Figure 3N). Scale bars, 500 mm.
(S) Density of rdLS cells positive for c-fos. 2 observations per mouse, 5 mice per group. Nested t test, p = 0.02.
(T) Percentage of layer 2/3 $ILA^{CRH}$ cells positive for c-fos (cf. Figure 3) vs. density of rdLS cells positive for c-fos following social interactions. Each dot is one mouse. Pearson's test, p = 0.007.
See also Figures S12, S13, and S14.

**CRH release in rdLS disinhibits rLS to suppress social interactions with familiar mice**

Does the activation of rLS during familiar encounters depends on CRH release from $ILA^{CRH}$ cells? We tested this hypothesis by measuring c-fos expression in mice where Crh was knocked down in ILA, similar to the approach used previously to disrupt memory retrieval.55 CRH-Cre mice were injected in ILA with Cre-dependent AAVs expressing anti-Crh shRNA or a scrambled shRNA control, as described above. Mice were then presented with a familiar littermate and sections containing the ILA, and rLS were labeled for c-fos (Figures 7A–7C). Importantly, mice expressing the anti-Crh shRNA interacted more with a familiar mouse than control mice, suggesting that Crh reduces social interaction with a familiar mouse (Figure 7D). Loss of Crh did not alter c-fos expression in layer 2/3 $ILA^{CRH}$ cells (Figure 7E) but reduced the density of c-fos expression in rLS (Figure 7F). As previously, control mice exhibited a correlation between c-fos levels in layer 2/3 $ILA^{CRH}$ and rLS neurons but mice depleted of Crh in ILA did not (Figure 7G). We next tested whether rdLSCRHR1 cells control the

disinhibition of rdLS following familiar social encounter. We expressed iDREADD in rdLSCRHR1 neurons and injected the mice with CNO before presenting them with a familiar mouse (Figures 7H and 7I). We then perfused the mice and labeled rLS slices against c-fos and mCherry (Figures 7J and 7K). Silencing rdLSCRHR1 neurons decreased the density of c-fos-labeled cells in rdLS (Figure 7L) while increasing the amount of social interaction (Figure 7I). Taken together, these experiments demonstrate that CRH release from ILA and activation of rdLSCRHR1 neurons during familiar encounters disinhibits a specific population of rLS cells bordering the lateral ventricles and suppress social interactions with a familiar mouse. Our findings suggest that rLS disinhibition suppresses social interactions. To explore this further, we examined the effects of optogenetic activation of rLS neurons. We injected an AAV expressing ChR tagged with mCherry or mCherry only in rLS of WT mice and implanted an optical ferrule above it (Figures 7M and 7N). We then presented a familiar mouse for 2 min while stimulating ChR using a 445-nm laser (1-ms stimulation at 20 Hz) and measured the interaction time as well as the mean duration of each interaction bout. As an additional control, we measured behavior in ChR-expressing mice without laser stimulation. Activation of rLS neurons decreased the amount of social interaction with familiar mice (Figure 7O) due to shorter interaction bouts each time the mice met (Figure 7P) but without affecting locomotion (Figure 7Q). This experiment demonstrates that rLS is able to decrease social interactions with familiar mice. Altogether our study shows that $ILA^{CRH}$ cells are activated during familiar mouse encounters, leading to release of CRH in rdLS and causing its disinhibition. Disinhibition of rLS in turn suppresses social interaction, which leads to the decrease in social interaction observed during familiarization. Finally, inhibition of social interaction with familiar mice indirectly promotes SNP when novel and familiar mice are presented simultaneously.

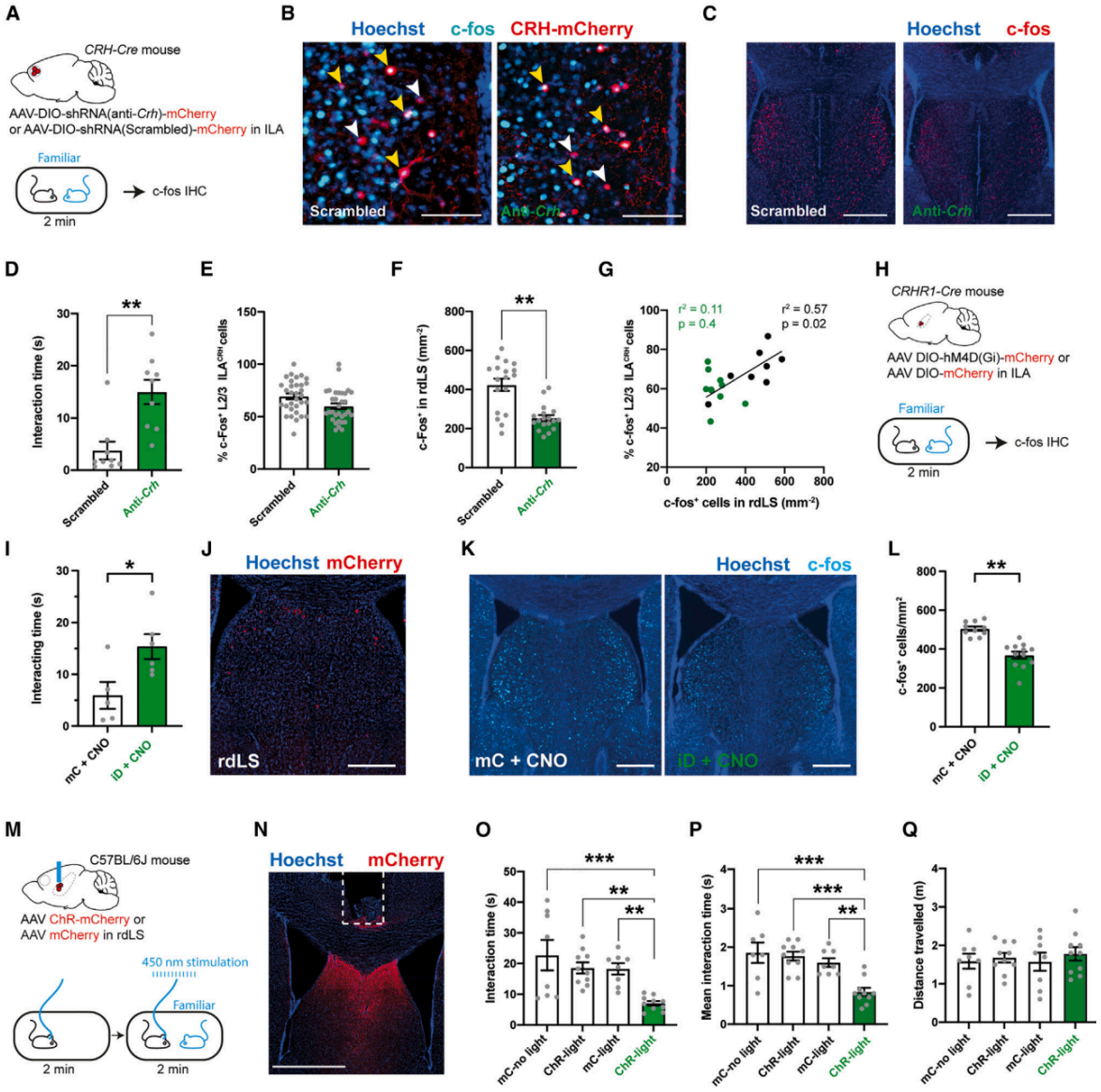


**Figure 7. CRH release from ILA and rdLS$^{CRHR1}$ neurons regulate rdLS disinhibition and social interaction with a familiar mouse**

(A) CRH-Cre mice injected in ILA with AAV2/9 CMV-DIO-(mCherry-U6)-shRNA(anti-Crh) or AAV2/9 CMV-DIO-(mCherry-U6)-shRNA(scrambled) presented with a familiar mouse before c-fos labeling.

(B and C) Immunohistochemistry images of c-fos labeling in ILA (B) and rdLS (C). Yellow arrowheads: c-fos+ / tdTomato+ cells. White arrowheads: c-fos$^{+}$ /tdTomato$^{+}$ cells. Scale bars, 100 and 300 mm.

(D) Duration of interaction during familiar presentation. Each dot is one mouse. Unpaired t test, p = 0.001.

(E) Percentage of layer 2/3 ILA$^{CRH}$ cells positive for c-fos in layer 2/3 of ILA. 3 to 4 observations per mouse, 9 mice per group. Nested t test, p = 0.06.

(F) Density of rdLS cells positive for c-fos. 2 observations per mouse, 9 mice per group. Nested t test, p = 0.002.

(G) Percentage of layer 2/3 ILA$^{CRH}$ cells positive for c-fos vs. density of rdLS cells positive for c-fos

following social interaction with a familiar mouse. Each dot is one mouse. Pearson's tests: Anti-Crh, p = 0.4; scrambled, p = 0.02.
(H) CRHR1-Cre mice injected in rdLS with AAV2/8 hSyn.DIO.hM4D(Gi)-mCherry (iDREADD) or AAV2/8 hSyn.DIO.mCherry presented with a familiar mouse before c-fos labeling.
(I) Interaction time with familiar mouse. Each dot is one mouse. Unpaired t test, p = 0.03.
(J) Immunohistochemistry picture of mCherry expression in rdLS. Scale bars, 400 mm.
(K) Immunohistochemistry pictures of c-fos expression in rdLS. Scale bars, 400 mm.
(L) Density of rdLS cells positive for c-fos. 2 observations per mouse, 5 and 6 mice per group. Nested t test, p = 0.002.
(M) C57BL/6J wild-type mice were injected with AA2/2 hSyn1.hChR2(H134R)-mCherry or AA2/2 hSyn1.mCherry as control and an optical fiber was implanted above the injection site. Mice were then presented to a familiar mouse for 2 min meanwhile 450 nm light or no light was applied (20 Hz, 1 ms).
(N) Immunohistochemistry picture of viral injection. Scale bars, 1 mm.
(O) Total interaction time with familiar mouse. Each do is one mouse. One-way ANOVA: $F_{3,32} = 7.01$, $p < 0.0001$. Dunnett's multiple comparison tests: p = 0.0005, 0.006, and 0.01.
(P) Average duration of each bout of social interaction. One-way ANOVA: $F_{3,31} = 10.62$, $p < 0.0001$. Dunnett's multiple comparison tests: p = 0.0001, 0.0001, and 0.003.
(Q) Total distance traveled. For the entire figure, bar graphs represent mean ± SEM.

**Increased CRH expression in ILA supports a shift in social preference in young mice**

In contrast to adults, young rodents prefer to interact with their familiar siblings compared with novel pups.[3,4,56] We tested when the shift in social preference occurs in mice by giving young WT mice the choice to interact with their familiar siblings or with unfamiliar non-siblings every day from post-natal days 7 to 21 (P7 to P21). Between P7 and P15, mice preferred to interact with their siblings (Figure 8A), and social preference was strongly skewed toward familiarity (Figure 8B). Social preference then gradually shifted toward novel mice (Figure 8A) with a clear preference for novel mice after P16 (Figure 8B). Both PFC and LS have been shown to control SNP and the LS is also involved in the preference young rats display for their own (familiar) kin compared with non-kin.3 We then asked when ILA neurons begin to express CRH and whether the emergence of the ILA to rdLS circuit described above contributes to the shift in social preference. We counted CRH-tdTomato$^{+}$ cells at P7, P15, and P21 in CRH-Cre;Ai9 mice (Figures 8C and 8D) and observed a strong increase in the density of ILA$^{CRH}$ cells from P7 to P21 (Figure 8E). Interestingly, the increase was the strongest in ILA compared with other prefrontal regions (Figure 8F). Within ILA, the increase of CRH+

cells proceeded mostly from an increase in CRH+ cells located in layer 2/3 (Figure 8G), which is the layer containing $ILA^{CRH}$ cells projecting to rdLS (Figures 1K and S3D). Comparing the number of $ILA^{CRH}$ cells per section with the retrogradely labeled ones (Figure S3D) suggests that at least 60% of these cells project to rdLS. Closer inspection of $CRH^{+}$ cells in PLA and ACA revealed less or no increase in layer 2/3 (Figures S15A and S15B). In situ hybridization against Crh in WT mice demonstrated a similar increase in Crh+ neuron density in mPFC in general and PLA and ILA in particular (Figures S15C–S15F). Overall, these experiments demonstrate that the strengthening of the $ILA^{CRH}$ to rdLS circuit correlates with the shift from social familiarity to SNP in young pups. We next probed whether the maturation of the $ILA^{CRH}$ cells to LS circuit causes the shift in social preference. P5 pups were injected with AAVs expressing the anti-Crh or the scrambled shRNAs. We reasoned the AAVs would be taken up by many ILA neurons so that, as soon as Crh expression begins, so would the Cre expression and therefore shRNA expression under the control of the fast-expressing U6 promoter.[57] 2 days after the injection, we began testing the injected pups for social preference and observed a shift in preference at P14 in the control group (Figure 8H), similar to our previous experiment on WT mice (Figure 8A). The test group lacking Crh in ILA however continued to exhibit familiar preference until P21 when the mice had to be weaned, and the experiment interrupted (Figure 8H). Consistently, the choice index for the control group inverted before and after P16, reflecting the shift in social preference while the index for the Crh-depleted group remained oriented toward familiar choices (Figure 8I). We performed in situ hybridization against Crh and mCherry at the end of the behavioral testing (P21) in order to verify the efficacy of the shRNA-mediated Crh depletion technique in young pups (Figure S15G). Similar to our results in adults (Figure 4B), cells expressing the anti-Crh shRNA exhibited a strong decrease in Crh labeling intensity (Figure S15H). Overall, these experiments suggest that increased CRH expression in ILA during the second and third post-natal weeks is responsible for the shift in social preference displayed by young mice.

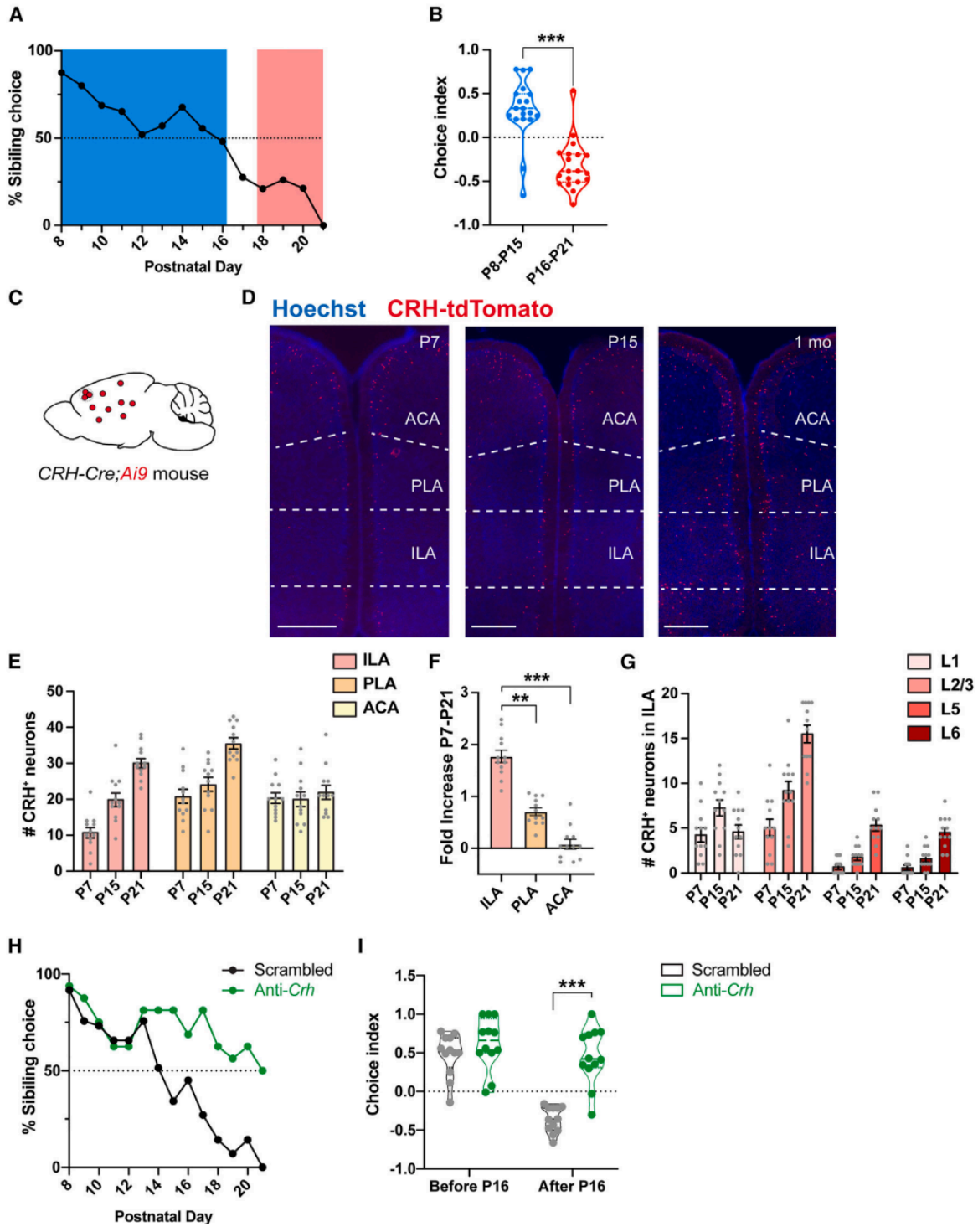


**Figure 8. Increased CRH expression in ILA supports a shift in social preference in young mice**

(A) Percentage of familiar choice during development, 19 mice.

(B) Discrimination index for familiar kin before and after post-natal day 16. Each dot is one mouse. Unpaired t test, $p < 0.0001$.

(C) CRH-Cre;Ai9 mouse.

(D) mPFC images of CRH-Cre;Ai9 mice at P7, P15, or P21. Scale bars, 500 mm.

(E) Number of CRH+ cells in ILA, PLA, and ACA during development. 4 observations per mouse, 3

mice per group. Nested one-way ANOVA tests comparing $CRH^+$ cells along post-natal day: F(ILA)2,6 = 18.64, p = 0.003; F(PL)2,6 = 11.47, p = 0.009; F(ACA)2,6 = 0.22, p = 0.8.
(F) Fold-increase of CHR+ cells between P7 and P21. P21 values compared with the average P7 value. Nested one-way ANOVAF2,6 = 52.51, p = 0.0002. Post-hoc Tukey's multiple comparison tests: p = 0.001 and p < 0.0001.
(G) Number of CRH+ cells per ILA layers during development. 4 observations per mouse, 3 mice per group.
(H) Percentage of familiar choice during development in CRH-Cre mice injected in ILA with AAV2/9 CMV-DIO-(mCherry-U6)-shRNA(anti-Crh) to downregulate Crh or control AAV2/9 CMV-DIO-(mCherry-U6)-shRNA(scrambled) (12 pups per group). Chi-squared test: p < 0.0001.
(I) Discrimination index for familiar kin before and after post-natal day 16. Each dot represents a mouse. Two-way ANOVA: F(virus x age)1,44 = 15,45, p = 0.0003; F(virus)1,44 = 34,54, p < 0.0001; and F(virus)1,44 = 14,73, p = 0.6 and p < 0.0001. Tukey's multiple comparison test: p < 0.0001. For the entire figure, bar graphs represent mean ± SEM.
See also Figure S15.

## DISCUSSION

We show that $ILA^{CRH}$ cells respond to social interaction with familiar over novel mice and release CRH into rLS in order to suppress social interactions with familiar mice through LS disinhibition. During familiarization, increasingly responsive $ILA^{CRH}$ cells control the decrease in interaction as a novel mouse becomes familiar. When given the choice between a familiar and a novel mouse, this circuit suppresses social interaction with the familiar mouse to support SNP. We asked previously whether $ILA^{CRH}$ cells control social memory or rather downstream processes, including SNP, that utilize social memory cues. Silencing $ILA^{CRH}$ cell terminals to rdLS during the recall trial but not during the learning trial disrupts SNP (Figures 4L and 4M), suggesting that $ILA^{CRH}$ cells do not contribute to social memory formation. This is in line with previous work showing that the CRH-binding protein is critical for the recall but not for the learning phase of social recognition.32 Knocking down Crh expression in ILA increases social interactions with familiar mice (Figures 4C and 7D) while keeping c-fos expression in ILA intact (Figure 7E), suggesting that $ILA^{CRH}$ neurons integrate social familiarity cues before releasing CRH in order to regulate social interaction with familiar mice. Previous hypotheses about the mechanisms underlying SNP supposed the existence of a circuit promoting social interactions with novel mice, probably under control of the rewarding properties of social

novelty. In addition, the kin preference toward mothers or siblings displayed by young mice[19,56] supposes the existence of other circuits controlling social preferences. Very little is known however about the mechanisms supporting the rewarding properties of social cues. The lateral habenula, nucleus accumbens, dorsal raphe nucleus, and ventral tegmental area modulate social reward,[58–62] some of them under the control of oxytocin.[58–60] Subsequent studies should aim to characterize how social novelty can facilitate interactions with novel mice. The LS, which is heavily modulated by dopamine, vasopressin, and oxytocin,[20] is likely to also integrate inputs facilitating interactions with novel mice in order to promote SNP. Interestingly, Liu et al.[63] showed that silencing dLS neurons (located posterior to rLS) suppresses social approach and facilitates avoidance with novel but not familiar mice. This confirms the importance of LS to modulate social interactions and suggests that different LS regions can regulate different types of social interactions and may work together to promote SNP. How specific is the regulation of social preference by $ILA^{CRH}$ cells? We demonstrate that $ILA^{CRH}$ cells control memory-based SNP but not memory-based novel object preference. Since the three stimulus mice used during our SNP test are siblings from the same cage (and thus also from the same strain, same age, and same sex), mice must discriminate between novel and familiar individuals based on the idiosyncratic identity of each individual, that is, based on true individual recognition and not a more general class recognition. Whether $ILA^{CRH}$ cells control other social preferences such as preferences based on sex, strain, kinship, or anxiety (mice prefer to interact with non-stressed mice)[13] remains to be determined. The associative nature of the mPFC and our rabies tracing experiment (data not shown) suggest that $ILA^{CRH}$ cells integrate information from many brain regions which are likely to provide various social cues about the nature and identity of the stimulus mice. In this framework, we suppose that social cues of negative valence activate excitatory neurons projecting to $ILA^{CRH}$ cells. For example, social memories of previous encounters are known to be stored in the pyramidal neurons of the ventral CA1 (vCA1) region of the hippocampus64 and vCA1 projection to mPFC is necessary for behaviors relying on social memory

such as SNP.[65,66] Consistently, rabies tracing demonstrates that ILA$^{CRH}$ cells receive direct inputs from vCA1 pyramidal neurons (data not shown). However, whether the vCA1 neurons projecting to ILA$^{CRH}$ cells carry social familiarly information remains to be confirmed. Unlike adults, young rats and mice display kin preference for mother and siblings during the first weeks of life.[3,19] Here, we show how young mice reliably display social preference toward their siblings vs. age-matched pups until maturation of the CRH circuit triggers a shift in preference toward the normotopic adult behavior. Indeed, while defenseless pups need to rely on the safety of their nest and company of their siblings, older and more able young mice will benefit from leaving their kin and venture out of the nest in order to sample resources (feeding behavior) and interact with novel conspecifics (reproductive behavior).[67] Overall, orchestrating a wide range of sometimes antagonistic motivated behaviors including safety, feeding, novel social interactions, and mating is essential and the LS has been proposed to play a key role in setting up priorities between motivated behaviors.[68] Unlike mice, monogamous prairie voles exhibit SNP only during short-term tests, but partner preference can be observed during long-term tests.[69,70] This difference in social preference might be due to the fact that the prairie vole mPFC does not express CRH.[71] Furthermore, CRH intra-cerebroventricular injections in prairie voles prior to short-term tests induces preference for a familiar vole over a novel one.[72] These experiments demonstrate the role of CRH in regulating social preferences in several rodent species and suggest that differences in mPFC CRH systems can be responsible for novelty or partner preference. Humans can suffer from social separation anxiety disorder, which manifests itself as an ‘‘unusually strong fear or anxiety to separating from people they feel a strong attachment to.’’[73] Patients present unusual distress at the discussion or experience of being parted from their attachment figure and a refusal to leave the attachment figure. Similarly, patients affected with avoidant personality disorder are unwilling to interact with novel individuals because of fear of being rejected and favor interacting with familiar ones.[73] In addition, CRH has been involved in various anxiety disorders, including social phobia.[35,74] Similar to our findings, familiarity cues

activate the human PFC[75,76] and septal[77] regions, supporting the idea that the circuit we described in the mouse is conserved in humans. A potential cause for social anxiety disorders such as separation anxiety disorder or avoidant personality disorder could then be that patients exhibit low CRH level in the PFC, preventing them from seeking social novelty.

**Limitations of the study**

The exact demarcations of the rodent PFC are subjected to debate, including the demarcations of its sub-regions such as the ILA are unclear.[78] In this study, we used the Paxinos atlas (4th edition) to delineate separations between brain regions.[47] Furthermore, even though shRNA-mediated silencing of vGAT decreased the intensity of vGAT labeling by 2-fold, we cannot exclude the possibility that enough vGAT remained to mediate some GABAergic transmission and perhaps participate in familiarization and SNP as well.

STAR+METHODS

Detailed methods are provided in the online version of this paper and include the following:

- KEY RESOURCES TABLE
- RESOURCE AVAILABILITY
    - Lead contact
    - Material availability
    - Data and code availability
- EXPERIMENTAL MODEL AND STUDY PARTICIPANT DETAILS
- METHOD DETAILS
    - Anti-Crh shRNA design and in vitro validation
    - Virus injections
    - Optical ferrule implants
    - Cannula guide implantation and micro-infusion
    - Immunohistochemistry (IHC)

- In situ hybridization (ISH)
- In vitro electrophysiological recordings
- Behavioral tests
- Fiberphotometry data acquisition

- QUANTIFICATION AND STATISTICAL ANALYSIS
  - Fiberphotometry data analysis
  - Classifier analysis

SUPPLEMENTAL INFORMATION Supplemental information can be found online at https://doi.org/10.1016/j.cell. 2023.08.010.


## ACKNOWLEDGMENTS

Our co-author Jay Shulkin sadly passed away during the final stage of the reviewing process. We would like to acknowledge his lifetime dedication to science, his good humor, and boundless motivation to discuss experiments and results. We miss him dearly. We thank Christina Fregola and Georg Keller for providing viral vectors, Jan Deussing for sharing the CRHR1-Cre mouse line, and Yulong Li for providing the CRF1.0 biosensor. We also thank Antoine Besnard, Claudio Elgueta, Azahara Oliva, Isabel Otan˜ o-Perez, Francesco Papaleo, and Steve Siegelbaum for critical reading of the manuscript and insightful comments. F.L. acknowledges support from an ERC starting investigator grant (H202O-ERC-STG/0784-Ref.949652), a CIDEGENT grant from the Valencian Community, the Severo Ochoa Foundation, and a NARSAD young investigator grant from the Brain and Behavior Research Foundation, funded by the Osterhaus Family. R.N. is supported by NSF Neuronex (1707398) and the Gatsby Charitable Foundation (GAT3708).


## AUTHOR CONTRIBUTIONS

Conceptualization, N.S.d.L.R., J.S., A.A., and F.L.; investigation, F.L.; intracellular recordings, N.S.d.L.R. and F.L.; behavioral assays and viral injections, N.S.d.L.R., P.S.D., A.A., and F.L.; immunohistochemistry and in situ hybridization, N.S.d.L.R., A.R.-P., Y.N., and F.L.; shRNA design

C.A.d.S.; fiber photometry, N.S.d.L.R. and Y.N.; classifier analysis, R.N.; writing – original draft, N.S.d.L.R. and F.L.; writing – review & editing, N.S.d.L.R., A.A., and F.L.; visualization, N.S.d.L.R. and F.L.; supervision, F.L.; funding acquisition, F.L.

## DECLARATION OF INTERESTS

C.A.d.S. is currently an employee of Rejuvenate Bio, San Diego, USA. A.A. is currently an employee of Exponent Inc, Philadelphia, USA. Their current work is unrelated to the contents of this manuscript, and their contributions to this manuscript were made while previously employed at Columbia University. We have deposited a patent request related to the content of this manuscript.

## INCLUSION AND DIVERSITY

We support inclusive, diverse, and equitable conduct of research. Received: August 29, 2022 Revised: May 13, 2023 Accepted: August 8, 2023 Published: September 4, 2023

## REFERENCES


1. Amdam, G.V., and Hovland, A.L. (2012). Measuring animal preferences and choice behavior. Nat. Educ. Knowl. 3, 74.

2. Blaustein, A.R., and O'Hara, R.K. (1981). Genetic control for sibling recognition? Nature 290, 246–248. https://doi.org/10.1038/290246A0.

3. Clemens, A.M., Wang, H., and Brecht, M. (2020). The lateral septum mediates kinship behavior in the rat. Nat. Commun. 11, 3161. https://doi.org/ 10.1038/s41467-020-16489-x.

4. Hepper, P.G. (1983). Sibling recognition in the rat. Anim. Behav. 31, 1177– 1191. https://doi.org/10.1016/S0003-3472(83)80024-4.

5. Kogo, H., Kiyokawa, Y., and Takeuchi, Y. (2021). Rats show a preference for unfamiliar strains of rats. Preprint at bioRxiv. https://doi.org/10.1101/ 2021.02.18.431764.

6. Stowers, L., Holy, T.E., Meister, M., Dulac, C., and Koentges, G. (2002). Loss of sex discrimination and mal-male aggression in mice deficient for TRP2. Science 295, 1493–1500. https://doi.org/10.1126/science.1069259.

7. Liu, Y., Jiang, Y.A., Si, Y., Kim, J.-Y., Chen, Z.-F., and Rao, Y. (2011). Molecular regulation of sexual preference revealed by genetic studies of 5-HT in the brains of male mice. Nature 472, 95–99. https://doi.org/10.1038/ nature09822.

8. Kingsbury, L., Huang, S., Raam, T., Ye, L.S., Wei, D., Hu, R.K., Ye, L., and Hong, W. (2020). Cortical representations of conspecific sex shape social behavior. Neuron 107, 941–953.e7.

https://doi.org/10.1016/J.NEURON. 2020.06.020.

9. Mossman, C.A., and Drickamer, L.C. (1996). Odor preferences of female house mice (Mus domesticus) in seminatural enclosures. J. Comp. Psychol. 110, 131–138. https://doi.org/10.1037/0735-7036.110.2.131.

10. Moy, S.S., Nadler, J.J., Perez, A., Barbaro, R.P., Johns, J.M., Magnuson, T.R., Piven, J., and Crawley, J.N. (2004). Sociability and preference for social novelty in five inbred strains: an approach to assess autistic-like behavior in mice. Genes Brain Behav. 3, 287–302. https://doi.org/10. 1111/J.1601-1848.2004.00076.X.

11. Watanabe, S. (2014). The dominant/subordinate relationship between mice modifies the approach behavior toward a cage mate experiencing pain. Behav. Processes 103, 1–4. https://doi.org/10.1016/J.BEPROC. 2013.10.005.

12. van Loo, P.L.P., de Groot, A.C., van Zutphen, B.F.M., and Baumans, V. (2010). Do male mice prefer or avoid each other's company? Influence hierarchy, kinship, and familiarity. J. Appl. Anim. Welf. Sci. 4, 91–103. https://doi.org/10.1207/S15327604JAWS0402_1

13. Scheggia, D., Manago` , F., Maltese, F., Bruni, S., Nigro, M., Dautan, D., Latuske, P., Contarini, G., Gomez-Gonzalo, M., Requie, L.M., et al. (2020). Somatostatin interneurons in the prefrontal cortex control affective state discrimination in mice. Nat. Neurosci. 23, 47–60. https://doi.org/10. 1038/S41593-019-0551-8.

14. Nadler, J.J., Moy, S.S., Dold, G., Trang, D., Simmons, N., Perez, A., Young, N.B., Barbaro, R.P., Piven, J., Magnuson, T.R., and Crawley, J.N. (2004). Automated apparatus for quantitation of social approach behaviors in mice. Genes Brain Behav. 3, 303–314. https://doi.org/10.1111/ J.1601-183X.2004.00071.X.

15. Oliva, A., Ferna´ ndez-Ruiz, A., Leroy, F., and Siegelbaum, S.A. (2020). Hippocampal CA2 sharp-wave ripples reactivate and promote social memory. Nature 587, 264–269. https://doi.org/10.1038/s41586-020-2758-y.

16. Gheusi, G., Bluthe´ , R.M., Goodall, G., and Dantzer, R. (1994). Social and individual recognition in rodents: methodological aspects and neurobiological bases. Behav. Processes 33, 59–87. https://doi.org/10.1016/ 0376-6357(94)90060-4.

17. Manduca, A., Carbone, E., Schiavi, S., Cacchione, C., Buzzelli, V., Campolongo, P., and Trezza, V. (2021). The neurochemistry of social reward during development: what have we learned from rodent models? J. Neurochem. 157, 1408–1435. https://doi.org/10.1111/JNC.15321.

18. Domı´nguez, S., Rey, C.C., Therreau, L., Fanton, A., Massotte, D., Verret, L., Piskorowski, R.A., and Chevaleyre, V. (2019). Maturation of PNN and ErbB4 signaling in area CA2 during adolescence underlies the emergence of PV interneuron plasticity and social memory. Cell Rep. 29, 1099– 1112.e4. https://doi.org/10.1016/j.celrep.2019.09.044.

19. Laham, B.J., Diethorn, E.J., and Gould, E. (2021). Newborn mice form lasting CA2-dependent memories of their mothers. Cell Rep. 34, 108668. https://doi.org/10.1016/j.celrep.2020.108668.

20. Menon, R., Su¨ ß, T., Oliveira, V.E.M., Neumann, I.D., and Bludau, A. (2022). Neurobiology

of the lateral septum: regulation of social behavior. Trends Neurosci. 45, 27–40. https://doi.org/10.1016/j.tins.2021.10.010.

21. Bielsky, I.F., Hu, S.-B., Ren, X., Terwilliger, E.F., and Young, L.J. (2005). The V1a vasopressin receptor is necessary and sufficient for normal social recognition: a gene replacement study. Neuron 47, 503–513. https://doi. org/10.1016/j.neuron.2005.06.031.

22. Lukas, M., Toth, I., Veenema, A.H., and Neumann, I.D. (2013). Oxytocin mediates rodent social memory within the lateral septum and the medial amygdala depending on the relevance of the social stimulus: male juvenile versus female adult conspecifics. Psychoneuroendocrinology 38, 916–926. https://doi.org/10.1016/J.PSYNEUEN.2012.09.018.

23. Gutzeit, V.A., Ahuna, K., Santos, T.L., Cunningham, A.M., Sadsad Rooney, M., Mun˜ oz Zamora, A., Denny, C.A., and Donaldson, Z.R. (2020) Optogenetic reactivation of prefrontal social neural ensembles mimics social buffering of fear. Neuropsychopharmacology 45, 1068–1077. https:// doi.org/10.1038/s41386-020-0631-1.

24. Levy, D.R., Tamir, T., Kaufman, M., Parabucki, A., Weissbrod, A., Schneidman, E., and Yizhar, O. (2019). Dynamics of social representation in the mouse prefrontal cortex. Nat. Neurosci. 22, 2013–2022. https://doi.org/ 10.1038/s41593-019-0531-z.

25. Kingsbury, L., Huang, S., Wang, J., Gu, K., Golshani, P., Wu, Y.E., and Hong, W. (2019). Correlated neural activity and encoding of behavior across brains of socially interacting animals. Cell 178, 429–446.e16. https://doi.org/10.1016/J.CELL.2019.05.022.

26. Park, G., Ryu, C., Kim, S., Jeong, S.J., Koo, J.W., Lee, Y.S., and Kim, S.J. (2021). Social isolation impairs the prefrontal-nucleus accumbens circuit subserving social recognition in mice. Cell Rep. 35, 109104. https://doi. org/10.1016/j.celrep.2021.109104.

27. Yizhar, O., and Levy, D.R. (2021). The social dilemma: prefrontal control of mammalian sociability. Curr. Opin. Neurobiol. 68, 67–75. https://doi.org/ 10.1016/j.conb.2021.01.007.

28. Carus-Cadavieco, M., Gorbati, M., Ye, L., Bender, F., van der Veldt, S., Kosse, C., Bo¨ rgers, C., Lee, S.Y., Ramakrishnan, C., Hu, Y., et al. (2017). Gamma oscillations organize top-down signalling to hypothalamus and enable food seeking. Nature 542, 232–236. https://doi.org/10.1038/ nature21066.

29. Vale, W., Spiess, J., Rivier, C., and Rivier, J. (1981). Characterization of a 41-residue ovine hypothalamic peptide that stimulates secretion of corticotropin and beta-endorphin. Science 213, 1394–1397. https://doi.org/ 10.1126/SCIENCE.6267699.

30. Schulkin, J. (2017). The CRF Signal: Uncovering an Information Molecule (Oxford University Press). https://doi.org/10.1093/acprof:oso/9780198793694.001.0001.

31. Hostetler, C.M., and Ryabinin, A.E. (2013). The CRF system and social behavior: a review. Front. Neurosci. 0, 92. https://doi.org/10.3389/ FNINS.2013.00092/BIBTEX.

32. Heinrichs, S.C. (2003). Modulation of social learning in rats by brain corticotropin-releasing factor. Brain Res. 994, 107–114. https://doi.org/10. 1016/J.BRAINRES.2003.09.028.

33. Dinan, T.G., Lavelle, E., Scott, L.V., Newell-Price, J., Medbak, S., and Grossman, A.B. (1999). Desmopressin normalizes the blunted adrenocorticotropin response to corticotropin-releasing hormone in melancholic depression: evidence of enhanced vasopressinergic responsivity. J. Clin. Endocrinol. Metab. 84, 2238–2240. https://doi.org/10.1210/JCEM.84.6.5723.

34. Raadsheer, F.C., Hoogendijk, W.J.G., Stam, F.C., Tilders, F.J.H., and Swaab, D.F. (1994). Increased numbers of corticotropin-releasing hormone expressing neurons in the hypothalamic paraventricular nucleus of depressed patients. Neuroendocrinology 60, 436–444. https://doi.org/ 10.1159/000126778.

35. Risbrough, V.B., and Stein, M.B. (2006). Role of corticotropin releasing factor in anxiety disorders: a translational research perspective. Horm. Behav. 50, 550–561. https://doi.org/10.1016/J.YHBEH.2006.06.019.

36. Dedic, N., Ku¨ hne, C., Gomes, K.S., Hartmann, J., Ressler, K.J., Schmidt, M.V., and Deussing, J.M. (2019). Deletion of CRH from GABAergic forebrain neurons promotes stress resilience and dampens stress-induced changes in neuronal activity. Front. Neurosci. 13, 986. https://doi.org/10. 3389/fnins.2019.00986.

37. Campbell, B.M., Morrison, J.L., Walker, E.L., and Merchant, K.M. (2004). Differential regulation of behavioral, genomic, and neuroendocrine responses by CRF infusions in rats. Pharmacol. Biochem. Behav. 77, 447–455. https://doi.org/10.1016/J.PBB.2003.12.010.

38. Dunn, A.J., and File, S.E. (1987). Corticotropin-releasing factor has an anxiogenic action in the social interaction test. Horm. Behav. 21, 193–202. https://doi.org/10.1016/0018-506X(87)90044-4.

39. Elkabir, D.R., Wyatt, M.E., Vellucci, S.V., and Herbert, J. (1990). The effects of separate or combined infusions of corticotrophin-releasing factor and vasopressin either intraventricularly or into the amygdala on aggressive and investigative behaviour in the rat. Regul. Pept. 28, 199–214. https://doi.org/10.1016/0167-0115(90)90018-R.

40. Gehlert, D.R., Shekhar, A., Morin, S.M., Hipskind, P.A., Zink, C., Gackenheimer, S.L., Shaw, J., Fitz, S.D., and Sajdyk, T.J. (2005). Stress and central urocortin increase anxiety-like behavior in the social interaction test via the CRF1 receptor. Eur. J. Pharmacol. 509, 145–153. https://doi.org/10. 1016/J.EJPHAR.2004.12.030.

41. Mele, A., Cabib, S., Oliverio, A., Melchiorri, P., and Puglisi-Allegra, S. (1987). Effects of corticotropin releasing factor and sauvagine on social behavior of isolated mice. Peptides 8, 935–938. https://doi.org/10.1016/ 0196-9781(87)90083-0.

42. Zhao, Y., Valdez, G.R., Fekete, E.M., Rivier, J.E., Vale, W.W., Rice, K.C., Weiss, F., and Zorrilla, E.P. (2007). Subtype-selective corticotropinreleasing factor receptor agonists exert contrasting, but not opposite, effects on anxiety-related behavior in rats. J. Pharmacol. Exp. Ther. 323, 846–854. https://doi.org/10.1124/JPET.107.123208.

43. Bagosi, Z., Cze´ bely-Le´ na´rt, A., Karasz, G., Csabafi, K., Ja´ szbere´ nyi, M., and Telegdy, G. (2017). The effects of CRF and urocortins on the preference for social novelty of mice. Behav. Brain Res. 324, 146–154. https:// doi.org/10.1016/J.BBR.2017.02.009.

44. Kasahara, M., Groenink, L., Kas, M.J.H., Bijlsma, E.Y., Olivier, B., and Sarnyai, Z. (2011). Influence of transgenic corticotropin-releasing factor (CRF) over-expression on social recognition memory in mice. Behav. Brain Res. 218, 357–362. https://doi.org/10.1016/J.BBR.2010.12.029.

45. Chen, P., Lou, S., Huang, Z.-H., Wang, Z., Shan, Q.-H., Wang, Y., Yang, Y., Li, X., Gong, H., Jin, Y., et al. (2020). Prefrontal cortex corticotropinreleasing factor neurons control behavioral style selection under challenging situations. Neuron 106, 301–315.e7. https://doi.org/10.1016/J. NEURON.2020.01.033.

46. van Pett, K., Viau, V., Bittencourt, J.C., Chan, R.K., Li, H.Y., Arias, C., Prins, G.S., Perrin, M., Vale, W., and Sawchenko, P.E. (2000). Distribution of mRNAs encoding CRF receptors in brain and pituitary of rat and mouse. J. Comp. Neurol. 428, 191–212. https://doi.org/10.1002/ 1096-9861(20001211)428:23.0.CO;2-U.

47. Paxinos, G., and Franklin, K.B.J. (2012). Paxinos and Franklin's the Mouse Brain in Stereotaxic Coordinates, Fourth Edition (Elsevier Science).

48. Bernardi, S., Benna, M.K., Rigotti, M., Munuera, J., Fusi, S., and Salzman, C.D. (2020). The geometry of abstraction in the hippocampus and prefrontal cortex. Cell 183, 954–967.e21. https://doi.org/10.1016/J.CELL.2020. 09.031.

49. Yu, X., Ye, Z., Houston, C.M., Zecharia, A.Y., Ma, Y., Zhang, Z., Uygun, D.S., Parker, S., Vyssotski, A.L., Yustos, R., et al. (2015). Wakefulness is governed by GABA and histamine cotransmission. Neuron 87, 164–178. https://doi.org/10.1016/J.NEURON.2015.06.003.

50. Pomrenze, M.B., Giovanetti, S.M., Maiya, R., Gordon, A.G., Kreeger, L.J., and Messing, R.O. (2019). Dissecting the roles of GABA and neuropeptides from rat central amygdala CRF neurons in anxiety and fear learning. Cell Rep. 29, 13–21.e4. https://doi.org/10.1016/J.CELREP.2019.08.083.

51. Wang, H., Qian, T., Zhao, Y., Zhuo, Y., Wu, C., Osakada, T., Chen, P., Ren, H., Yan, Y., Geng, L., et al. (2022). A toolkit of highly selective and sensitive genetically encoded neuropeptide sensors. Preprint at bioRxiv. https:// doi.org/10.1101/2022.03.26.485911.

52. Dedic, N., Ku¨ hne, C., Jakovcevski, M., Hartmann, J., Genewsky, A.J., Gomes, K.S., Anderzhanova, E., Po¨ hlmann, M.L., Chang, S., Kolarz, A., et al. (2018). Chronic CRH depletion from GABAergic, long-range projection neurons in the extended amygdala reduces dopamine release and increases anxiety. Nat. Neurosci. 21, 803–807. https://doi.org/10.1038/ s41593-018-0151-z.

53. Wang, Y., Chen, Z.-P., Zhuang, Q.-X., Zhang, X.-Y., Li, H.-Z., Wang, J.-J., and Zhu, J.-N. (2017). Role of corticotropin-releasing factor in cerebellar motor control and ataxia. Curr. Biol. 27, 2661–2669.e5. https://doi.org/10. 1016/J.CUB.2017.07.035.

54. Asok, A., Schulkin, J., and Rosen, J.B. (2016). Corticotropin releasing factor type-1 receptor antagonism in the dorsolateral bed nucleus of the stria terminalis disrupts contextually conditioned fear, but not unconditioned fear to a predator odor. Psychoneuroendocrinology 70, 17–24. https:// doi.org/10.1016/j.psyneuen.2016.04.021.

55. Tanaka, K.Z., Pevzner, A., Hamidi, A.B., Nakazawa, Y., Graham, J., and Wiltgen, B.J. (2014).

Cortical representations are reinstated by the hippocampus during memory retrieval. Neuron 84, 347–354. https://doi.org/10. 1016/J.NEURON.2014.09.037.

56. Clemens, A.M., and Brecht, M. (2021). Neural representations of kinship. Curr. Opin. Neurobiol. 68, 116–123. https://doi.org/10.1016/j.conb.2021. 02.007.

57. Lambeth, L.S., Moore, R.J., Muralitharan, M., Dalrymple, B.P., McWilliam, S., and Doran, T.J. (2005). Characterisation and application of a bovine U6 promoter for expression of short hairpin RNAs. BMC Biotechnol. 5, 13. https://doi.org/10.1186/1472-6750-5-13.

58. Do¨ len, G., Darvishzadeh, A., Huang, K.W., and Malenka, R.C. (2013). Social reward requires coordinated activity of nucleus accumbens oxytocin and serotonin. Nature 501, 179–184. https://doi.org/10.1038/ NATURE12518.

59. Hung, L.W., Neuner, S., Polepalli, J.S., Beier, K.T., Wright, M., Walsh, J.J., Lewis, E.M., Luo, L., Deisseroth, K., Do¨ len, G., and Malenka, R.C. (2017). Gating of social reward by oxytocin in the ventral tegmental area. Science 357, 1406–1411. https://doi.org/10.1126/SCIENCE.AAN4994.

60. Gunaydin, L.A., Grosenick, L., Finkelstein, J.C., Kauvar, I.V., Fenno, L.E., Adhikari, A., Lammel, S., Mirzabekov, J.J., Airan, R.D., Zalocusky, K.A., et al. (2014). Natural neural projection dynamics underlying social behavior. Cell 157, 1535–1551. https://doi.org/10.1016/j.cell.2014. 05.017.

61. Li, Y., Zhong, W., Wang, D., Feng, Q., Liu, Z., Zhou, J., Jia, C., Hu, F., Zeng, J., Guo, Q., et al. (2016). Serotonin neurons in the dorsal raphe nucleus encode reward signals. Nat. Commun. 7, 10503. https://doi.org/10. 1038/NCOMMS10503.

62. Golden, S.A., Heshmati, M., Flanigan, M., Christoffel, D.J., Guise, K., Pfau, M.L., Aleyasin, H., Menard, C., Zhang, H., Hodes, G.E., et al. (2016). Basal forebrain projections to the lateral habenula modulate aggression reward. Nature 534, 688–692. https://doi.org/10.1038/nature18601.

63. Liu, Y., Deng, S.-L., Li, L.-X., Zhou, Z.-X., Lv, Q., Wang, Z.-Y., Wang, F., and Chen, J.-G. (2022). A circuit from dorsal hippocampal CA3 to parvafox nucleus mediates chronic social defeat stress-induced deficits in preference for social novelty. Sci. Adv. 8, eabe8828. https://doi.org/10.1126/ sciadv.abe8828.

64. Okuyama, T., Kitamura, T., Roy, D.S., Itohara, S., and Tonegawa, S. (2016). Ventral CA1 neurons store social memory. Science 353, 1536– 1541. https://doi.org/10.1126/science.aaf7003.

65. Phillips, M.L., Robinson, H.A., and Pozzo-Miller, L. (2019). Ventral hippocampal projections to the medial prefrontal cortex regulate social memory. Elife 8, e44182. https://doi.org/10.7554/eLife.44182.

66. Sun, Q., Li, X., Li, A., Zhang, J., Ding, Z., Gong, H., and Luo, Q. (2020). Ventral hippocampal-prefrontal interaction affects social behavior via parvalbumin positive neurons in the medial prefrontal cortex. iScience 23, 100894. https://doi.org/10.1016/J.ISCI.2020.100894.

67. Castelhano-Carlos, M.J., Sousa, N., Ohl, F., and Baumans, V. (2010). Identification methods

in newborn C57BL/6 mice: a developmental and behavioural evaluation. Lab Anim. 44, 88–103. https://doi.org/10.1258/la.2009. 009044.

68. Besnard, A., and Leroy, F. (2022). Top-down regulation of motivated behaviors via lateral septum sub-circuits. Mol. Psychiatry 27, 3119–3128. https://doi.org/10.1038/S41380-022-01599-3.

69. Beery, A.K., Christensen, J.D., Lee, N.S., and Blandino, K.L. (2018). Specificity in sociality: mice and prairie voles exhibit different patterns of peer affiliation. Front. Behav. Neurosci. 12, 50. https://doi.org/10.3389/ FNBEH.2018.00050.

70. Lee, N.S., Goodwin, N.L., Freitas, K.E., and Beery, A.K. (2019). Affiliation, aggression, and selectivity of peer relationships in meadow and prairie voles. Front. Behav. Neurosci. 13, 52. https://doi.org/10.3389/fnbeh. 2019.00052.

71. Lim, M.M., Tsivkovskaia, N.O., Bai, Y., Young, L.J., and Ryabinin, A.E. (2006). Distribution of corticotropin-releasing factor and urocortin 1 in the vole brain. Brain Behav. Evol. 68, 229–240. https://doi.org/10.1159/ 000094360.

72. DeVries, A.C., Guptaa, T., Cardillo, S., Cho, M., and Carter, C.S. (2002). Corticotropin-releasing factor induces social preferences in male prairie voles. Psychoneuroendocrinology 27, 705–714. https://doi.org/10.1016/ S0306-4530(01)00073-7.

73. American Psychiatric Association (2013). Cautionary statement for forensic use of DSM-5. In Diagnostic and Statistical Manual of Mental Disorders (American Psychiatric Publishing, Inc). https://doi.org/10.1176/ appi.books.9780890425596.744053.

74. Laryea, G., Arnett, M.G., and Muglia, L.J. (2012). Behavioral studies and genetic alterations in corticotropin-releasing hormone (CRH) neurocircuitry: insights into human psychiatric disorders. Behav. Sci. (Basel) 2, 135–171. https://doi.org/10.3390/BS2020135.

75. Aly, M., Yonelinas, A.P., Kishiyama, M.M., and Knight, R.T. (2011). Damage to the lateral prefrontal cortex impairs familiarity but not recollection. Behav. Brain Res. 225, 297–304. https://doi.org/10.1016/j.bbr.2011. 07.043.

76. Horn, M., Jardri, R., D'Hondt, F., Vaiva, G., Thomas, P., and Pins, D. (2016). The multiple neural networks of familiarity: a meta-analysis of functional imaging studies. Cogn. Affect. Behav. Neurosci. 16, 176–190. https://doi.org/10.3758/S13415-015-0392-1/TABLES/3.

77. Moll, J., Bado, P., de Oliveira-Souza, R., Bramati, I.E., Lima, D.O., Paiva, F.F., Sato, J.R., Tovar-Moll, F., and Zahn, R. (2012). A neural signature of affiliative emotion in the human septohypothalamic area. J. Neurosci. 32, 12499–12505. https://doi.org/10.1523/JNEUROSCI.6508-11.2012.

78. Laubach, M., Amarante, L.M., Swanson, K., and White, S.R. (2018). What, if anything, is rodent prefrontal cortex? eNeuro 5. ENEURO.0315-18.2018. https://doi.org/10.1523/ENEURO.0315-18.2018.

79. Sherathiya, V.N., Schaid, M.D., Seiler, J.L., Lopez, G.C., and Lerner, T.N. (2021). GuPPy, a Python toolbox for the analysis of fiber photometry data. Sci. Rep. 11, 24212. https://doi.org/10.1038/s41598-021-03626-9.

80. Botta, P., Demmou, L., Kasugai, Y., Markovic, M., Xu, C., Fadok, J.P., Lu, T., Poe, M.M., Xu, L., Cook, J.M., et al. (2015). Regulating anxiety with extrasynaptic inhibition. Nat. Neurosci. 18, 1493–1500. https://doi.org/10. 1038/nn.4102.

81. Owen, S.F., and Kreitzer, A.C. (2019). An open-source control system for in vivo fluorescence measurements from deep-brain structures. J. Neurosci. Methods 311, 170–177. https://doi.org/10.1016/J.JNEUMETH.2018.10.022.

82. Boyle, L., Posani, L., Irfan, S., Siegelbaum, S.A., and Fusi, S. (2022). The geometry of hippocampal CA2 representations enables abstract coding of social familiarity and identity. Preprint at bioRxiv. https://doi.org/10. 1101/2022.01.24.477361. 83. Nogueira, R., Rodgers, C.C., Bruno, R.M., and Fusi, S. (2023). The geometry of cortical representations of touch in rodents. Nat. Neurosci. 26, 239–250. https://doi.org/10.1038/S41593-022-01237-9.

**STAR+METHODS**

**KEY RESOURCES TABLE**

| Reagent or Resource | Source | Identifier |
|---|---|---|
| Antibodies | | |
| Anti-c-fos antibody produced in rabbit | Abcam | #ab190289; RRID:AB_2737414 |
| Anti-GFP antibody produced in chicken | AVES Labs | #GFP-1020; RRID:AB_10000240 |
| Anti-GFP polyclonal antibody, Alexa Fluor 488 | Thermo-Fisher Scientific | #A21311; RRID:AB_221477 |
| Anti-RFP antibody produced in rabbit | Rockland Antibody | #600-401-379; RRID:AB_2209751 |
| Anti-mCherry antibody produced in goat | Biorbyt | #orb153320 |
| Anti-GABA antibody produced in guinea-pig | Abcam | #ab17413; RRID:AB_443865 |
| Donkey anti-goat IgG (H+L) secondary antibody, Alexa Fluor 568 conjugate | Thermo-Fisher Scientific | #A11057; RRID:AB_2534104 |
| Goat anti-rabbit IgG (H+L) secondary antibody, Alexa Fluor 568 conjugate | Thermo-Fisher Scientific | #A11011; RRID:AB_143157 |
| Goat anti-rabbit IgG (H+L) secondary antibody, Alexa Fluor 647 conjugate | Thermo-Fisher Scientific | #A32733; RRID: AB_2633282 |
| Goat anti-guinea-pig IgG (H+L) secondary antibody, Alexa Fluor 647 conjugate | Thermo-Fisher Scientific | #A21450; RRID:AB_2735091 |
| Goat anti-mouse IgG1 (H+L) secondary antibody, Alexa Fluor 647 conjugate | Thermo-Fisher Scientific | #A21240; RRID:AB_2536165 |

| | | |
|---|---|---|
| Goat anti-rat IgG (H+L) secondary antibody, Alexa Fluor 488 conjugate | Thermo-Fisher Scientific | #A48262; RRID:AB_2896330 |
| Goat Anti-chicken IgG (H+L) secondary antibody, Alexa Fluor 488 Conjugate | Thermo-Fisher Scientific | #A11039; RRID:AB_142924 |
| Chemicals, Peptides, and Recombinant Proteins | | |
| Stressin-1 | Tocris | #1608 |
| Antalarmin | Tocris | #2778 |
| DMSO | Sigma-Aldrich | #D8418 |
| CNO | Cayman Chemical | #16882 |
| CGP 55845 | Tocris | Cat# 1248 |
| SR 95531 | Tocris | Cat# 1262 |
| ISH probe Mm-Crh | ACD Bio | #316091 |
| ISH probe mCherry-C2 | ACD Bio | #431201-C2 |
| Experimental Models: Organisms/Strains | | |
| C57BL/6J Mus musculus | Jackson Laboratories | RRID:IMSR_JAX:000664 |
| B6(Cg)-Crhtm1(cre)Zjh/J | Jackson Laboratories | RRID:IMSR_JAX:012704 |
| B6-Crhr1tm4(cre)Jde | Jackson Laboratories | RRID:MGI:6281608 |
| B6.Cg-Gt(ROSA)26Sortm9(CAG-tdTomato)Hze/J | Jackson Laboratories | RRID:IMSR_JAX:007909 |
| Recombinant DNA | | |
| AAV2/DJ hSyn.FLEX.mGFP.2A.Synatophysin-mRuby | Stanford vector core | Addgene #1930 / Addgene #71760 |
| AAV2/9 EF1a.DIO.hChR2(E123T/T159C).eYFP | Massachusetts General Hospital | #35505-AAV9 |
| HSV hEF1a.LSIL.GFP (HT) | Massachusetts General Hospital | #RN406 |
| HSV hEF1a-Cre (HT) | Massachusetts General Hospital | #RN242 |
| Software | | |
| AxoGraph | AxoGraph | Ref. 51 |
| PRISM 9 | Graphpad | #V-124 |
| Microsoft Office Word | Microsoft | 2019 |
| Microsoft Office Excel | Microsoft | 2019 |

| | | |
|---|---|---|
| Adobe Illustrator | Adobe | 2020 v24.1 |
| FIDJI | GPL v2 | 1.6.4 |
| MATLAB | Mathworks | 9.0.1 (128) |
| Python | Lerner Lab | 3.10.2 |

## RESOURCE AVAILABILITY

### Lead contact

Further information and requests for resources and reagents should be directed to and will be fulfilled by the lead contact, Felix Leroy (felxfel@aol.com).

### Material availability

Plasmids generated in this study are available upon request to the lead contact and will be deposited to Addgene.

### Data and code availability

All data reported in this paper will be shared by the lead contact upon request. The code used to create the classifiers analysis of the fiber-photometry data is available at https://github.com/ramonnogueira/decode_familiarity. Any additional information required to reanalyze the data reported in this paper is available from the lead contact upon request.

## EXPERIMENTAL MODEL AND STUDY PARTICIPANT DETAILS

All animal procedures were performed in accordance with the regulations of the UMH-CSIC IACUCs. We used P5 to 16-week-old C57BL6/J wild-type (Jackson Laboratories, #000664) mice as well as mice of the same age range from the following transgenic mouse lines: CRH-Cre mice (Jackson Laboratories, #012704) and CRHR1-Cre mice (courtesy of Jan Deussing). CHR-Cre were crossed to the Ai9 tdTomato Cre-reporter mice (Jackson Laboratories, #007909) in order to visualize CRH+ neurons. All transgenic mice were on the C57BL6/J background. During social interaction tests, stimulus mice were C57BL6/J wild-type mice of the same gender and age than the test mouse. We observed no difference related to sex and the results were pooled together. Table S1 summarizes the number of male and female mice used in each behavioral experiment.

## METHOD DETAILS

### Anti-Crh shRNA design and in vitro validation

Three different shRNAs that target Crh (shRNA1: GCCCTTGAATTTCTTGCAGCC; shRNA2: GCATGGGTGAAGAATACTTCC; shRNA3: GGAAACTGATGGAGATTATCG) were cloned into the PX552 plasmid (Addgene #60958) to make rAAV-U6-shRNA1,2,3(CRH)-CMV-EGFP-SV40-polyA (Brain VTA #PT-2784, #PT-2785 and #PT-2786). In addition, a scrambled shRNA control was cloned into the

same plasmid to make rAAV-U6-shRNA(scrambled)-CMV-EGFP-SV40-polyA (Brain VTA #PT-0916). To overexpress CRH mRNA, the sequence for mouse CRH was cloned into a plasmid to construct rAAV-CMV-CRH-P2A-EGFP-WPRE-hGH-polyA (Brain VTA #PT-2827). For validation, HEK293T cells were transfected, in triplicate, with one of the 3 plasmids containing anti-Crh shRNAs or the scrambled shRNA construct along with the overexpression plasmid for Crh (CMV-CRH-GFP). The cells were collected 48hr post-transfection and RNA was purified (MiniBEST Universal RNA Extraction Kit; Takara,9767) and subjected to RT-PCR (One Step SYBR PrimeScript RT-PCR Kit II; Takara,RR086A) using primers for CRH (F: CCCCGCAGCCCTTGAATTTCTTG; R: GGGCGTG GAGTTGGGGGACAG) and GAPDH (F: GCAAATTCCATGGCACCGTCAAGG; R: CGCCAGCATCGCCCCACTTG) as a control. The RT-PCR results revealed that all three of the anti-Crh shRNAs showed robust decreases of Crh mRNA relative to the scrambled shRNA control. The anti-Crh shRNA-2 showed the highest knockdown efficiency and was selected for in vivo knockdown experiments. The anti-Crh shRNA-2 and the scrambled shRNA were cloned into a Cre-dependent plasmid80 to make rAAV-CMV-DIO-(mCherry-U6)- shRNA(anti-Crh)-WPRE-hGH-polyA (Brain VTA, #PT-2787) and rAAV-CMV-DIO-(mCherry-U6)-shRNA(scrambled)-WPRE-hGH-polyA (Brain VTA, #PT-2788) which were subsequently packaged into AAV9.

**Virus injections**

For all injections, animals were anesthetized using isoflurane and given analgesics. A craniotomy was performed above the target region and a glass pipette was stereotaxically lowered down the desired depth. Injections were performed using a nano-inject II (Drummond Scientific). 23 nL were delivered 10 s apart until the total amount was reached. The pipette was retracted after 5 min. With homozygous animals (C57BL/6J wild-type or CRH-Cre mice), injection of the virus injection expressing DREADD, ArchT, shRNA(anti-Crh) and their control viruses (fluorophore only) was randomized within each cage.

**AAVs injections in ILA**

Injection coordinates were the following (in mm from Bregma): AP: 1.65, ML: ±0.1, DV: -2.6. Injections were done bilaterally with 100nl injected per site. We injected AAV2/DJ hSyn.FLEX.mGFP.2A.Synatophysin-mRuby (Addgene #71760 prepared by the Stanford University vector core #1930), AAV2/8 hSyn.DIO.hM4D(Gi)-mCherry (Addgene #44362-AAV8), AAV2/8 hSyn.DIO.mCherry (Addgene #50459-AAV8), AAV2/5-hSyn-DIO-hM3D(Gq)-mCherry (Addgene, #44361-AAV5), AAV2/5 hsyn.DIO.mCherry (Addgene #50459- AAV5), AAV2/1 syn.FLEX.GCaMP6f.WPRE.SV40 (Addgene #100833-AAV1), AAV2/9 CMV-DIO-(mCherry-U6)-shRNA(anti-Crh) (VTA brain), AAV2/9 CMV-DIO-(mCherry-U6)-shRNA(scrambled) (VTA brain), AAV2/9 hSyn.FLEX.dsRed-shRNA(Vgat) (Addgene #67845), AAV 2/9 hSyn-flex-dsRed-shRNA(scrambled) (Addgene #71383), AAV2/2 CAG.FLEX.ArchT-tdTomato (Addgene #28305 prepared by the University of North Carolina vector core) and AAV2/2 CAG.FLEX.tdTomato (Addgene #28306 prepared by the University of North Carolina vector core) into the ILA of CRH-Cre mice. Viruses expressed for a minimum of 2 weeks.

**ACA and PLA anterograde tracing injections**

We injected AAV2/DJ hSyn.FLEX.mGFP.2A.Synatophysin-mRuby(Stanford vector core #1930 / Addgene #71760A) in ACA and PLA of CRH-Cre mice. Injections were done unilaterally with 100 nl injected per site. Injection coordinates were the following (in mm from Bregma): PLA: 1.65, ML: ±0.1, DV: -1.4 and ACA 1.65, ML: ±0.1, DV: -0.6. Viruses expressed for a minimum of 2 weeks.

**AAV injections in rdLS**

Unless specified otherwise, viruses were injected at the following coordinates in mm from Bregma: AP: 0.9, ML: ±0.2, DV: -2.8. We injected bilaterally 100 nL of HSV hEF1a.LSIL.mCherry, (Rachel Neve, Massachusetts General Hospital #RN406) into the rdLS of CRH-Cre mice. We injected 100 nL of AAV2/5 DIO.mGFP (University of North Carolina, #AV4310i) unilaterally into CRHR1-Cre mice. We injected unilaterally 200 nL of AAV2/1 syn.GCaMP6f.WPRE.SV40 (University of Pennsylvania, #AV-1-PV2822) or AAV2/9 syn.CRF1.051 into C57BL/6J WT mice. We injected bilaterally 100 nL of AA2/2 hSyn1.hChR2(H134R)-mCherry.WPRE (University of Zurich #V-124) or AA2/2 hSyn1.mCherry.WPRE (Addgene #114472-AAV2) into C57BL/6J WT mice. We injected bilaterally 100 nL of AAV2/8 hSyn.DIO.hM4D(Gi)-mCherry (Addgene #44362) or AAV2/8 hSyn.DIO.mCherry (Addgene #50459) into the rdLS of CRHR1-Cre mice. All viruses expressed for a minimum of 2 weeks.

Dual injection in rdLS and ILA

We injected C57BL/6 mice with 200 nL of HSV hEF1a.Cre in rdLS (coordinates in mm from Bregma: AP: 0.9, ML: 0, DV: -2.8). We also injected bilaterally 100 nL of AAV2/9 CMV-DIO-(mCherry-U6)-shRNA(anti-Crh) or AAV2/9 CMV-DIO-(mCherry-U6)-shRNA(scrambled) in ILA (coordinates in mm from Bregma): AP: 1.65, ML: ±0.1, DV: -2.6). We waited 3 weeks for viral expression.

**Optical ferrule implants**

Animals were anesthetized using isoflurane and given analgesics. The scalp was removed and we applied Vetbond (3M#7000002814) along the cut. A craniotomy was performed above the target region and the optical ferrule was lowered until the desired depth. Superglue was applied to hold the lens in position and then dental cement (GC FujiCEM 2) was applied to cover the exposed skull and keep the optical ferrule in position. Animal were allowed to recovered for 5 days before being used.

For fiberphotometry recording of $ILA^{CRH}$ cells in the right hemisphere we implanted the optical ferrule (B280-4419-3, Doric) at the following coordinates: AP: 1.65, ML: 0.1, DV: -2.4.

For fiberphotometry recording of rdLS cells we implanted the optical ferrule at the following coordinates: AP: 0.9, ML: 0, DV: -2.65.

For silencing of $ILA^{CRH}$ cells fibers in rdLS cells we implanted optical ferrules (Thorlab # FT200UMT and # CFLC230-10) bilaterally at the following coordinates: AP: 0.9, ML: ±0, DV: -2.65.

For excitation rdLS cells we implanted the optical ferrule (Thorlab # FT200UMT and # CFLC230-10) at the following coordinates: AP: 0.9, ML: 0, DV: -2.65

**Cannula guide implantation and micro-infusion**

The mouse scalp was removed and scored before a hole was drilled (AP +0.9, ML ±0). A cannula guide extending 2.4 mm below the pedestal (Plastics One #C315G 2-G11-SPC) was lowered slowly and kept in place using superglue. The skull was then covered with dental cement (GC FujiCEM 2) and dummy cannulas (Plastics One #C315DC-SPC) were inserted into the guides. The mice were returned to their home cages and left to recover for at least 1 week. For rdLS infusion, mice were placed under light isoflurane anes- thesia (2%) and the dummy cannula was removed. A cannula (Plastics One #C315I-SPC) projecting 2.5 mm from the tip of the cannula guide was mounted. 0.6 mL of a solution containing 2 mg of antalarmin dissolved in DMSO or DMSO (Sigma-Aldrich # D8418) only were infused over 5 min using the Fusion 200 syringe pusher (Chemix Inc.) mounted with a 2-ml syringe (Hamilton #88511). The cannula was removed 2 min after the end of the micro-infusion. Mice typically recovered fully from the light anesthesia within 5 min. Mice were returned to their home cages 20 min before the test began.

**Immunohistochemistry (IHC)**

Mice were anesthetized using isoflurane then perfused in the heart with 10 mL saline and their brains were quickly extracted and incubated in 4% PFA overnight. After 1 h washing in PBS, 60 mm slices were prepared using a Leica VT1000S vibratome (Leica Biosystems). Unless indicated otherwise, slices were permeabilized for 2h in PBS with 0.5% Triton-X100 (T9284, Sigma-Aldrich) in PBS before being incubated overnight at 4 C with primary antibodies diluted in PBS with 0.5% Triton-X in PBS. The slices were washed in PBS for 1 h then incubated overnight at 4C with secondary antibodies from Thermo-Fisher Scientific at a concentration of 1:500 diluted in PBS with 0.1% Triton-X. Hoechst counterstain was applied (Hoechst 33342 at 1:1000 for 30 min in PBS at RT) prior to mounting the slice using fluoromount (Sigma-Aldrich). Images were acquired using inverted confocal microscopes (lsm 900, Zeiss and SPII, Leica) or an epifluorescent microscope (Thunder, Leica). For post-hoc immunocytochemistry after patch-clamp recordings, slices were fixed for 1 h in PBS with 4% PFA and streptavidin was applied during secondary incubation.

Figures 1B–1E: For mRuby and GFP labelling, primary incubation was performed overnight at 4C with rabbit anti-RFP (1:500, Rockland Antibody, #600-401-379) and chicken anti-GFP (1:1000, Aves, #GFP-1020) antibodies. Secondary incubation was performed with anti-rabbit antibody conjugated to Alexa 568 (#A11036) and anti-chicken antibody conjugated to 488 (#A11039).

Figures 1M, S1, S4, S11, and S14: For YFP, GFP,GCaMP or CRF1.0 labelling, incubation was performed overnight at 4 C with anti-GFP antibody conjugated to Alexa 488 (1:500, Thermo-Fisher Scientific #A21311). No immunohistochemistry was performed against mCherry.

Figure S3E: For GABA labelling, incubation was performed during 2 days at 4C with an anti-GABA antibody (1:200, Abcam, #ab17413). Secondary incubation was performed with anti-guinea-pig antibody conjugated to Alexa 647 (#A21450). No immunohistochemistry was performed against GFP.

Figures 2B and 5E: For mCherry labelling, primary incubation was performed overnight at 4 C with

an anti-RFP antibody (1:500, Rockland Antibody, #600-401-379). Secondary incubation was performed with anti-rabbit antibody conjugated to Alexa 568 (#A11036).

Figures 3P, 7B, 7G, S14B, and S14E: For c-fos labelling, primary incubation was performed overnight at 4C with anti-c-fos antibody (1:1000, Abcam, #ab190289). Secondary incubation was performed with an anti-rabbit antibody conjugated to Alexa 568 (#A11036).

Figures 5I, 7F, and S6A: For c-fos labelling, primary incubation was performed overnight at 4 C with an anti-c-fos antibody (1:1000, Abcam, #ab190289). Secondary incubation was performed with anti-rabbit antibody conjugated to Alexa 647 (#A32733). No immunohistochemistry was performed against mCherry or tdTomato.

Figures 4L, 7R, and S9I: For tdTomato or mCherry labelling, primary incubation was performed overnight at 4 C with an anti-RFP antibody (1:500, Rockland Antibody, 600-401-379). Secondary incubation was performed with anti-rabbit antibody conjugated to Alexa 568 (#A11036).

Figure S10B: For tdTomato and CRF1.0 labelling, primary incubation was performed overnight at 4 C with an anti-RFP antibody (1:500, Rockland Antibody, 600-401-379). Secondary incubation was performed with anti-rabbit antibody conjugated to Alexa 568 (#A11036) and anti-GFP antibody conjugated to Alexa 488 (1:500, Thermo-Fisher Scientific #A21311).

Figures 5A, S8A, S13B, and S13C: For GFP or GCaMP6f labelling, incubation was performed overnight at 4C with an anti-GFP antibody conjugated to Alexa 488 (1:500, Thermo-Fisher Scientific, #A21311).

Figures 7I and 7J: For c-fos and mCherry labelling, primary incubation was performed overnight at 4C with an anti-c-fos antibody (1:1000, Abcam, #ab190289) and anti-mCherry antibody (1:1000, Biorbyt, #orb153320). Secondary incubation was performed with anti-rabbit antibody conjugated to Alexa 647 (#A32733) and anti-goat secondary antibody conjugated to Alexa 568 (#A11057).

**Fluorescence quantification in CRH-Cre mice injected in the PFC with AAV2/DJ**

**hSyn.FLEX.mGFP.2A.Synatophysin-mRuby**

Images were acquired using an epifluorescent microscope (Thunder, Leica). Images at 8 bits (0 to 255 intensity units/pixel) were analyzed using the software Image J. For each picture, we measure the mean fluorescence value of the background and then sub- tracted it from the mean fluorescence value of the region of interest (ROI). Fluorescence intensity = (Mean fluorescence of ROI – Mean fluorescence of the background).

**In situ hybridization (ISH)**

Mice were anesthetized using isoflurane then decapitated and their brain quickly extracted. Brains were then immersed in dry-ice cold Butan X for 6 s before being stored at -80 C. 16 mm-thick slices were prepared using a Leica cryostat (CM3050 S, Leica Biosystems) and mounted on Superfrost Plus microscope slides (12-550-15, FisherBrand). For Crh and mCherry labelling (Figure 4A), we processed the slices using the RNAscope Multiplex Fluorescent Detection kit v1 (ACD Bio,

#320851) with the probes for Crh in C1 (#316091), mCherry in C2 (#431201-C2). We applied Protease IV for 30 s and used the Amp4 Alt-A color module. The first version of the kit was discontinued and we performed the Crh only labelling (Figure S15C) using the RNAscope Multiplex Fluorescent Detection kit v2 (#323110) with Crh in C1 (#316091) with 30 s of Protease IV for and used the TSA Vivid Dye 520 at 1:750. We also performed Vgat/dsRed (Figure S9C) labelling using the RNAscope Multiplex Fluorescent Detection kit v2 (ACD Bio, #323110) vGATin C1 (#319191) and dsRed in C2 (#481361-C2) with 2 min of Protease IV. Weused fluorescent dyes TSA Vivid Dye 520 at 1:750 for vGAT and TSA Vivid Dye 650 at 1:750 for dsRed. DAPI was apply for 30 s prior to mounting using fluoromount. Images were acquired using a confocal microscope (SPII, Leica).

**In vitro electrophysiological recordings**

We prepared coronal brain slices from 8- to 12-week-old C57BL6/J mice. Animals were killed under isoflurane anesthesia by perfusion into the right ventricle of ice-cold solution containing the following (in mM): 125 NaCl, 2.5 KCl, 22.5 glucose, 25 NaHCO3,1.25NaH2PO4,3Na Pyruvate,1Ascorbic acid,2CaCl2 and 1 MgCl2). ACSF was saturated with 95% O2 and 5% CO2,pH7.4.Brainswere cut into 400 mm slices with a vibratome (VT1200S, Leica) in the same ice-cold dissection solution. Slices were then transferred to an incubation chamber containing the same ACSF solution. The chamber was kept at 34C for 30min and then at room temperature for at least 1 h before recording. All experiments were performed at room temperature. Slices were mounted in the recording chamber under a microscope. Recordings were acquired using the Multiclamp700B amplifier (Molecular Device), data acquisition interface ITC-18 (Instrutech) and the Axograph software. We targeted CA2 PNs based somatic location and size in both deep and superficial layer. Whole-cell recordings were obtained from LS neurons in voltage-clampmode at -70mV patch pipette (3–5 MU) containing the following (in mM): 135 Cs-gluconate, 5 KCl, 0.2 EGTA-Na, 10 HEPES, 2 NaCl, 5 ATP, 0.4 GTP, 10 phosphocreatine, and 5 mM biocytin, pH 7.2 (280–290 mOsm). The liquid junction potential was 1.2 mV and was left uncorrected. Inhibitory currents were recorded in voltage-clamp configuration at +10 mV. We recorded rdLS neurons in septal slices from CRH-Cre mice expressing channelrhodopsin and applied 2 mMSR95531 (Tocris, # 1262) and 1 mMCGP55845 (Tocris, #1248) to block GABAA and GABAB receptors, respectively while monitoring the light induced IPSCs in rdLS neurons. We also applied a tetanic light stimulation (3 times 100 pulses of 1 ms at 100 Hz) with or without 300 nM antalarmin (Tocris, #2778) present in the bath.

We also recorded LS neurons from WT mice. After 10 min of stable baseline recording, stressin-1 (300 nM, Tocris # 1608) was applied following a 1:1000 dilution from stock solution into the ACSF. We used the Axograph software for data acquisition, and Excel (Microsoft) and PRISM (Graphpad) for data analysis.

**Behavioral tests**

Based on our experience conducting similar social behavior experiments, we used group size of 10-15 animals. Animals that had viral expression outside of ILA or rdLS were excluded from analysis. This criterion was pre-established since we wanted to investigate the role of local neurons. The observer was blind to the identity of the mice while performing the behavioral experiments and the subsequent analyses.

**Acknowledgments**
Reconocimientos

A mi madre, padre,

Natalia, Laura, Oscar y a Camilo.

Hoy reconozco que la decisión de dividir mi corazón entre los Andes y el Mediterráneo me ha enseñado a vivir en gratitud.

Gracias, Felix, por ser una guía en este camino, por tus extraordinarias habilidades mayéuticas y por brindarme el espacio para gestar mis propias ideas. Gracias, Noe, por ser la mejor y más cercana referente en la construcción de ciencia, sin olvidar el gran amor del que todos formamos parte.

Agradezco a mis padres por su incondicionalidad; a mis hermanas, inspiradoras mujeres brillantes; y a los “Frijoles”, por darle tanto sazón como humor a la vida. Gracias Camilo por navegar tantos kilómetros, emociones y pensamientos en este camino cambiante, sabiendo ser luz y serenidad.

Finalmente, pero no menos importante: gracias a mí.

*…cuando no sabemos medir lo importante,*

*le damos importancia a lo que medimos.*